The Development of an Antibody-Drug Conjugate to Specifically Target and Soften the Crystalline Lens *in vivo*

by

Gah-Jone Won

A thesis
presented to the University of Waterloo
in fulfillment of the
thesis requirement for the degree of
Doctor of Philosophy
in
Vision Science & Biology

Waterloo, Ontario, Canada, 2016

EXAMINATION COMMITTEE

The following served on the Examining Committee for this thesis. The decision of the Examining Committee is by majority vote.

External Examiner   Dr. Judith West-Mays, Ph.D.
             Professor, Faculty of Health Sciences
             McMaster University

Supervisor(s)   Dr. Vivian Choh, Ph.D.
             Associate Professor, School of Optometry
             University of Waterloo

Internal Member   Dr. Trefford Simpson, Ph.D.
             Professor, School of Optometry
             University of Waterloo

Internal-external Member   Dr. Jim Frank, Ph.D.
             Professor, Department of Kinesiology
             University of Waterloo

Other Member(s)   Dr. Brendan McConkey, Ph.D.
             Associate Professor, Department of Biology
             University of Waterloo

             Dr. David McCanna, Ph.D.
             Research Associate, School of Optometry
             University of Waterloo

AUTHOR'S DECLARATION

This thesis consists of material all of which I authored or co-authored: see Statement of Contributions included in the thesis. This is a true copy of the thesis, including any required final revisions, as accepted by my examiners.

I understand that my thesis may be made electronically available to the public.

STATEMENT OF CONTRIBUTIONS

I would like to acknowledge the names of my co-authors who contributed to this thesis:

1) Dr. Vivian Choh, Ph.D.

   Associate Professor, School of Optometry and Vision Science

   University of Waterloo, Ontario, Canada

2) Dr. Douglas Fudge, Ph.D.

   Adjunct Professor, Department of Integrative Biology

   University of Guelph, Ontario, Canada

ABSTRACT

Helmholtz's classical theory of accommodation states that, within the eye, contraction of the annular ciliary muscle releases the passive tension of zonules that hold the lens in a flattened state. As a result, the surface curvature of the lens steepens, and so too does dioptric power of the eye, allowing for nearby vision. It was also hypothesized that presbyopia, the age-related loss of accommodation, is due to the loss of ability for the lens to deform with age. Recently, the crystalline lens has been shown to possess a network of actomyosin filaments that are organized to help give the lens structural integrity. Given that cytoskeletal proteins are known to contribute to the integrity and biomechanical properties of cells, the question is raised of whether lenticular cells and the lens as a whole are affected by changes to these proteins and their distributions, and if so, whether a drug therapy can be designed to specifically target and soften the crystalline lens by inhibiting cytoskeletal protein interactions. This study was carried out in three stages:

(1) Investigating the effects of various physiological inhibitors on the overall stiffness of the crystalline lens.

(2) The development of a targeted drug therapy using one of the aforementioned inhibitors.

(3) Testing the newly synthesized targeted drug therapy on an in vivo system, and assessing its effect on the accommodative system.

ACKNOWLEDGEMENTS

DEDICATIONS

This work is dedicated to my mother, my father, my sister, and Virginie. None of what I have accomplished would be possible without your love, support, and encouragement. I am incredibly grateful to have you as my family.

TABLE OF CONTENTS

LIST OF FIGURES

LIST OF TABLES

LIST OF ABBREVIATIONS AND ACRONYMS

ADC   antibody-drug conjugate
ADP   adenosine diphosphate
ANOVA   analysis of variance
AQP0   aquaporin-0
AQP0ab   aquaporin-0 antibody
AQP0Fab   aquaporin-0 antigen-binding fragment
ATP   adenosine triphosphate
ATPase   adenosine triphosphatase
b-AQP0ab blebbistatin-aquaporin-0 antibody (initial ADC)
b-AQP0Fab blebbistatin-aquaporin-0 antigen-binding fragment (refined ADC)
BFSP   beaded filament structural protein
Blebbistatin 1-phenyl-1,2,3,4-tetrahydro-4-hydroxypyrrolo[2.3-b]-7-methylquinolin-4-one
BMC   basal membrane complex
BSA   bovine serum albumin
BVFL   back vertex focal length
Ca^{2+} calcium ion
CFA   complete Freund's adjuvant
D   dioptre
Da   dalton
DMSO   dimethyl sulfoxide
DTT   dithiothreitol
ELISA   enzyme-linked immunoabsorbant assay
Fab   antigen-binding fragment
F-actin   filamentous actin
FBS   fetal bovine serum
FDA   U.S. Food and Drug Administration
FGF   fibroblast growth factor
FITC   fluorescein isothiocyanate
FL   focal length
g   g-force
G-actin   globular actin
GAG   glycosaminoglycan
GRAVY   grand average hydropathicity
GRIN   gradient refractive index
Hz   hertz
IF   intermediate filament
IFA   incomplete Freund's adjuvant
IgG   immunoglobulin G
kDa   kilodalton

LAT-A	latrunculin A; [1R-[1R*, 4Z, 8E, 10Z, 12S*, 15R*, 17R*(R*)]]-4-(17-Hydroxy-5,12-dimethyl-3-oxo-2,16-dioxabicyclo[13.3.1]nonadeca-4,8,10-trien-17-yl)-2-thiazolidinone
mA	milliampere(s)
MIP	major intrinsic protein
ML-7	1-(5-Iodonaphthalene-1-sulfonyl)-1H-hexahydro-1,4-diazepine hydrochloride
MLCK	myosin light chain kinase
mm	millimetre(s)
MS	mass spectrometry
ms	millisecond
MT	microtubule
MW	molecular weight
MYH9	myosin heavy chain 9
NNA	nearest neighbour analysis
OD	optical density
PAGE	polyacrylamide gel electrophoresis
PBS	phosphate buffered saline
P_i	inorganic phosphate
pI	isoelectric point
POI	points of interest
PS	peptide sequence
PVDF	polyvinyldene fluoride
RIPA	radioimmunoprecipitation assay
Rn	nearest neighbour value
ROS	reactive oxygen species
RPE	retinal pigmented epithelium
RT	room temperature
SA	spherical aberration
SD	standard deviation
SDS	sodium dodecyl sulphate
SEC	size exclusion chromatography
SEM	standard error of the mean
TEMED	tetramethylethylenediamine
TM	theoretical mass
TS	Tyrode's solution
UV	ultraviolet
v/v	volume/volume
w/v	weight/volume
WB	Western blot
α	alpha
β	beta
γ	gamma

I.   INTRODUCTION

Within the anterior segment of the human eye, there exists a transparent biconvex structure known as the crystalline lens. The crystalline lens assists the cornea with the refraction of incident light onto the retina such that objects at a distance are perceived to be in focus. In order for vision to transition from distance to near, the lens must undergo a shape change to steepen its surface curvatures, which leads to increases in the focusing power of the eye as a whole. The aforementioned process is known as accommodation, and is achieved via the contraction of an annular muscle surrounding the equator of the crystalline lens (Helmholtz, 1962). However, as the eye ages, the mechanism of accommodation becomes increasingly compromised, which results in the eventual loss of near vision (Atchison, 2002; Duane, 1908). The inability to focus on nearby objects is a condition known as presbyopia, and is presently considered to be the most common refractive disorder in later life (Davies, Croft, Papas, & Charman, 2016). The onset of presbyopia typically occurs at 38 to 45 years of age, with a prevalence rate of 100% by the age of 55 (Koretz, Cook, & Kaufman, 2002). All individuals eventually require intervention for presbyopia, regardless of any pre-existing refractive conditions in the eye (Holden et al., 2008; The Eye Diseases Prevalence Research, 2004). However, unlike normal (emmetropic) and farsighted (hyperopic) individuals, short-sighted (myopic) individuals benefit slightly from their near-sightedness, and may not require intervention until slightly later on in life, although their amplitude of accommodation diminishes with age in a similar manner (Koretz & Cook, 2001).

The current non-invasive solutions to presbyopia include bifocal or progressive spectacles, multifocal contact lenses, and monovision correction (Meister & Fisher, 2008). However, a small percentage of presbyopic individuals that dislike the use of ocular prosthetics require or elect to have

either multifocal corneal refractive surgery, implantation of corneal inlays that increase depth of focus, or implantation of accommodative intraocular lenses (Charman, 2014; Davidson et al., 2016; Gil-Cazorla, Shah, & Naroo, 2016; Ong, Evans, & Allan, 2014). These solutions to presbyopia are considered management strategies rather than treatment options because they do not treat the underlying physiological cause of presbyopia; rather, they provide an optical solution to which the majority of the presbyopic population is content with.

It is likely that an actual physiological cure for presbyopia has not yet been resolved because of the residual uncertainty that still remains regarding the mechanism of accommodative degradation with age. In general, there are three schools of thought for presbyopia, which are based on Helmholtz's theory of accommodation (Atchison, 2002): (1) lens and capsule based theories, which consider the continued lens fibre deposition and the loss of capsule elasticity with age, (2) extralenticular theories, which consider ongoing choroidal development and ciliary muscle atrophy, and (3) geometric theories, which consider changes in the zonular attachment positions to the lens with age. The consensus is that the onset of presbyopia occurs as a result of these three theories acting in synchrony, and although the importance of each individual factor remains heavily disputed, it is widely believed that presbyopia is primarily caused by a loss of lenticular elasticity with age (Glasser & Campbell, 1998; Strenk, Strenk, & Koretz, 2005).

In an attempt to further understand lenticular biomechanics, several groups have investigated the composition and distribution of cytoskeletal proteins within the lens (Bassnett, Missey, & Vucemilo, 1999; Yeh, 1986). In 1999, Bassnett et al. (1999) imaged a hexagonal network of extracellular cytoskeletal proteins that serves to anchor lens fibre cells to the surrounding lens capsule, known as the basal membrane complex (BMC). The composition and architecture of the BMC suggest that it plays a critical role in maintaining the biomechanical integrity of the lens.

Furthermore, the distribution of actomyosin elements in the BMC, along with the presence of myosin light chain kinase (MLCK), suggests that the BMC may have two-dimensional contractile tones (Bassnett et al., 1999).

The objectives of this thesis are threefold: (1) to investigate the disruptive effects of cytoskeletal inhibitors on the biomechanical integrity of the crystalline lens, if so, (2) to identify whether an inhibitor could be modified to target and soften the crystalline lens, and finally (3) to assess the in vivo effects of the modified inhibitor on the accommodative mechanism of the eye.

II. LITERATURE REVIEW

2.1 THE EYE

The eye of any eukaryotic organism is an organ that is fundamentally responsible for the detection of light in order to form an image. However, the complexity of the eye varies greatly in nature, and as a result, some visual systems are able to perceive more than others (Prince, 1956; Walls, 1942). The simplest versions of eyes are found among single-cell organisms, such as the aquatic protozoan *Euglena* (Oyster, 1999). *Euglenas* possess a single eye, known as a stigma, which is located at the base of their flagella, and is more of an organelle that can only recognize the direction from which incident light arises. When stimulated, the stigma directs the *Euglena* towards light energy and nutrients.

In contrast to the *Euglena*, the ability to process visual details and form images of surrounding environments requires a much more complicated eye; a multicellular organ has an aperture to regulate the amount of incident light, fixed and adjustable refractive elements to focus light from varying distances, and a network of diverse photosensitive cells that converts images into electrical signals to be received by a central nervous system (Oyster, 1999). To that end, the human eye exemplifies a complex visual organ, and yet, it is well known that the design of the human eye is far from perfect. For example, the photoreceptor cells of the human eye do not face the direction of incoming light. Instead, they are embedded in a layer of surrounding tissue, and their neurons run towards the direction of incoming light. As a result of this awkward directionality, the neurons must then exit the eye in order to reach the brain by passing back through the layer of photoreceptor cells from which they originally received their signals, thereby effectively creating a blind spot. The blind

spot represents one of only a number of shortcomings in the human eye. It is therefore crucial to understand the anatomy and physiology of the visual system in order to improve upon and develop remedies for the human eye.

2.2 FUNCTIONAL ANATOMY OF THE HUMAN EYE

The human eye, for the most part, is a spherical structure formed by three layers of tunics that encapsulate a pressurized chamber filled with a jelly-like substance (Fig. II-1) (Oyster, 1999). The outermost tunic consists of a tough white scleral tissue that surrounds the posterior and majority of the eye. Anteriorly, the sclera is continuous with the cornea, which is a transparent window that allows light to enter into the chamber. The middle tunic, also known as the uvea, consists of the iris, an aperture that regulates the amount of light entering the eye, and the ciliary body, a muscle which
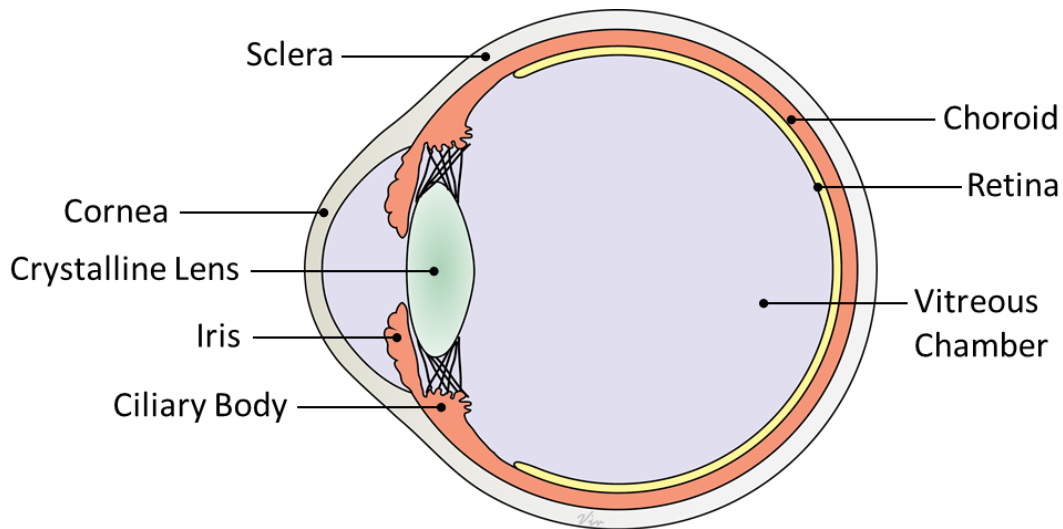
Figure II-1: Schematic diagram of the human eye. Anterior side facing left. The outer tunic consists of the cornea and sclera, the middle tunic consists of the iris, ciliary body, and choroid, and the inner tunic is known as the retina. The crystalline lens is suspended on the optical axis by the ciliary body.

suspends the crystalline lens at the front and centre of the chamber, just posterior to the iris. The posterior end of the ciliary body is continuous with the choroid, which acts as a black body that absorbs stray light and provides the vascular supply to the retina, which is the innermost tunic.

2.2.1 THE CORNEA AND THE SCLERA

Although the cornea and the sclera are continuous with one another and are composed predominantly of the same components, their structures and functions are quite different. The cornea is transparent and serves as the primary refractive element in the eye, whereas, the sclera is opaque, tougher to penetrate, and serves as the attachment point for various extraocular muscles (Oyster, 1999). These dissimilarities are primarily due to the organizational differences of collagen fibrils between the two tissues (Borcherding et al., 1975; Komai & Ushiki, 1991). In both the cornea and the sclera, collagen fibrils are organized into lamellae. However, the diameter and spacing of individual fibres in the cornea are much smaller (< 200 nm apart) and more consistent than the sclera, whose fibres vary greatly in both characteristics. The difference in mechanical strength and optical properties of the two tissues can be attributed to the lamellae of the cornea being stacked neatly on top of one another in order to allow for light to pass through easily, while the lamellae of the sclera is interwoven chaotically to increase tissue integrity at the cost of transparency (Borcherding et al., 1975; Maurice, 1957, 1970).

The air-water interface on the surface of the cornea, along with the cornea and its surface curvature, represents the most powerful refractive element in the eye (Holly & Lemp, 1977). Together, they provide two thirds of the total dioptric power of the eye. The cornea is often referred to as the window of the eye, as it is the clear structure through which light first passes in order to

form an image. The cornea is approximately 500-600 µm thick, depending on the region, and from anterior to posterior, it is composed of five distinct layers: (1) the corneal epithelium, (2) Bowman's membrane, (3) the corneal stroma, (4) Descemet's membrane, and (5) the corneal endothelium (Fig. II-2) (Maurice, 1957). The corneal epithelium contains squamous cells, wing cells, and basal cells with each cell type originating from the layer below. Basal cells, in turn, originate from stem cells that are found at the transition between the cornea and sclera, a region known as the corneal limbus (Kruse, 1994; Pellegrini et al., 1999); these cells can develop into any of the aforementioned cell types (Li et al., 2007).

Aside from damage caused by trauma or surgery, the importance of the corneal regenerative mechanism arises due to squamous epithelial cells normally lost while blinking (Thoft & Friend,
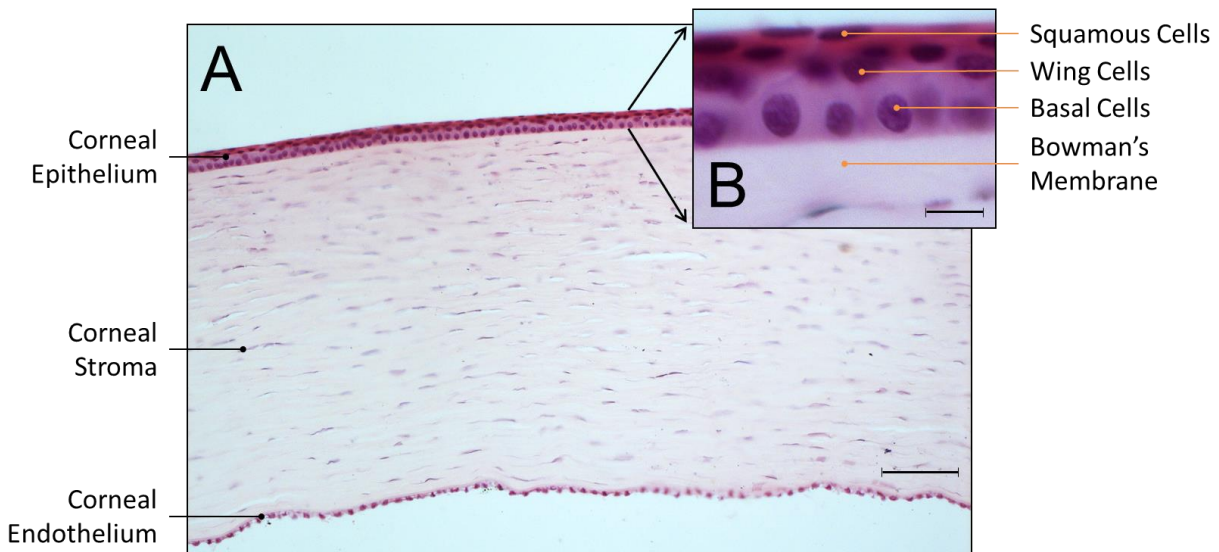
Figure II-2: Light micrograph of a histological cross-section of the primate cornea. Images taken with a (A) 10x objective lens, scale bar = 100 µm, and (B) 40x objective lens, scale bar = 5 µm. Anterior side facing up. Under low magnification, 3 layers of the cornea are visible: the corneal epithelium, the corneal stroma, and the corneal endothelium. The corneal epithelium is composed of 3 cells types: squamous cells, wing cells, and basal cells. The basement membrane of the epithelium is known as Bowman's membrane. Photo taken from a Turtox slide of the primate eye.

1983). The basement membrane of basal epithelial cells interacts intimately with the subsequent corneal layer, known as Bowman's layer, an 8-12 µm layer composed predominantly of collagen fibrils that is speculated to serve as a protective sheet for the corneal stroma and endothelium. The corneal stroma constitutes approximately 90% of the total corneal thickness, and is composed primarily of keratocytes and collagen fibrils. The posterior most layer of the cornea is known as the corneal endothelium, and is composed of a single-cell layer of simple cuboidal cells. The metabolic activity of the endothelium helps with the essential role of maintaining a detergesced state in the cornea, so that over-hydration of corneal stromal cells does not cause losses in transparency. The basement membrane of the endothelial cell layer is known as Descemet's membrane, and lies between the endothelial cells and the posterior corneal stroma. As Descemet's membrane does not affect the metabolic interchange between the endothelium and stroma, its function is speculated to be primarily protection against perforation of the cornea (Yurchenco & Schittny, 1990).

2.2.2 THE IRIS

The iris of the eye is the coloured diaphragm that rests gently on the anterior surface of the crystalline lens. The aperture or hole formed by the iris is known as the pupil, whose diameter can be varied by a set of muscles found within the iris in order to regulate the amount of light that enters the eye (Campbell, Robson, & Westheimer, 1959). From a cross-sectional point of view (Fig. II-3), the iris consists of a large stromal body primarily composed of pigmented fibrous connective tissue (Freddo, 1996; van der Zypen, 1978). At the posterior surface of the stroma is a stratified double layer of pigmented epithelial cells (Oyster, 1999). At the pupil margin, a small length of the pigmented epithelial cell layers, known as the pupillary ruff, curls over to the anterior side of the iris
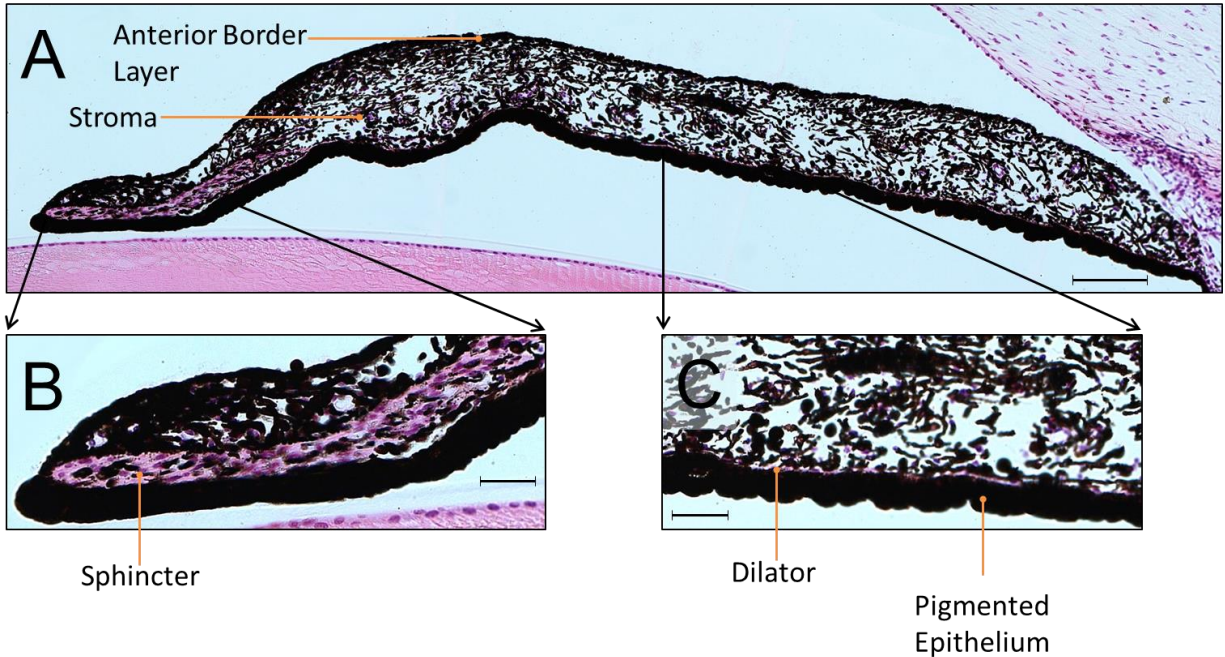
Figure II-3: Light micrograph of a histological cross-section of the primate iris.
Images taken at with a (A) 10x objective lens, scale bar = 100 μm, (B) 20x objective
lens, scale bar = 5 μm, and (C) 20x objective lens, scale bar = 5 μm. Anterior side
facing up. The bulk of the iris consists of stroma which resides posterior to the anterior
border layer. The sphincter muscle resides within the stroma, closest to the pupillary
end, whereas the dilator is a thin layer just anterior to the pigmented epithelium. Photo
taken from a Turtox slide of the primate eye.

to increase the sharpness of the aperture stop (Oyster, 1999).

Within the stroma of the iris, there exists an intricate network of vasculature with two arterial

circles as its foundation. Additionally, the expansion and contraction of the iris, which control the

size of the pupillary aperture, are mediated by two muscles found in the stroma that act oppositely

from one another (Lowenstein & Loewenfeld, 1950). The dilator muscle, which is a thin

myoepithelium produced by the more anterior of the two irideal epithelial layers, is arranged along

the length of the iris; this muscle, sympathetically innervated, acts as an antagonist to the sphincter

muscle, and functions to increase the radius of the pupil in order to augment the amount of light

entering the eye. The sphincter muscle, found at the margins of the pupil and arranged

circumferentially around the pupil is parasympathetically innervated, and functions to decrease the radius of the pupil in order to limit the amount of light entering the eye. At the other end of the pupillary margin, the root of the iris is joined to the ciliary body of the middle tunic (Oyster, 1999).

2.2.3 THE ANTERIOR CHAMBER

Within the eye, between the cornea and the iris, is a fluid-filled compartment known as the anterior chamber (Oyster, 1999). The fluid, known as aqueous humour, is produced by the ciliary body, and flows from the posterior chamber to the anterior chamber, where it is drained (Bill & Hellsing, 1965). The drainage system for the aqueous humour, known as the trabecular meshwork (Oyster, 1999) is located at the lateral sides of the anterior chamber, the cornea and the iris meet at a junction known as the anterior angle (Fig.II-4). The trabecular meshwork, in turn, has two drainage routes: (1) the corneoscleral meshwork, which accounts for 90% of the aqueous drainage, and (2) the uveal meshwork, which accounts for the remaining 10% of aqueous drainage (Weinreb, 2000). Aqueous humour running out of the corneoscleral meshwork enters a large tubular canal of Schlemm, which is connected to the veins of the external sclera, that join the venous system (Bill, 1984; Tripathi, 1971). In contrast, aqueous humour exiting through the uveoscleral meshwork is removed by the smaller veins of the ciliary body after travelling through the interstitial space of the ciliary muscle. (Alm, 2000; Bill & Hellsing, 1965).

2.2.4 THE CILIARY BODY

Posterior and lateral to the iris root, the uvea continues as the ciliary body, an annular structure that
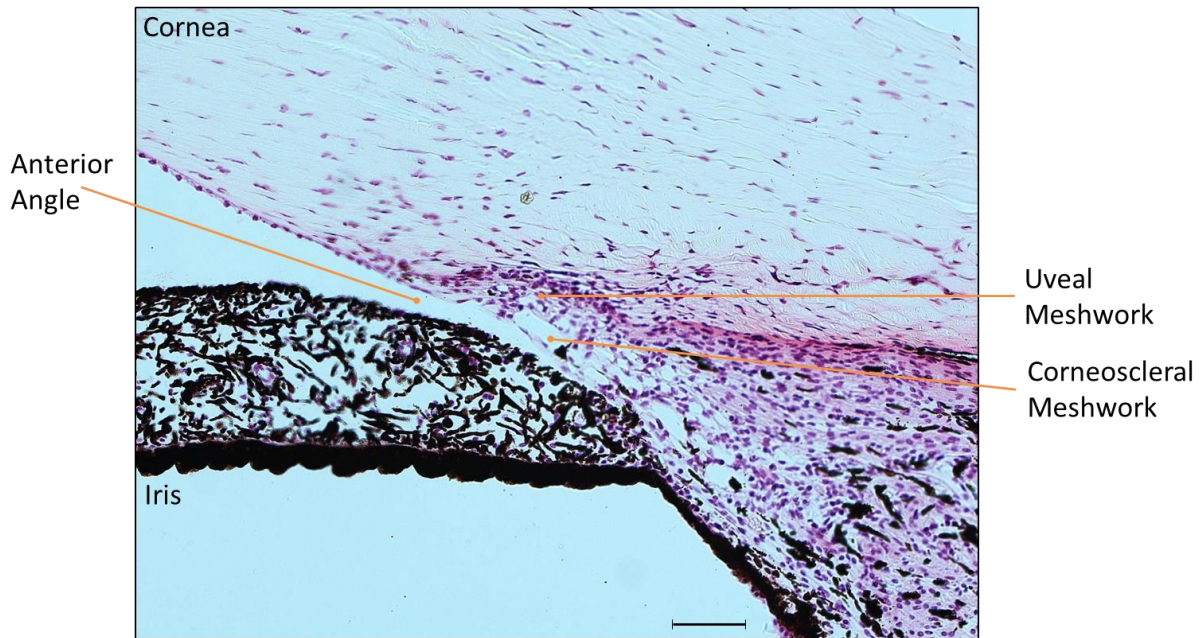
Figure II-4: Light micrograph of a histological cross-section of the primate anterior angle. Images taken with a 10x objective lens, scale bar = 100 μm, anterior side facing up. At the junction between the cornea, sclera and uvea, a trabecular meshwork (also known as corneoscleral meshwork) and a uveaoscleral meshwork exists to drain aqueous fluid form the anterior chamber of the eye. Photo taken from a Turtox slide of the primate eye.

suspends the crystalline lens at the centre of the optical axis (Fig. II-5) (Oyster, 1999). In addition to

supporting the lens, the ciliary body functions to change the shape of the lens, as well as to produce a

nutrient-rich fluid, known as aqueous humour, for the anterior ocular structures. The stromal tissue

of the ciliary body is highly vascularized, with a majority of the stroma composed of smooth muscle

responsible for manipulating the shape of the lens in a process known as accommodation (Chapter

II-1.5). The ciliary muscles vary in length, with the circular fibres staying in the pars plicata, a

region of the ciliary body containing finger-like projections known as ciliary processes, the oblique

muscle ending in the pars plana, the region just posterior to the pars plicata containing flat ciliary

body surfaces, (Fisher, 1977; Tamm, Tamm, & Rohen, 1992) and the longitudinal fibres terminating

beyond the ciliary body, at the choroid. The ciliary processes of the pars plicata project towards the

11
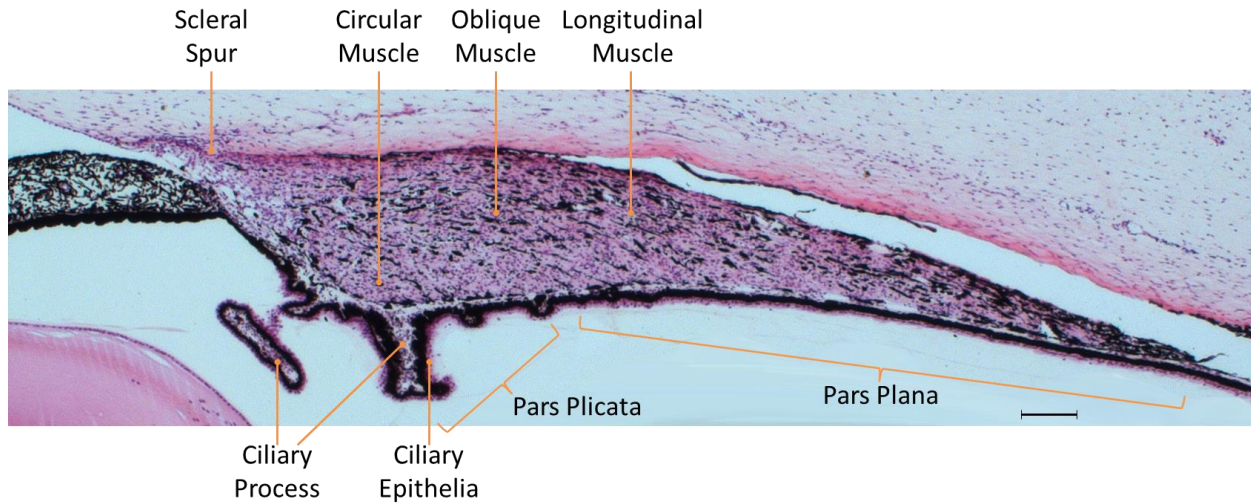
Figure II-5: Light micrograph of a histological cross-section of the primate ciliary body. Image taken with a 10x objective lens, scale bar = 100 μm, anterior side facing up. The bulk of the ciliary body is composed of 3 ciliary muscles that run in circular, oblique, and longitudinal orientations. The region formed by the projections of the ciliary processes is known as the pars plicata, while the flat posterior underside is known as the pars plana. Photo taken from a Turtox slide of the primate eye.

lens and extend suspensory ligaments that attach to the lens equator. Blood circulating through the ciliary processes are filtered through the ciliary epithelium, to produce aqueous humour, which is secreted into the posterior chamber for circulation through the pupil and in to the anterior chamber. At the tail end of the pars plana, towards the back of the eye, the epithelial cells expand to become the retina and the retinal pigmented epithelium, while the stroma continues as the choroid.

2.2.5 THE CRYSTALLINE LENS

The crystalline lens is a transparent ellipsoid structure that is centred on the optical axis by the annular ciliary muscle (Fig. II-6). The anterior surface of the lens is less curved than that of the posterior surface. In the adult, the lens is typically 10 mm in diameter with an axial length of 4 mm.

It is, however, important to note that the size and shape of the lens can change due to accommodation (Chapter II-2.5) and because the lens continues to grow throughout life. The structure of the crystalline lens can be divided into three main components; (1) the lens capsule, (2) the lens epithelium, and (3) the lens fibres (Rafferty, 1985). The lens capsule is a thin (~2-28 μm) layer of collagen and sulfated glycosaminoglycans (GAGs) that surrounds the entirety of the lens (Kuwabara, 1975) and maintains the rigidity and shape of the lens as a whole. Underneath the lens capsule, a single-cell layer of epithelial cells cradles anterior face of the lens (Taylor et al., 1996). At the equator of the lens, increasing concentrations in fibroblast growth factor (FGF) stimulate
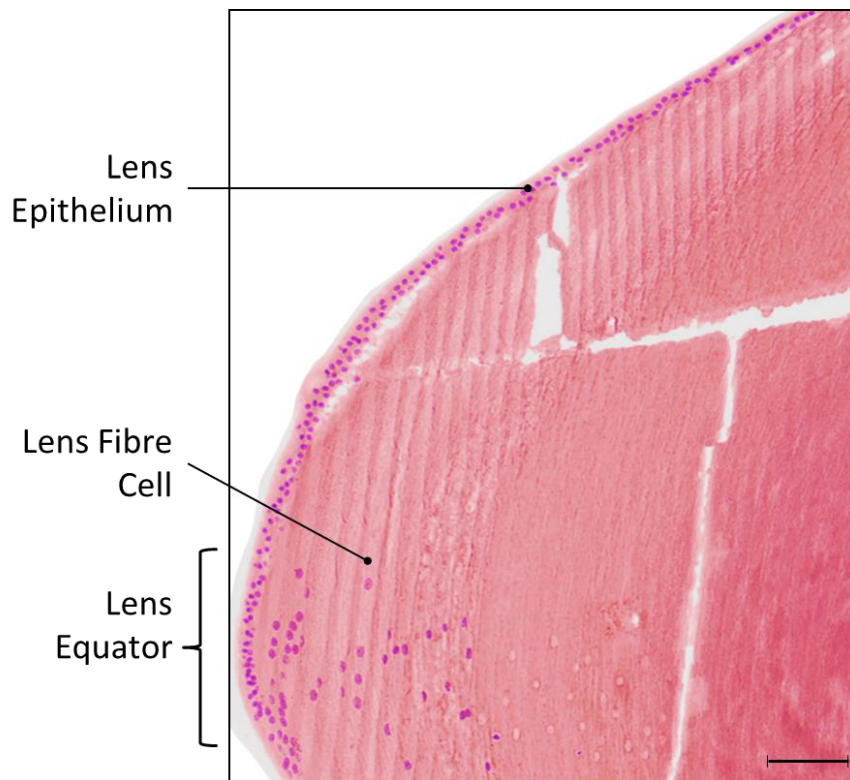

Figure II-6: Light micrograph of a histological cross-section of the primate crystalline lens. Image taken with a 10x objective lens, scale bar = 100 μm, anterior side facing up. The anterior side of the crystalline lens is cradled by a layer of epithelial cells. At the lens equator epithelial cells divide, differentiate, and elongate to become lens fibre cells that migrate towards the centre of the lens. Photo taken from a Turtox slide of the primate eye.
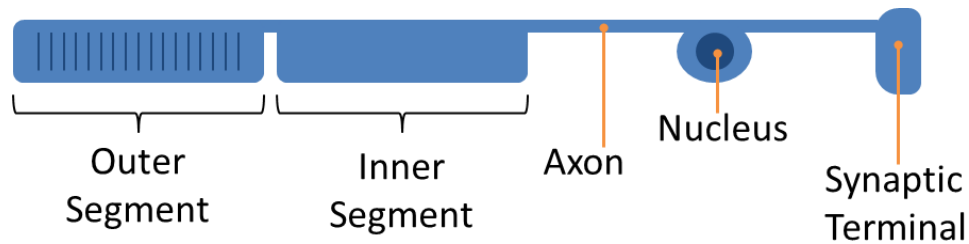
Figure II-7: Schematic diagram of a photoreceptor cell. Photons are absorbed by a photopigment that resides in the outer segment which produces an electrical signal that travels down the axon, past the nucleus, to the synaptic terminal where it is passed on to other cells.

epithelial cells to divide, differentiate, and elongate, respectively, to become lens fibre cells (McAvoy & Chamberlain, 1989), all of which occur simultaneously while they migrate posteriorly (Kuwabara, 1975). The bulk of the lens is composed of lens fibre cells, with the oldest cells residing in the central lens nucleus, and the youngest cells residing close to the equator of the lens. As they migrate, lens fibre cells undergo a modified apoptotic procedure in order to lose organelles while also maintaining the minimum requirements to survive so that light may pass unscattered through the centre of the lens (Kuwabara, 1975).

2.2.6 THE RETINA

In order for light to be perceived, it must be detected by a specialized light-sensitive cell known as a photoreceptor. In brief, there are two types of photoreceptors in the human eye: (1) rods, which are responsible for low light (scotopic), achromatic, low spatial acuity vision, and (2) cones, which are responsible for high light (photopic), chromatic, high spatial acuity vision. A photoreceptor has five main anatomical regions (Baylor, 1996; Nathans, 1987) (Fig II-7): (1) the outer segment, which contains an excitable photopigment, (2) the inner segment, a site of metabolically driven pumps that

sustains electric-current flow throughout the photoreceptor, (3) the nucleus, which controls the cells gene expression and interrupts, (4) the axon, which carries electrical impulses in the form of slow potentials to (5) the synaptic terminal, which produces neurotransmitters to communicate with other retinal neurons further downstream.

The structure within the eye that houses photoreceptors is known as the retina, and is responsible for receiving, regulating, and transmitting light information from the eye to the visual cortex and the brain. Of the various intraocular structures, the retina is certainly the most anatomically complicated, however, due to the specific nature in which light information is received and travels out of the eye, the retina is organized into 10 distinct functional layers (Boycott, Dowling, & Kolb, 1969; Dowling & Boycott, 1966; y Cajal, 1893) (Fig. II-8). The RPE is a single layer of melanin-rich epithelial cells just outside the photoreceptor layer. Pigmented processes from the RPE extend into the photoreceptor layer and isolate the outer segments of each photoreceptor, which helps to increase the resolution of images by absorbing stray photons that have the potential to stimulate multiple photoreceptor cells. Just anterior to the RPE is the photoreceptor layer, which contains the inner and outer segments of the photoreceptors. The nuclei of these photoreceptors are found in the outer nuclear layer and are separated from their inner segments by an external limiting membrane. The axons of photoreceptors continue through the outer plexiform layer, where their synaptic terminals meet the dendrites of receiving intermediate neurons. The inner nuclear layer houses the nuclei of three intermediate neurons: bipolar cells, horizontal cells, and amacrine cells, which are responsible for the vertical and horizontal transmission and regulation of signals running through the retina. The nuclei of Müller cells, which are the principle glial cells of the retina that form the internal and external limiting membranes, also reside in this layer. The inner plexiform layer houses the axons of neurons synapsing with ganglion cells and amacrine cells. The
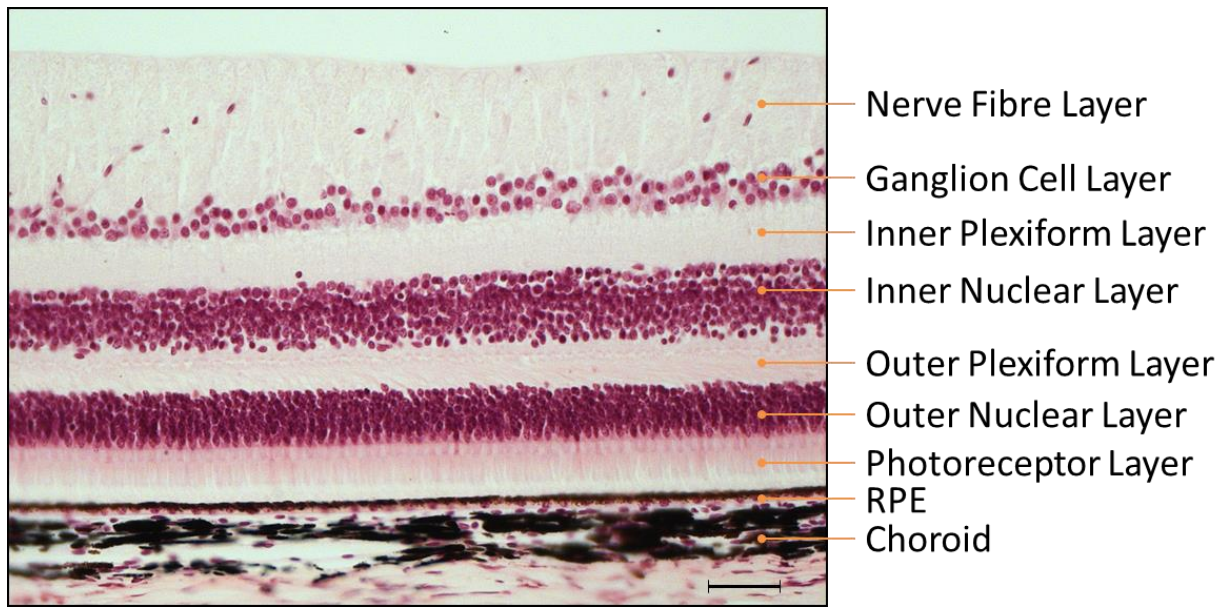
Figure II-8: Light micrograph of a histological cross-section of the primate retina. Image taken with a 20x objective lens, scale bar = 50 μm, anterior side facing up. From interior to exterior, the retina is composed of 10 layers: (1) internal limiting membrane, (2) nerve fibre layer, (3) ganglion cell layer, (4) inner plexiform layer, (5) inner nuclear layer, (6) outer plexiform layer, (7) the outer nuclear layer, (8) the external limiting membrane, (9) the photoreceptor layer, (10) the retinal pigmented epithelium (RPE). Photo taken from a Turtox slide of the primate eye.

final nuclear layer of the retina is known as the ganglion cell layer, and houses the cell bodies of ganglion cells and displaced amacrine cells. The axons of ganglion cells run anteriorly and horizontally in the nerve fibre layer, and eventually exit the eye as the optic nerve in order to reach the brain. Because the nerve fibre layer exits through the retina, a region exists where no photoreception is possible, effectively creating a blind spot in the eye (Fig. II-9).

A special region of the retina exists for high spatial acuity vision, known as the fovea, whose centre occurs approximately 4.9 mm temporally from the centre of the optic disc (Williams & Wilkinson, 1992). The fovea is approximately 1500 μm in diameter, with a central region of about 200 μm known as the foveola (Fig. II-10). At the foveola, the retina is approximately 100 μm thick and consists of only 6 of the 10 retinal layers: the RPE, the photoreceptor layer, external limiting

Figure II-9: Light micrograph of a histological cross-section of the primate optic nerve head. Image taken with a 10x objective lens, scale bar = 100 μm, anterior side facing up. At the optic nerve head, nerve fibre cells exit through the retinal layers, creating a blind spot. Photo taken from a Turtox slide of the primate eye.
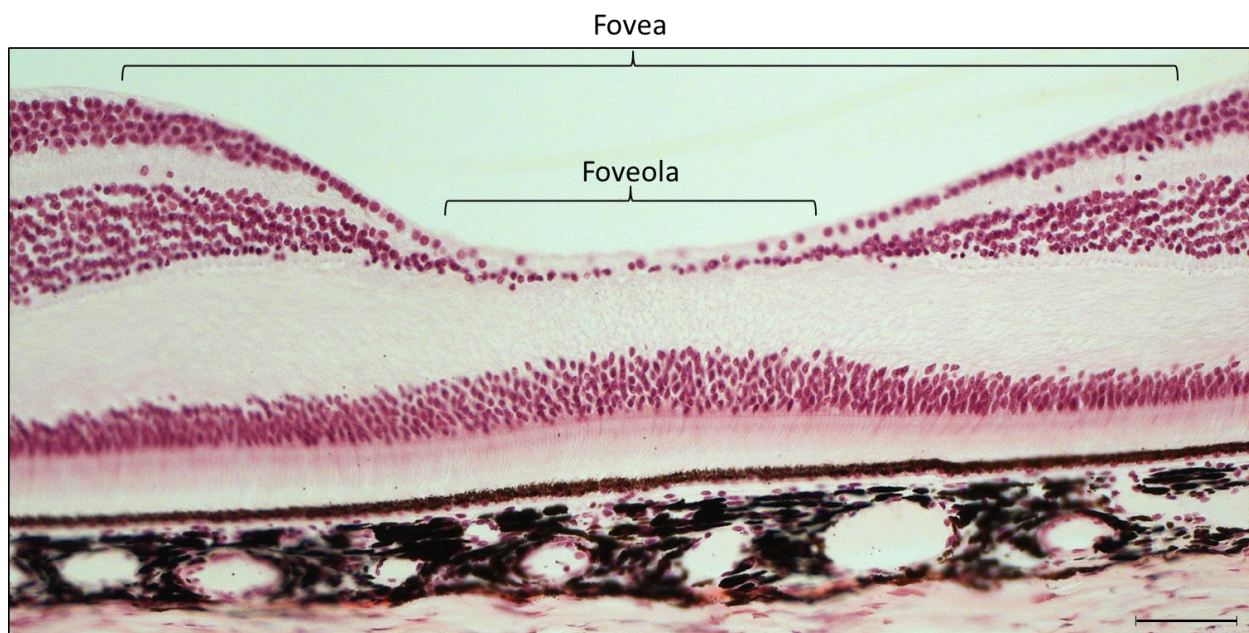
**Figure II-10: Light micrograph of a histological cross-section of the primate fovea.** Image taken with a 20x objective lens, scale bar = 75 μm, anterior side facing up. At the fovea, only the RPE, the photoreceptor layer, external limiting membrane, outer nuclear layer, outer plexiform layer, and the inner limiting membrane are present. Photo taken from a Turtox slide of the primate eye.

membrane, outer nuclear layer, outer plexiform layer, and the inner limiting membrane. The missing layers of the retina at the foveola have been pushed aside to optimize photoreception in this region, and can be observed at the edge of the foveal rim. The principle reason for the sharp central vision of the fovea is due to the high density and exclusive presence of cones in the photoreceptor layer. Furthermore, almost no horizontal dispersion of light information occurs as the photoreceptors in the fovea are connected in a near 1:2:2 ratio with bipolar and ganglion cells, respectively (Mollon & Bowmaker, 1992).

2.2.7 THE CHOROID

Surrounding the retina, just outside of the photoreceptor cells, is a heavily pigmented layer of vascular tissue known as the choroid (Fig. II-11), which is the continuation of the uveal tract at the posterior end of the ciliary body (Oyster, 1999). The vasculature of the choroid provides nutrients and metabolic exchange to the photoreceptor cells (Oyster, 1999). Furthermore, the heavy pigmentation serves to absorb stray light that is not received by the photoreceptor layer.

2.3 COMPARATIVE ANATOMY AND EVOLUTION OF THE EYE

Although modern day discussions about evolution utilise the phylogenetic descriptions, a good number of investigations concerning the evolution of the eye also use the Linnaean system. Discussions on evolution of the eye in this thesis follow the conventions of the references. Given that early references to evolution were written before phylogenetic advances, the descriptions in this thesis are organised in the classical Linnaean system, unless otherwise noted.

18
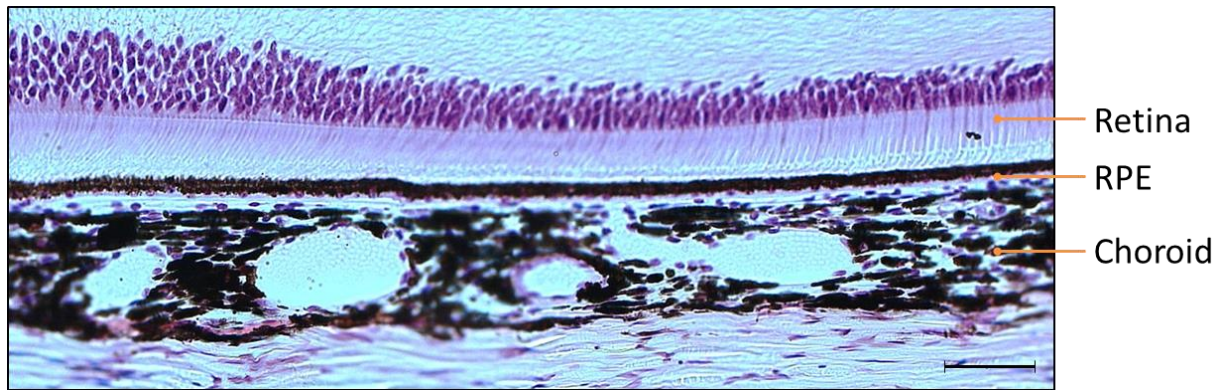
Figure II-11: Light micrograph of a histological cross-section of the primate choroid. Image taken with a 20x objective lens, scale bar = 50 μm, anterior side facing up. The vasculature of the choroid is organized into three layers in which the diameters of the vessels progressively become smaller as they approach the photoreceptor layer; Haller's layer is the outermost region and contains the largest blood vessels of the choroid, Sattler's layer is immediately interior to this layer and contains blood vessels with medium sized diameters, and finally, the choriocapillaris layer is closest to the RPE and contains the capillaries that nourish the photoreceptor layer. Between the choriocapillaris and the RPE, a basement membrane composed of equal parts choroid and RPE exists, and is known as Bruch's membrane.

In comparison with other visual organs in the animal kingdom, the human eye is not the most highly evolved visual structure, nor is it the most fundamental. It cannot detect wavelengths outside the visible spectrum (about 390 nm to 700 nm), unlike American kestrels (Rajchard, 2009), nor does it have the incredible distance vision of red-tailed hawks (Jones, Pierce, & Ward, 2007), nor the ultra-rapid tracking of flycatchers (Boström et al., 2016). The human eye is, perhaps surprisingly, average. And yet, with only materials such as cells, water, and jelly, nature has created a diverse number of optical systems delicately tuned to allow survival of each species. Therefore, in order to understand, research, and improve upon the human eye, it is important to compare and contrast the human visual organ to that of others in the animal kingdom.

2.3.1 THE AQUATIC EYE

Regardless of the vertebrate type, whether it be mammalian, amphibian, or avian, its eye originated and emerged from the water. It is for this reason that the physical and chemical properties of water have such a profound relationship with the vertebrate eye. Indeed, the refractive structures, as well as the aqueous and vitreous substance of vertebrate eyes are composed of and rely predominately on water and its special properties. The origin of water in the vertebrate eye, in turn, arose from the phenomenon known as osmosis, or the passive movement of water through membranes towards higher concentrations of dissolved substances.

One aquatic species that still takes advantage of the osmotic phenomenon is the Petromyzontidae (Collin, 2009), also known as lampreys, of the Cyclostomata clade (Gabbott & Donoghue, 2016). Their semi-permeable corneas allow for the influx of water to help maintain a desired intra-ocular pressure (Collin & Collin, 2001). In addition to this mechanism, the cornea, along with an overlying sheath known as the spectacle, is also responsible for accommodation in lampreys (Sivak & Woo, 1975). The cornealis muscle, which is extra-ocular, inserts into the skin of the spectacle from the posterior side. Contraction of the cornealis muscle causes a flattening of the cornea, whose interior surface simultaneously pushes on the lens, resulting in its translational movement. The majority of aquatic eyes are required to accommodate by translation of the lens due to the refractive properties of the cornea being rendered neutral by the surrounding water. As a result, aquatic lenses are considerably more spherical than human lenses, and so accommodation by a change in lens shape would not be as effective at changing focal lengths as a translational movement. Aside from the delicately balanced corneal osmotic mechanism, and the translational accommodation mechanism, however, the lamprey eye is rather primitive, and considered the

simplest amongst non-degenerate eyes of vertebrates.

Amongst the more complex of the aquatic eyes are those of the teleosts, which make up 96% of the fish population (Walls, 1942). Due to the overwhelming diversity of species in this class, the eyes of teleosts are incredibly diverse; therefore, only the anatomical structures found amongst the majority of these fish will be highlighted. The teleost eye, like that of the lampreys, has a clear dermal sheath that sits on top of the corneal layer; however, this sheath is not responsible for accommodation (Sivak, 1975; Tamura, 1957). Instead, the spherical lens, which is held in place by a suspensory ligament, is attached at its equator to a retractor lentis muscle that pulls it temporally and backwards in order to increase refractive power in the eye (Somiya, 1987; Somiya & Tamura, 1973). The retractor lentis originates from the falciform process, which is a protrusion of the choroid into vitreal space that helps nourish and aid with the metabolic exchange of the inner retina. In nearly all teleosts, the retina contains three types of visual cells: rods, single cones, and twin cones (Levine & MacNichol, 1979). As a result, most teleosts have colour vision, and are able to see in both scotopic and photopic conditions. The exact function of the twin cones is not known, however, it is speculated by Lyall (1957) and Walls (1942), that they are associated with vision in deeper waters. In 1953, Wilmer found that the twin cones share a similar function as but are more sensitive than their single cone counterpart. Additionally, Wilmer demonstrated that both cod and whiting fish, which are both species that live in considerable depths, have almost exclusively double cones in their retinas. These two pieces of evidence suggest that the twin cones most likely serve as an intermediate light receptor, between that of rods and single cones, to provide colour vision in low light conditions, such as that of a deep water environment (Lyall, 1957).

Elasmobranchs, which is the subclass that contains sharks and rays, possess the largest of the non-mammalian aquatic eyes (Hodgson & Mathewson, 1978). For the most part, the elasmobranch

eye possesses the typical characteristics of an aquatic eye; they have a flatter anterior segment, with an inner surface of the cornea that rests on the anterior surface of a spherical lens (Sivak, 1990). However, accommodation in elasmobranchs is extraordinarily different from that of the cyclostomes and teleosts. A translational movement of the lens is achieved by a bowing out of the suprachoroidea, which pulls the entire anterior segment backwards, while leaving the retina and its curvature in place (Sivak, 1978). In addition to this mechanism, almost all elasmobranchs possess a specialized reflective layer in their choroids known as the tapetum lucidum, which allows for increased sensitivity in low light conditions (Best & Nicol, 1967; Heath, 1990).

2.3.2 THE AMPHIBIOUS EYE

During the transition of vertebrates from aquatic to terrestrial living, the most important adaptation was that of the anterior surface. The corneal interface with air immediately presented refractive advantages to the eye; however, certain disadvantages arose as well. The corneal surface had to remain transparent, and safe from injury. As a result, it became necessary to evolve lids that would protect and wipe the eye, coat it in tear film, and distribute that tear film evenly (Walls, 1942). Because the lens was no longer the essential refractive element in the eye, it receded further back, towards the retina, allowing for the development of an aperture and diaphragm mechanism, that are the pupil and iris, respectively. Additionally, the shape of the lens became less spherical, allowing for the accommodative system to go from a translational movement to a shape change mechanism (Walls, 1942). Due to the aquatic and terrestrial nature of amphibians, the evolution of their eyes is caught in an awkward state between the two environmental paths. According to Walls (1942), "the Amphibia have never felt fully the penalties, nor completely realized the possibilities of either

situation." Their eyelids and associated glands are suboptimal, and at times, barely functional (Walls, 1942). Additionally, they still use a translational system for accommodation, without ever having developed a muscular ciliary body.

Anurans, the order to which frogs belong, demonstrate a very interesting path of ocular development, as they are hatched aquatically, as tadpoles, and transition through metamorphosis to become terrestrial adult frogs. During the transition from water to land, the eye of the anuran develops lids and a nictitating membrane to protect and lubricate the eye. Additionally, the dermal spectacle, like those typically found in aquatic eyes, either fuses with the dural cornea or atrophies, to produce a single corneal structure. Finally, a massive Harderian gland develops, which secretes mucous, serous, and/or lipid components to the tear film depending on the species (Chieffi et al., 1992; Payne, 1994; Shirama, Kikuyama, Takeo, Shimizu, & Maekawa, 1982). Adult frogs possess a broad bifurcation of the external rectus muscle, known as the retractor bulbi, which is so powerful that in some species, can help with mastication and ingestion of food while also protecting the eyeball (Levine, Monroy, & Brainerd, 2004). The accommodation mechanism in frogs is quite unique in that they possess two muscles, one dorsal and one ventral, both of which originate from the iris root and insert near the posterior side of the ciliary triangle (Douglas, Collett, & Wagner, 1986). Contraction of these muscles draws the zonule anchors forward, resulting in the approximation of the lens moving towards the cornea (Douglas et al., 1986). Therefore, the unaccommodated state of the frog eye, unlike humans, allows for near vision, and accommodation allows for distance vision. The retinal pigmented epithelium (RPE) of certain frogs that have suboptimal eye lids contains an interesting pigment migration mechanism. During intense photopic conditions, pigment from the RPE migrates over the photoreceptor layer in order to prevent bleaching of photopigments. In contrast, a transition to scotopic conditions leads to the retraction of mechanical pigments back to the

RPE layer (Bäck, Donner, & Reuter, 1965; Burnside & Nagle, 1983).

The urodeles, or salamanders, possess eyes that are similar in structure to that of anurans, however, the visual organs of salamanders are considerably smaller and simpler than that of frogs (Walls, 1942). It is uncertain whether or not these differences are a result of salamanders not requiring as much vision as frogs, or because they are the ancestral precursors of frogs. The urodele extraocular muscles, accommodative system, and retina possess the same morphological elements as anurans (Jordan, Luthardt, Meyer-Naujoks, & Roth, 1980; Ott, 2006). However, salamanders differ primarily by having photoreceptors that are larger in size and smaller in number. Furthermore, they have the most extensive ability in the animal kingdom to regenerate complex structures (Reyer, 1977; Stone & Farthing, 1942), such as the lens (Reyer, 1954) and the retina (Mitashov, 1996; Mitsuda, Yoshii, Ikegami, & Araki, 2005), in addition to many other parts of their body (Ghosh, Thorogood, & Ferretti, 1994; Tassava & Huang, 2005). The regenerative mechanism in salamanders is thought to be initiated by local activation of thrombin, which signals cell cycle re-entry and regeneration (Imokawa & Brockes, 2003; Simon & Brockes, 2002; Tanaka & Brockes, 1998). In contrast, mammalian liver regeneration is initiated by serotonin release, which signals proliferation in residual hepatocytes (Lesurtel et al., 2006). The differences in signalling pathways is speculated to be an important clue as to why mammalian regeneration is so distinctly limited (Godwin & Brockes, 2006).

2.3.3 THE TERRESTRIAL EYE

The link from amphibians to reptiles would be all but lost if it were not for the discovery of the Seymouria, an extinct amphibious descendant considered to be the first reptile (Watson, 1918). The

Seymouria was found to have adapted the necessary organs to exclusively live on terrain. The Seymouria are thought to have evolved the lens-squeezing mechanism of accommodation, and with it, striated muscle in the ciliary body, attachment points of the ciliary muscle to the scleral spur, scleral ossicles, and a thickening of the lens equator, known as an annular pad (Walls, 1942). Reptilian descendants of the Seymouria would eventually develop striated muscle in their irises, along with a pigmented and vascular conical protrusion from the optic nerve head known as the conus papillaris. Due to their lack of a central retina artery, the conus papillaris serves to nourish the innermost layers of the retina by diffusing nutrients through the vitreous, much like the falciform process in teleosts (Walls, 1942).

Although snakes belong to the reptilian class, their eyes are widely different than any other reptilian suborder, and even differ greatly from their lizard ancestors (Walls, 1942). Of all the reptilian species, only snakes have the dermal spectacles that are found universally in aquatic eyes. In addition, the choroid and the sclera are so firmly fused, that it appears as if no embryological differentiation has occurred (Walls, 1942). The lens of snakes is much more spherical than that of other reptiles, and also develops sutures with age (Phillips, 2009). Furthermore, aside from certain aquatic snakes that accommodate by a translational movement of the lens, most species of snakes have hard lenses, and uncertain mechanisms of accommodation (Sivak, 1977; Walls, 1942). One characteristic that snakes do share with other reptiles is their reversion from diurnality and pure-cone retinas to nocturnal lifestyles supported by rod-rich or even pure rod-retinas (Davies et al., 2009).

Similar to reptiles, the majority of non-primate mammals are either nocturnal or crepuscular. The nocturnality of these animals is speculated to have evolved as a survival mechanism during the triassic-jurassic period to avoid the diurnal dinosaurs (Gerkema, Davies, Foster, Menaker, & Hut, 2013; Walls, 1942); this concept, proposed by Walls in 1942, is known as the bottleneck theory, and

25

is supported to this day (Gerkema et al., 2013). As a result of switching from photopic to scotopic vision, a reflecting structure within the eye, known as the tapetum, was evolved (Ollivier et al., 2004; Walls, 1942). In most mammals and reptiles, the tapetum is a reflective layer that appears between the choroid and retinal pigmented epithelium, and in scoptopic conditions, provides the photoreceptors of the retina with a second opportunity for stimulation, thereby enhancing visual sensitivity (Braekevelt, 1986, 1990). Most of the noctural mammals, such as the monotremes and marsupials possess tapeta, and operate almost exclusively in dim light conditions (Walls, 1942). The monotreme eye is, in fact, so similar to the reptilian eye (O'Day, 1952), that it alone can prove the reptilian origin of the entire mammalian class. The only difference between the eyes of reptiles and monotremes is the lack of a ciliary body in the latter. Instead, monotremes possess a ciliary web (Walls, 1942), which is essentially a thin iris, void of muscle, interconnecting the ends of the ciliary processes. This small difference, however, indicates that no monotreme has any demonstratable mechanism of accommodation. In fact, the majority of mammals, including placentals such as mice and rats, display little to no accommodative ability (Barrett, 1938). Accommodation was not considerably present in mammals until its necessity arose in predatory or high-functioning species (Barrett, 1938; Walls, 1942).

Despite the large differences in appearances between birds and reptiles, the bird eye also contains no important feature that does not already occur in the reptilian eye. The reason is likely to be because no evolutionarily beneficial structure was required since its separation from its reptilian common ancestor. The avian class, however, relies much more on its visual organs, and it is perhaps for this reason that the bird eye is so significantly larger, on average, than that of the reptiles. The eyes of a fully developed hawk or owl, whose body sizes are a fraction of adult humans, are comparable in size, if not larger, than of humans. Because of their relatively large eyes, there is only

26

room for a small cranial cavity. The eyes of birds fall in to one of three categories: (1) flat, such as those found in swans and chickens; (2) globose, such as those found in hawks, eagles, and buzzards, or (3) tubular, such as those found in owls. In all three categories, the eye exhibits a region of concavity, directly peripheral to the corneal limbus, which is shaped by a ring of bones known as the scleral ossicles. The scleral ossicles, in turn, support the anterior eye during accommodation, which is particularly strong in birds due to the immense striated muscle found in the avian ciliary body. The majority of birds are non-predatory, and thus, are capable of surviving with the short axis offered by the flat eye (Sillman, 1973). Birds of prey, however, need high resolution sight at great distances in order to hunt and survive, and therefore require a longer axis, such as that of the globose eye (Hocking & Mitchell, 1961). The longest axis is found in the tubular eye, so named due to the shape the lengthy eye must adopt in order to fit within the meagre skull. The owl, however, does not require the axial length of its eyes to view great distances, but more so for higher visual acuity, and a broadening of the image at the visual-cell level (Hocking & Mitchell, 1961). Interestingly, the superior nocturnal vision of owls does not arise from a direct difference in anatomical structure, but from secondary neural processing of the larger retinal image produced by the tubular eye (Bowmaker & Martin, 1978; Hocking & Mitchell, 1961).

Aside from the differences of ocular morphology in the various bird species based on visual activity, the anatomical structures within the avian eye are quite uniform. The cornea of birds is histologically similar to that of humans; however, it is not wiped by their eye lids, but by a nictitating membrane that runs beneath the lids in a perpendicular direction. The sclera, in turn, is substantially more rigid due to the presence of a hyaline cartilage that extends from the peripheral edge of the ossicles to the back of the eye. The entry position of the optic nerve into the eye is protected by a bone in the shape of a washer known as Gemminger's ossicle. The choroid of birds is

27

substantially thicker than that of any other class, however, even in nocturnal species, they never contain a tapetum lucidum (Jones et al., 2007; Sillman, 1973). At its anterior, the choroid thins to become the ciliary body, which, like reptiles, is more closely associated with the sclera than it is with the uvea (Walls, 1942). The reason for this difference is due to the stronger lens-squeezing accommodation mechanism in birds and reptiles than that of higher marsupials and primates. Because the ciliary body in birds is composed of skeletal, rather than smooth, muscle, its forceful contraction requires anchoring to the sclera so as not to damage the middle tunic (Levy & Sivak, 1980). Additionally, accommodation in birds is highly effective due to direct contact, and therefore direct contraction, of the ciliary body on to the lens equator; instead of relying on intrinsic forces for the lens to change shape, as do higher mammals, the avian eye exerts direct equatorial force, using skeletal muscle, to steepen the lens surface curvature (Levy & Sivak, 1980).

Interestingly, it has been shown that certain avian species have corneal in addition to lenticular accommodation. Schaeffel and Howland (1991) demonstrated that up to half of the full range of accommodation in chickens and pigeons could be accounted for by corneal accommodation. The mechanism and optical change of avian corneal accommodation, however, remains heavily disputed. In 1831, Crampton, as reported by Walls (1942), hypothesized that a contraction of the ciliary muscle would flatten the cornea for distance vision. In 1846, Brücke (1846) challenged this hypothesize by proposing that the central corneal curvature would steepen as a result of the contraction in, ironically, Crampton's muscle. Since then, a multitude of corneal accommodation theories have been proposed, including one which hypothesizes that the curvature of the avian cornea changes with increases in hydrostatic pressure within the eye. However, other investigators (Glasser, Pardue, Andison, & Sivak, 1997; Glasser, Troilo, & Howland, 1994; Pardue & Sivak, 1997) have demonstrated that contraction of the ciliary muscle in birds is, indeed, responsible for

steepening the curvature of the corneal surface. Furthermore, Glasser et al. (1994) found that during

in vivo accommodation, the hydrostatic pressure changes in the eye could not account for the

changes in shape of the cornea.

2.4 THE CRYSTALLINE LENS

2.4.1 THE AVIAN LENS

The avian lens is a highly refractive structure and soft structure, particular in species where the range

of accommodation is great (Jones et al., 2007; Sillman, 1973). Unlike primates, the avian lens has a

thick pad called the ringwulst (or annular pad), which takes up half the area of a coronal section of

the whole lens, that serves to increase accommodative amplitude through direct contact with the

ciliary body (Walls, 1942). Between the ringwulst and the lens proper, a slender space exists into

which the inner ends of the ringwulst fibres secrete a lubritive substance (Walls, 1942); this

lubricated space is speculated to allow the surrounding structures to shift past one another during

contraction of the ciliary muscle to increase deformation of the of the lens and increase

accommodative amplitudes (Walls, 1942).

2.4.2 EMBRYOLOGICAL DEVELOPMENT

During early stages of ocular development, the optic cup, a structure that eventually becomes the

retina, induces a thickening of surface ectoderm that gives rise to the lens placode (Oyster, 1999)

(Fig. II-12A). The lens placode then invaginates and buckles inward, forming the lens pit (Oyster,
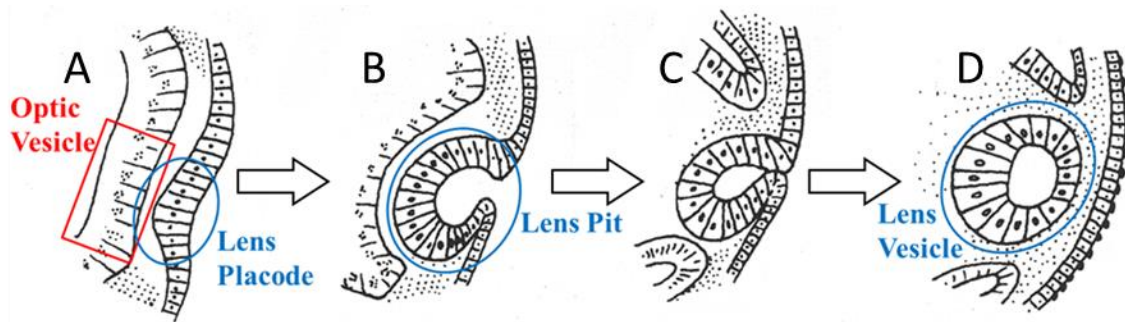
Figure II-12: Formation of the lens vesicle. The optic vesicle induces the formation of the lens vesicle. Throughout the formation of the lens vesicle, the optic vesicle invaginates simultaneously to produce the primitive retina (modified with permission from Figure 1.8, Oyster, CW (1998). The Human Eye, Sinauer Associates Inc.).

1999) (Fig II-12B). The mouth of the lens pit eventually closes (Fig. II-12C) and the entire structure buds off of the surface ectoderm, eventually forming the lens vesicle (Fig. II-12D), a single-cell layered sphere with a hollow cavity in its centre (Oyster, 1999).

At this stage, the epithelial cells of the lens vesicle secrete a collagenous outer layer that encapsulates the lens, which gives rise to the lens capsule (Oyster, 1999) (Fig. II-13A). The posterior-most epithelial cells of the crystalline lens begin to differentiate into primary lens fibre cells and elongate towards the anterior surface (Fig. II-13B), filling the empty lumen of the lens vesicle (Fig. II-13C) (Oyster, 1999). Secondary fibres arise from the proliferation, migration and
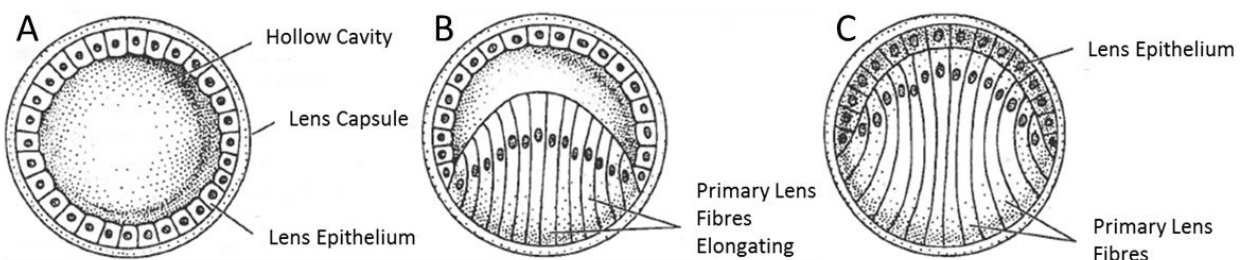
Figure II-13: Formation of the primitive lens. Posterior epithelial cells elongate anteriorly, filling the hollow cavity (with permission from Figure 1.12, Oyster, CW (1998). The Human Eye, Sinauer Associates Inc.).

30

differentiation of cells at the equator of the lens (Section 2.2.5).

2.4.3 CRYSTALLINS

The dry weight of the crystalline lens is composed of approximately 95% protein, making it a reservoir for one of the highest protein concentrations in the human body. The proteins in the lens are often categorized as (1) water soluble or (2) water insoluble types. As the lens plays a vital role in the refraction of light, it requires a very high concentration of water soluble proteins in order to create a refractive index greater than water, while also maintaining overall lens transparency; the most abundant of these proteins, making up over 90% of the total protein concentration in the lens, are the crystallins (Horwitz, 2009). Crystallins are responsible for the transparency and precise refractive index of the lens, and as with the cornea, organization is the key to these optical properties (Oyster, 1999). The three-dimensional structure of crystallins allows for them to form dense, high-molecular weight aggregates that pack tightly into lens fibre cells, thereby increasing the refractive index while maintaining lens transparency (Oyster, 1999). Additionally, crystallins are self-maintaining, as certain crystallins act as molecular chaperones which are responsible for maintaining the native state of other crystallins (Horwitz, 2009), achieved by either preventing denaturation of other crystallins or guiding the proper reassembly of denatured crystallins (Horwitz, 2009). With age, chaperone crystallins lose their effectiveness in the reassembly of fellow proteins, and together with increasing amounts of reactive oxygen species (due to long-term ultraviolet light exposure) could result in the inability of lenses to maintain transparency and the eventual development of cataracts (Li & Spector, 1996). Since their discovery and implication in cataractogenesis, they have been the focus of lens and cataract research. However, providing the lens with its optical properties

is not the sole function of these crystallins. The secondary roles they perform are largely dependent on the superfamily from which they were recruited (Table II-1) (Piatigorsky, 1993). Indeed, crystallins are not proteins unique to the lens, nor did they appear spontaneously throughout the course of evolution. They are enzymes and stress proteins recruited from outside the eye to help the lens perform its optical function in addition to their native role in the body.

In the human lens, there exist three groups of crystallins that fall into one of two major superfamilies; α- or βγ- crystallins. α-crystallins are the most abundant of the three, and are also known as heat shock protein 70 (HSP70), a 70 kDa heat shock protein found ubiquitously throughout the body. In contrast, β- and γ- crystallins are found primarily in the lens, but have analogs that are speculated to help protect the body against certain microbial infections (Lee et al., 1993; Wistow, 1993).

2.4.3.1 α-CRYSTALLINS

From the late 1980s to the early 2000s, a significant amount of lens research was dedicated to uncovering the structure and function of α-crystallins. It was found that two genes existed for α-crystallins: alpha A (αA-) and alpha B (αB-), with an amino acid sequence similarity of 57%

Table II-1: Crystallin diversity and their respective functions

Crystallins	Species	Recruited Protein
α-	Vertebrates	Small heat shock protein
β- and γ-	Vertebrates	Microbial stress protein
	Scallop	Aldehyde dehydrogenase
δ-	Birds, Reptiles	Argininosuccinate lyase
	Birds, Crocodiles	Lactate dehydrogenase
	Frogs	NADPH reductases
	Guinea Pigs	Alcohol dehydrogenase
	Camels	Lactate dehydrogenase

between the two isoforms (Bloemendal, 1981). In 1989, researchers discovered that αA-crystallins were found primarily in the lens with trace amounts in other tissues, while αB-crystallins are found ubiquitously throughout the body (Bloemendal & Bloemendal, 1998; Srinivasan, Nagineni, & Bhat, 1992). Additionally, it was shown that αB-crystallins were completely homologous to heat shock protein 70 (Klemenz, Fröhli, Steiger, Schäfer, & Aoyama, 1991). Shortly afterwards, it was demonstrated that αA-crystallins, αB-crystallins, and other small heat shock proteins, could assist in the folding/unfolding and assembly/disassembly of other macromolecules (Horwitz, 1992; Jakob, Gaestel, Engel, & Buchner, 1993) – properties that are attributed to proteins known as molecular chaperones.

Because lens fibre cells never truly die, that is, they undergo a modified apoptosis to shed organelles as they migrate towards the centre of the lens, nuclear fibre cells of adult lenses contain crystallins synthesized during the embryogenesis (Bassnett & Winzenburger, 2003; Kusak & Brown, 1994). Additionally, due to the lack of vascularisation, macromolecules such as α-crystallins remain physically stagnant throughout life (Derham & Harding, 1997). For these reasons, chaperone activity of α-crystallins is vital for maintaining proper protein assembly in order to preserve both optical and structural properties of the aging lens (Carver, Nicholls, Aquilina, & Truscott, 1996; P. Vasantha Rao, Huang, Horwitz, & Zigler, 1995; Takemoto & Boyle, 1994; K. Wang & Spector, 1994).

α-crystallins function by recognizing unfolded or denatured proteins that have a high risk of aggregating with other molecules. Upon recognition, the α-crystallins prevent further disassembly of the protein and maintain a refoldable confirmation that is energetically favourable (Haslbeck, Peschek, Buchner, & Weinkauf, 2016). However, it is speculated that the chaperone system of α-crystallins at the centre of the lens lacks the ability to repair proteins that have been extensively

33

unfolded or disassembled. Additionally, it has been shown that the aging lens contains a much lower concentration of functional α-crystallins in their nuclei, and as a result of rampant protein misfolding, leads to a loss in the ability to prevent the development of nuclear cataracts (Vasantha Rao et al., 1995; Roy & Spector, 1976).

In a study by Hanson et al. (2000), it was found that 50-65 year old lenses contained high levels of α-crystallins bound to γS-, γD-, and various β-crystallins. This observation indicates that α-crystallins have a high affinity for other crystallins that require repairing. Additionally, it has been shown that α-crystallins can also bind to housekeeping enzymes, such as glyceraldehyde-3-phosphate dehydrogenase and enolase (Horwitz, 2003) as well as various water-soluble cytoskeletal components (Quinlan et al., 1999a). Furthermore, a study by Muchowski et al. (1999) that subjected lenticular cells to thermal stress resulted in αB-crystallins selectively binding to intermediate filament proteins. Together, these results indicate that αB-crystallins are perhaps tailored to repairing the lens cytoskeleton, whereas αA-crystallins are responsible for repairing other crystallins.

2.4.3.2 βγ-CRYSTALLINS

Not much is known about the function of β- and γ-crystallin families, however, their structures have been extensively studied in an attempt to reveal homologous proteins that may occur elsewhere in the body. βγ-crystallins are constructed from four homologous Greek key motifs organized into two domains (Lubsen, Aarts, & Schoenmakers, 1988). They were originally thought to be unique to the lens, however, a study by Wang et al. (2004) showed that βγ-crystallins occur not only in lens fibre cells and lens epithelial cells, but also in various tissues outside the lens. The expression site and patterns of certain βγ-crystallins indicate that they function in response to some form of stress.

Additionally, two microbial proteins, spherulin 3a and protein S, share their tertiary structure and resemble the topology of βγ-crystallin (Clout, Kretschmar, Jaenicke, & Slingsby, 2001). However, the resemblance of βγ-crystallin to these microbial proteins gives no further indication of its potential function.

2.4.3.3 δ-Crystallins

δ-crystallin is a major structural protein that occurs within the lenses of birds and reptiles, but is absent from the lenses of teleost, amphibia, and mammals (Chiou, Chang, Lo, & Chen, 1987; Piatigorsky, 1984). In the embryonic lens, it comprises 70-80% of the total soluble protein concentration, however, that percentage diminishes shortly thereafter as synthesis ceases upon maturation of the lens; thus, the study of δ-crystallin synthesis is important, as it offers the opportunity to investigate the switching on and off of a gene product during normal development (Piatigorsky, 1984). In 1988, Piatigorsky et al. (1988) demonstrated the similarity of δ-crystallin to the enzyme argininosuccinate lyase (ASL). Furthermore, it was shown that duck δ-crystallin demonstrates high ASL activity, indicating the possibility that ASL may have been recruited, through gene sharing, for their ideal properties to serve as the transparent, water-soluble protein within the lenses of birds and reptiles (Piatigorsky et al., 1988). Like all vertebrates, bird lenses also contain α- and ß-crystallins, although delta-crystallins remains the predominant crystallin in the bird lens (Slingsby, Wistow, & Clark, 2013).

2.4.4 GRADIENT REFRACTIVE INDEX (GRIN)

The optics of the crystalline lens is quite unique in that, unlike the cornea, the refractive index is not uniform throughout the entire structure (Pierscionek & Chan, 1989). The lens cortex has an index of 1.37 which gradually increases to approximately 1.5 in the lens nucleus (Pierscionek & Chan, 1989). Although much uncertainty exists as to how this gradient is achieved, it is speculated that the difference in crystallin concentration throughout the lens is responsible for this phenomenon (Delaye & Tardieu, 1982). Because the refractive index is a function of protein concentration, this model works quite nicely; crystalline concentrations are highest within the lens nucleus, and gradually decrease towards the cortex.

In lenses with a gradient refractive index, the refraction near the centre of the lens is greater than lenses with a uniform refractive index, leading to a greater total refractive power of the lens (Moore, 1980;Pierscionek, 1989). As a result, peripheral rays have a shorter focal length than central rays, which forms an optical effect known as spherical aberration. However, the gradient refractive index, with the highest index at the centre of the lens in the crystalline lens refracts light more at the centre and less at the periphery. Together, the shape of the lens and the gradient can nearly abolish spherical aberrations in some vertebrate lenses (Sivak & Kreuzer, 1983). It should be noted spherical aberrations in chickens are negatively aberrated (Sivak, Ryall, Weerheim, & Campbell, 1989b) and this aberration becomes more prominent with age (Priolo, Sivak, & Kuszak, 1999).

2.4.5 SUTURES

Sutures form at the anterior and posterior poles of the lens where fibre cells growing from opposite sides of the lens abut at their apical and basal ends. In human embryos, elongated lens fibre cells meet at three planes, forming an upright "Y" at their anterior ends (with respect to the superior–inferior axis of the eye) and an inverted "Y" posteriorly (Oyster, 1999). As the human lens grows, the suture planes formed by more superficial shells of fibres become increasingly complex (Oyster, 1999). The first evidence of this new pattern typically occurs soon after birth, when two new suture planes form at the ends of each of the three branches of the Y sutures (Oyster, 1999). As new fibres are added during lens growth, the branch points of the newly formed sutures gradually "migrate" towards the centre, eventually forming the adult stellate structure (Oyster, 1999). In some species, particularly of birds (Kuszak, 1995; Walls, 1942) and reptiles (Walls, 1942), all fibre cells meet near the midline of the lens, forming an "umbilical" or point suture (Kuszak, Bertram, Macsai, & Rae, 1984). Similar to humans, with age, sutures in bird lenses become less organized (Priolo et al., 1999b).

2.4.6 METABOLISM

As the lens is an avascular structure, it must receive its essential nutrients from and expel metabolic waste through the surrounding aqueous and vitreous humours. In addition, lens fibre cells lack the usual sodium channels and sodium-potassium pumps for circulation of critical ions (Cheng & Chylack, 1985; van Heyningen, 1969). The pathway by which nuclear lens fibre cells receive their nutrients is heavily debated even to this day. There are currently two schools of thought in this

debate: (1) that a fluid microcirculatory system exists for the flow of ionic current, and (2) that a circulatory system is unnecessary, as nuclear lens fibre cells do not require nutrients to carry out their function. As early as 1982, Robinson and Patterson (1982) proposed a fluid microcirculatory system of the lens that was subsequently theoretically tested more thoroughly as a model to explain the functions of intercellular components of the lens, such as the gap junctions, and the mechanisms for cataractogenesis (Donaldson, Musil, & Mathias, 2010; Mathias, Kistler, & Donaldson, 2007; 2004; Mathias, 1997). In brief, sodium ions are actively pumped into the lens at the anterior pole, and trickle in passively through extracellular clefts of fibre cells at the posterior pole (Fig. II-14). The sodium ions then flow towards the centre of the lens via an intracellular pathway mediated by gap junction channels. Because gap junction coupling conductance in the outer shell of differentiating fibres is concentrated at the equator, the intracellular current is then directed to the equatorial epithelial cells where the highest densities of sodium-potassium pumps reside to actively transport sodium out of the lens.

In a recent debate, Beebe et al (2010) stated that mature fibre cells have no need for metabolic activity, and that empirical evidence demonstrates that little to no metabolic activity exists in the lens nucleus. Furthermore, fluid flow from the centre to the periphery of the lens would be detrimental to the lens, as glutathione, an antioxidant responsible for removing harmful reactive oxygen species, would be inadvertently removed from the nucleus, where it is most required. In support of this counter-argument, Beebe et al. pointed to work by Shestopalov and Bassnett (2000) who injected a fluorescent dye into individual lens fibres at various distances from the nuclear centre. At all points of injection, the fluorescent dye diffused radially, which demonstrated that a unidirectional current flow within the lens was non-existent. While there is a substantial amount of evidence in favour of the lens not requiring metabolic activity, the lens microcirculatory system
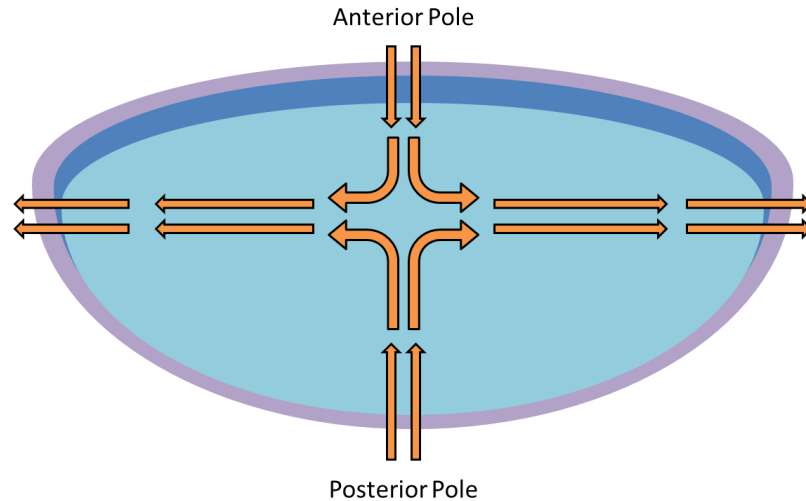
Figure II-14: The lens microcirculatory system theory. The ionic current enters at the anterior and posterior poles of the lens and exits at the equator of the lens. After Journal of Membrane Biology, The Lens Circulation, 216, 2007, 1-16, Mathais, R.T., Kistler, J. and Donaldson, P.J., (© Springer Science+Business Media, LLC 2007). With permission of Springer.

remains to be disproven. It should be noted that the optimal system has yet to be observed.

2.4.7 CATARACTS

Although there are a number of mechanisms within the lens that exist to maintain its transparency throughout life, a variety of factors can overcome these mechanisms and cause the lens to become opaque or cataractous. These opacities occur due to the unfolding, aggregation, and precipitation of proteins within the lens, which manifest as a result of ultraviolet (UV) light exposure or aging.

Under normal circumstances, the lens contains yellow pigments (3-hydroxy kynurenine and its glucoside) which function to absorb and subsequently dissipate day-to-day levels of UV radiation (Roberts, 2011). However, if the lens undergoes acute exposure to intense UV radiation or chronic exposure to mild UV radiation, the lenticular pigments get overwhelmed, photooxidation occurs, and

39

harmful reactive oxygen species (ROSs), such as free radicals or singlet oxygen, are produced (Ji et al., 2015; Linetsky & Ortwerth, 1996; Zigman, 2000). ROSs cause extensive protein unfolding and aggregation, which eventually leads their precipitation and lenticular cataractogenesis. Molecular chaperones, such as α-crystallins, repair unfolded proteins, but over time, the amount of functional crystallins within the lens deteriorates, resulting in nuclear and cortical cataracts, the two most prevalent forms of this condition (Sperduto & Hiller, 1984). A third less-common form of this condition exists, known as posterior subcapsular cataracts, in which exposure to UV radiation causes erroneous differentiation and elongation of equatorial lens fibre cells (Bochow et al., 1989; Drews, 1979). The abnormal cells migrate posteriorly, where their irregular morphology causes a breach in fibre cell organization resulting in an opacity of the lens.

2.5 THEORIES OF ACCOMMODATION

The primary function of the crystalline lens is to maintain a sharp image on objects that transition from distant to nearby locations, a process known as accommodation (Helmholtz, 1855; Helmholtz, 1962). The most widely accepted theory of accommodation is that proposed by Helmholtz in 1909 (Gullstrand & Helmholtz, 1909), wherein, the accommodative process is parasympathetically controlled by the ciliary muscle that surrounds the lens (Helmholtz & Southall, 1924). In its resting state, the ciliary muscle draws tightly on the zonules and maintains a taut and flattened lens shape while in its contracted state, the zonules lose tension and the lens becomes thick and round (Helmholtz, 1855; Strenk et al., 2005). Therefore, while the ciliary muscle is contracted, the lens curvatures steepen, ultimately increasing the refractive power of the eye as a whole and allowing for near-sighted vision (Helmholtz, 1962). The age-related loss of accommodative power is known as

presbyopia, and can be primarily attributed to the loss of elasticity of the lens as a whole (Koretz et al., 2002).

In diametric opposition of Helmholtz's theory, a proposal by Schachar suggests that contraction of the ciliary muscle results in increasing tension on the zonules at the equator, leading to a thickening and steepening of the central portion of the lens. In addition, the peripheral surfaces of the lens flatten and the equator of the lens moves toward the sclera (Schachar, 1992). In light of this controversy, Glasser and Kaufman (1999) demonstrated that the equatorial diameters of both human and non-human primate crystalline lenses decreased during accommodation using various imaging techniques, thereby disproving Schachar's theory of accommodation and presbyopia. Additionally, *in vitro* laser imaging showed that the crystalline lens did not change focal length when increasing and decreasing radial stretching forces were applied, thus supporting Helmholtz's classical theory of accommodation (Glasser & Kaufman, 1999).

In terms of the neural pathway for accommodation, the afferent loop of accommodation begins with the detection of a blurred image in the retina (Atchison, 2002). The signal of the blurred image travels down the optic fibres and synapses with the lateral geniculate nucleus, which subsequently relays the signal to the visual cortex. The signal is then relayed to the Edinger-Westphal (oculomotor) nucleus of the brain stem, which is the origin of the efferent loop of the accommodative reflex; signals carried by the fibres of the occulomotor nerve synapse with the ciliary nerve which causes contraction of the ciliary muscles (Nolte, 2002).

2.5.1 PRESBYOPIA

Children approximately 5 years of age possess the highest amplitudes of accommodation, reaching

41

values upwards of 14 dioptres (Garner, 1983). Perhaps surprisingly, from this age onwards, accommodative amplitude declines steadily at about 1 dioptre every 5 years until the age of 30, where the rate of decline accelerates to just under 4 dioptres at age 45 (Garner, 1983). It is at this point that the near work becomes difficult; the accommodative amplitude becomes less than the normal reading or working distance and objects must be extended further away to be seen clearly. Therefore, with age, the loss of accommodation is inevitable, and the subsequent inability to focus on near objects is a condition known as presbyopia.

To this day, the exact mechanism of presbyopia remains uncertain (Richdale et al., 2013; Schachar, 2015). However, several theories on the development of this condition have come to light, and can be divided into two categories: lenticular and extralenticular. Lenticular theories, such as the Hess-Gullstrand, and Fincham theories, propose the idea that the lens hardens or becomes more rigid with age (Fincham, 1937; Fincham, 1951; Gullstrand, 1924). As a result, the lens becomes increasingly resistant to the elastic forces of the capsule during accommodation. In contrast, the geometric theory attributes the loss of accommodation to changes of size and shape of the lens, particularly with regards to the steepening of anterior surface curvature and posterior shifts of zonular insertions. Koretz and Handelman (1982) propose that a combination of these two factors results in the relaxation of zonules having a smaller effect on the lens shape.

Extralenticular theories, such as that proposed by Duane, suggest that the ciliary muscle becomes weaker with age (Duane, 1925, 1931). However, evidence by Fisher demonstrates that the contractile force of the ciliary muscle, in fact, reaches a maximum during the onset of presbyopia, and a weakening does not occur until well after this 45 years of age (Fisher, 1988). It has also been proposed that the deterioration of the elastic components of the ciliary body and choroid may be responsible for the decline of accommodation with age, however, evidence of this deterioration has

yet to be demonstrated (Bito, 1988). The most widely accepted theory is that of Weale, who claims that presbyopia has more than one cause; it arises due to a combination of changes in the lens capsule and lenticular elasticity combined with a change in lens geometry (Weale, 1962).

Despite the major differences in anatomy between birds and primates (Walls, 1942), specifically the direct contact of the ciliary muscle of birds onto their lens equator, the chicken eye is also susceptible to presbyopia (Choh, Sivak, & Meriney, 2002). Although it remains unclear which exact mechanism causes the loss of accommodative amplitude in chickens, this study demonstrates the possibility of using chicken eyes as a model for presbyopia.

2.6 ACTIN, MYOSIN, AND THEIR INTERACTIONS

The interaction between actin filaments and myosin motors is responsible for an array of biological movements. The effects of these movements can be observed both microscopically, such as the division of cells during mitosis and meiosis, as well as macroscopically, such as the contraction of skeletal muscles.

Actin is a family of structural, globular proteins that assembles amongst themselves to form microfilaments, the thinnest of biological cables. Each monomeric actin subunit, known as globular (g-)actin, has a plus end and a minus end. When bound to adenosine triphosphate (ATP), the monomeric actin binds head-to-tail with other g-actin in order to form a strand of filamentous (f-)actin (Silverthorn, Ober, Garrison, & Johnson, 2009). As f-actin is the smallest of the biological tubules, it is quite flexible when compared to larger intermediate, and microtubules. However, the thinner diameter allows for an ideal surface on which motor proteins, such as myosin, can traverse.

Myosin II, which is the conventional myosin, was the first motor protein to be identified, and

is responsible for the contraction of all muscle types (Alberts et al., 1995); it is an elongated protein that resembles two golf clubs with their shafts coiled around one another. In this analogy, the double club heads are the force-generating machinery that form the N-terminus of the protein, and that interact with the actin microfilaments to generate movement (Silverthorn et al., 2009). The C-terminus is therefore found at the opposite end of the shaft. The long axes of myosin proteins are aligned parallel to one and other, and are connected tail-to-tail, in order to form a myosin filament, which resembles a long strand with multiple myosin heads protruding out of its sides. The interaction of myosin strands with actin filaments is responsible for the contraction of muscle.

2.6.1 MUSCLE CONTRACTION

In vertebrates, there are three different types of muscle tissues: (1) skeletal muscle, which is attached to the bones of the skeleton, (2) smooth muscle, which controls the movement of internal organs and tubes, and (3) cardiac muscle, which controls beating of the heart (Silverthorn et al., 2009). Skeletal and cardiac muscle are often referred to as having striations, due to the alternating light and dark bands that they are observed to have when examining these tissues under a light microscope. Because the contractile fibres in smooth muscle are considerably less organized, no striations are observed in their tissue.

Skeletal muscle is often described as being voluntary, while cardiac and smooth muscle are involuntary (Silverthorn et al., 2009). It is well known, however, that movement of skeletal muscle may occur unconsciously, and a certain degree of control over cardiac and smooth muscle may be learned. Therefore, a more precise way of describing skeletal muscle is that they can only contract in response to a signal from a somatic motor neuron. In contrast, cardiac and smooth muscle are

controlled primarily by the autonomic nervous system, and their activities are subject to modulation by hormones of the endocrine system (Silverthorn et al., 2009).

2.6.1.1 SKELETAL MUSCLE CONTRACTION

The functional units in skeletal muscle are known as fascicles, which are bundles of muscle fibres sheathed in a tube of connective tissue. Each muscle fibre, in turn, contains a thousand or more myofibrils that occupy a majority of the intracellular space, leaving little room for the organelles. The primary contractile proteins in myofibrils are actin and myosin, where bundles of actin form thin filaments, and bundles of myosin form thick filaments (Silverthorn et al., 2009). The overlapping arrangement of thick and thin filaments in skeletal and cardiac muscle create an alternating light and dark pattern, which are the striations observed under light microscopy. A single repetition of this pattern forms what is known as a sarcomere, which is the contractile unit found within myofibrils, and the basis for the sliding filament theory of contraction. In this model, actin and myosin filaments use adenosine triphosphate (ATP) energy to slide past one another, which, in synchrony with other sarcomeres and myofibrils, results in muscle contraction.

At rest, myosin heads form tight crossbridges with actin in a rigor state. During muscle contraction, myosin heads interact with f-actin by, quite literally, stepping along each individual actin subunit by the following mechanism:

1. ATP binds to myosin, causing the myosin head to lose affinity towards actin.

2. While unbound, myosin hydrolyzes ATP to produce adenosine diphosphate (ADP) and inorganic phosphate (P_i), causing a rotation of the myosin head and a subsequent reattachment further along the f-actin filament. The rotational movement of myosin causes a

coiling of its shafts, resulting in the increase of potential energy.

3. Calcium ions (Ca^{2+}) signal the beginning of a power stroke, which causes myosin to adhere tightly to its new position, and a subsequent release of P_i from the myosin head. Release of P_i discharges the coiled energy in the myosin molecule and causes the heads to swivel, resulting in the entire myosin filament sliding forward along the actin filament.

4. Upon completion of the power stroke, the myosin head releases the ADP to once again become tightly bound with actin in a low-energy rigor state.

2.6.1.2 SMOOTH MUSCLE CONTRACTION

Although the contractile fibres in smooth muscle cells are not arranged in sarcomeres, they possess the same contractile proteins as those found in skeletal muscle tissue, with the exception of having a different myosin II isoform. In smooth muscle fibres, the actin and myosin filaments crisscross diagonally around the cell periphery, resembling a water balloon inside of a fish net. Due to this oblique arrangement of myofibrils, smooth muscle fibres become more globular during contraction, rather than shortening as skeletal muscle fibres do.

During muscle contraction, the interaction between actin and myosin filaments is identical in both smooth and skeletal muscle fibres. However, the signalling cascade for the onset of contraction in smooth muscle tissues is slightly different than that of skeletal muscle tissue, and occurs as follows:

1. An increased level of intrinsic Ca^{2+} initiates the contraction process.

2. Ca^{2+} binds to calmodulin, which begins a signal transduction pathway that activates myosin light chain kinase (MLCK)

3. MLCK enhances myosin ATPase activity by phosphorylating light protein chains of the myosin head, which results in muscle contraction.

Note that the onset of contraction in smooth muscle tissues has a variety of influences. Muscle contraction may be influenced by physical stretch

2.6.1.3 CARDIAC MUSCLE CONTRACTION

Cardiac muscle tissue shares features with both skeletal and smooth muscle tissues. Like skeletal muscle fibres, cardiac muscle fibres are striated due to the organization of their myofibrils into sarcomeres. Thus, they share a similar contraction mechanism with that of skeletal muscle. However, because of the smaller area that cardiac muscle has to cover, their muscle fibres are shorter than those of skeletal muscle and branch out in accordance with the shape of the heart. Additionally, cardiac muscle fibres are specially linked to one another via intercalated disks, which enable rapid transmission of electrical impulses throughout the network. As a result, coordinated contractions can be made in rapid succession in order to sequentially pump blood through the various chambers of the heart.

2.6.2 NON-MUSCLE MYOSIN

Myosin is not only found in the fibres of muscle tissue, but is also present and interacts with actin in non-muscle cells. The majority of non-muscle myosin are, like muscle myosin, part of the class II double-headed family, in addition to being of similar isoforms (IIA and IIB). Together with actin, these contractile proteins are responsible for a variety of important cellular functions such as

intracellular transportation, support, and cytokinesis. For example, interaction of myosin II with corticol actin filaments increases the stiffness of the plasma membrane, reducing the chance of cell surface deformation. In addition, during cytokinesis, actin and myosin II form a contractile ring around the dividing cell in order to pinch the cell into two halves. Finally, myosin I and V have been demonstrated to help with intracellular translocation of membrane-limited vesicles along actin filaments (Lodish et al., 2000; Woolner & Bement, 2009).

2.7 THE LENS CYTOSKELETON

Much like other cells in the human body, the cytoskeleton of the crystalline lens is composed of three categories of filaments; microfilaments (otherwise known as actin filaments, ~6-8 nm in diameter), intermediate filaments (~10 nm in diameter), and microtubules (~25 nm in diameter) (Quinlan et al., 1999b). The majority of these filaments function similarly to those in other extralenticular cells. Microfilaments in the lens facilitate changes in cell shape, strengthen cell-to-cell/cell-to-extracellular matrix interactions, and define plasma membrane compartments (Quinlan et al., 1999a). Microtubules in the lens help with intracellular transport processes and the distribution of organelles (Quinlan et al., 1999a). Intermediate filaments are perhaps the most distinctive of the three cytoskeletal systems within the lens, as they not only contribute for maintaining the structural integrity and transparency of the lenticular system as a whole, but also resist the physical strain brought on by the accommodative mechanism of the eye (Quinlan et al., 1999b; Song et al., 2009). Bradley et al. (1979) showed that age-related changes in the cytoskeleton of human lenses included redistributions of intermediate filaments and proteins thought to microfilaments. Despite these studies suggesting a possible role for cytoskeletal proteins in accommodation and therefore presbyopia, not many studies have examined how these proteins may affect the biomechanical

properties or accommodative capabilities of the lens. A study by Luck and Choh (2010) hinted at a role for low concentrations of myosin light chain kinase in softening lenses. Recent work by Fudge et al. (2011) showed that lenses from knock-out mice without beaded intermediate filaments showed lenses that were less stiff and more resilient than wild-type mice. Of the three major classes of cytoskeletal proteins, actin and its interacting proteins show the most promise in the potential to facilitate lenticular shape changes.

2.7.1 MICROFILAMENTS

Since the late 1970's, it has been known that an abundance of actin filaments exists within the crystalline lens (Ireland, Lieska, & Maisel, 1983; Kibbelaar, Selten-Versteegen, Dunia, Benedetti, & Bloemendal, 1979). In addition to either participating in or regulating a variety of biological functions, such as morphogenesis, cell migration, cell adhesion, cell movement, and cell division (Burridge & Wennerberg, 2004; Hall, 1998; Ridley et al., 2003; Tapon & Hall, 1997), actin filaments are known to interact with myosin to form a rigid structure that could offer tensile strength in order to maintain lens shape and accommodative function in the eye (Bassnett et al., 1999; Kibbelaar et al., 1980; Rafferty, Scholz, Goldberg, & Lewyckyj, 1990). In epithelial cells, actin filaments are organized as bands or belts that wrap around the cell just inside the cell membrane. Tightening the actin belt of an epithelial cell will force a rearrangement of the cytoskeleton and a corresponding change in cell shape (Oyster, 1999) whose length may increase on the order of several hundred-folds during the process of differentiating into a lens fibre cell (Piatigorsky, 1981; Taylor et al., 1996). As the lens fibre cells elongate and mature, lamellipodial extensions from the cell surface help fibre cells migrate from the equator of the lens to the centre (Taylor et al., 1996).

The apical surface of the lens fibre cells are anchored to the anterior layer of epithelial cells while the basal surface of the lens fibre cells are anchored to the posterior lens capsule (Taylor et al., 1996). The basal surface of lens fibre cells are anchored to a set of structures known as the basal membrane complex (BMC) (Bassnett et al., 1999). In addition to adhering the lens fibre cells to the posterior lens capsule, the BMC facilitates migration of lens fibres during their differentiation process (Bassnett et al., 1999). The BMC was first observed by Rafferty's group (Rafferty et al., 1990; Yeh, 1986) as early as 1986 (Fig. II-15A), where these investigators determined that the structure was composed primarily of filamentous-actin (f-actin) arranged in a polygonal array. Further investigation by Bassnett's group revealed that the polygonal array is co-localized with non-muscle myosin II and N-cadherin, forming a hexagonal lattice (Fig. II-15B). The specific arrangement of actin and myosin in the BMC, along with the adhesive protein N-cadherin, suggests that the polygonal array may have contractile properties of its own (Fig. II-16), that is, the lens produces a contractile force independent of the surrounding ciliary muscle.
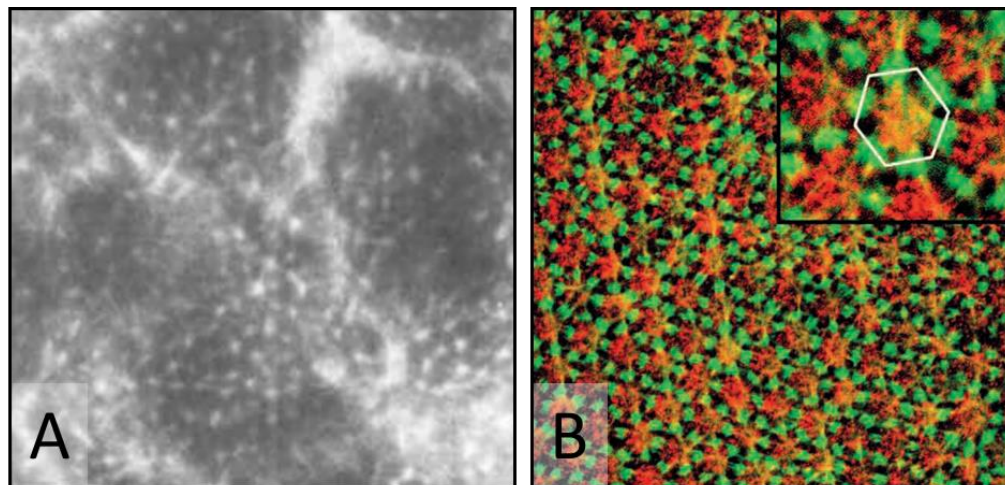
Figure II-15: Confocal images of actin microfilaments found at the lens capsule. (A) Anterior (Rafferty et al. in 1990) and (B) posterior surfaces (Bassnett et al. in 1999) both exhibit polygonal arrays of actin. (A) Republished with permission of the Association for Research in Vision and Ophthalmology from Rafferty et al. (1990), (B) Republished with permission of The Company of Biologists Ltd from Bassnett et al. (1999).
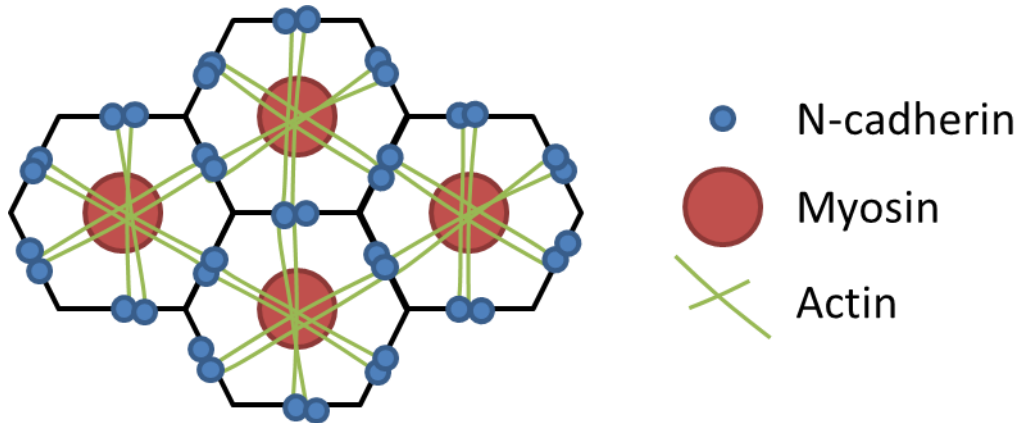
Figure II-16: Schematic diagram of a potential two-dimensional muscle. The specific arrangement of actin (green), myosin (red), and N-cadherin (blue) in the basal membrane complex suggests that the structure as a whole can contract laterally to increase the tension of the crystalline lens surface as a whole. Redrawn after (Bassnett et al., 1999).

2.7.2 INTERMEDIATE FILAMENTS

Unlike microfilaments, which are simply polymerized strands of actin monomers, there are numerous types of intermediate filaments (IFs) that vary in shape and function based on their protein architecture (review by Quinlan et al., 1999b). However, intermediate filament proteins share the same general structure (Fig. II-17) in that they are composed of a central rod domain flanked by two terminal domains (Quinlan et al., 1999a). The central rod domain consists of one or more α-helical domains with an N-terminal head on one end and a C-terminal tail on the other. The N-terminal domain is essential for assembly of IFs, whereas the C-terminal domain's function varies depending on the role of the particular IF in question. Conserved sequences LNDR and TYRKLLEGE are found at the N- and C- terminal ends, respectively, of the central rod domain, and are essential to IF assembly (Perng, Zhang, & Quinlan, 2007).
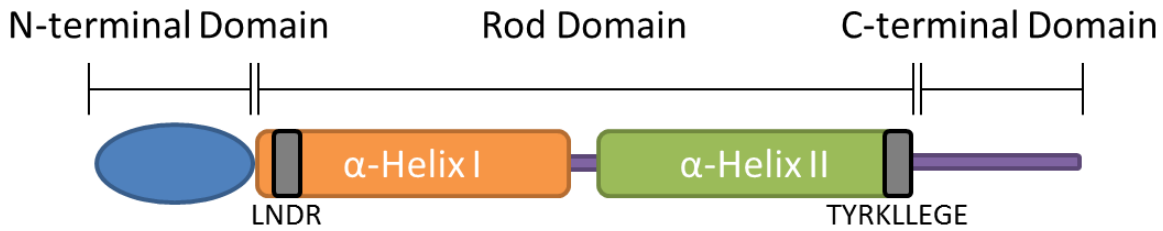
Figure II-17: Schematic representation of the general structure of an intermediate filament (IF). Each IF is composed of a rod domain flanked by N-terminal and C-terminal domains.

Intermediate filaments are not essential for cell survivability (Perng et al., 2007; Song et al., 2009). In fact, single cell eukaryotes do not have intermediate filaments whatsoever, suggesting that these filaments have a more recent emergence on the evolutionary stage and perhaps a more specialized role in the cell (Song et al., 2009). The notion that the lenticular cell is specialized is exemplified by the expression of a unique intermediate filament, the beaded filament, that are crucial for maintaining both the structural integrity as well as the optical clarity of the lens as a whole. Although a number of IF families found within the lens occur throughout the human body and the crystalline lens contains a wide variety of intermediate filaments (see Table II-2), the beaded filament, first discovered by Maisel and Perry in 1972 (1972), is by far the most abundant and is found exclusively within lens fibre cells (Ireland & Maisel, 1983; Rao & Maddala, 2006). These

Table II-2: Intermediate filaments found in the developing and adult crystalline lens

Intermediate Filament Protein	Developing Lens		Adult Lens	
	Epithelium	Fibres	Epithelium	Fibres
Filensin (CP115)	-	+	-	+
Phakinin (CP49)	-	+	-	+
Vimentin	+	+	+	+
GFAP	+	-	+	-
K8/K18/K19	+	-	+	-
Nestin	+	+	-	-
Synemin	+	+	+	+

Data compiled from Maisel and Perry (1972), Ireland & Maisel (1983), and Rao & Maddala (2006)

lens-specific IFs are crucial for maintaining both the structural integrity as well as the optical clarity of the lens as a whole.

The term "beaded filament" was first used by Maisel and Perry in 1972, to describe the oddly shaped filaments that they observed in cryogenic sections of chick lenses (Maisel & Perry, 1972). At the time of discovery, the identity of these beads were unknown and simply thought to be artefacts. It is now known that the beads are organized clusters of α-crystallins, the crucial proteins found within the lens that are responsible for maintaining lenticular transparency (Song et al., 2009).

Interestingly, the *in vitro* assembly of beaded filament structural proteins (BFSPs) into 10 nm intermediate filaments requires the presence of both filensin (BFSP1) and phakinin, also known as CP49 (BFSP2) (Quinlan et al., 1999b) (Fig. II-18A). Furthermore, the addition of α-crystallins to filensin and CP49 results in the complete assembly into beaded filaments (Quinlan et al., 1999b) (Fig. II-18B), indicating an inherent mechanism of assembly amongst these three components. However, perhaps unsurprisingly, the *in vitro* assembly of filensin, CP49, and α-crystallins is unregulated and produces disorganized branches of beaded filaments, as opposed to the organized columns observed *in vivo* (Quinlan et al., 1999a).

The specific assembly of BFSPs along with their unique structural features are likely due to their distinct motifs (LGER and RYHRIIEIE in mammalian BFSP1 and LGGC and SYHALLDRE in mammalian BFSP2) in place of the highly conserved LNDR and TYRKLLEGE motifs, which set them apart from other IFs. This theory is reinforced by the close resemblance of BFSP structures to the general structure of IFs with only the conserved sequences that differ.

The collective data thus far on CP49 and filensin indicate that they are two key lens-specific intermediate filament proteins, and are vital for both the transparency and structural integrity of the crystalline lens as a whole (Quinlan et al., 1999b). Therefore, interactions of CP49 and filensin, with
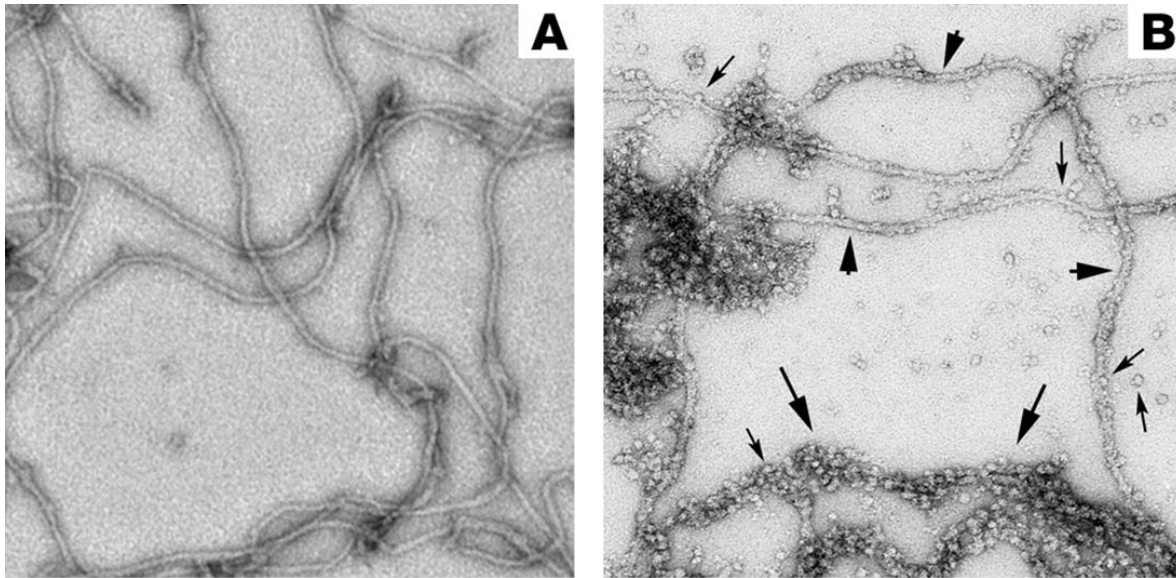
Figure II-18: Electron micrographs of beaded filament assembly. (A) *in vitro* assembly without α-crystallins and (B) native filaments in the lens. Large arrowheads denote smooth 10-nm filaments, while large arrows denote beaded filaments. Small arrows indicate α-crystallin particles. Republished with permission of the American Society of Clinical Investigations, from Functions of the intermediate filament cytoskeleton in the eye lens, Song, S., Landsbury, A., Dahm, R., Liu, Y., Qingjiong, Z. and Quinlan, R.A., 2009, 119(7), 1837-1848 (permission conveyed through Copyright Clearance Center, Inc.).

both cytoplasmic and plasma membrane proteins, may be important in the prevention of lens abnormalities.

2.7.3 MICROTUBULES

Microtubules (MTs) were first observed in the crystalline lens by Cohen (1965). As the formation of the adult lens involves continuous mitosis of lens epithelial cells, in addition to complex migration and extensive elongation of lens fibre cells, it was speculated at the time that the role of lens microtubules was largely developmental. Evidence that MTs were primarily intracellular

developmental agents was presented by Pearce and Zwaanby in 1970, when they treated chicken embryos with colcemid, a microtubule-dissociating agent (Pearce & Zwaan, 1970); lenticular cells of colcimid-treated embryos were arrested in metaphase and further elongation of interphase cells ceased. Additionally, colcimid-treated tissues maintained a pseudostratified columnar appearance, indicating that microtubules are not needed to maintain the columnar shape, but are absolutely necessary for fibre cell elongation. Further support for microtubule involvement in lens cell elongation was shown by Piatigorsky et al. in 1972, when they cultured primary explants of epithelial cells and found that elongation was correlated with longitudinally-oriented microtubules (Piatigorsky, Webster, & Wollberg, 1972). Additionally, lenticular cell elongation in this experiment was shown to be prevented by treatment with colchicine or vinblastine sulphate, agents that dissociate cytoplasmic microtubules.

Despite these findings, the role of MTs within the lens was heavily debated in the early 1980s, when Farnsworth, Shyne, and Caputo (1980) showed an abundance of MTs in lenses of normal post-mortem human eyes ranging in age from 6 to 54. As the lenses in the study maintained their transparency and viscoelastic properties post-mortem, it was speculated that MTs played a major role in lens clarity and structural integrity. However, it is now known that the integrity, modulus, and transparency of the lens are results of the interaction between microfilaments, intermediate filaments and lenticular crystallins; studies of microfilaments in the crystalline lens to date suggest that MTs are only responsible for cell migration, mitosis, and development (Piatigorsky, 1981)

2.8.1 BLEBBISTATIN

Blebbistatin (1-phenyl-1,2,3,4-tetrahydro-4-hydroxypyrrolo[2.3-b]-7-methylquinolin-4-one) (Fig. II-19) is a small molecule inhibitor with high affinity to myosin II. It is permeable to cell membranes, and is a potent inhibitor of skeletal and non-muscle myosin II isoforms. It preferentially binds to myosin heads within the aqueous cavity between the nucleotide pocket and the cleft of the actin-binding interface. This binding blocks myosin II in an actin-detached state and slows down phosphate release, blocking the myosin heads in the ATPase intermediate (with ADP and phosphate bound at the active site) with low actin affinity. Because of this property, blebbistatin prevents rigid actomyosin crosslinking.

A recent study by Kovacs et al. (2004) demonstrated that blebbistatin has little to no effect on several unconventional myosins, such as myosin I, V, and X, although the sequence of the structural elements comprising the ATP-binding site is highly conserved through the myosin superfamily (Kovacs, 2004) (Fig. II-20). This absence of an effect indicates that the inhibitor does not directly
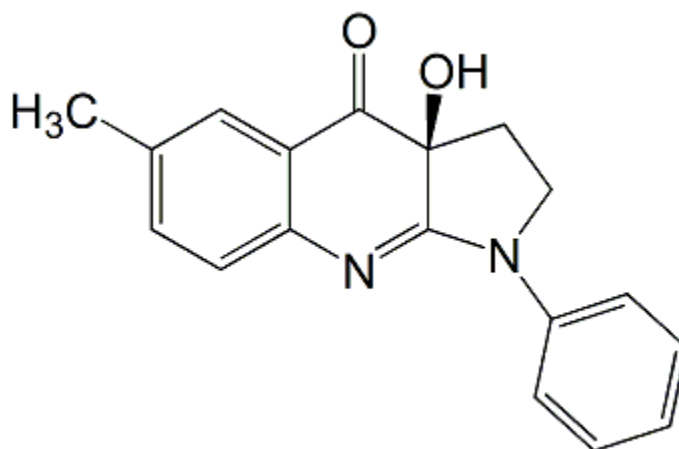
Figure II-19: Chemical structure of blebbistatin.
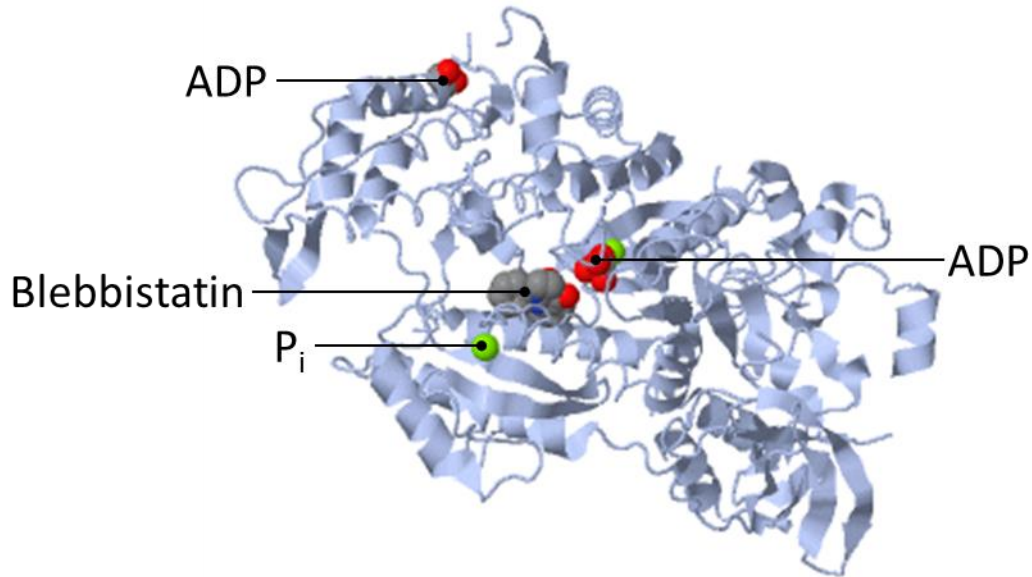
Figure II-20: Binding site of blebbistatin, ATP, ADP and P$_i$ in myosin II.

bind into the nucleotide pocket of myosin II but, instead, causes specific perturbations in the structure of that region, which decreases the rate of inorganic phosphate released, ultimately blocking myosin in a low actin affinity products complex.

2.8.2 LATRUNCULIN A

Latrunculia magnificans, is a Red Sea sponge that exudes a noxious, red fluid that kills fish within minutes. Latrunculin-A ([1R-[1R*, 4Z, 8E, 10Z, 12S*, 15R*, 17R*(R*)]]-4-(17-Hydroxy-5,12-dimethyl-3-oxo-2,16-dioxabicyclo[13.3.1]nonadeca-4,8,10-trien-17-yl)-2-thiazolidinone) (Fig. II-21) is a drug purified from this fluid, and is capable of rapidly, reversibly, and specifically disrupting the actin cytoskeleton by associating with globular (g-)actin monomers, and preventing polymerization into filamentous (f-)actin.
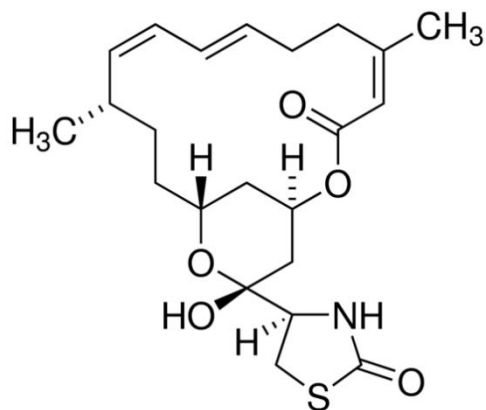
Figure II-21: Chemical structure of Latrunculin-A

2.8.3 ML-7

ML-7 (1-(5-Iodonaphthalene-1-sulfonyl)-1H-hexahydro-1,4-diazepine hydrochloride) (Fig. II-22) has been shown to inhibit Ca^{2+}-dependent and independent smooth muscle MLCK (myosin light chain kinases) via competitive inhibition of ATP and also inhibits protein kinases C and A. ML-7 also inhibits cell transporters activated by shrinkage and affects the osmotic volume regulation of cells. Mechanistic studies suggest that both processes are mediated via stimulation of potassium chloride co-transport, a cell volume regulating ion (Tian, Brumback, & Kaufman, 2000). ML-7 has also been reported to affect the superoxide O_2-producing system of human neutrophils in a myosin light chain kinase independent manner.
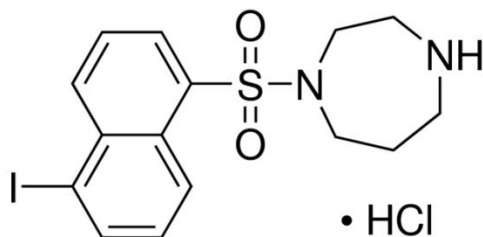
Figure II-22: Chemical structure of ML-7

III. THE EFFECTS OF ACTOMYOSIN DISRUPTORS ON THE MECHANICAL INTEGRITY OF THE AVIAN CRYSTALLINE LENS

This chapter was published in Won G, Fudge DS and Choh V (2015). The effects of actomyosin disruptors on the mechanical integrity of the avian crystalline lens. Mol. Vis., 21: 98-109.* [Won: designed experiments, conducted experiment, analysed/interpreted data, wrote manuscript and proofed/revised manuscript; Fudge: provided materials, proofed/revised manuscript; Choh: designed experiments, analysed/interpreted data, provided materials, proofed and edited manuscript].

Addendum: 10 µM is the dosage that was used for all inhibitors as it in the range that has been used in a variety of other studies (Zhang, 2011; Feng, 2010; Luck, 2010; Yin, 2010)

3.1 OVERVIEW

Purpose: Actin and myosin within the crystalline lens maintain the structural integrity of lens fibre cells and form a hexagonal lattice cradling the posterior surface of the lens. The actomyosin network was pharmacologically disrupted to examine the effects on lenticular biomechanics and optical quality.

Methods: One lens of 7-day-old White Leghorn chickens was treated with 10 µM of disruptor and the other with 0.01% dimethyl sulfoxide (vehicle). Actin, myosin, and myosin light chain kinase (MLCK) disruptors were used. The stiffness and the optical quality of the control and treated lenses were measured. Western blotting and confocal imaging were used to confirm that treatment led to disruption of the actomyosin network. The times for the lenses to recover stiffness to match control values were also measured.

Results: Disruptor-treated lenses were significantly less stiff than their controls ($p \leq 0.0274$ for all disruptors). The disruptors led to changes in the relative protein amounts as well as distributions of proteins within the lattice. However, the disruptors did not affect the clarity of the lenses ($p \geq 0.8051$ for all disruptors) and spherical aberration differences were only observed for myosin-inhibited lenses ($p=0.0500$). The effects of all

three disruptors were reversible, with lenses recovering from treatment with actin, myosin and MLCK disruptors after 4 hours, 1 hour, and 8 minutes, respectively.

Conclusion: Cytoskeletal protein disruptors led to a decreased stiffness of the lens, and the effects were reversible. Optical quality was mostly unaffected but the long-term consequences remain unclear. Our results raise the possibility that the mechanical properties of the avian lens may be actively regulated in vivo via adjustments to the actomyosin lattice.

3.2 INTRODUCTION

The process of accommodation allows for the eye to focus on nearby objects. The mechanism by which accommodation occurs in vertebrates involves either a translation of the lens or a change in lens curvature in order to increase the optical power of the eye (Helmholtz, 1962). Humans and birds are similar in that both species use the latter method to accommodate (Helmholtz, 1962; Sivak, 1980), however, the changes in the human lens occur via relaxation of zonules attached to the ciliary muscle (Helmholtz, 1962; Zinn & Wrisberg, 1780), whereas the ciliary muscle in the avian eye directly articulates with the equator of the lens (Sivak, 1980), resulting in squeezing of the lens in the equatorial plane.

The lens maintains its integrity and transparency due to the organization of its cells, which are epithelial in origin (Bettelheim, 1985; Clark, Matsushima, David, & Clark, 1999; Maddala et al., 2004). Similar to other epithelial cells in the body, lens epithelial cells contain cytoskeletal filaments, the smallest of which are known as microfilaments and are found throughout the lens (Ireland et al., 1983). Microfilaments are composed largely of filamentous (f-)actin and are responsible for an array of essential biological functions, including facilitating changes in cell shape,

fortifying cell-cell and cell-extracellular matrix interactions, as well as the compartmentalization of plasma membranes (Alberts, 2008; Quinlan et al., 1999b).

In most cells, f-actin function relies on its ability to interact with myosin II, a non-muscle and smooth muscle motor protein, to form actomyosin assemblies (Rao & Maddala, 2006). In smooth- and non-muscle systems, contraction of actin and myosin is triggered by myosin light chain kinase (MLCK), an upregulator of ATPase activity and a catalyst for actin-myosin cross-linking (Hai & Murphy, 1988; Kamm & Stull, 1985; Yuen, Ogut, & Brozovich, 2009). The ATP is used by myosin heads to move along actin filaments and results in contractile movement of myofilaments. In squirrel, rabbit, and humans, f-actin is arranged in polygonal arrays at the anterior face of crystalline lenses and is associated with myosin within the epithelium (Rafferty et al., 1990). Similarly, at the posterior surface of the avian crystalline lens, f-actin, non-muscle myosin, and N-cadherin are arranged in a hexagonal lattice resembling a "two-dimensional muscle" (Bassnett et al., 1999). The actomyosin complex at the anterior epithelium has been speculated to facilitate accommodation by allowing the epithelial cells to change shape or by permitting the lens as a whole to change into a more spherical shape (Yeh, 1986) while the proteins collectively at the basal membrane complex of the posterior lens surface have been shown to mediate fibre cell migration across, and anchor fibre cells to, the lens capsule (Bassnett et al., 1999). In addition, the presence of highly regular actomyosin lattices in the lens raises the possibility that these networks are involved in setting the passive biomechanical response of the avian lens to external forces such as those exerted by the ciliary muscle. Indeed, previous research using knockout mice has shown that in the murine lens, beaded filaments, which are intermediate filaments unique to the lens, contribute significantly to lens stiffness (Fudge et al., 2011). Furthermore, the fact that the actomyosin network has the potential to be contractile raises two even more intriguing possibilities - that lens stiffness could be actively

tuned by adjusting the amount of tension in the network, and that the shape of the lens itself could be similarly adjusted (Bassnett et al., 1999; M. A. Kibbelaar et al., 1980; Kuszak, Zoltoski, & Tiedemann, 2004; Ramaekers, Poels, Jap, & Bloemendal, 1982; Yeh, 1986). The demonstration that the MLCK inhibitor, ML-7, has significant effects on the focal length, and therefore almost certainly the shape, of avian lenses seems to support this idea (Luck & Choh, 2010). The purpose of this study was to test the hypothesis that lenticular actomyosin networks affect the biomechanics and optics of the whole avian lens by pharmacologically disrupting them and measuring the effects on lens stiffness and optical clarity.

3.3 METHODS

3.3.1 ANIMALS

White leghorn (Gallus gallus domesticus) hatchling chicks were obtained from the Maple Leaf hatchery in New Hamburg, Ontario and were fed *ad libitum*. They were housed in stainless steel brooders with a heat source, and kept on a 14:10 day:night light cycle. Chicks were raised in accordance to the Guidelines of the Canadian Council on Animal Care and conform to the ARVO Statement for the Use of Animals in Ophthalmic and Vision Research. As the focus of this study was to test the fundamental question of whether disrupting cytoskeletal proteins could have an effect on lenticular biomechanics, chicks with robust amounts of accommodation (about a week old) were used instead of older birds, which will be considered for a future study once the functions of disruptors have been well established. Week-old chicks also show highly monotonic spherical aberrations (Choh, Sivak, & Meriney, 2002) thereby providing a model for which optical changes

could be assessed.

3.3.2 LENS DISSECTIONS

Six to eight day old chicks were sacrificed by decapitation and their eyes were enucleated. Eyes were placed in chilled oxygenated Tyrode's solution (TS: 134 mM NaCl, 3 mM KCl, 20.5 mM NaHCO3, 1 mM MgCl2, 3 mM CaCl2) before removal of the posterior globe and vitreous humour. The exposed lens was then separated from the surrounding ciliary body and extracted from the anterior segment, taking care to minimize damage to the lens capsule.

3.3.3 DISRUPTORS

Latrunculin A (LAT-A) is a drug that rapidly, reversibly, and specifically disrupts actin cytoskeleton by preventing polymerization (Morton, 2000; Spector, 1983). 1-phenyl-1,2,3,4-tetrahydro-4-hydroxypyrrolo[2.3-b]-7-methylquinolin-4-one (blebbistatin) is a reversible inhibitor with specificity and high-affinity for several class II myosins and acts by reducing the actin affinity of the myosin heads (Kovacs, 2004). 1-(5-Iodonaphthalene-1-sulfonyl)-1H-hexahydro-1,4-diazepine hydrochloride (ML-7) selectively disrupts myosin light chain kinase activity by preventing myosin II light-chain phosphorylation (Saponara, 2012).

3.3.4 LENS TREATMENTS

For each bird, one eye was treated for 15 minutes with either 10 μM latrunculin (n=18), in 0.01%

(v/v) dimethyl sulfoxide (DMSO) in TS, 10 μM blebbistatin (n=16), in 0.01% (v/v) DMSO in TS or

10 μM ML 7 (n=14) in 0.01% (v/v) DMSO in TS. The lenses from the opposite eyes were subjected

to vehicle (0.01% (v/v) DMSO in TS; 15 min). Assignment to the treatment group alternated

between left and right eyes. All lenses were briefly rinsed in TS prior to biomechanical testing,

Western blot analysis, immunocytochemical processing, or assessment of optical quality.

3.3.5 LENS COMPRESSIONS

The mechanical properties of the lens were measured using a universal testing machine (Instron,

Norwood, MA, USA). Each lens was placed anterior side down on a pedestal located in the

compression chamber containing chilled TS. Lenses were then compressed 0.75 mm using an

aluminum compression element connected to a 10-N load cell (Fig. III-1) and measurements of the

resultant force exerted by the lens were collected. For experiments examining whether the effects

on the biomechanics were reversible, a 5-N sensitive load cell was used and compressions were
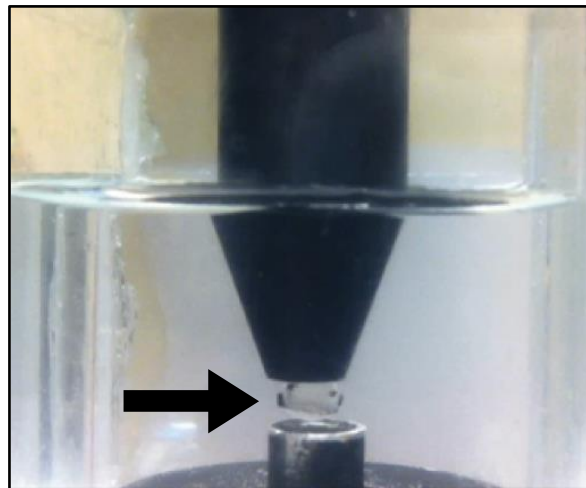
Figure III-1: Image of a lens in the compression chamber. The lens (arrow) is
submerged in TS, sitting anterior side up on a pedestal and compressed from above by
an aluminum compression element connected to a load cell.

carried out immediately after the 15 minute disruptor/vehicle treatment at the following time points: 1 min., 2 min., 4 min., 8 min., 16 min., 32 min., 1 hr., 2 hr., 4 hr., 8 hr., 16 hr., and 32 hr. after treatment. Force-compression data for each lens were collected using Bluehill software (ver. 9, Instron, Norwood, MA, USA).

3.3.6 ANALYSIS OF STIFFNESS

Force data were adjusted to account for buoyancy exerted by the surrounding solution on the compression element, as it displaced more or less test solution during compression and relaxation of the lens. The resulting force-compression curves that were generated for each lens were then best-fit to a 3-parameter exponential curve with the equation $y = y_0 + ae^{bx}$. As the b-coefficient of the exponential equation is a unitless constant that describes a relationship of how rapidly the force increases as compression distance increases, it was used to assess the relative stiffness between lenses (Demer & Yin, 1983; Higashita et al., 1996) with larger numerical values for the b-coefficient representing steeper curves, and thus stiffer lenses. B-coefficients from each curve were extracted and means and standard deviations were calculated from these data. Dimensionless b-coefficient values for whole lenses should not be confused with the Young's Modulus, which is known to vary in different parts of the lens (Weeber & van der Heijde, 2008) and was not measured in this study. It should be noted that there were no significant differences in the size of control and treated lenses, thus differences in b-coefficient likely correspond with differences in the Young's Modulus of at least part of the lens, although our data cannot tell us which part.

3.3.7 WESTERN BLOT ANALYSIS

Western blot analysis was carried out to confirm that disruptors had the expected effects on the lens. Disruptor and vehicle treatments were identical to those for the compression trials. Lenses were dissected and separated into 1) posterior capsule samples, and 2) decapsulated lens fibre samples (composed of cortical+nuclear fibres). Each sample was separately ground using mini pestles, and lysed with Radioimmunoprecipitation Assay Buffer (RIPA; R0278, Sigma-Aldrich Co., Oakville, ON, Canada) containing a general use protease inhibitor cocktail (P2714, Sigma-Aldrich Co., Oakville, ON, Canada). The total protein of lens tissue samples was quantified using the BioRad DC protein assay (500-0111; BioRad Laboratories, Inc., Mississauga, ON, Canada). Samples were prepared with Laemmli sample buffer, run on 10% precast gels (456-1033, BioRad Laboratories, Inc., Mississauga, ON, Canada) in the BioRad Mini-Protean System (165-8000, BioRad Laboratories, Inc., Mississauga, ON, Canada), transferred to a polyvinyldene fluoride (PVDF; 162-0175, BioRad Laboratories, Inc., Mississauga, ON, Canada) membrane and visualized with antibodies specific to the protein being blotted. Mono- and polymeric actin levels in the lens capsule were quantified using a globular (g-)actin/filamentous (f-)actin in vivo assay biochemistry kit (BKO37, Cytoskeleton, Inc., Denver, CO, USA). In brief, lens samples were homogenized and a detergent-based lysis buffer that stabilizes and maintains the globular and filamentous forms of cellular actin was added. The lysate containing each sample was then centrifuged ($21,100 \times$ g, Thermo Scientific Sorvall Legend Micro 21), with the resulting supernatant and pellet containing g-actin and f-actin, respectively. Actin levels in both supernatant and pellet were then quantified by Western blot analysis for three replicates. ML-7 inhibits MLCK, which phosphorylates myosin, therefore antibodies against phosphorylated myosin (M6068, Sigma-Aldrich Co., Oakville, ON, Canada) were used for ML-7-treated samples. Secondary antibodies conjugated with horseradish

peroxidase were detected by enhanced chemiluminescence using Amersham ECL prime (RPN2236, GE Healthcare, Mississauga, ON, Canada). Western Blots were visualized using a Storm 860 scanner (GE Healthcare, Mississauga, ON, Canada), and assessed using ImageQuant software (GE Healthcare, Mississauga, ON, Canada).

3.3.8 OPTICAL QUALITY

The optical quality of lenses was assessed using a ScanTox© scanning laser monitor. In brief, lenses were placed anterior side down in a rectangular glass chamber in TS and 5% fetal bovine serum, the latter to visualize the helium-neon laser beams passing through the lens at various eccentricities from the optical axis. Refracted beams were captured and recorded with a camera and back vertex focal lengths were calculated using software associated with the scanner. Beams passing through the sutures were omitted, as they produce highly inaccurate back vertex focal lengths. The optical quality of lenses was assessed based on changes in scatter and spherical aberration. For calculations of spherical aberration, data were first converted to dioptric values (vergences) using a thin lens approximation in water; the refractive index of water (n_w = 1.33) was divided by the back vertex focal lengths (in meters). The vergences were then fitted using a 3rd order polynomial line of regression to determine the back vertex distance at the optical axis (Fig. III-2). The amounts of spherical aberration were determined for a 1.5 mm pupil size by averaging the spherical aberration calculations for the positive (0 to 0.75 mm) and negative (0 to -0.75 mm) eccentricities. As bird lenses typically show a high negative spherical aberration (SA) (Choh et al., 2002; Glasser & Howland, 1995; Sivak & Kreuzer, 1983; Sivak, Ryall, Weerheim, & Campbell, 1989a), scatter was quantified as the mean deviation of the various focal lengths from the best fitting 3rd order

$$y = 3.0581x^2 - 0.1903x + 12.589$$
$$R^2 = 0.9864$$
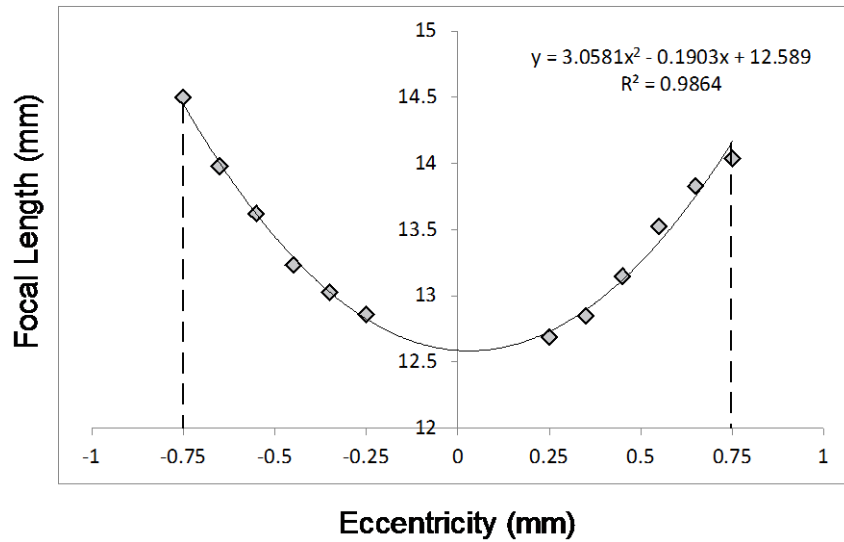
Figure III-2: Effects of disruptors on lenticular optics. Line graph showing the focal length (mm) at various eccentricities (mm) of a typical avian crystalline lens. Graphs were fitted with third-order polynomial equations to calculate the amount of scatter and SA.

polynomial line of regression. Higher deviations indicated higher degrees of scatter.

3.3.9 CONFOCAL MICROSCOPY

Blebbistatin- and latrunculin-treated lenses and the controls for these lenses were fixed with 2% (v/v) paraformaldehyde in TS. Lenses were permeabilized *in toto* using 0.05% v/v Triton X-100 in phosphate buffered saline (PBS) before addition of mouse anti-myosin-light-chain antibody (M4401, Sigma-Aldrich, 1:100 dilution in PBS, 2 hrs. at 37°C) followed by rabbit anti-mouse secondary antibody conjugated to Texas Red (1:500 in PBS, overnight at RT). Following a 3 x 5 minutes wash, lenses were counterstained with phalloidin FITC (P5282, Sigma-Aldrich, 1:400 dilution in PBS, 15 min, RT). Lenses were mounted *in toto* posterior pole up onto slides using 5% (w/v) agar solution in water with 0.05 mg/ml phenylenediamene (P6001, Sigma-Aldrich; in 50% (v/v) glycerol

in water). A coverslip coated with ProLong Gold (P36934, Life Technologies) was then placed on top of the posterior pole of the lens and adhered to the slide with the agar. The protein distribution of lenses was visualized using a Zeiss LSM 510 confocal microscope and images were captured and processed using the Zen 2011 software (Zeiss).

Protein distributions were quantified using nearest neighbour analysis, which assesses the closeness of points of interest (POIs) on an image and assigns a value between 0 and 2.15, where a score of 0 represents clustered POIs, a score of 1 represents random distribution of POIs, and a score of 2.15 is highly regular distribution of POIs. For latrunculin-treated lenses (n=3), the POIs used were the vertices of actin hexagons, while for blebbistatin-treated lenses (n=3), the POIs used were the centre of myosin globules. POIs were targeted and selected using NIH Image or Scion Image software. Nearest neighbour values (R_n) were calculated using the equation $R_n = \frac{D(obs)}{0.5\sqrt{a/n}}$, where D(Obs) is the mean observed nearest neighbour distance, a is the area, and n is the total number of POIs.

3.3.10 STATISTICAL ANALYSIS

The effects of the disruptors on the stiffness and optical quality of the lenses were analysed using mixed-model analysis of variance, with disruptor versus vehicle as the repeated measure and the type of disruptor used as a factor. For the longitudinal (reversibility) study, a two-way repeated measured analysis of variance (ANOVA) was used with the disruptor versus vehicle as one measure, and time as the other. Tukey or Bonferroni-corrected post-hoc multiple comparison tests were carried out where applicable. Comparisons of the optical quality of the lenses, and of nearest neighbour values were assessed using paired t-tests. For all statistical tests, results were considered significant at p ≤

0.05.

3.4 RESULTS

Force-compression curves were generated for each lens (Fig. III-3). Linear regression of the data to a 3-parameter exponential curve ($y = y_0 + ae^{bx}$) yielded mean r^2 values ($\pm$ SEM) of 0.9861 ± 0.0217 (range: 0.8787 and 0.9999). For most pairs of lenses, treatment with disruptors was associated with a decrease in stiffness of the lens, as indicated by the shallower force-compression curves (Fig. III-3, filled symbols). Specifically, for 15 of the 18 pairs of eyes in the latrunculin group, treated lenses exhibited relatively lower stiffness values for the latrunculin-treated lenses compared to its vehicle-control, while 3 pairs showed the opposite trend, with stiffness in latrunculin-treated lenses relatively higher than those exposed to vehicle. The mean stiffness values reflected the general trend (Fig. III-4), with latrunculin-treated lenses significantly lower ($\pm$ SEM) at 2.64 ± 1.28 compared to the vehicle-treated lenses at 4.15 ± 1.15 (p=0.0011; Fig. III-4A). Similarly, 14 of 16 pairs of lenses showed relatively lower stiffness values for the blebbistatin-treated lenses compared to the vehicle-treated counterpart, with 2 pairs showing the opposite trend. Again, the mean stiffness values ($\pm$ SEM) were lower for blebbistatin-treated lenses (3.25 ± 0.23) compared to those exposed to vehicle (4.47 ± 0.57; p=0.0274; Fig. III-4B). Finally, for 12 out of 14 pairs of lenses, the stiffness of ML-7 treated lenses were relatively lower compared to the vehicle-treated lenses, while lenses for 2 pairs were relatively higher. The mean stiffness for ML-7-treated lenses were, again, lower than of their fellow eyes (2.90 ± 1.19 vs. 4.49 ± 1.23, respectively; p=0.0027; Fig. III-4C). Mixed model analysis revealed no significant difference in stiffness levels between the disruptors (p=0.2379) nor was there an interaction effect (p=0.7483).

70
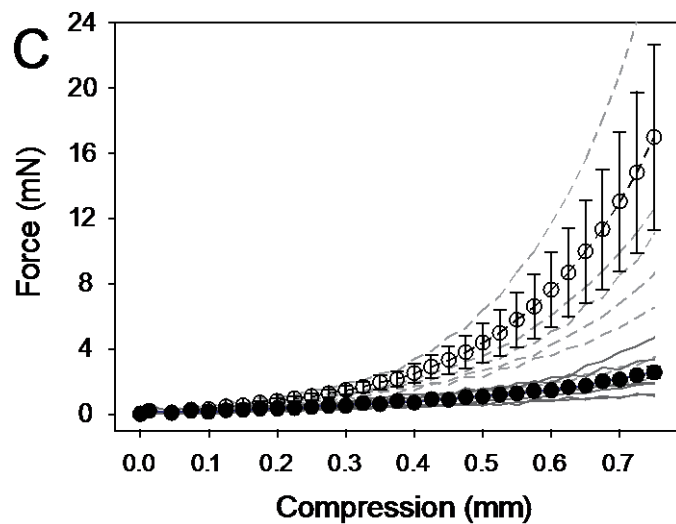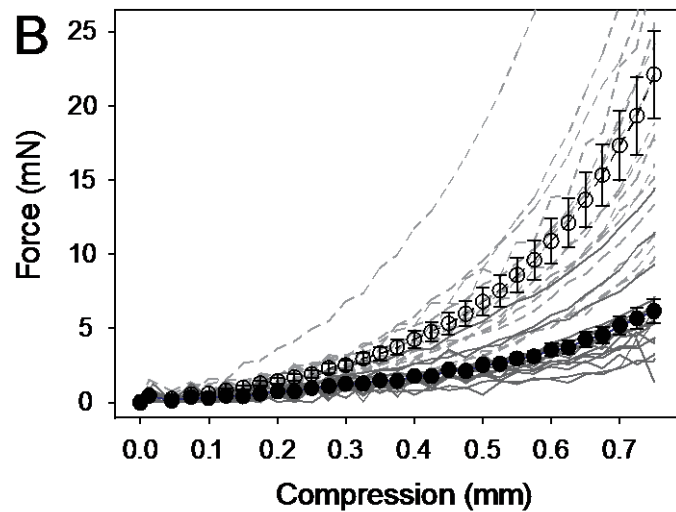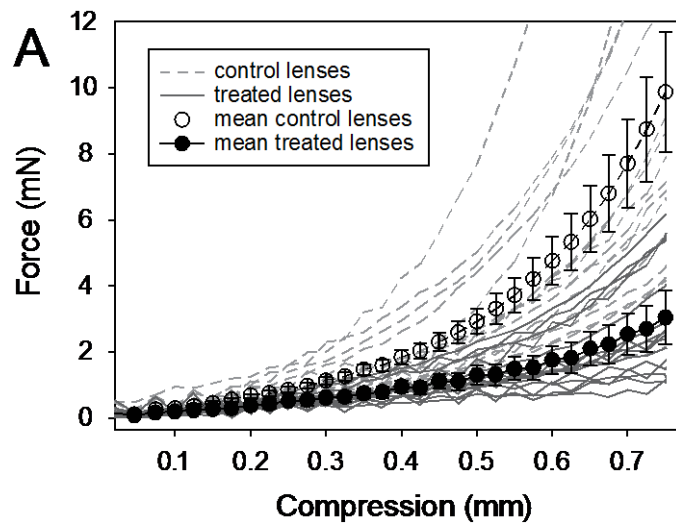
Figure III-3: Force-compression curves of all lenses. Mean force ± SEM of (A) latrunculin-, (B) blebbistatin-, and (C) ML-7-treated lenses (filled symbols) and their controls (empty symbols), as a function of compression. Force-compression curves of individual disruptor-treated (solid gray lines) and vehicle-treated (dashed gray lines) lenses are also included.
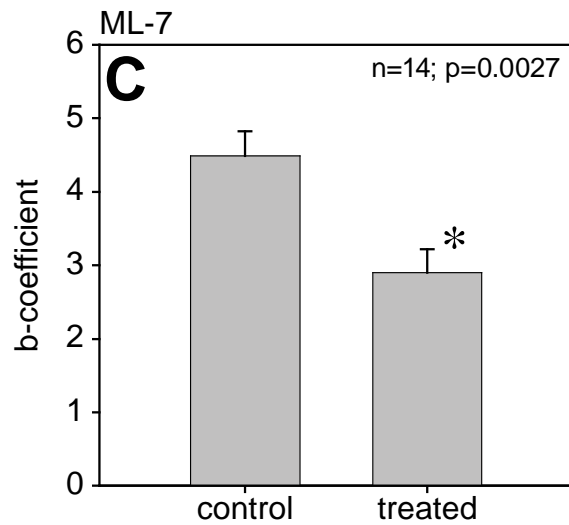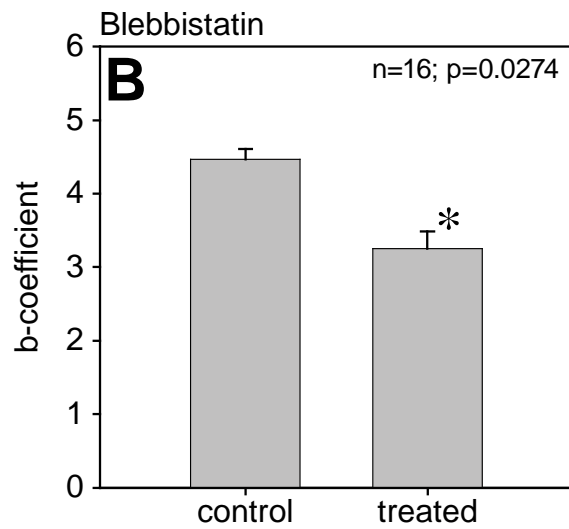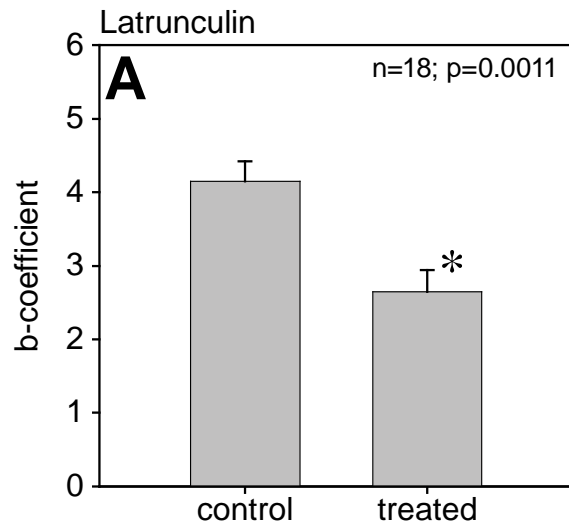
Figure III-4: Effects of disruptors on lenticular stiffness. Mean stiffness values ± SEM of disruptor- and vehicle-treated lenses for (A) 10 μM latrunculin (n = 18), (B) 10 μM blebbistatin (n = 16), and (C) 10 μM ML-7 (n = 14). Asterisks denote significant differences (all groups p≤0.0274).

Western blot analysis indicated that latrunculin and ML-7 treatments were effective in disrupting actin levels and myosin phosphorylation, respectively, at both the basal membrane complex (BMC) and the cortical lens fibres (Fig. III-5). Actin levels in latrunculin-treated lenses were quantified using a g-actin/f-actin in vivo assay kit, which revealed a large decrease in f-actin at both the BMC and in the lens fibre cells as a result of lens tissue treatment. In BMC samples treated with Western blot analysis indicated that latrunculin and ML-7 treatments were effective in
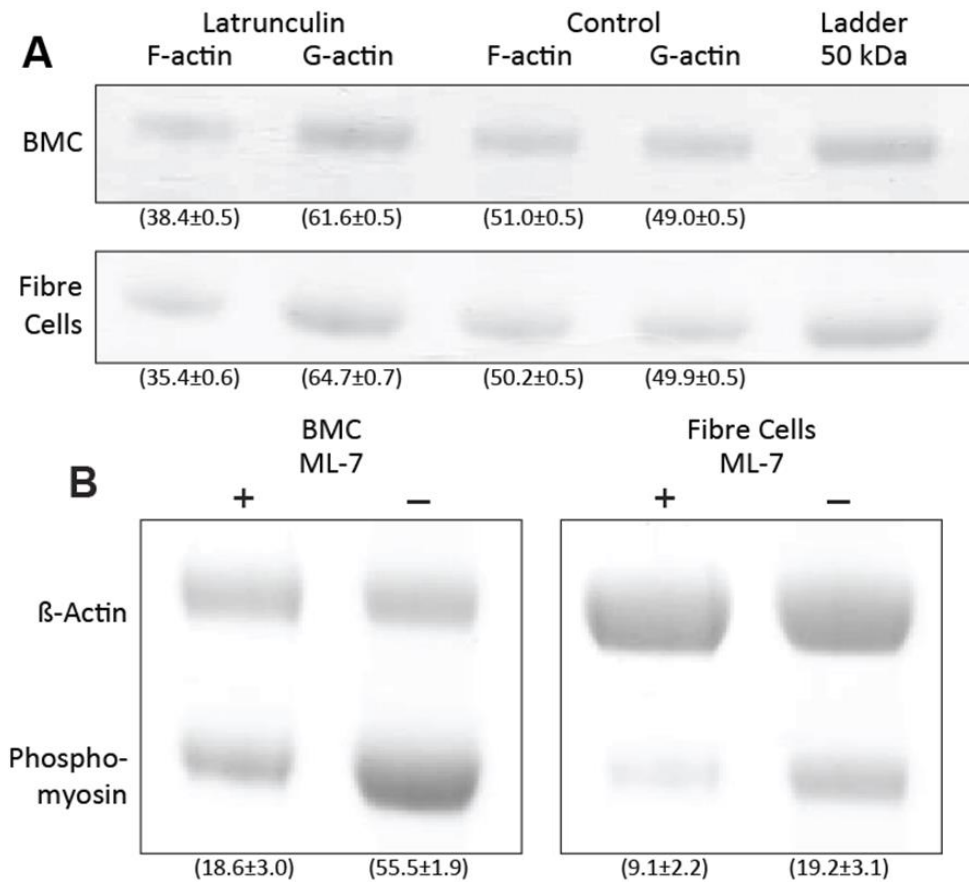
Figure III-5: Effects of disruptors on protein concentrations in the lens. (A) Western blots of f- and g-actin in BMC and lens fiber cell samples treated with latrunculin. Numbers in parentheses represent the mean percentage optical density (±SEM) relative to the total amount of actin. (B) Western blots of phosphomyosin in BMC and lens fiber cell samples treated with ML-7 (+) and vehicle (-). Numbers in parentheses represent the mean optical densities (±SEM). β-actin was used as the loading control.

73

disrupting actin levels and myosin phosphorylation, respectively, at both the basal membrane complex (BMC) and the cortical lens fibres. Actin levels in latrunculin-treated lenses were quantified using a g-actin/f-actin in vivo assay kit, which revealed a large decrease in f-actin at both the BMC and in the lens fibre cells as a result of lens tissue treatment. In BMC samples treated with latrunculin, the mean intensity ($\pm$ SEM) of f-actin was 12.0 ± 1.2, while the mean intensity of g-actin was 19.3 ± 1.9, representing $38.4 \pm 0.5\%$ and $61.6 \pm 0.5\%$ of the total actin amount, respectively, indicating substantial depolymerization of f-actin as a result of latrunculin treatment (Fig. III-5A). In comparison, control samples showed a ratio of approximately 1:1, with mean intensities of f- and g-actin at 14.2 ± 1.4 and 13.7 ± 1.4, representing $51.0 \pm 0.5\%$ and $49.0 \pm 0.5\%$ of the total actin amount, respectively. In cortical fibre samples treated with latrunculin, the mean intensity ($\pm$ SEM) of f-actin was 10.0 ± 1.55, while the mean intensity of g-actin was 18.3 ± 1.9, representing $35.4 \pm 0.55\%$ and $64.7 \pm 0.7\%$ of the total actin amount, respectively (Fig. III-5B). In comparison, control samples again showed a ratio of approximately 1:1, with mean intensities of f- and g-actin at 13.4 ± 1.3 and 13.3 ± 1.2, representing $50.2 \pm 0.5\%$ and $49.9 \pm 0.5\%$ of the total actin amount, respectively. The relative intensities of phospho-myosin were lower in both BMC (by 21.1%) and lens fibre cell (by 15.6%) samples when treated with ML-7 (Fig. III-5C, 5D, respectively), indicating ML-7-dependent inhibition of myosin phosphorylation.

Confocal images indicated that latrunculin led to rearrangement and thinning of the actin cables at the basal membrane (Fig. III-6). Actin in the latrunculin-treated lenses appeared different from vehicle-treated lenses, which showed the typical punctate staining of the highly regular hexagonal vertices. Additionally, myosin bundles localized at the centre of the actin formations appeared more variable in size and neighbouring distance. Nearest neighbour analysis indicated a significant increase in the disorder of the myosin associated with the actin lattice (R_n for treated
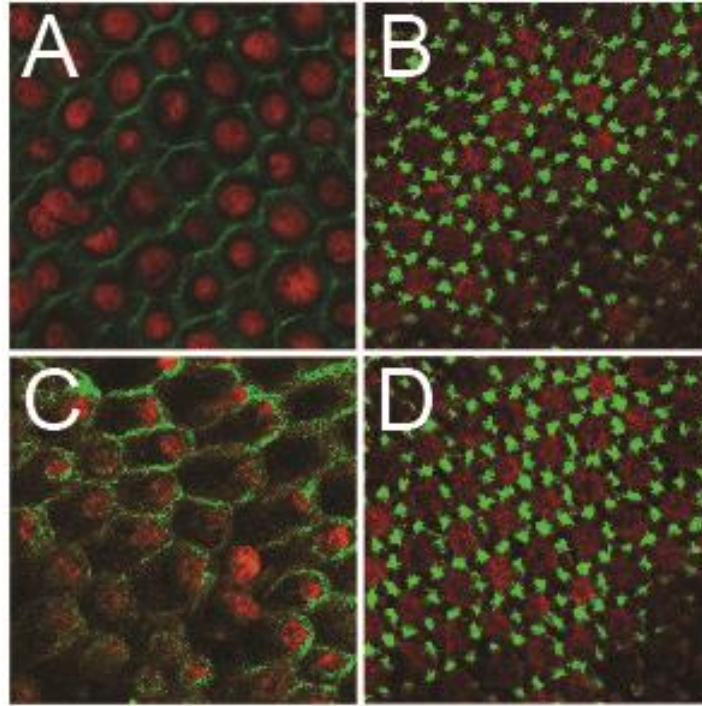
Figure III-6: Effects of disruptors on actin and myosin distributions in the lens.
Confocal images of posterior lens capsules showing the distribution of actin (green) and myosin (red) in a (A) latrunculin-treated lens and (B) its vehicle-treated counterpart, as well as a (C) blebbistatin-treated lens and (D) its vehicle-treated counterpart. Scale bar = 5 µm for all images. R_n values for actin (R_{na}, green) and myosin (R_{nm}, red) distributions are included.

lenses: 1.75 ± 0.02 vs. R_n for control lenses: 2.06 ± 0.05; p=0.0025). The actin distribution in lenses

treated with latrunculin had an R_n ($\pm$ SEM) of 1.83 ± 0.05, while its vehicle counterpart had an R_n of

2.09 ± 0.05, indicating a small increase in f-actin disorder (Fig. III-6A and B), although these

changes were not significant (p = 0.0593). Both actin and myosin organization were adversely

affected by blebbistatin. The myosin distributions in lenses treated with blebbistatin were even less

ordered than those observed in latrunculin-treated lenses, and treated lenses showed an even lower

R_n of 1.58 ± 0.08, while its vehicle counterpart had an R_n of 2.05 ± 0.03 (p=0.0183, Fig. III-6C and

D). The actin distribution was also affected; blebbistatin-treated lenses lost the regular repeating

arrays of punctate staining and the R_n of 1.52 ± 0.02 in these lenses was significantly different from

75

that of control lenses, at an R_n of 2.00 ± 0.005 (p=0.0183), indicating a large increase in disorder.

Despite the rearrangement of the cytoskeletal proteins at the BMC, the optical quality of disruptor-treated lenses, assessed using two criteria, scatter and spherical aberration (Table III-1), were unaffected; none of the disruptor-treated lenses showed a difference in the amounts of scatter compared to its respective control nor did any disruptor treatments result in differences in the amount of spherical aberration.

Table III-1: Mean spherical aberration (D) ± SEM and mean scatter (mm) ± SEM for latrunculin-, blebbistatin-, and ML-7-treated lenses and their controls.

Disruptor	Spherical aberration (D)			Scatter (Mean deviation; mm)		
	Treated	Control	p-value	Treated	Control	p-value
Latrunculin	-11.80±0.50	-11.57±0.48	0.6093	1.15 ± 0.03	1.15 ± 0.04	0.9858
Blebbistatin	-11.62±0.31	-11.59±0.26	0.9212	1.19 ± 0.07	1.14 ± 0.02	0.4696
ML-7	-11.94±0.69	-12.44±0.78	0.2245	1.15 ± 0.03	1.13 ± 0.05	0.7526

In the longitudinal (reversibility) compression trials, it was found that lenses treated with latrunculin took the longest to recover, showing significant differences in stiffness up until the four-hour mark, (mean stiffness ± SEM at 4 hours: control lenses, 6.17 ± 0.43 vs. treated lenses, 4.98 ± 0.56; p=0.0730; Fig. III-7A). Lenses treated with blebbistatin were found to have a recovery time of 1 hour (mean stiffness at 1 hour: control lenses, 5.37 ± 0.19 vs. treated lenses, 5.27 ± 0.51; p=1.000; Fig. III-7B). Lenses treated with ML-7 had the quickest recovery time at 8 minutes (mean stiffness at 8 minutes: control lenses, 6.02 ± 0.36 vs. treated lenses, 5.17 ± 0.40; p=1.000; Fig III-7C).
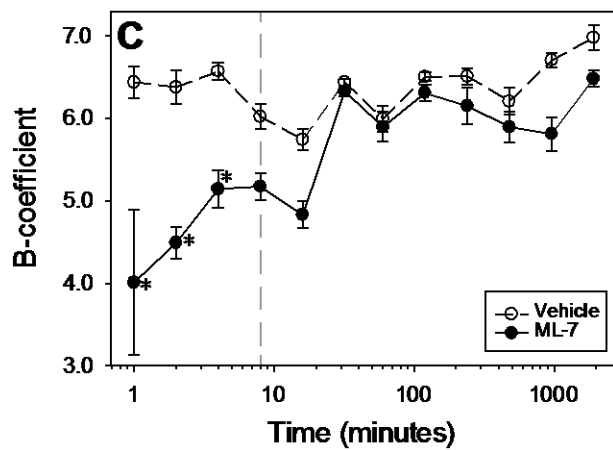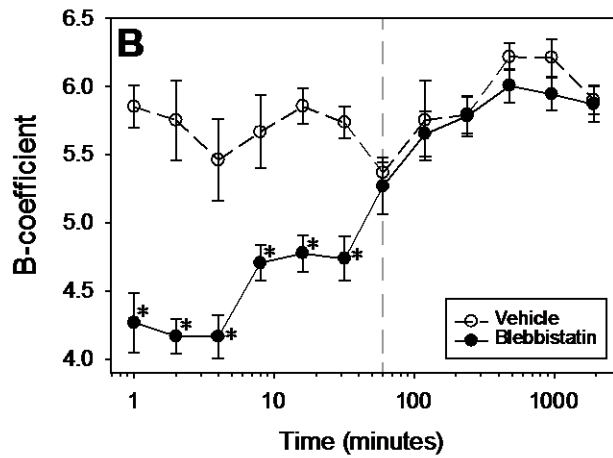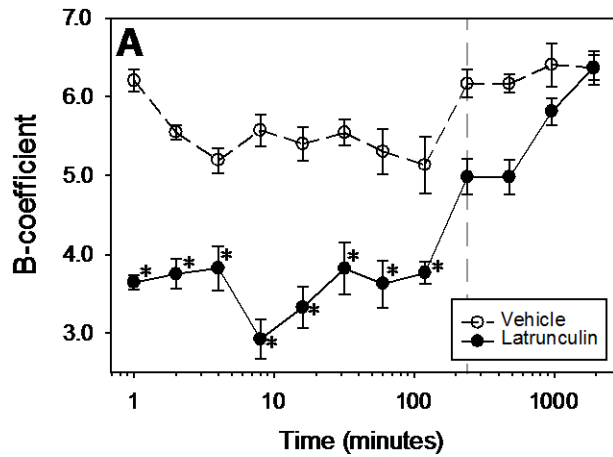
Figure III-7: Time course of lenticular stiffness following disruptor removal. Longitudinal recovery effects of (A) 10 μM latrunculin (n = 6), (B) 10 μM blebbistatin (n = 6), and (C) 10 μM ML-7 (n = 6) on lens stiffness compared to vehicle controls. Asterisks (*) indicate significant differences between disruptor- and vehicle-treated lenses.

77

3.5 DISCUSSION

The compression trials showed that treatment with actomyosin disruptors results in significant changes in the distributions of actin and myosin and significant decreases in the stiffness of the whole lens. While it is possible that other mechanisms were responsible for lens softening, the simplest explanation is that the decrease in stiffness was a direct result of the changes to the structure of the actomyosin lattice wrought by the disruptors.

Responses were reversible for all three disruptors, but the kinetics of recovery differed. Latrunculin-treated lenses recovered the slowest, perhaps due to the ubiquitous presence of actin microfilaments, found not only at the lens capsule and BMC, but also within the lens cortex and nucleus, the latter two of which form the bulk of the lens (Ireland et al., 1983). More actin would presumably require more time to reassemble. Although optimal assembly conditions for actin and myosin differ, it should be noted that, at least theoretically, actin has a slower association rate than that of myosin II, with the elongation rates of actin filaments of 11.6 ± 1.2 x 10-6 M-1s-1 at the barbed ends and 1.3 ± 0.2 x 10-6 M-1s-1 at the pointed ends (Pollard, 1986) compared that for myosin II at ≥ 2.0 x 108 M-1s-1 (Sinard & Pollard, 1990). It is most likely that, blebbistatin and ML-7-treated lenses were much faster in their recovery times because these disruptors do not physically segregate the target protein into its monomeric components. Instead, the myosin disruptors act by preventing phosphorylation and competitively binding to key structures in the actomyosin cascade, a process that is presumably easier and quicker to reverse (Kovacs, 2004; Kuhn & Pollard, 2005).

It should be noted that preliminary trials in which acute treatment of lenses with a higher concentration of ML-7 (100 µM) resulted in lens stiffening, with 4 of 16 lenses physically bursting

during force-compression trials (data not shown). Stiffening as a result of high concentrations of ML-7 could be due to a biphasic dose response of the MLCK-inhibitor. Indeed, in the case of cell spreading, another process mediated by dynamics of the actomyosin network, ML-7 had opposite effects in COS7 carcinoma cells when its dose was increased by a factor of five (Takizawa, Ikebe, Ikebe, & Luna, 2007). Moreover, results of two-dimensional gel electrophoresis of 100 μM ML-7-treated posterior lens capsule tissues suggests increases in protein phosphorylation compared to a samples treated with10 μM ML-7 (data not shown).

In a related study on lens shape changes by Luck and Choh (2010), low and high concentrations of ML-7 resulted in longer and shorter avian lens focal lengths, respectively. Although the directionality of 10 and 100 μM changes is in agreement with the stiffening observed in our experiment, we did not observe any focal length changes with these two ML-7 concentrations. One difference may be that Luck and Choh conducted the optical trials on lenses in situ, where the lens was still in its accommodative apparatus, while we conducted our optical trials on lenses in vitro, i.e., on lenses that had been extracted from its surrounding tissue. In our experiments, lenses may have "rounded up", a phenomenon that has been described before for lenses separated from their surrounding anatomy (Glasser, Murphy, Troilo, & Howland, 1995). This idea seems to be supported by the average focal length of our vehicle treated lenses (14.1 ± 0.2 mm; data not shown), which was shorter and therefore more powerful than the vehicle-treated lenses in Luck and Choh's study (19.6 mm). It is possible that, in our experiment, lenses were maximally rounded and therefore any further release of tension associated with the actin-myosin network would be too small to detect.

Indications that cytoskeletal proteins might play a role in lenticular biomechanics were noted by Rafferty et al. (1994), who showed that increasing intracellular calcium levels in rabbit anterior

epithelial cells in the lens resulted in changes in actin stress fibre distributions. Although the concentration of myosin is generally lower than actin in contractile networks, such as that found in lens epithelial cells (Rafferty et al., 1990), it is nonetheless crucial for structural integrity. Two of the disruptors used targeted myosin or myosin function and both were able to exert effects that were similar to that exerted by the actin disruptor. However, it should also be noted that cytoskeletal integrity is not limited to the actomyosin system; intermediate filaments and microtubules also play a role in maintaining cellular architecture (Quinlan et al., 1999b). Lenses from mice in which a gene for beaded filaments, which belong to the intermediate filament gene family, is knocked out, are less stiff than those from wild-type mice (Fudge et al., 2011). Our results add to the growing body of evidence showing the importance of cytoskeletal protein integrity to lenticular biomechanics. While studies by Fudge (2011) and the present study examined how disrupting cytoskeletal integrity affects the biomechanics of the lens as a whole, a previous study investigated their effects on lenticular cells individually. Unlike our results, Hozic and colleagues (2012) showed no difference in the stiffness of the individual lenticular cells with cytochalasin, an actin disruptor. The difference between the present study and that of Hozic and colleagues (2012) may be related to the disruptor used (latrunculin vs. cytochalasin B); cytochalasin works by inhibiting actin polymerization, essentially preventing the formation of actin networks (blocks monomer addition) while latrunculin depolymerizes f-actin.

In both the acute and longitudinal compression trials, lenses were kept in Tyrode's solution in temperatures upwards of 5°C in order to retard cell metabolism and prevent the tissue from degrading, particularly for the longitudinal trials that required ex vivo viability for upwards of 32 hours. It should be noted that lenses in situ would be closer to body temperature (Al-Ghadyan & Cotlier, 1986) and, moreover, that cold temperatures could promote depolymerization of actin

microfilaments. Hall et al. (1996; 1994) showed that cells exposed to a temperature of 4°C for 2-4 hours exhibit a marked thinning of actin filaments. However, Matthews et al (2005) found no effects of these conditions on actin structure. Our lenses were exposed to a minimum of 5°C for a maximum of 15 minutes, and thus cold-induced depolymerization of f-actin should have been minimal. Furthermore, any cold-induced depolymerization was accounted for by our control lenses, which experienced identical conditions aside from the disruptor treatment.

The confocal imaging and Western blots together indicate that the disruptors penetrated the lens at a deep enough level to affect the cytoskeletal distribution at the BMC in addition to the lens fibre cells. Given that confocal images were acquired between 12-13 µm below the lens capsule, it is known that the depth of disruptor penetration is at least to this extent. It is unclear how deeply the disruptors penetrate the lens, and whether they diffuse uniformly throughout the lens, however, it is sure to be different as a disparity between the diffusion patterns at the surface of the lens compared to the lens core syncytium exists and has been shown by Shestapolov and Bassnett (2000, 2003).

While f-actin depolymerization was an expected outcome of latrunculin treatment, myosin organization was also affected (Fig. 6A). It has been proposed that in order for myosin II to remain in the cytoskeleton, it must be bound to stable actin (Kolega & Kumar, 1999). Similarly, blebbistatin also appears to enhance depolymerization of f-actin (Fig. 6C). Blebbistatin is known to disassemble actin (Martens & Radmacher, 2008), presumably by reducing myosin activity and therefore actin cross-linkings. Although ML-7 affects phosphorylation and therefore the ability of actin and myosin to interact, it would not be expected to physically alter the architecture of the actomyosin network, which was indeed the case (ML-7-treated R_n = 2.02±0.02 vs. vehicle-treated R_n=2.01 ± 0.02; data not shown).

Our results showed that despite the cytoskeletal distribution changes at the BMC and the

81

measured changes in stiffness, the optics of the isolated lenses was unaffected by the disruptors (Table 1) and during the acute study trials, it was noted that lenses maintained transparency (note clarity of the lens in Fig. 2). Either the disruption at the BMC was too small to confer a change in spherical aberration and scatter, or the regular arrangement and tight packing of the lens fibre cells rendered any disruption of the actomyosin distributions negligible. However, while lenses were clear during the acute experiment, the long-term effects of disruptors on lenticular transparency remain unknown; qualitative assessment of the lenses indicated that incubation with disruptors for about an hour resulted in turbidity and development of cataracts (data not shown). Whether turbid lenses can recover optical clarity also remains unknown, therefore, the use of cytoskeletal disruptors as permanent effectors for changing lens biomechanics must take into account other possible effects on functions such as optical clarity.

Other questions that need to be answered include whether these disruptors can be as effective on older lenses. As mentioned above, the focus of this experiment was to determine whether disruption of the actomyosin lattice could alter lenticular biomechanics, and for experimental convenience we used young chicks. While it is tempting to relate our results to presbyopia, which is accompanied by profound increases in lenticular stiffness with age (refs), further investigation will require the use of older experimental animals.

We have found that by targeting the cytoskeletal proteins that are known to have structural roles in cells, lenses become less stiff, but whether the lens plays more than a passive role during accommodation remains unclear. The physiology and cellular arrangement of the lens are mostly dedicated to maintaining optical clarity, by ordering the fibre cells into a regular arrangement, and reducing the intercellular spaces between them, so that light is less scattered. The hexagonal shape conferred upon the lens fibre cells fulfils both of these functions and therefore the finding that a

geodesic hexagonal network is present at the posterior surface may simply reflect the shape of the highly organized fibres cells and function to resist deformations that could disrupt this organization.

In summary, we found that disruption of actomyosin networks in young avian lenses causes significant decreases in the stiffness of isolated lenses, but no differences in their optical properties. These results are consistent with the hypothesis that lens stiffness may be actively tuned via adjustments to the actomyosin networks in lens cells. The lack of an effect on lens optical properties may have been due to a "rounding up" artefact caused by isolation of the lens from the eye.

IV. DEVELOPING AN ANTIBODY-DRUG CONJUGATE TO SPECIFICALLY TARGET AND SOFTEN THE CRYSTALLINE LENS *IN VIVO*

4.1 OVERVIEW

Purpose: The purpose of this study was to synthesize a novel drug delivery platform designed to specifically target and soften the lens. Given that blebbistatin, a selective myosin II inhibitor, was shown to be able to soften the crystalline lens by disrupting the lenticular cytoskeletal network, a lens-specific antibody was hybridized to blebbistatin to form b-AQP0Fab. Validation of b-AQP0Fab and its *in vitro* effects on various ocular tissues were also investigated.

Methods: Blebbistatin was hybridized to a fragmented (Fab) custom anti-AQP0 antibody via a labile crosslinker to produce b-AQP0Fab, an antibody-drug conjugate. Successful hybridization of b-AQP0Fab was verified by non-denaturing polyacrylamide gel electrophoresis (PAGE), and its binding capacity was assessed by direct enzyme-linked immunoabsorbant assay (ELISA). The effects of b-AQP0Fab on myosin II levels of various intraocular tissues were assessed by Western blot analysis.

Results: SDS-PAGE indicated a successful hybridization of blebbistatin to anti-AQP0 using a PDPH crosslinker when compared to unconjugated anti-AQP0. Additionally, direct ELISA analysis indicated that b-AQP0Fab retained its binding strength to AQP0. Western blot analysis demonstrates that, despite treatment of global intraocular structures, only lenticular tissue exhibited a change in myosin II activity.

Conclusion: b-AQP0Fab was synthesized successfully and shows specificity towards lenticular aquaporin-0. Additionally, extra-lenticular tissues were not affected by b-AQP0Fab. Further studies should be conducted to investigate the *in vivo* specificity of b-AQP0Fab and its effects on the accommodative mechanism in the eye.

4.2 INTRODUCTION

In 1900, Paul Ehrlich, a German physician and Nobel laureate, proposed that "if a compound could be made that selectively targeted a disease-causing organism, then a toxin for that organism could be delivered with the agent of selectivity" – he would eventually coin the term *magische kugel* or "magic bullet" for this idea (Ehrlich & Herter, 1904). In essence, the magic bullet is a targeted drug delivery theory that has: (1) a selective component that can specifically recognize a target, and (2) a pharmaceutical payload to treat the target. The advantage of this delivery system is that it increases the specificity and efficacy of a drug to diseased or pathogenic tissues, while exhibiting low or no toxicity on healthy tissues in the body.

There are currently three categories of targeting drug delivery systems: (1) physical targeting, which localizes agents to target areas by using their biophysical characteristics, such as size and composition, (2) chemical targeting, which localizes agents to target areas using prodrugs, enzyme, or chemical reactions, and (3) biological targeting, which allows localized agents to target areas through antibodies, peptides, or any other molecules that have an affinity towards receptors, tissues, or organs (Mills & Needham, 1999).

Due to their remarkable specificity, antibodies have received the most attention and have the greatest potential to realize Ehrlich's proposal of a magic bullet. Recently, with the development of extraction, isolation, and engineering procedures for monoclonal antibodies, biological targeting, particularly against cancerous tissue, has seen rapid increases in research and development (Troy, 2015). One targeting therapy in particular takes advantage of the site-specific binding properties of antibodies to localize the delivery of a therapeutic agent using an antibody-drug conjugate (ADC) (Zolot, Basu, & Million, 2013); ADCs delivers biological payloads attached to monoclonal

antibodies in order to specifically target and destroy tumours without affecting healthy tissues. At present, there are only two ADCs approved by the U.S. Food and Drug Administration (FDA): Trastuzumab emtansine (Kadcyla®) and Brentuximab vedotin (Adcetris®) (Sassoon & Blanc, 2013). Trastuzumab emtansine arrests the growth of cancer cells by binding to tumour-specific HER2/neu receptors and delivering emtansine (DM1), a tubulin inhibitor. Brentuximab vedotin functions by binding specifically to CD30 proteins found specifically in Hodgkin's and systemic anaplastic large cell lymphomas, and delivers a dosage of Monomethyl auristatin E (MMAE), an anti-mitotic agent, that inhibits cell division by block the polymerization of tubulin. Although there are only two ADCs on the market, there are currently over 40 new ADCs in clinical development (Donaghy, 2016; Schumacher, Hackenberger, Leonhardt, & Helma, 2016). None of these ADCs, however, are designed to treat the eye.

Presbyopia is an age-related deterioration of the eye's ability to focus on nearby objects. It is believed that the predominant physiological mechanism by which presbyopia occurs is by a loss of elasticity in the crystalline lens of the eye, and as a result, the eye is unable to increase in dioptric power (Beers & Van der Heijde, 1996; Glasser & Campbell, 1998). The current solutions to presbyopia only serve to manage its symptoms and do not cure the physiological cause, primarily because restoring elasticity to the lens has several complications; the various factors contributing to lens elasticity are not completely understood (Strenk et al., 2005), and few attempts have been made to investigate biological agents capable of restoring lens elasticity. Additionally, the lens is an internal structure, and studying the mechanical properties of the isolated lens has serious limitations; post-mortem changes, artefactual deformation, and application of non-physiological forces all contribute to discrepancies between *in vivo* and *in vitro* lens traits (Strenk et al., 2005). However, developing an antibody-drug conjugate capable of specifically targeting and softening the crystalline

86

lens would allow for the treatment of the physiological cause of presbyopia. The ADC would require three components (Fig. IV-1): (1) an antibody capable of recognizing an antigen unique to the crystalline lens, (2) a cytotoxic agent or drug capable of softening the crystalline lens, and (3) a crosslinker with the appropriate functional groups to attach the antibody with the cytotoxic agent.
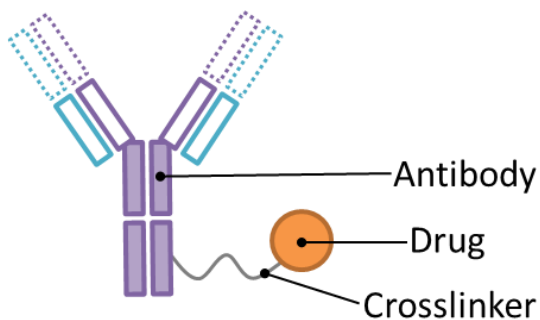
Figure IV-1: Schematic representation of an antibody-drug conjugate. The antibody (purple) is attached to the drug (orange) via a crosslinker (grey line).

As the targeting mechanism of ADCs is dependent on the antigen-binding site of the antibody component, the antibody component can be engineered to target any protein or peptide sequence, provided that the sequence of the amino acids is known. Because the crystalline lens contains several unique proteins that are not found elsewhere in the human body, the principle of the ADC and its targeting mechanism can be applied to the crystalline lens within the eye. AQP0 is a transmembrane water channel found uniquely in the lens that is expressed prolifically in fibre cell membranes (Broekhuyse, Kuhlmann, & Winkens, 1979; Chepelinsky, 2003; Goodenough, 1979). Although it was initially demonstrated that AQP0 had weaker water permeation than those observed in other aquaporins, it was later discovered that under low pH conditions, such as that within the lens, a drastic increase in water channel activity was observed (Németh-Cahalan, Kalman, & Hall, 2004). For this reason in addition to its prolific expression within fibre cell membranes, it was speculated that AQP0 could provide anchors for cytoskeletal structures, such as beaded filaments, to

confer fibre cell shape, architecture, and integrity (Sindhu Kumari et al., 2015). The extracellular portion of AQP0 is therefore an ideal antigen site for an antibody-drug conjugate to target. The selection of peptide sequences found on AQP0 to which an antibody should be conjugated against requires careful consideration to increase the chances of an immune reaction. Several factors that increase antigen binding strength include: longer amino acid chains, appropriate three-dimensional conformations, and increased hydrophilicity of peptide sequences. The total size of the ADC, to which the antibody carrying the specific peptide sequence is conjugated, may also play a role in antigen affinity, as the limited pore size of the lens capsule restricts transit of larger molecules. The lens capsule has, however, been observed to diffuse positively charged molecules and neutral dextrans, of up to 147.8 kDa in size, quite quickly (Lee et al., 2006). Furthermore, proteins of similar molecular weight carrying a net negative charge have also been observed to pass through the lens capsule, although, at a much slower rate (Danysh, Czymmek, Olurin, Sivak, & Duncan, 2008), indicating that ADCs of approximately 150 kDa in size should pass through the lens capsule.

Antibodies can, however, be cleaved into various components using fragmentation kits. A standard immunoglobulin G (IgG) antibody consists of two light chains and two heavy chains which, together, form the Y-shaped structure. On each antibody, two variable domains exist, and are responsible for recognizing antigenic peptide sequences. The tail of the body is known as the constant domain and functions to recruit secondary immune responses, which may not be necessary in certain applications. A pepsin digestion kit can be used to separate the constant domain from the body in order to form an $F(ab')_2$ fragment. Further digestion of $F(ab')_2$ with β-mercaptoethanol cleaves the molecule in half, resulting in an $F(ab')$ fragment. In cases where the disulphide bond in $F(ab')$ are not required, a papain digestion kit may be used to produce an $F(ab)$ fragment, despite its smaller size, stills consists of the variable domain capable of binding to antigenic peptide sequences

88

(Fig. IV-2).
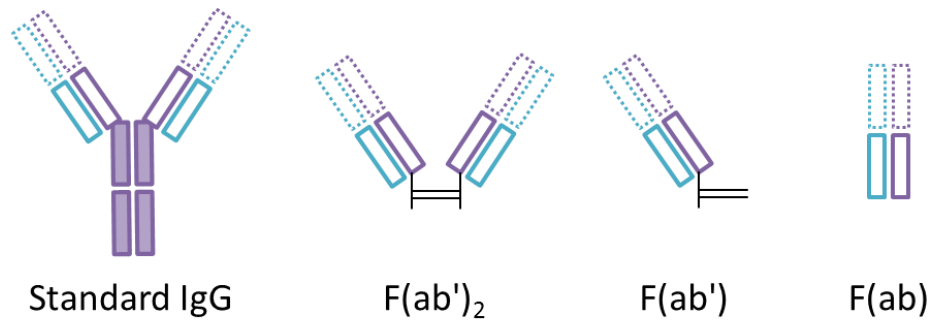
Figure IV-2: Schematic representation of a standard IgG antibody along with the various fragments that it may be cleaved into using appropriate digestion kits. The standard IgG antibody consists of 2 light chains (blue outlines), and 2 heavy chains (purple outlines). The antigen recognition sites occur at the tips of each variable domain (dotted outlines) of the antigen binding regions (empty squares). The tail of the IgG is known as the constant region (filled squares).

It was previously demonstrated that treatment of the crystalline lens using several cytoskeletal inhibitors (latrunculin, blebbistatin, and ML-7) to disrupt the lenticular actomyosin network causes the lens to soften as a whole (Won, Fudge, & Choh, 2015) (Chapter III). Moreover, treated lenses did not show changes in light scatter or spherical aberration, and were not found to develop any form of turbidity or cataracts, indicating that these inhibitors could potentially be used to treat lenses that have lost their elasticity. The chemical structures of these inhibitors will therefore be examined to determine the best candidate for hybridization; ideal characteristics include: accessibility, appropriate and reactive functional groups, small molecule size, and attenuated functionality while hybridized. It should be noted that only limited types of crosslinkers are commercially available, and therefore, only certain functional groups are compatible. Additionally, certain crosslinkers are labile, allowing the release of the hybridized payload under appropriate physiological conditions, a characteristic that can be taken advantage of in order to increase ADC specificity.

The purpose of this study was to identify an ideal antigen binding site, crosslinker, and biological agent to successfully develop an antibody-drug conjugate that is able to target and soften the avian crystalline lens *in vivo*.

4.3 MATERIALS

4.3.1 SELECTION OF PEPTIDE SEQUENCE FOR ANTI-PEPTIDE CONJUGATION:

Several factors were considered to determine the optimal peptide sequence for anti-peptide conjugation in order to elicit an appropriate antigenic response; (1) peptide amino acid composition, (2) peptide length, (3) peptide solubility, and (4) peptide secondary structure. In brief, the peptide sequence should contain amino acids that are found on the surface of the native protein with both hydrophobic and hydrophilic residues (Lee et al., 2010). Longer peptide sequences are harder to synthesize and purify, however, they generally result in better antigenic responses (Lee et al., 2010). The major caveat for lengthy peptide sequences is the formation of incompatible secondary structures that reduce antigenicity. Finally, the hydrophobicity of each individual amino acid heavily influences the solubility of the peptide sequence, and should be kept below 50% (Hopp & Woods, 1981).

Chicken AQP0 (Uniprot ID P28238, NCBI 989597) was determined to exist solely within the crystalline lens using the basic local alignment search tool (BLAST). Interestingly, BLAST analysis of protein alignment revealed a 68.4% similarity with AQP0 in the Mississippi alligator lens, a 65.4% similarity with AQP0 in yak and cattle, and a 65% similarity with AQP0 in sheep. Chicken AQP0 was further characterized using the Genscript® antigen profiler to determine optimal peptide

sequences (PSs) for targeting purposes. Based on the topology of AQP0 (Fig. IV-3), three external peptide sequences of the transmembrane water channel are exposed for possible binding: (1) RWAPGP (PS01; 033-038), (2) TPAAVRGTLGLSALHPSVG (PS02; 108-126), (3) TRNFTN (PS03; 195-200).
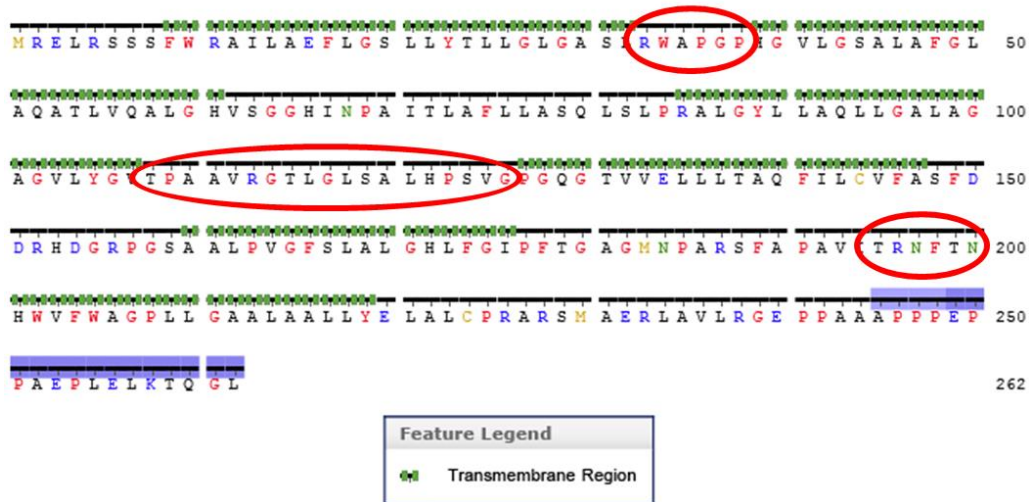
Figure IV-3: Schematic representation of the AQP0 peptide sequence. External sequences of interest circled in red. Transmembrane regions are denoted with green squares, and the first sequence (1-8) occurs interiorly.

Optimal sequences were further screened using the ThermoFisher® peptide synthesis and proteotypic peptide analyzing tool in order to determine the best candidates for antigenic response. The characteristics of interest in peptide sequences include: sequence length, hydrophobicity, grand average of hydropathicity (GRAVY), average molecular weight, and monoisotopic molecular weight (results summarized in Table IV-1).

As longer, higher molecular weight peptide sequences are generally considered more likely to specifically attach antigenic sites, PS02 (TPAAVRGTLGLSALHPSVG) was selected for antibody conjugation (Frahm et al., 2004). Additionally, PS02 only contains one of the unstable amino acids (C, M, W, N, P, D and Q, E at N-termimus) that can cause side reactions during

91

Table IV-1: Summary of PS01, PS02, and PS03 peptide characteristics

	PS01: RWAPGP	**PS02**: TPAAVR…	**PS03**: TRNFTN
Sequence Length	6	19	6
Hydrophobicity	13.61	33.02	7.79
GRAVY	-1.200	0.532	-1.683
Average MW	682.7863 g/mol	1804.0963 g/mol	751.8043 g/mol
Monoisotopic MW	682.3551	1803.0004	751.3613

immunization and thereby alter the purity of the end product. PS02 is also moderately hydrophobic (Fig. IV-4, green line in blue box), and so is compatible for antibody conjugation. Of the two shorter chains, PS01 (RWAPGP) is more hydrophobic, however, it is not a sequence unique to chicken biology, and contains several unstable amino acids. Alternatively, PS03 (TRNFTN) is unique to the chicken lens, but it is the least hydrophobic (Fig. IV-4, green line in orange box) of the three sequences, and contains several unstable amino acids. It has, however, been shown that unstable amino acids are less problematic for conjugation of short-chain amino acids. For these reasons, PS03 was also selected for antibody conjugation.

Anti-AQP0-peptide synthesis and validation was conducted by Cedarlane labs using a standard 2-rabbit (New Zealand White) 70-day immunization protocol. In brief, TRNFTN and TPAAVRGTLGLSALHPSVG peptide sequences, conjugated to keyhole limpet hemocyanin to boost immune response, were synthesized prior to immunization. On day 0, approximately 5 mL of control serum was collected per rabbit. On day 1, each rabbit was immunized with 0.50 mg of either TPAAVRGTLGLSALHPSVG or TRNFTN in Complete Freund's Adjuvant (CFA). On days 14 and 28, both rabbits received a booster shot with 0.25 mg of the appropriate peptide antigen in Incomplete Freund's Adjuvant (IFA). On day 35, approximately 25 mL of serum was collected per
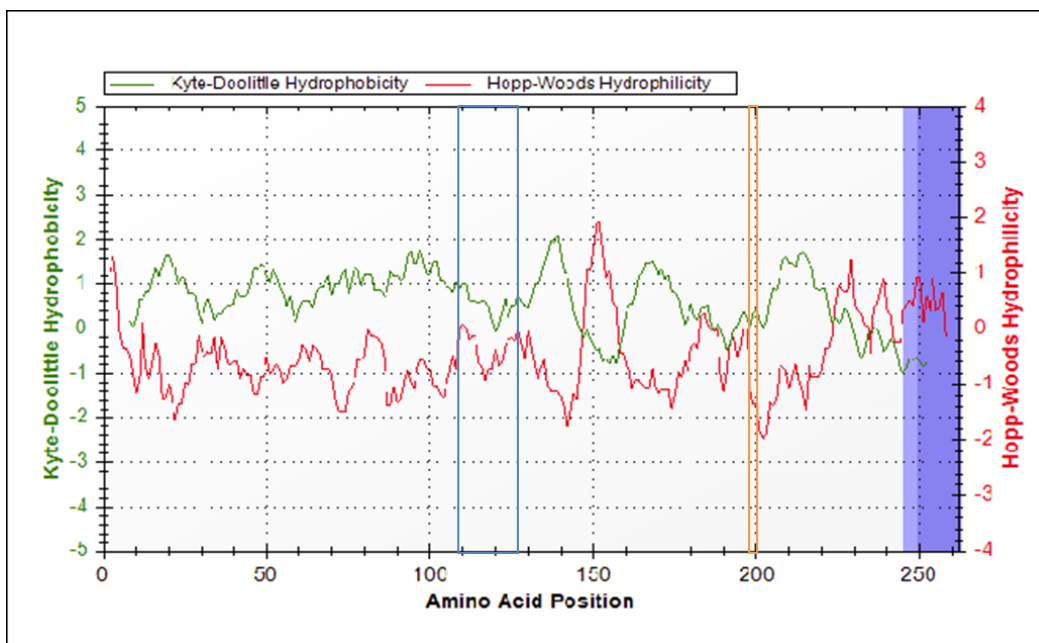
Figure IV-4: Hydrophobicity (green line) and hydrophilicity (red line) chart of the entire AQP0 peptide sequence. PS02 sequence located within blue bars, PS03 sequence located within orange bars.

rabbit. On day 42, a third booster shot, identical to previous boosts, was given to each rabbit. On days 56 and 58, approximately 50 mL of serum was collected per rabbit. On day 60, ELISA titrations were conducted, and rabbits were euthanized.

4.3.2 SELECTION OF BIOLOGICAL PAYLOAD

Of the three cytoskeletal inhibitors (latrunculin A, blebbistatin, and ML-7) that were shown to soften the lens (Won et al., 2015), only blebbistatin was selected. Although latrunculin A has an array of ketones, amines, and alcohol groups to use as reactive groups for crosslinking, the three-dimensional structure and large size of the molecule are detrimental to conjugation with a crosslinker. Additionally, the numerous reactive groups present could form various isomers that would require purification and individual analysis of functionality, rendering the molecule more complicated to

use. In contrast, ML-7 has a small and simple chemical structure, however, its most reactive functional group, the sulphonamide, is relatively inert, and is nestled between a large aromatic and azocane ring, rendering it inaccessible. Due to its relatively simple chemical structure and effectiveness at softening the crystalline lens, blebbistatin was selected as the biological agent for ADC conjugation. The exposed carbonyl group on the piperidine ring provides easy access for binding with an aldehyde-reactive crosslinker chain. Furthermore, few isomers are likely to form as both reactive ends of the crosslinker chain do not favourably bind to the amine or hydroxyl groups of blebbistatin.

4.3.3 SELECTION OF CROSSLINKER

With the advent of antibody derived therapeutics, the understanding of reactive amino acids within antibodies became increasingly important. The most notable amino acid group occurring in IgG_1 antibodies are cysteine residues, as they are highly conserved throughout evolution, occur in abundance, and contain reactive sulfhydryl groups for chemical manipulation (Lee et al., 2010).. In its native state, the cysteine residues of IgG_1 are bridged to form cystine groups connected by a disulphide bond (Fig. IV-5). Reduction of cystine using thiols, such as β-mercaptoethanol or dithiothreitol (DTT) opens the disulphide bridge for chemical manipulation (Lee et al., 2010).
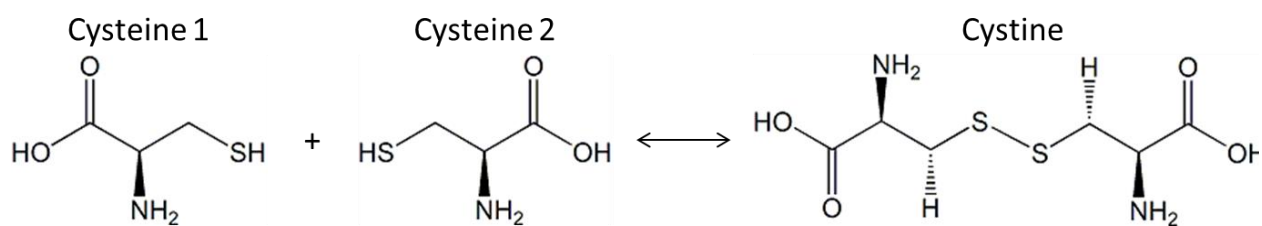
Figure IV-5: Schematic representation of cystine (disulphide bond) formation by two cysteine residues.

Within the IgG_1 molecule, 16 disulphide bonds are present (Fig. IV-6); 12 occur within chains (2 in each light chain, and 4 in each heavy chain), while 4 occur between chains (1 connecting each antigen binding region, and 2 connecting the constant region) (Lee et al., 2010). It should be noted that interchain cysteine groups are rarely used for conjugation, as their reduction would result in cleavage of the antibody, and an ultimate loss of antibody function (Bjork & Tanford, 1971; Burton, 1985; Chan & Cathou, 1977). Fortunately, it has been demonstrated that under mild reduction conditions, interchain bridges of IgG structures remain intact but intrachain disulphide bonds reduce to allow for conjugation (Schroeder, Tankersley, & Lundblad, 1981; Willner et al., 1993). Studies on individual domains without the complete intrachain disulphide bond have demonstrated lower stability and biological function (Harris, 2005; McAuley et al., 2008; Ouellette et al., 2010; Thies et al., 1999). Therefore, although it is theoretically possible to attach a total of 12 crosslinkers to a single IgG_1 antibody, a maximum of 6 attachments can be made without affecting
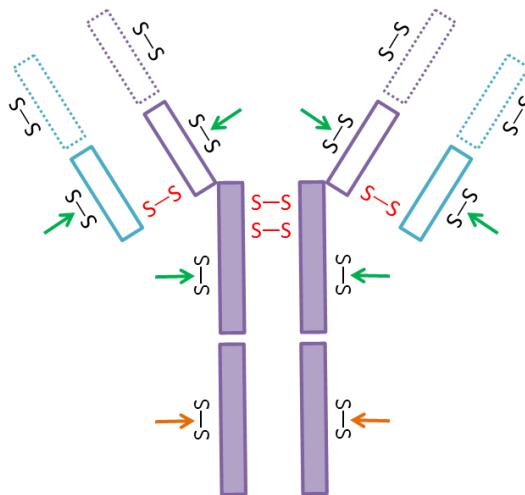
Figure IV-6: Schematic representation of disulfide bonds found in conventional IgG_1. Each IgG_1 contains 12 intrachain cysteine residues (black S-S), and 4 interchain cysteine residues (red S-S). Green arrows indicate disulfide bridges that may be used for conjugation without affecting antibody functionality. Orange arrows indicate disulfide bridges that may cause a loss of secondary immune response if used for conjugation.

antibody functionality (Lee et al., 2010). If the antibody conjugation is not required to elicit a secondary immune response from its constant region, a maximum of 8 attachments can be made.

In order to attach the reduced cysteine sulfhydryl groups of IgG antibodies to the carbonyl ketone on blebbistatin, a heterobifunctional crosslinker, which is a crosslinker with two different reactive ends, must be used. Of the non-cleavable crosslinkers reactive to sulfhydryl and carbonyl groups, three lengths were available: (1) N-β-maleimidopropionic acid hydrazide (BMPH, MW: 297.19, spacer arm: 8.1Å), (2) N-ε-maleimidocaproic acid hydrazide (EMCH, MW: 339.27, spacer arm: 11.8Å), and (3) N-κ-maleimidoundecanoic acid hydrazide (KMUH, MW: 409.40, spacer arm: 19.0Å). Because of its shorter spacer arm and lower molecular weight, BMPH (Fig. IV-7i) was selected to reduce the chance of homodimerization, and decrease the total weight of the final ADC product. Several options were available for labile crosslinkers reactive to sulfhydryl and carbonyl groups, however, only 3-(2-pyridyldithio)propionyl hydrazide (PDPH, MW: 229.32, spacer arm: 9.1Å, Fig. IV-7ii) contained a disulphide cleavage site that can potentially be cleaved by lenticular conditions.
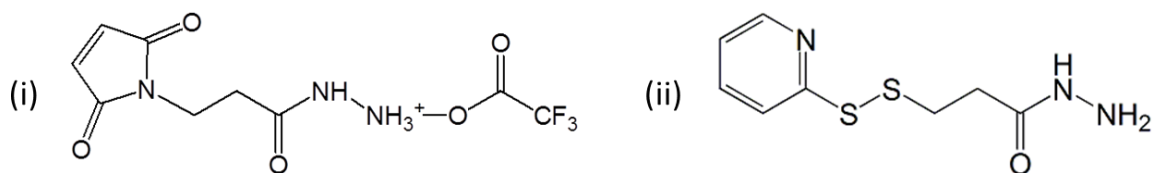
Figure IV-7: Chemical structures of (i) N-β-maleimidopropionic acid hydrazide (BMPH) and (ii) 3-(2-pyridyldithio)propionyl hydrazide (PDPH)

4.4 METHODS

4.4.1 SYNTHESIS OF ADC: b-AQP0ab

10 mM N-β-maleimidopropionic acid hydrazide (BMPH, crosslinker) solvent was prepared. A 5-fold molar excess of crosslinker reagent over protein was mixed with 1mg/mL DTT-reduced AQP0ab, and the reaction mixture was incubated for 2 hours at room temperature for 4 hours at 4°C (Reaction 1; Fig. IV-8). Samples were dialyzed overnight at room temperature against a coupling buffer (0.1M sodium phosphate, 0.15M NaCl, pH 7.2) to remove excess reagent and exchange crosslinker buffer. Crosslinker-modified sulhydryl proteins were mixed with blebbistatin in a 1:10 molar ratio, respectively (Reaction 2; Fig. IV-8). The reaction mixture was incubated for 2 hours at room temperature.
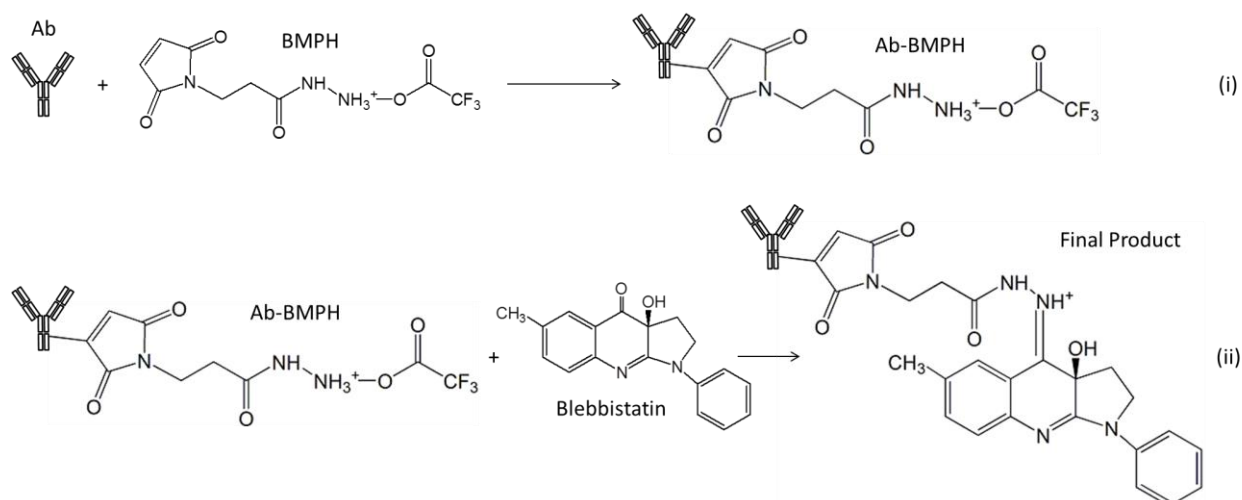
Figure IV-8: Schematic representation of the b-AQP0ab reaction mechanism. The conjugation reaction occurred in two steps: (1) attaching the AQP0 antibody (ab) to the BMPH crosslinker, and (2) attaching the product of reaction (i) to blebbistatin to form b-AQP0ab.

4.4.2 ANTIBODY FRAGMENTATION

Whole anti-peptide antibodies were fragmented using the Pierce Fab Preparation Kit (Thermo Scientific #44985). Immobilized papain was equilibrated by centrifuge at 5000 x *g* for 1 minute. The resulting resin was washed with 0.5 mL of digestion buffer, and centrifuged for 5000 x g for 1 minute. Anti-AQP0 samples were prepared by centrifugation in a Zeba Spin Desalting Column at 5000 x g for 2 minutes. Approximately 0.5 mL of 4 mg/mL IgG was collected. Fragments were generated by adding the anti-AQP0 sample to the spin column containing equilibrated immobilized papain. The digestion reaction was incubated for 7 hours (4 mg/mL rabbit IgG) on a tabletop rocker at 37°C, and centrifuged in a column at 5000 x g for 1 minute to separate digest from immobilized papain. The resulting resin was washed with 0.5 mL phosphate buffered saline (PBS), and centrifuged in a column at 5000 x *g* for 1 minute, and the fragmented anti-AQP0 (anti-AQP0Fab) was collected.

4.4.3 REFINEMENT OF ADC: b-AQP0Fab

11 mg of 3-[2-Pyridyldithio]propionyl hydrazide (PDPH) was dissolved in 1 mL of dimethylsulfoxide (DMSO) to produce 50 mM PDPH in crosslinker solvent. 0.5 mL of 8 mg/mL Fab was added to 0.5 mL of the 50 mM PDPH solution and incubated for 2 hours at room temperature (Reaction 3; Fig. IV-9). The Fab-PDPH mixture was purified using a size exclusion column (Superdex 75) to remove unbound PDPH, and dialyzed overnight against 0.1 M PBS (pH 7.4). 1 mL of the dialyzed Fab-PDPH sample was added to 1 mL of 0.05 M blebbistatin under sulfhydryl reducing conditions (5mM dithiothreitol) (Reaction 4; ; Fig. IV-9). The reaction mixture
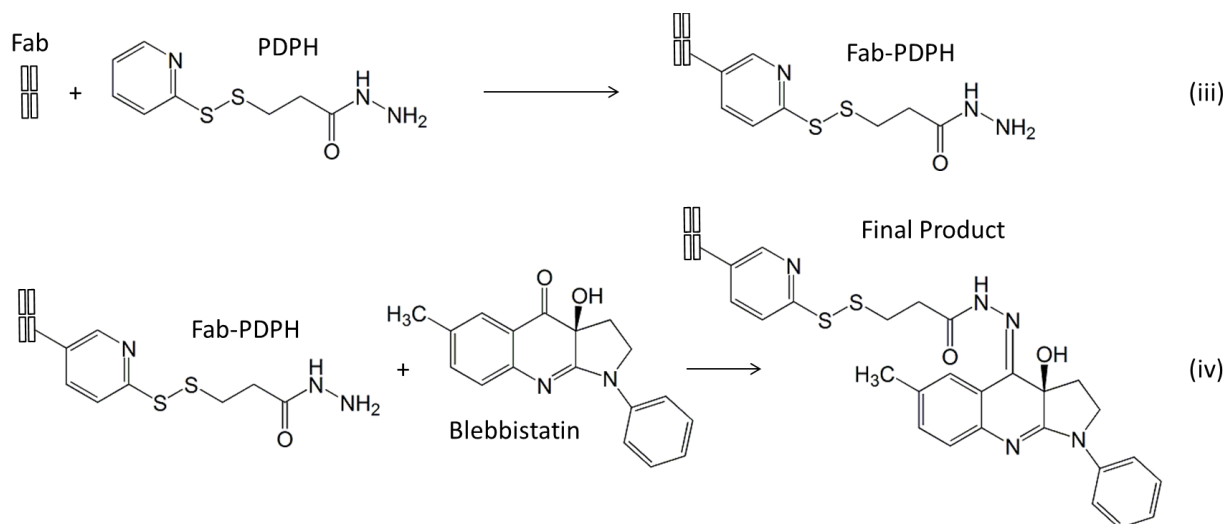
Figure IV-9: Schematic representation of the b-AQP0Fab reaction mechanism. The conjugation reaction occurred in two steps: (1) attaching the fragmented AQP0 antibody (Fab) to the PDPH crosslinker, and (2) attaching the product of reaction (iii) to blebbistatin to form b-AQP0Fab.

was incubated for 2 hours at room temperature and purified using a size exclusion column (Superdex 75) to remove unbound blebbistatin from the final product, b-AQP0Fab. Two isoforms of b-AQP0Fab were synthesized, one with antigenic response to the TPAAVRGTLGLSALHPSVG peptide sequence and the other to the TRNFTN peptide sequence.

4.4.4 LABELLING B-AQP0FAB WITH FLUORESCEIN ISOTHIOCYANATE

The reaction product b-AQP0Fab was fluorescently labelled with fluorescein isothiocyanate (FITC) isomer I (Sigma-Aldrich F2502) for detection purposes in validation experiments. A 4 mg/mL solution of b-AQP0Fab was prepared in 0.1 sodium carbonate buffer (pH 9). 1 mg/mL of FITC was dissolved in anhydrous dimethyl sulfoxide (DMSO). 50 μL of FITC solution was slowly added (in 5 μL aliquots) for every 1 mL of b-AQP0Fab solution during continual stirring. The reaction was incubated for 8 hours at 8°C in the dark. After incubation, 50 mM of NH_4Cl was added, and the

reaction was incubated again for 2 hours at 8°C in the dark. Unbound FITC was separated from fluorescently labelled b-AQPOFab using a Sephadex G-10 column (GE Life Sciences #17-0010-01), and stored at 8°C in a lightproof container.

4.4.5 Non-Reducing Sodium Dodecyl Sulphate Polyacrylamide Gel Electrophoresis (SDS-PAGE)

In order to observe the successful conjugation of b-AQP0ab and b-AQP0Fab, non-reducing, sodium-dodecyl-sulfate polyacrylamide gel electrophoresis (PAGE) was used to indicate the approximate size of the final products. Gels were freshly prepared before each assay. 10 mL of 15% separating gel (3 kDa to 100 kDa molecular weight range) was prepared by mixing 5 mL of acrylamide/bis-acrylamide (30%/0.8% w/v), 4.89 mL 0.375M Tris-HCl (pH 8.8), 100 µL of ammonium persulfate (AP, 10% w/v), and 10 µL tetramethylethylenediamine (TEMED). The separating gel mixture was pipetted into gel casting plates, and allowed to polymerize for 30 minutes. The remainder of the plate was filled with isopropanol to prevent evaporation and to ensure even surface gelation. 5 mL of stacking gel was then prepared by mixing 4.275 mL of 0.375 M Tris-HCl (pH 8.8), 0.67ml acrylamide/bis-acrylamide (30%/0.8% w/v) 0.05 mL of 10% (w/v) AP, and 5 µL TEMED. The isopropanol atop of the separating gel was drained, the stacking gel was pipetted on top, and a gel comb (15-well, 40 µL, custom 3D printed) was inserted into the mixture. The stacking gel was allowed to polymerize for 30 minutes.

Protein solutions were individually mixed in a 1:1 volume ratio with 2x sample buffer (62.5 mM Tris-HCl (pH 6.8), 25% glycerol, 10% sodium dodecyl sulphate, and 1% bromophenol blue), and loaded into wells. Running buffer for electrophoresis was composed of 25 mM Tris and 192

mM glycine at a pH of 8.3. The electrophoresis was conducted at low voltage and on ice to prevent degradation of proteins. Completed gels were stained with Coomassie blue to visualize protein bands.

4.4.6 SIZE EXCLUSION CHROMATOGROPHY – MASS SPECTROMETRY (SEC–MS)

Samples of b-AQP0Fab were separated using a Superdex 75 increase 10/300 GL column (GE Healthcare Life Sciences #17-5174-01). Mass spectral data for the ADC was acquired on an Agilent 6510 QTOF (Agilent, Santa Clara, CA) in positive electrospray ionization (ESI) mode in the range of 1000−8000 mass to charge ratio (m/z). Nitrogen gas was used as both drying and nebulizing gasses. The drying gas temperature was 350 °C, and flow rates for the drying gas and the nebulizer gas pressure were 12 Litres/hour and 35 psi, respectively. The capillary, fragmentor, and octupole radio frequency voltages were set at 5000, 450, and 750, respectively.

4.4.7 ENZYME–LINKED IMMUNOABSORBANT ASSAY (DIRECT)

The binding capability of b-AQP0Fab to aquaporin peptide sequence was assessed by a custom direct enzyme-linked immunoabsorbant assay (ELISA). 96-well plates were coated with 2 μg/mL of BSA either conjugated with TPAAVRGTLGLSALHPSVG or conjugated with TRNFTN and incubated for 2 hours at room temperature. TPAAVRGTLGLSALHPSVG- and TRNFTN- conjugated BSA were provided with the custom anti-peptide antibodies ordered from Cedarlane Labs. Coated wells were then washed 3x with PBS and blocked with unconjugated BSA. Triplicates of b-AQP0Fab samples were added to the coated wells in 10 dilution ratios: 1:256k,

1:128k, 1:64k, 1:32k, 1:16k, 1:8k, 1:4k, 1:2k, 1:1k, 1:500. Wells were then washed 3x with PBS.

Samples were viewed using a SpectraMax M5^e (Molecular Devices, Sunnyvale, CA, USA)

4.4.8 WESTERN BLOT ANALYSIS

Western blot analysis was conducted to evaluate the disruptive strength of blebbistatin on lenticular

tissue after antibody hybridization. In brief, lenses from 7-day-old chickens were ground using mini

pestles, and lysed with Radioimmunoprecipitation Assay Buffer (RIPA; R0278, Sigma-Aldrich Co.,

Oakville, ON, Canada) containing a general use protease inhibitor cocktail (P2714, Sigma-Aldrich

Co., Oakville, ON, Canada). The total protein of lens tissue samples was quantified using the

BioRad DC protein assay (500-0111; BioRad Laboratories, Inc., Mississauga, ON, Canada).

Samples were prepared with Laemmli sample buffer, run on 10% precast gels (456-1033, BioRad

Laboratories, Inc., Mississauga, ON, Canada) in the BioRad Mini-Protean System (165-8000,

BioRad Laboratories, Inc., Mississauga, ON, Canada), transferred to a polyvinyldene fluoride

(PVDF; 162-0175, BioRad Laboratories, Inc., Mississauga, ON, Canada) membrane. The transferred

membrane was treated with a 1:100 dilution of rabbit anti-myosin heavy chain 9 (MYH9; Sigma-

Aldrich HPA001644), prior to treatment with a 1:400 dilution ratio of goat anti-rabbit IgG

conjugated with horseradish peroxidase (Sigma-Aldrich A0545). Treated membranes were then

visualized using Amersham ECL prime (RPN2236, GE Healthcare, Mississauga, ON, Canada),

imaged with a Storm 860 scanner (GE Healthcare, Mississauga, ON, Canada), and assessed using

ImageQuant software (GE Healthcare, Mississauga, ON, Canada).

4.4.9 IN VITRO ASSESSMENT OF b-AQP0Fab EFFECTS ON LENS STIFFNESS

The mechanical properties of lenses treated with b-AQP0Fab were measured using a universal testing machine (Instron, Norwood, MA, USA). Each lens was placed anterior side down on a pedestal located in the compression chamber containing chilled TS. Lenses were then compressed 0.75 mm using an aluminum compression element connected to a 10-N load cell and measurements of the resultant force exerted by the lens were collected.

4.5 RESULTS

Sodium dodecyl sulphate polyacrylamide gel electrophoresis (SDS-PAGE) on b-AQP0ab indicated that hybridization of whole anti-AQP0 to the BMPH crosslinker was successful (Fig. IV-10). However, due to the low molecular weight of blebbistatin, no conclusions were made regarding its conjugation. Additionally, the reaction of anti-AQP0, BMPH, and blebbistatin resulted in a product with an approximate molecular weight of 200 kDa, which is substantially greater than the unconjugated anti-AQP0 (by approximately 50 kDa), and possibly indicating homedimerization of BMPH.

Western blot (WB) analysis to verify the functionality of b-AQP0ab-conjugated blebbistatin indicated only a slight disruption of MYH9 activity (Fig. IV-11). Mean band intensities ($\pm$ SEM) of lens tissue treated with blebbistatin indicated a much lower concentration of MYH9 (9.74 ± 1.15) when compared to lens tissue treated with b-AQP0ab (24.69 ± 2.26) and untreated lens tissue (28.69 ± 2.18).
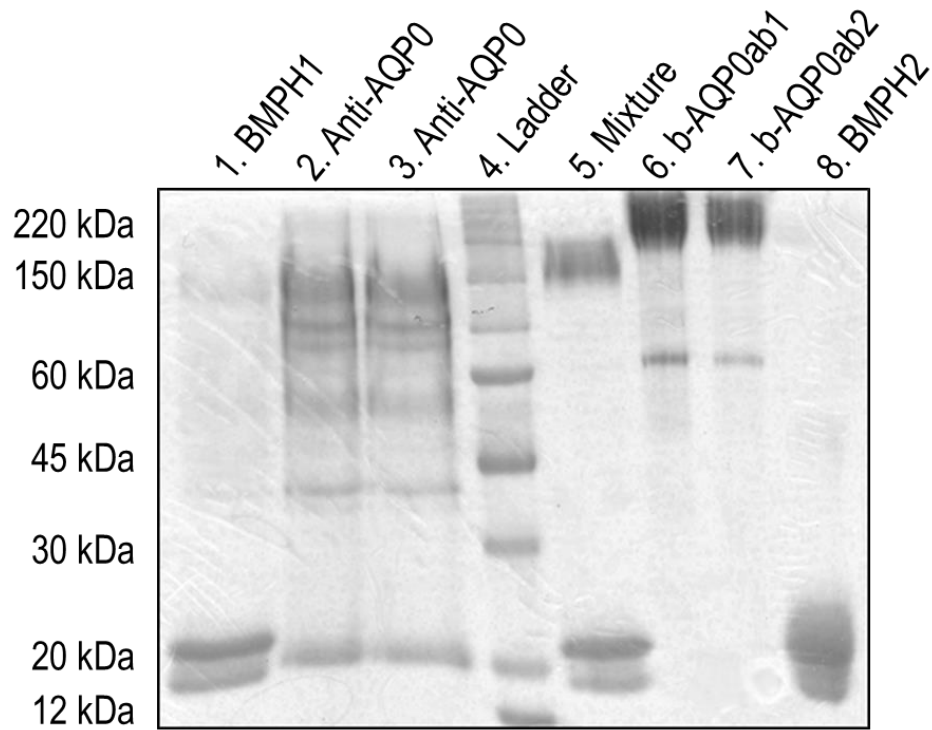
Figure IV-10: Non-reducing SDS-PAGE comparing the molecular weight of b-AQP0ab and its unconjugated constituents. Lanes 1 & 8: BMPH crosslinker, lanes 2 & 3: stock anti-AQP0 antibody, lane 4: molecular weight marker, lane 5: unconjugated mixture of b-AQP0ab components, lane 6 & 7: b-AQP0ab. Gel visualized using Coomassie brilliant blue stain.
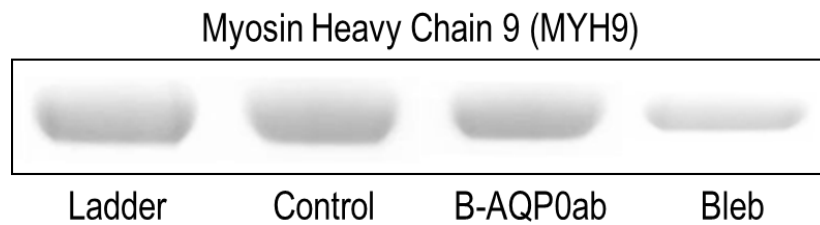
Figure IV-11: Western blot comparing myosin heavy chain 9 (MYH9) levels in lenticular tissue treated with dimethyl sulfoxide (DMSO, control), b-AQP0ab, and blebbistatin.

Furthermore, direct enzyme-linked immunoabsorbant assay (ELISA) analysis of antibody to AQP0 affinity indicated that both peptide isoforms of b-AQP0ab experienced a loss of recognition towards their respective antigen sequences (Fig. IV-12). At 1:500 dilution ratios, both TPAAVRGTLGLSALHPSVG- and TRNFTN-conjugated b-AQP0ab samples demonstrated a substantial loss of optical density (OD_{450}: 0.2740 ± 0.1010 and 0.2294 ± 0.0190, respectively) compared to their unconjugated counterparts (OD_{450}: 0.5350 ± 0.0210 and 0.3250 ± 0.0221, respectively).

Despite the low antigen affinity and low blebbistatin functionality of b-AQP0ab, whole lenses treated with b-AQP0ab exhibited a decrease in overall lens stiffness. Lenses treated with b-
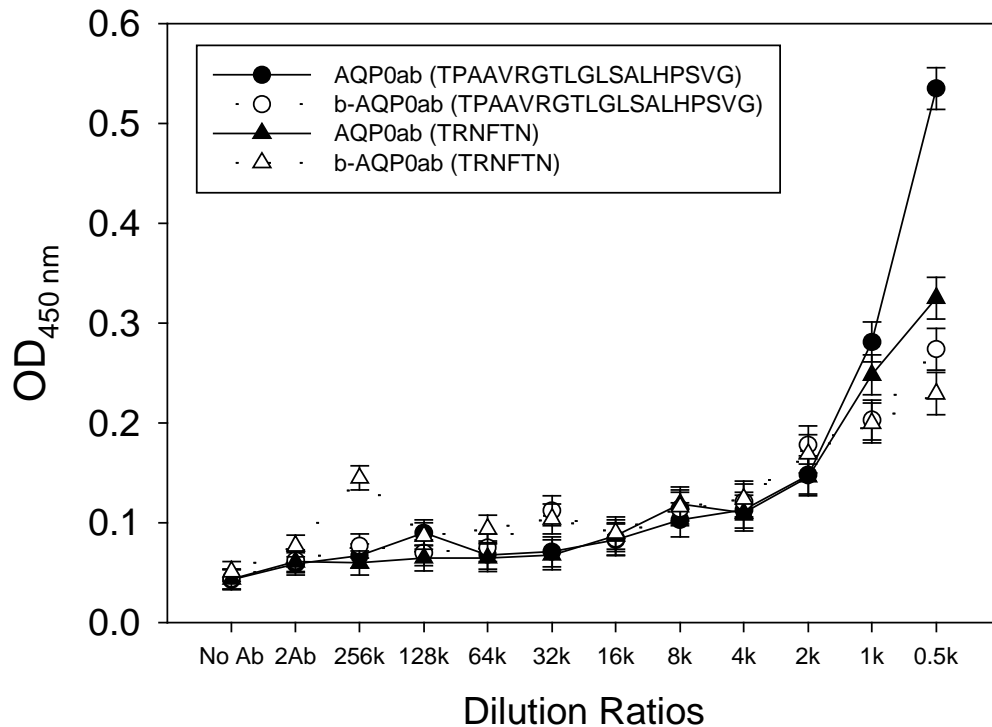
Figure IV-12: Binding strength of b-AQP0ab isoforms. Direct enzyme-linked immunoabsorbant assay (ELISA) indicated lower antigen affinity of TPAAVRGTLGLSALHPSVG- (empty circle) and TRNFTN- (empty triangle) isoforms of b-AQP0ab compared to their native IgG counterparts (filled circle and filled triangle, respectively).

AQP0ab showed significantly lower stiffness coefficients ($\pm$SEM) at 4.10 ± 0.25 when compared to lenses treated with anti-AQP0 at 5.05 ± 0.10 (Fig. IV-13A, p=0.0363). Similarly, lenses treated with b-AQP0ab also displayed a significantly lower stiffness coefficient ($\pm$SEM) when compared to lenses treated with vehicle control (Fig. IV-13B, compare 5.05 ± 0.07 and 3.93 ± 0.27, respectively, p=0.0262).

Following the refinement of b-AQP0ab to produce b-AQP0Fab, the new ADC was subjected to SDS-PAGE. The SDS-PAGE indicated proper cleaving and purification of the anti-AQP0 IgG into Fab fragments (Fig. IV-14, lane 4 band (approximately 45 kDa)) through the use of a papain digestion kit. Additionally, the native PAGE also demonstrated the successful hybridization of fragmented anti-AQP0 with the PDPH crosslinker (Figure IV-14, compare lane 4 band (approximately 45 kDa) with lane 5 band (approximately 50 kDa), respectively). The difference between the weight of Fab-AQP0 and Fab-ADC indicates multiple attachments of PDPH to Fab-
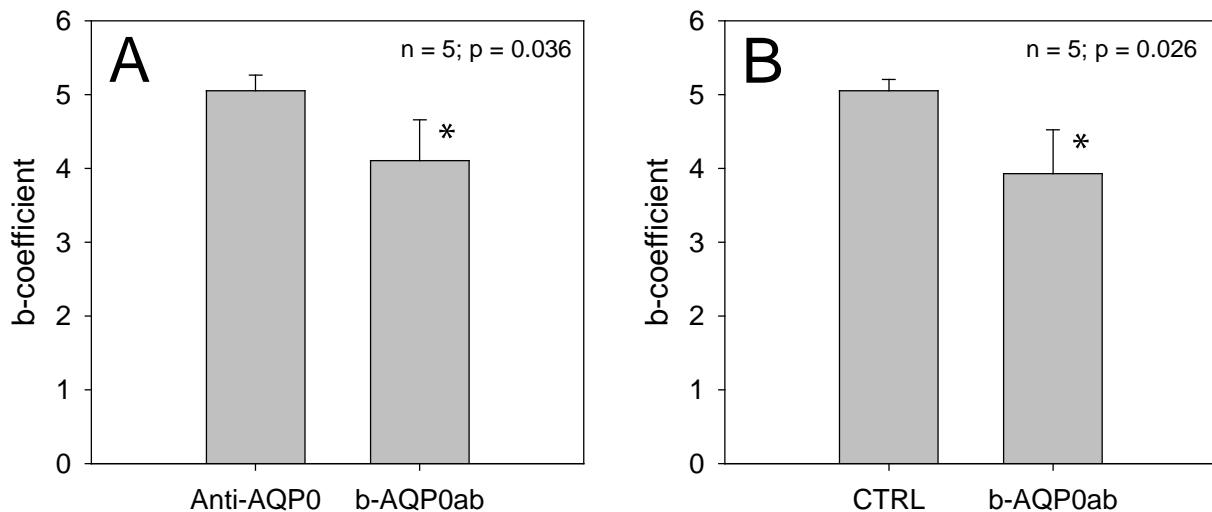
Figure IV-13: Bar graphs comparing stiffness of (b-)coefficients. Lenses treated with b-AQP0ab were less stiff than those treated with anti-AQP0 (A) and were less stiff than those treated with phosphate buffered saline (control) (B). Asterisks denote a significant decrease in lens stiffness.
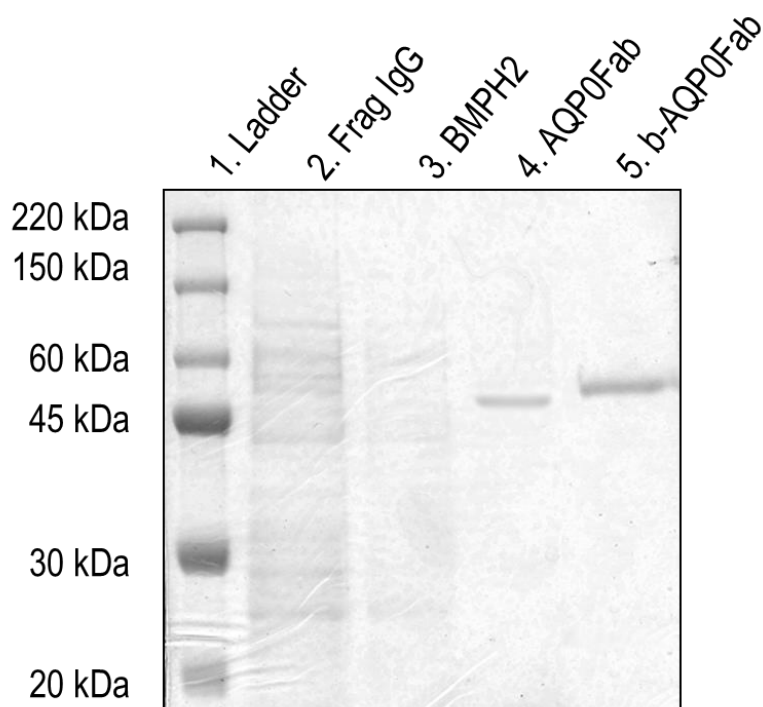
Figure IV-14: Non-reducing SDS-PAGE comparing the molecular weights of b-AQP0Fab and its unconjugated constituents. Lane 1: molecular weight marker, lane 2: native AQP0 antibody, lane 3: PDPH crosslinker, lane 4: papain digested AQP0, lane 5: b-AQP0Fab. Gels visualized using Coomassie brilliant blue stain.

AQP0 occurred; however, the difference in weight between the two lanes was not large enough to indicate homodimerization of PDPH.

Size exclusion chromatography – mass spectrometry (SEC-MS) revealed 4 peaks corresponding to 4 reaction products as a result of b-AQP0Fab conjugation (Fig. IV-15, data summarized in Table IV-2). Peak 1 corresponds to unconjugated Fab (theoretical mass (TM): 50,000 Da), peak 2 corresponds to Fab with 1 conjugation (TM: 50,521 Da), peak 3 corresponds to Fab with 2 conjugations (TM: 51,042 Da), and peak 4 corresponds to Fab with 3 conjugations (TM: 51,563 Da). No peaks were observed for Fab with 4 conjugations. Based on the percentage intensity of each peak, reaction samples were composed predominantly of Fab with 2 conjugations
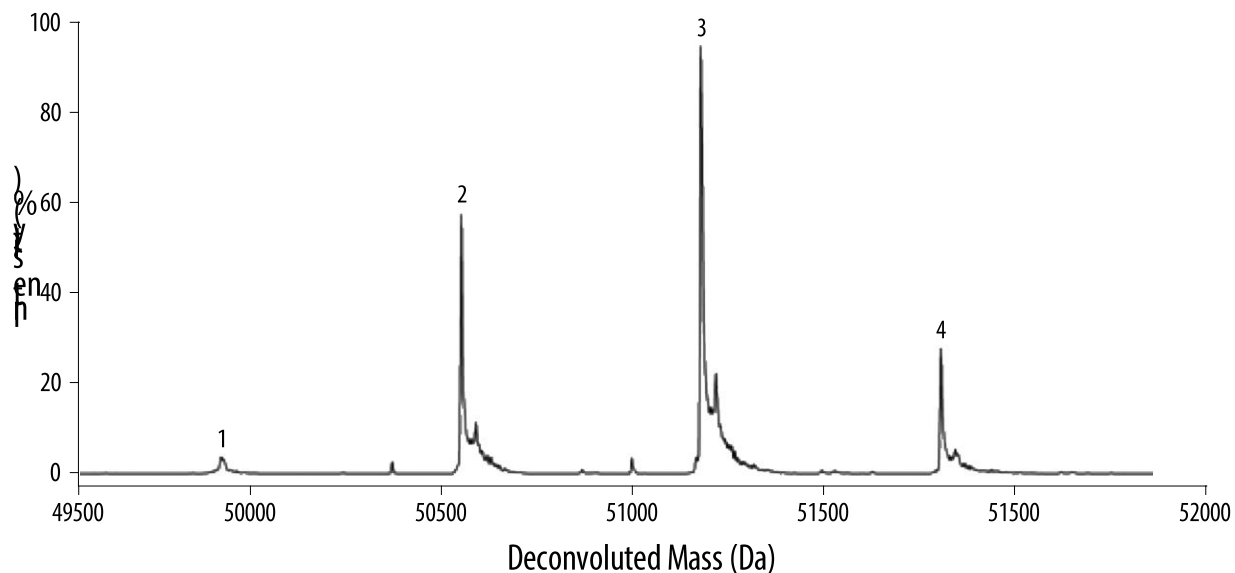
Figure IV-15: Characterization of b-AQP0Fab by size exclusion chromatography – mass spectrometry (SEC-MS). The various reaction products resulting from the conjugation of b-AQP0Fab were (1) unconjugated b-AQP0Fab, (2) b-AQP0Fab with 1 conjugation, (3) b-AQP0Fab with 2 conjugations, (4) b-AQP0Fab with 2 complete and 1 incomplete conjugation.

Table IV-2: Summary of SEC-MS Data

	Peak			
	1	2	3	4
Theoretical Mass (Da)	50,000	50,521	51,042	51,563
Deconvoluted Mass (Da)	50,007.51	50,540.78	51,071.47	51,611.46
Intensity	4.35%	56.67%	93.67%	27.92%
Sample Proportion	2.38%	31.03%	51.29%	15.29%

(51.29%), followed by Fab with 1 conjugation (31.03%), and Fab with 3 conjugations (15.29%). Only 2.38% of the sample remained unconjugated.

Once again, to verify the functionality of blebbistatin after conjugation to anti-AQP0Fab, the activity of lenticular MYH9 was assessed by Western blot analysis (Fig. IV-16). Mean band
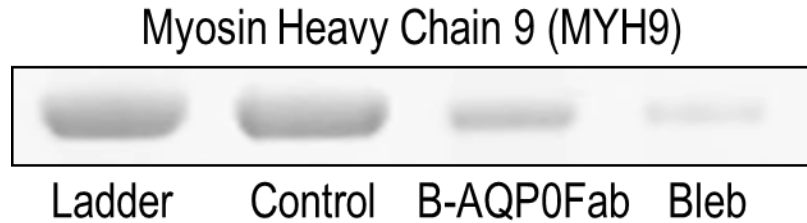
Figure IV-16: Western blot comparing myosin heavy chain 9 (MYH9) levels in lenticular tissue treated with dimethyl sulfoxide (DMSO, control), b-AQP0Fab, and blebbistatin. MYH9 expression was lower in b-AQP0Fab-treated lenses compared to its control, but was not as low as that of blebbistatin-treated lenses, indicating a slight loss of blebbistatin activity after ADC conjugation.

intensities (±SEM) of lens tissues treated with b-AQP0Fab (13.97 ± 1.81) indicated a decrease in MYH9 staining comparable to that of unconjugated blebbistatin (11.25 ± 0.42). Furthermore, both treatments resulted in a substantial decrease in MYH9 labelling when compared to untreated lens tissue (32.70 ± 2.97).

Direct ELISA indicated that the TPAAVRGTLGLSALHPSVG isoform of b-AQP0Fab (Fig. IV-17, empty circle) maintained a strong response towards its respective antigenetic site compared its unconjugated anti-AQP0Fab counterpart (Fig. IV-17, filled circle). At a 1:500 dilution ratio, TPAAVRGTLGLSALHPSVG-conjugated b-AQP0Fab demonstrated only a slight loss of optical density (OD_{450}: 0.4600 ± 0.0210) compared to its unconjugated counterpart (OD_{450}: 0.5780 ± 0.0219). Although the TRNFTN isoform of b-AQP0Fab retained comparable binding strength to its unconjugated anti-AQP0Fab counterpart (compare OD_{450}: 0.1700 ± 0.0130 and 0.1660 ± 0.1440, respectively), both antibodies show low overall affinity towards their respective TRNFTN antigenic sites.

Finally, the effects of the newly refined TPAAVRGTLGLSALHPSVG isoform of b-AQP0Fab on the biomechanics of the crystalline lens were assessed. Whole lenses treated with b-AQP0Fab exhibited a decrease in overall lens stiffness. Lenses treated with b-AQP0Fab showed
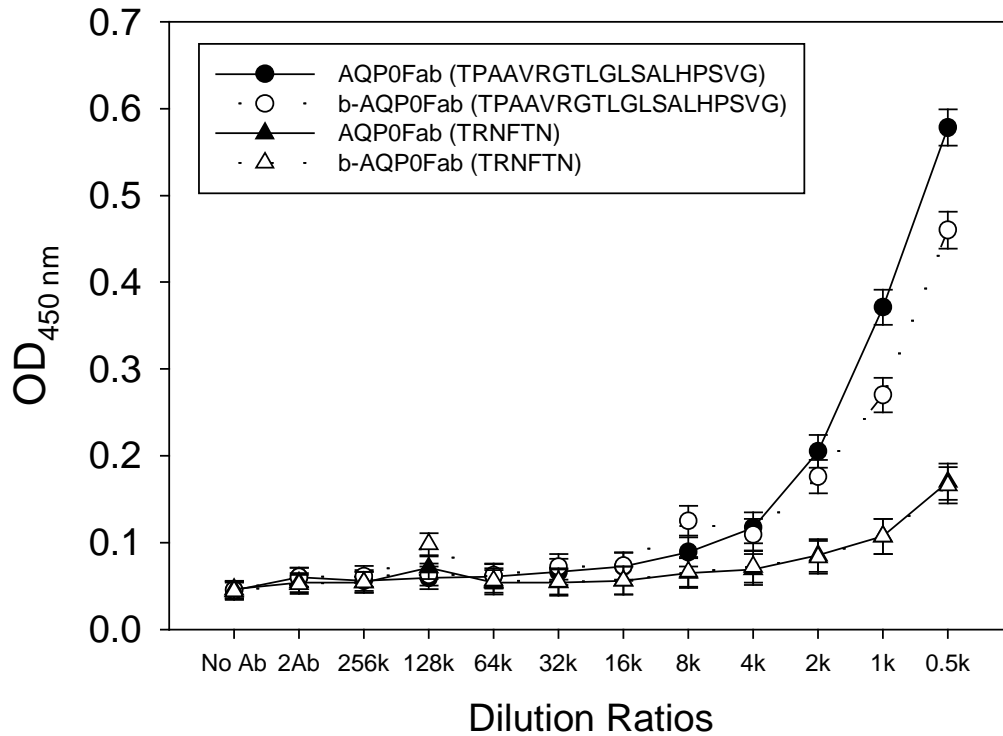
Figure IV-17: Direct enzyme-linked immunoabsorbant assay (ELISA) comparing the binding strength of TPAAVRGTLGLSALHPSVG- (empty circle) and TRNFTN- (empty triangle) isoforms of b-AQP0Fab with their unconjugated Fab counterparts (filled circle and filled triangle, respectively).

significantly lower stiffness coefficients ($\pm$SEM) at 3.53 ± 0.15 when compared to lenses treated with anti-AQP0 at 5.33 ± 0.16 (Fig. IV-18, $p = 0.0262$). Similarly, lenses treated with b-AQP0Fab also displayed a significantly lower stiffness coefficient ($\pm$SEM) when compared to lenses treated with vehicle control (compare 5.19 ± 0.13 and 3.53 ± 0.16, respectively, $p = 0.0161$).

4.6 DISCUSSION

An antibody-drug conjugate (ADC) was synthesized to specifically target and soften the crystalline
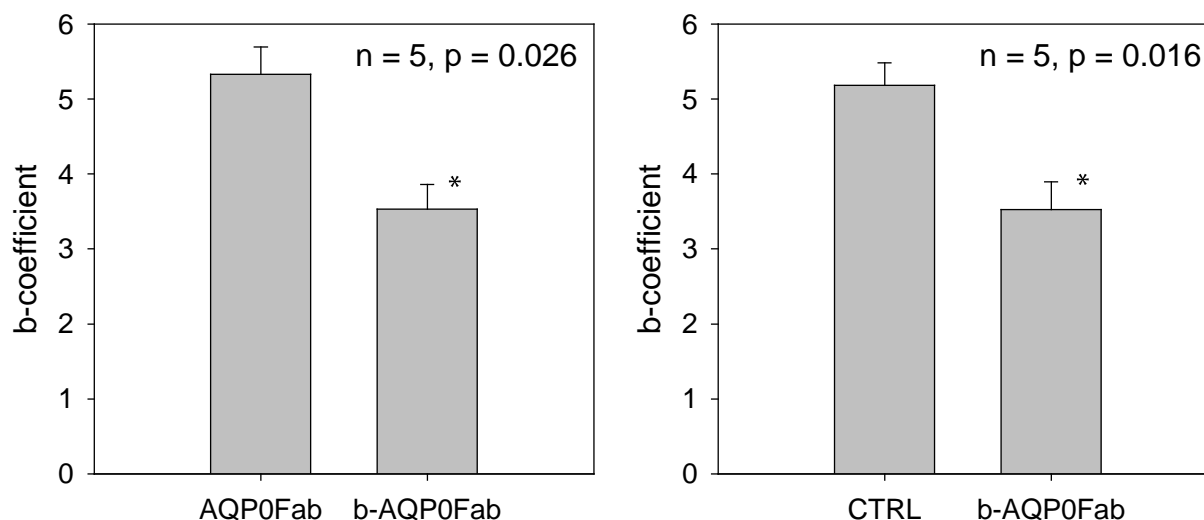
Figure IV-18: Bar graphs showing stiffness (b-)coefficients of (A) lenses treated with AQP0Fab vs. lenses treated with b-AQP0Fab, and (B) lenses treated with phosphate buffered saline (control) vs. lenses treated with b-AQP0Fab. Asterisks denote a significant decrease in lens stiffness.

lens. The ADC constituents were carefully selected in order to optimize the specificity, efficacy, and efficiency of the total compound. The first iteration of the ADC, b-AQP0ab, was composed of an unfragmented custom polyclonal IgG antibody (specific to the external TPAAVRGTLGLSALHPSVG- and TRNFTN-peptide sequences of AQP0) hybridized to blebbistatin using BMPH, an uncleavable hydrazide crosslinker. Non-reducing SDS-PAGE indicated that hybridization of the three components was successful; however, b-AQP0ab produced a band much heavier than the theoretical sum of the three components. The theoretical weight of unfragmented, unconjugated AQP0ab should have been approximately 150 kDa, which was observed. A total maximum of 12 BMPH crosslinker chains (at approximately 297 daltons each) and 12 molecules of blebbistatin (at approximately 292 daltons each) may be linked to AQP0ab to produce an ADC with a theoretical molecular weight of 157,068 daltons. The SDS-PAGE produced a band for b-AQP0ab with a range of approximately 160kDa to 200 kDa. The colossal difference

observed in the theoretical vs. observed molecular weights are speculated to be as a result of dimerization and oligomerization of the BMPH crosslinker, which arises in high crosslinker reaction concentrations (Hemaprabha, 2012).

Western blot analysis indicated that conjugation of blebbistatin to the BMPH crosslinker severely attenuated the disruptive effects of blebbistatin (Fig. IV-11). Direct enzyme-linked immunabsorbant assay (ELISA) of both b-AQP0ab isoforms demonstrated a substantial loss of binding specificity to their respective antigen peptide sequences (Fig. IV-12). However, despite the low characterized efficacy of antigen-binding and attenuated blebbistatin activity of the b-AQP0ab, treatment of whole lenses resulted in a significant decrease in their biomechanical integrity. Together, these results suggest a potent effect of blebbistatin on disrupting the cytoskeletal foundation of the crystalline lens.

As a result of this preliminary study, various refinements were made to b-AQP0ab to optimize its specificity and efficacy. The unconjugated AQP0ab was digested using a papain kit to produce smaller, yet still specific, fragments of the antibody. In brief, papain digestion cleaves the peptide bonds at the hinge region of the antibody, resulting in two 50 kDa Fab fragments and a 50 kDa Fc fragment. As Fab fragments retain both the variable heavy and light chain regions, and therefore, the antigen binding site, the targeting characteristic of the antibody is preserved. The Fc fragments, however, were discarded to reduce the overall size of the antibody and because their role in secondary immune response recruitment was not required. Note that as a result of papain digestion, Fab fragments can only have a total maximum of 4 conjugation sites. Furthermore, because intrachain disulphide reduction of variable domains causes a decrease in stability and specificity of the Fab fragment (McAuley et al., 2008; Ouellette et al., 2010), Fab conjugations must occur in the non-variable domains in order to function. As a result, a maximum of 2 conjugations

are possible per Fab fragment. The Fab fragments were then conjugated to a new cleavable crosslinker, PDPH, in an effort to bolster the effect of conjugated blebbistatin.

SDS-PAGE demonstrated that the second iteration of the ADC, b-AQP0Fab, was also successful in conjugation (Fig. IV-14). The Fab fragment of AQP0ab has a theoretical molecular weight of approximately 50 kDa, which was observed, while PDPH has a molecular weight of approximately 229 daltons, and blebbistatin has a molecular weight of 292 daltons. With four possible attachment sites, b-AQP0Fab has a total theoretical maximum weight of 52,084 daltons. A molecular band for b-AQP0Fab greater than AQP0Fab was observed, however, a close estimate was hard to make due to the limited space provided by the ladder for the large range of molecular weights. SEC-MS revealed that the conjugation protocol for b-AQP0Fab resulted in 4 products with differing molecular weights. The sample was composed predominantly of Fab with 2 conjugations (51.29%), followed by Fab with 1 conjugation (31.03%), and Fab with 3 conjugations (15.29%). As Fab was the limiting reagent for this reaction, it is logical that only 2.38% of the sample was unconjugated. It should be noted, however, that not all of the aforementioned conjugations may result in a functional ADC, as conjugation to cysteine groups within the variable domains reduces antibody specificity (Ouellette et al., 2010). Assuming an equal reaction chance of conjugation at each intrachain disulphide bond, only 2 of 4 Fabs with 2 conjugations are guaranteed to be functional. Similarly, only 2 of 4 Fabs with 1 conjugation will be functional. Unfortunately, none of the Fabs with 3 conjugations will be functional, as one variable domain must have been compromised. Nevertheless, 41.15% (½ of 1-conjugation Fab + ½ of 2-conjugation Fab) of the total sample contains b-AQP0Fab with functional antigen recognition. Further experimentation is required to yield a higher percentage of functional b-AQP0Fab.

Western blot analysis demonstrated that using the labile crosslinker PDPH, to hybridize

blebbistatin with AQP0Fab, resulted in a substantial increase in reactivity of conjugated blebbistatin towards lens tissue. The use of PDPH is advantageous for two reasons: its labile site is susceptible to cleavage in lenticular conditions, and following cleavage, blebbistatin may revert back to its native unconjugated structure. The labile site for PDPH is a disulphide bridge, which is cleavable by thiols such as reduced glutathione. Glutathione, in turn, is found in high concentrations within the lens (Reddy, 1990; Rosner, Farmer, & Bellows, 1938), and acts as an anti-oxidant to prevent cataractogenesis (Giblin, 2000; Reddy, 1990). Upon cleavage of the disulphide bridge, the electron cloud of the remaining spacer arm (of the crosslinker) attached to blebbistatin destabilizes. The existence of the strong double bond makes it unlikely for the blebbistatin molecule to revert back to its native conformation, although theoretically, a high level of thermal and/or mechanical energy could mediate such changes (Fig. IV-19). Although, lenses treated with b-AQP0Fab showed a substantially lower concentration of MYH9 when compared to untreated tissue, it should be noted that unconjugated blebbistatin remains as the most effective disruptor of MYH9. However, the effect of b-AQP0Fab on MYH9 levels of lenticular tissue is substantially greater than that of b-AQP0ab, indicating successful reactivation of blebbistatin upon crosslinker cleavage.

Direct ELISA of both b-AQP0Fab isoforms demonstrated that conjugated Fab fragments resulted in binding strengths that were comparable to their native fragmented states. Although
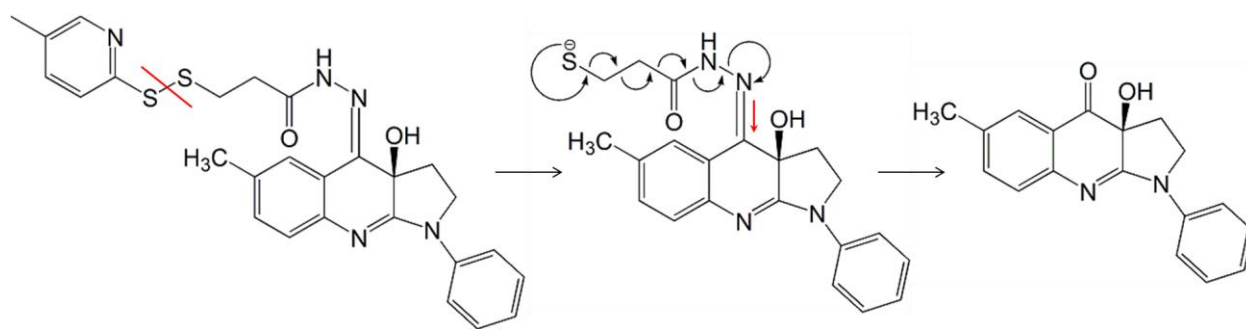
Figure IV-19: Proposed reaction schematic of blebbistatin release following cleavage of PDPH disulfide bonds.

TPAAVRGTLGLSALHPSVG-sequence b-AQP0Fab showed a slight loss of specificity when compared to its unconjugated counterpart, the overall binding strength was substantially higher than both native and conjugated TRNFTN-sequence b-AQP0Fabs. It is speculated that the difference in specificity is largely due to the difference in size of both peptide sequences, where the longer sequence has a higher potential of binding to its respective antigenic site. As a result, TPAAVRGTLGLSALHPSVG-sequence b-AQP0Fab was selected for further experimentation.

Lenses treated with TPAAVRGTLGLSALHPSVG-sequence b-AQP0Fab showed a significant decrease in biomechanical integrity, indicating that the blebbistatin component was effective at disrupting the interaction of lenticular actomyosin networks. Interestingly, the difference in efficacy of the refined TPAAVRGTLGLSALHPSVG-sequence b-AQP0Fab and b-AQP0ab on lens stiffness was negligible, indicating that a blebbistatin is highly effective at disrupting lens integrity and that lower concentrations of blebbistatin may be used should adverse effects be observed.

V. THE EFFECTS OF INTRAVITREALLY INJECTED B-AQP0AB ON THE ACCOMMODATIVE MECHANISM OF AVIAN EYES

5.1 OVERVIEW

Purpose: b-AQP0Fab, an antibody-drug conjugate designed to specifically target and soften the crystalline lens, was synthesized and validated in a previous study. In this study, 7-day-old birds were injected with b-AQP0Fab to investigate the in vivo effects of the ADC on the mechanism of accommodation and distribution of lenticular actomyosin lattice.

Methods: One eye of 7-day-old White Leghorn chickens was intravitreally injected with 100 µM of b-AQP0Fab and the other with 100 µM of anti-AQP0 conjugated with PDPH. Eyes were enucleated at 1 hour, 2 hour, 4 hour, and 8 hour time points. Enucleated eyes were attached to an electrophysiological stimulator, and the focal lengths of the eye were measured pre-, during-, and post accommodative stimulation. Additionally, confocal microscopy was used to assess changes in lenticular actomyosin distribution between control and treated eyes.

Results: b-AQP0Fab demonstrated the ability to penetrate the lens capsule and bind specifically to the lens fibre cell membrane. Furthermore, intravitreal injection of b-AQP0Fab into the eye resulted in disruption of the lens basal membrane complex. After 4 hours of treatment, intravitreally-injected eyes demonstrated a significant decrease in back vertex focal length (BVFL) during stimulation compared to control eyes ($P = 0.03$), in addition to an increase in BVFL during recovery ($p = 0.04$). No notable changes occurred during 1 hour, 2 hour, and 8 hour time groups.

Conclusions: b-AQP0Fab was successful in specifically targeting and softening the crystalline lens. However, the effects of the ADC wore off quickly, indicating the need for further optimization.

5.2 INTRODUCTION

Within recent years, intravitreally-injected sustained-release formulations have shown promise to become powerful delivery platforms for intraocular therapeutics (Gaudana, Ananthula, Parenky, & Mitra, 2010). Indeed, common diseases such as age-related macular degeneration, macular edema, and diabetic retinopathy have seen a marked decline in prevalence with the development of antibody-derived therapeutics, such as bevacizumab, ranibizumab, and aflibercept, which are injected into the vitreous chamber. As intravitreal injections offer a bypass to ocular surface barriers, the attention of most pharmacologists and drug delivery scientists has focused on treating diseases that affect the posterior segment of the eye. However, a number of anterior structures within the eye, such as the crystalline lens, remains difficult to target with topical drugs due to the exceptionally tight corneoscleral barrier (Leong & Tong, 2015). To date, there are no FDA-approved treatments that offer a cure to the physiological decline of lens elasticity with age. This inevitable, age-related loss of lens elasticity results in the eventual decline of accommodative power in the eye, and in the inability to focus on nearby objects, a condition known as presbyopia (Atchison, 2002; Strenk et al., 2005). Certain pharmaceutical groups have claimed the discovery of a small molecule eye drop that can soften the lens specifically, however, no refereed publications have been presented nor have the targeting and reaction mechanisms been revealed (Crawford, Garner, & Burns, 2014; W. H. Garner, Garner, Crawford, & Burns, 2014). Additionally, small molecule drugs that are able to circumvent the corneoscleral barrier demonstrate low or no specificity to the lens, and can cause adverse systemic effects that are even more detrimental to the eye. Alternatively, some presbyopia researchers have proposed the use of miotics, such as the muscarinic agonist pilocarpine (Kaufman, 2008; Wendt, He, & Glasser, 2013), or a combination of the cholinergic agonist carbachol with the α2-adrenergic agonist brimonidine, in order to constrict

the ciliary muscle and decrease the pupillary diameter, resulting in an improvement in the ocular depth of focus (Abdelkader, 2015). Unfortunately, intervention using miotics is unsustainable due to the inevitable build-up of receptor tolerance with prolonged treatment (Ostrin & Glasser, 2010).

Although the majority of the presbyopic population is content with a simple management solution, such as bifocal or progressive addition spectacles, it remains important to investigate and develop pharmaceutical methods of restoring the elastic modulus of the lens in order to revert the eye's accommodative machinery to a healthy, functioning state. A description of the synthesis of a custom antibody-drug conjugate (ADC), b-AQP0Fab, to specifically target and soften the crystalline lens was previously described (Chapter IV). In brief, b-AQP0Fab is a hybridization of a peptide antibody that recognizes a unique sequence of the extracellular region of the transmembrane protein aquaporin-0 (AQP0), linked to blebbistatin, a selective myosin II inhibitor, by a labile hydrazide linker that is cleaved by exposure to high thiolic conditions, such as that which may be found in the lens. *In vitro*, b-AQP0Fab was demonstrated to have high affinity towards native AQP0 in addition to retaining the disruptive capacity of blebbistatin. The purpose of this investigation was to examine the *in vivo* effects of intravitreally injecting b-AQP0Fab into the eye of chickens.

5.3 METHODS

5.3.1 ANIMALS

White leghorn (*Gallus gallus domesticus*) hatchling chicks were obtained from the Maple Leaf hatchery in New Hamburg, Ontario and were fed *ad libitum*. They were housed in stainless steel brooders with a heat source, and kept on a 14:10 day:night light cycle. Chicks were raised in

accordance to the Guidelines of the Canadian Council on Animal Care and conform to the ARVO Statement for the Use of Animals in Ophthalmic and Vision Research. As the focus of this study was to test the fundamental question of whether disrupting cytoskeletal proteins could have an effect on lenticular biomechanics, chicks with robust amounts of accommodation (about a week old) were used. Older birds, will be considered for a future study once the functions of disruptors have been well established. Week-old chicks also show highly monotonic spherical aberrations (V. Choh et al., 2002) thereby providing a model for which optical changes could be assessed.

5.3.2 INTRAVITREAL INJECTIONS

Six- to eight-day-old chicks were used for intravitreal injections. Prior to injections, chicks were anesthetized with 1.5% isoflurane in oxygen. Chicks were injected intravitreally with 20 μL of either 100 μM b-AQP0ab or 100 μM control (AQP0ab). Intravitreal injections were carried out using a 20 μL Hamilton 702N syringe (Sigma# 20735), and in order to ensure delivery into the vitreal chamber, the needle was fitted through Tygon tubing to limit the puncture depth to 2.47 mm. The site of injection was immediately rostral to the orbital notch on the lateral orbit. The site of injection was held closed by forceps for 20 seconds to prevent leakage and to maximize drug delivery after removal of the syringe. Intravitreally-injected chicks were sacrificed at 1 hour, 2 hour, 4 hour, and 8 hour time points to assess the effect of b-AQP0ab and control treatments.

5.3.3 LIGHT AND CONFOCAL MICROSCOPY

Seven-day-old chicks were sacrificed by decapitation and their eyes were enucleated. Eyes

were placed in oxygenated Tyrode's solution (TS: 134 mM NaCl, 3 mM KCl, 20.5 mM NaHCO$_3$, 1 mM MgCl$_2$, 3 mM CaCl$_2$) before removal of the posterior globe and vitreous humour. For light microscopy, the anterior segment was fixed in 4% (w/v) paraformaldehyde solution in 0.1M phosphate buffered saline (PBS) for 20 minutes. The tissue was then washed (3 x 5 mins) with 0.1M PBS and cryoprotected in 30% (w/v) sucrose in PBS overnight. The tissue was then embedded in 22x22 mm molds (Fischer Scientific #38-104-18) filled with optimal cutting temperature embedding medium (OCT medium, VWR #27900-246) before being frozen. Eyes were sectioned sagittally at 15 μm (Leica CM 1900 UV cryotome) and mounted onto Superfrost Plus glass slides (Fischer Scientific #12-550-15). Slides with sections were air-dried for 30 minutes and stained with Texas Red-phalloidin (1:400 dilution in PBS; ThermoFisher Scientific #T7471) for 15 mins at room temperature (RT; 21°C) before a coverslip coated with ProLong Gold (P36934, Life Technologies) was then placed on top. Coverslips were sealed onto slides using nail polish.

For confocal microscopy, after enucleation and removal of the posterior globe, the exposed lens was separated from the surrounding ciliary body and extracted from the anterior segment, taking care to minimize damage to the lens capsule. Lenses were permeabilized *in toto* using 0.05% (v/v) Triton X-100 in PBS before the addition of mouse anti-myosin-light-chain antibody (M4401, Sigma-Aldrich, 1:100 dilution in PBS, 2 hrs. at 37°C), followed by rabbit anti-mouse secondary antibody conjugated to Texas Red (1:500 in PBS, overnight at RT). Following a 3 x 5 minutes wash, lenses were counterstained with fluorescein isothiocyanate (FITC)-phalloidin (P5282, Sigma-Aldrich, 1:400 dilution in PBS, 15 min, RT). Lenses were mounted *in toto* posterior pole up onto slides using 5% (w/v) agar solution in water with 0.05 mg/ml phenylenediamene (P6001, Sigma-Aldrich; in 50% (v/v) glycerol in water). A coverslip coated with ProLong Gold (P36934, Life Technologies) was then placed on top of the posterior pole of the lens and adhered to the slide with the agar. The

protein distribution of lenses was visualized using a Zeiss LSM 510 confocal microscope and images were captured and processed using the Zen 2011 software (Zeiss).

Protein distributions were quantified using nearest neighbour analysis, which assesses the closeness of points of interest (POIs) on an image and assigns a value between 0 and 2.15, where a score of 0 represents clustered POIs, a score of 1 represents a random distribution of POIs, and a score of 2.15 represents a highly regular distribution of POIs. For latrunculin-treated lenses (n=3), the POIs used were the vertices of actin hexagons, while for blebbistatin-treated lenses (n=3), the POIs used were the centre of myosin globules. POIs were targeted and selected using NIH Image or Scion Image software. Nearest neighbour values (R_n) were calculated using the equation $R_n = \frac{D(obs)}{0.5\sqrt{a/n}}$, where D(obs) is the mean observed nearest neighbour distance, a is the area, and n is the total number of POIs.

5.3.4 OPTICAL MEASUREMENTS OF THE LENS DURING ACCOMMODATION

Chicks were euthanized by decapitation and their heads were bisected sagitally in order to enucleate the eyes while taking care to minimize any damage to the nerves. Enucleated eyes were submerged and subsequently dissected in oxygenated (95% O_2, 5% CO_2) Tyrode's solution (TS). For each eye, the optic nerve was removed to expose and isolate the ciliary nerve and ganglion. The anterior segment was left completely intact, while the posterior globe was removed, aside from a wedge containing the ciliary nerve and ganglion.

Optical measurements of the lens were taken using a ScanTox scanning laser monitor as previously described (Section 3.3.8.), however, a modified ScanTox chamber with an open-ended

tube was used in place of the normal chamber (Fig. V-1). The dissected eye was pinned anterior-side down to a Sylgard® (Dow Corning 184) washer, and placed into the modified ScanTox chamber. A suction electrode was passed through the open-ended tube of the modified chamber to connect the ciliary nerve and ganglion to an electrophysiological stimulator (Grass S48 Stimulator). The exit of the open-ended tube was plugged with dielectric tune-up grease, and the chamber was filled with 5% (v/v) fetal bovine serum in oxygenated TS.

The dissected eyes connected to the electrode were scanned pre-, during, and post-stimulation in order to determine back vertex focal lengths during the resting, accommodating, and recovering states of the eye. The stimulus for the ciliary nerve was carried out at a pulse rate of 0.4 ms at 40 Hz with a current of 2 mA. For scans during the accommodation state, the eye was stimulated immediately before capturing the beam image at each eccentricity. The step sizes for the eccentricities were set to 0.13 mm, and 13 radial steps were used in total. As the sutures of each lens
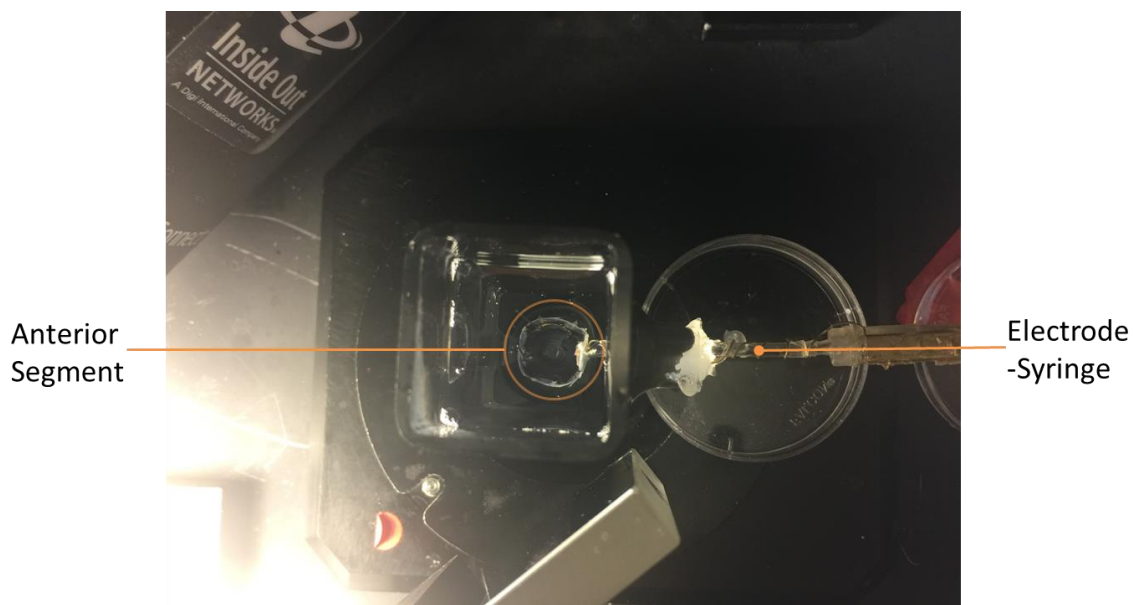
Figure V-1: Top-down view of the in situ accommodation system. The anterior segment of the eye sits anterior-side down inside the ScanTox chamber. The electrode-syringe enters through a tube fashioned into the side of the ScanTox chamber and contacts the ciliary nerve of the posterior wedge.

produce large variability of the central focal lengths (Bantseev, Herbert, Trevithick, & Sivak, 1999; Kuszak et al., 2004; Sivak, Herbert, Peterson, & Kuszak, 1994), the four central rays of each scan were omitted during the collection of data. Additionally, eccentricities where the iris hindered the peripheral beams during accommodation were omitted in all three states during the calculation of average focal lengths.

5.3.5 WESTERN BLOT ANALYSIS

Western blot analysis was carried out to confirm that b-AQP0Fab had the expected effects on lenticular myosin heavy chain 9 (MYH9) levels. ADC-injected eyes were dissected, and tissue from the lens, cornea, ciliary body, and retina were collected. Each sample was separately homogenized using mini pestles, and lysed with Radioimmunoprecipitation Assay Buffer (RIPA; R0278, Sigma-Aldrich Co., Oakville, ON, Canada) containing a general use protease inhibitor cocktail (P2714, Sigma-Aldrich Co., Oakville, ON, Canada). The total protein of lens tissue samples was quantified using the BioRad DC protein assay (500-0111; BioRad Laboratories, Inc., Mississauga, ON, Canada). Samples were prepared with Laemmli sample buffer, run on 10% precast gels (456-1033, BioRad Laboratories, Inc., Mississauga, ON, Canada) in the BioRad Mini-Protean System (165-8000, BioRad Laboratories, Inc., Mississauga, ON, Canada), transferred to a polyvinyldene fluoride (PVDF; 162-0175, BioRad Laboratories, Inc., Mississauga, ON, Canada) and incubated with a primary anti-MYH9 antibody. Secondary antibodies conjugated with horseradish peroxidase were detected by enhanced chemiluminescence using Amersham ECL prime (RPN2236, GE Healthcare, Mississauga, ON, Canada). Western Blots were visualized using a Storm 860 scanner (GE Healthcare, Mississauga, ON, Canada), and assessed using ImageQuant software (GE Healthcare,

Mississauga, ON, Canada).

5.3.6 STATISTICAL ANALYSIS

The effects of b-AQP0Fab on the accommodative properties of the lenses were analysed using repeated analysis of variance, with b-AQP0Fab versus vehicle one repeated measure and time as a second measure. Greenhouse-Geisser corrected values were used for epsilon values < 0.75. Bonferroni-corrected post-hoc multiple comparison tests were carried out where needed. Comparisons of the optical quality of the lenses, and of nearest neighbour values were assessed using paired t-tests. For all statistical tests, results were considered significant at $p \leq 0.05$.

5.4 RESULTS

Lenses of both b-AQP0Fab-treated and control eyes of intravitreally injected 7-day-old birds showed predominantly negative spherical aberrations during 1 hour, 2 hour, 4 hour, and 8 hour time points (Fig. V-2). Additionally, the pattern of spherical aberration remained largely negative for all three physiological states of accommodation, where paraxial rays were shorter than those of the periphery. Within the 4 hour group, 1 pair of lenses demonstrated positive spherical aberration (data not shown), causing the peripheral eccentricities of the 4 hour time point back vertex focal lengths (BVFLs) averages to taper positively (Fig. V-2C). Lenses undergoing accommodative stimulation demonstrated a trend towards a higher degree of negative spherical aberration for 1 hour, 2 hour, and negativity for spherical aberrations were observed within the physiological states of these groups (Fig. V-3, 1 hour: $p = 0.0921$; 2 hour: $p = 0.8352$; 4 hour: $p = 0.9701$; 8 hour: $p = 0.8003$). Spherical
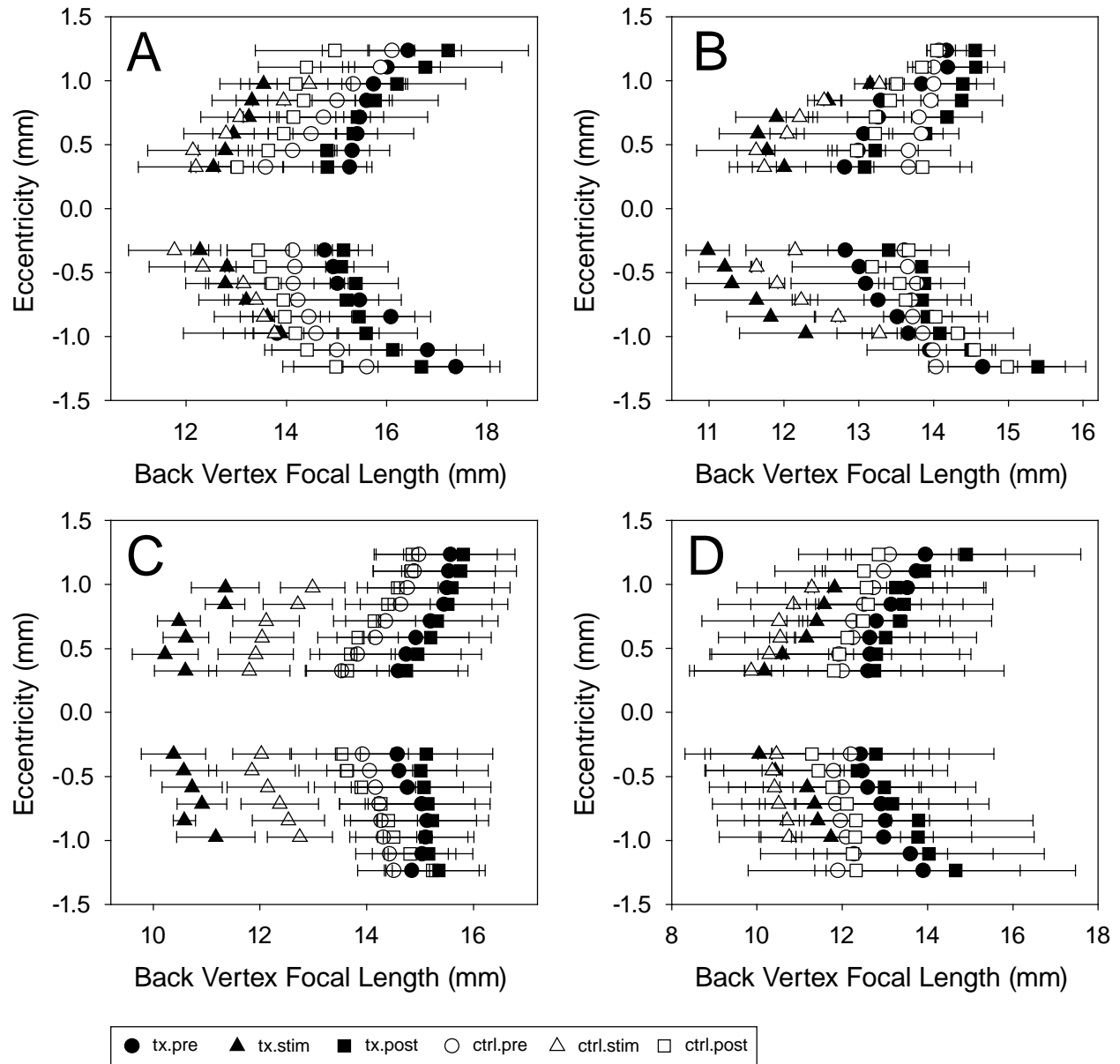
Figure V-2: Mean back vertex focal lengths (± SEM) at various eccentricities of lenses from intravitreally injected eyes. (A) 1 hour, (B) 2 hours, (C) 4 hours, and (D) 8 hours after treatments. Lenses from treated (filled) and control (empty) eyes were scanned prior to stimulation (circle), during stimulation (triangle), and after stimulation (square).

aberrations were measured with a pupil size of 1.95 mm.

Assessment of the mean back vertex focal lengths demonstrated that changes in focal lengths for both treated and control eyes were shorter during ciliary nerve stimulation for the 1 hour, 2 hour,
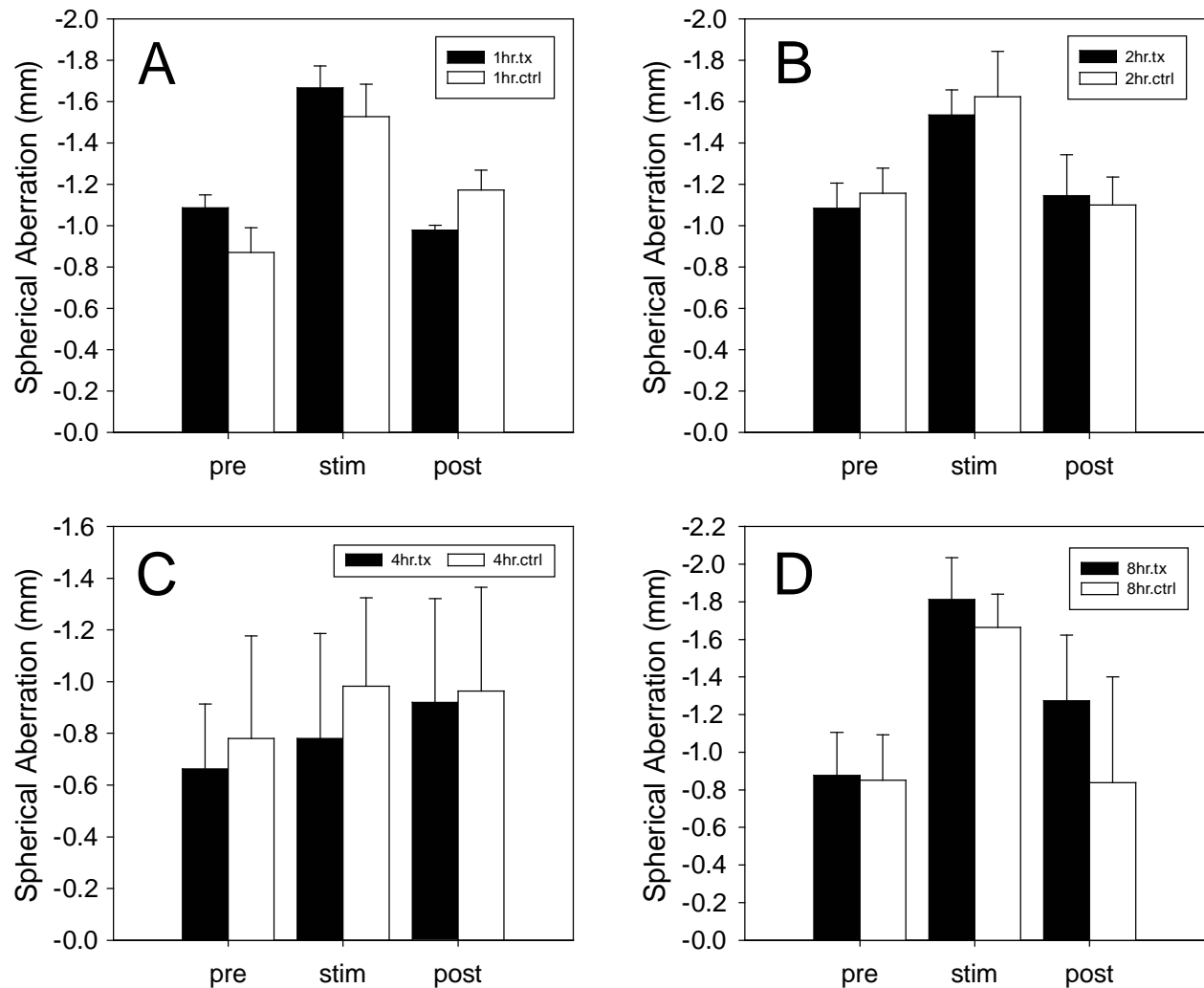
Figure V-3: Mean spherical aberrations (± SEM) of lenses from intravitreally injected eyes after (A) 1 hour, (B) 2 hour, (C) 4 hour, and (D) 8 hour treatments. Note the general increase in negative spherical aberration during stimulation compared to pre- and post- accommodation values for 1 hour, 2 hour, and 8 hour time point groups.

and 4 hour groups (Fig. V-4); however, ADC-associated differences in focal lengths were observed only in the 4 hour group (Fig. V-4C). At 1 hour, both treated and control eyes demonstrated shorter focal lengths during stimulation than at resting states (treated eye at rest vs. during stimulation: 15.24 ±0.51 mm vs. 13.31 ± 0.54 mm, respectively, p = 0.0265; control eyes at rest vs. during stimulation: 14.42 ± 1.07 vs. 13.04 ± 0.91 mm, respectively, p = 0.0312; Fig. V-4A), however, no differences were observed as a result of treatment (p = 0.7110). Similarly, at 2 hours, stimulated
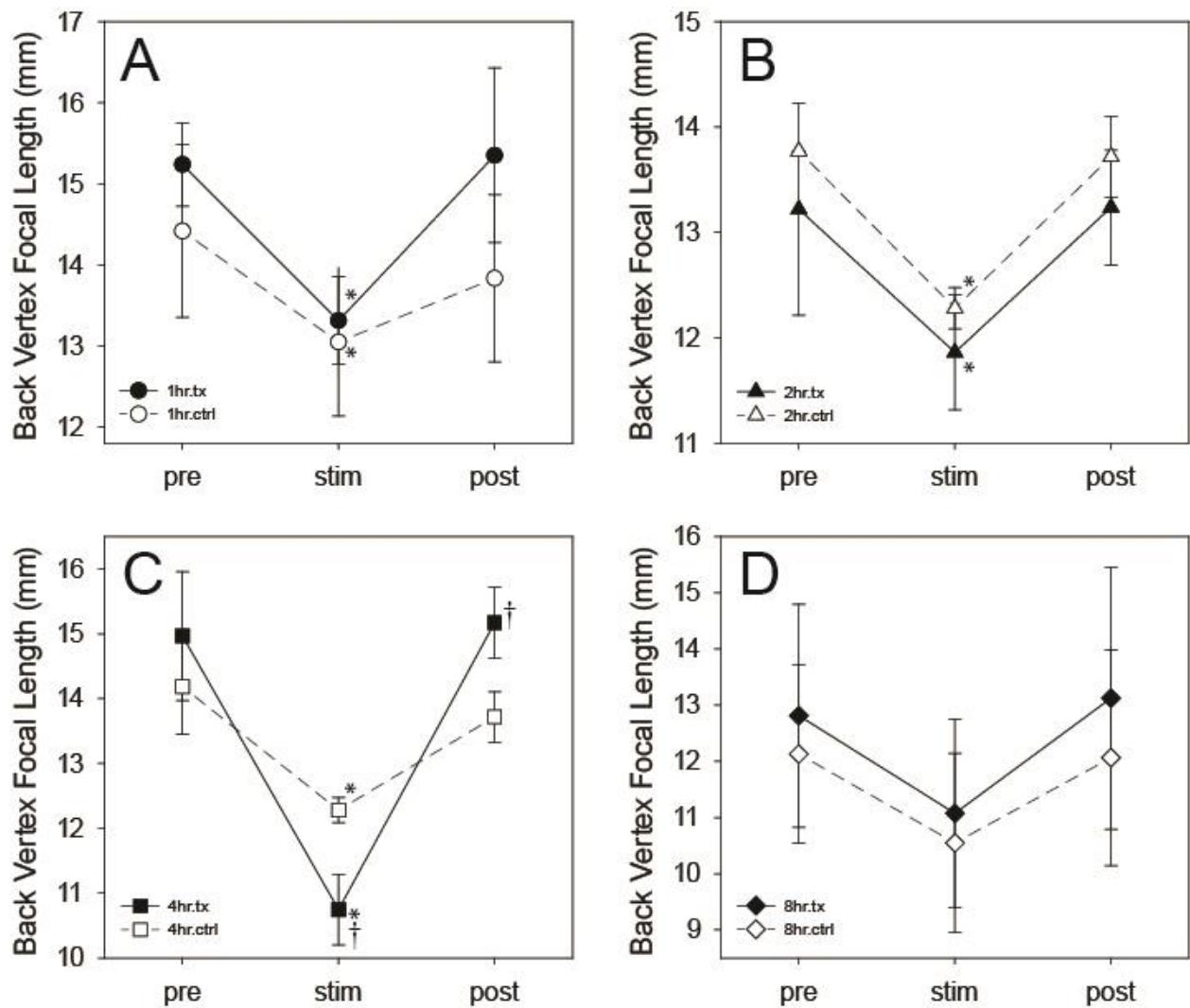
Figure V-4: Mean back vertex focal lengths (±SEM) of lenses from intravitreally injected eyes (A) 1 hour, (B) 2 hours, (C) 4 hours, and (D) 8 hours after treatment. For each eye, asterisks denote a significant change in focal lengths compared to the pre-stimulation state, while daggers represent significant differences between treated (filled symbol) and control (empty symbol) samples at that physiological state.

eyes in both treated and control groups demonstrated shorter focal lengths when compared to their resting states (treated eye at rest vs. during stimulation: 13.77 ± 0.71 mm vs. 12.28 ± 0.20 mm, respectively, $p = 0.0227$; control eyes at rest vs. during stimulation: 13.22 ± 1.00 mm vs. 11.86 ± 0.55 mm, respectively, $p = 0.0419$; Fig. V-4B). At 4 hours, both treated and control eyes also demonstrated shorter focal lengths during stimulation than at resting states (treated eye at rest vs.

127

during stimulation: 14.97 ± 0.99 mm vs. 10.75 ± 0.55 mm, respectively, p = 0.0519; control eyes at rest vs. during stimulation: 14.19 ± 0.74 mm vs. 12.28 ± 0.20 mm, respectively, p = 0.0321; Fig. V-4C), however, a significant decrease in focal length was demonstrated during stimulation as a result of treatment (compare 10.75 ± 0.55 mm to 12.28 ± 0.99 mm; p = 0.0346; Fig. V-4C). Furthermore, during the recovery state, focal lengths of treated eyes were significantly longer than those of control eyes (compare 15.17 mm $\pm$ 0.54 to 13.72 ± 0.39 mm; p = 0.0431; Fig. V-4C). At 8 hours, no changes in the focal lengths of both treated and control eyes were observed during stimulation than at resting state (treated eye at rest vs. during stimulation: 12.81 ± 1.98 mm vs. 11.07 ± 1.68 mm, respectively, p = 0.2814; control eyes at rest vs. during stimulation: 12.13 ± 1.56 mm vs. 10.55 ± 0.50 mm, respectively, p = 0.0358; Fig. V-4D). No changes in focal lengths were observed as a result of treatment in this group (p = 0.5613).

After 1 hour of b-AQP0Fab treatment, birds exhibited a slight increase in accommodative and recovery amplitudes (treated eye accommodation vs. recovery: 14.44 ± 1.68 D vs. 10.21 ± 1.36 D, respectively, p = 0.0212; control eyes accommodation vs. recovery: 14.65 ± 0.74 D vs. 6.14 ± 1.29 D, respectively, p = 0.0013; Fig. V-5A), however, after 2 hours of b-AQP0Fab treatment, the increase in amplitudes was no longer observed (treated eye accommodation vs. recovery: 11.03 ± 1.27 D vs. 12.05 ± 1.27 D, respectively, p = 0.531; control eyes accommodation vs. recovery: 12.56 ± 1.38 D vs. 10.18 ± 1.14 D, respectively, p = 0.117; Fig. V-5B). Birds treated with 4 hours of b-AQP0Fab exhibited a large increase in both amplitudes of accommodation and recovery when compared to control groups (treated eye accommodation vs. recovery: 34.89 ± 0.85 D vs. 15.09 ± 0.61 D, respectively, p = 0.0021; control eyes accommodation vs. recovery: 35.70 ± 0.99 D vs. 13.98 ± 0.48 D, respectively, p = 0.0015; Fig. V-5C). However, after 8 hours of treatment, no changes in the amplitudes of accommodation and recovery were observed (treated eye accommodation vs.
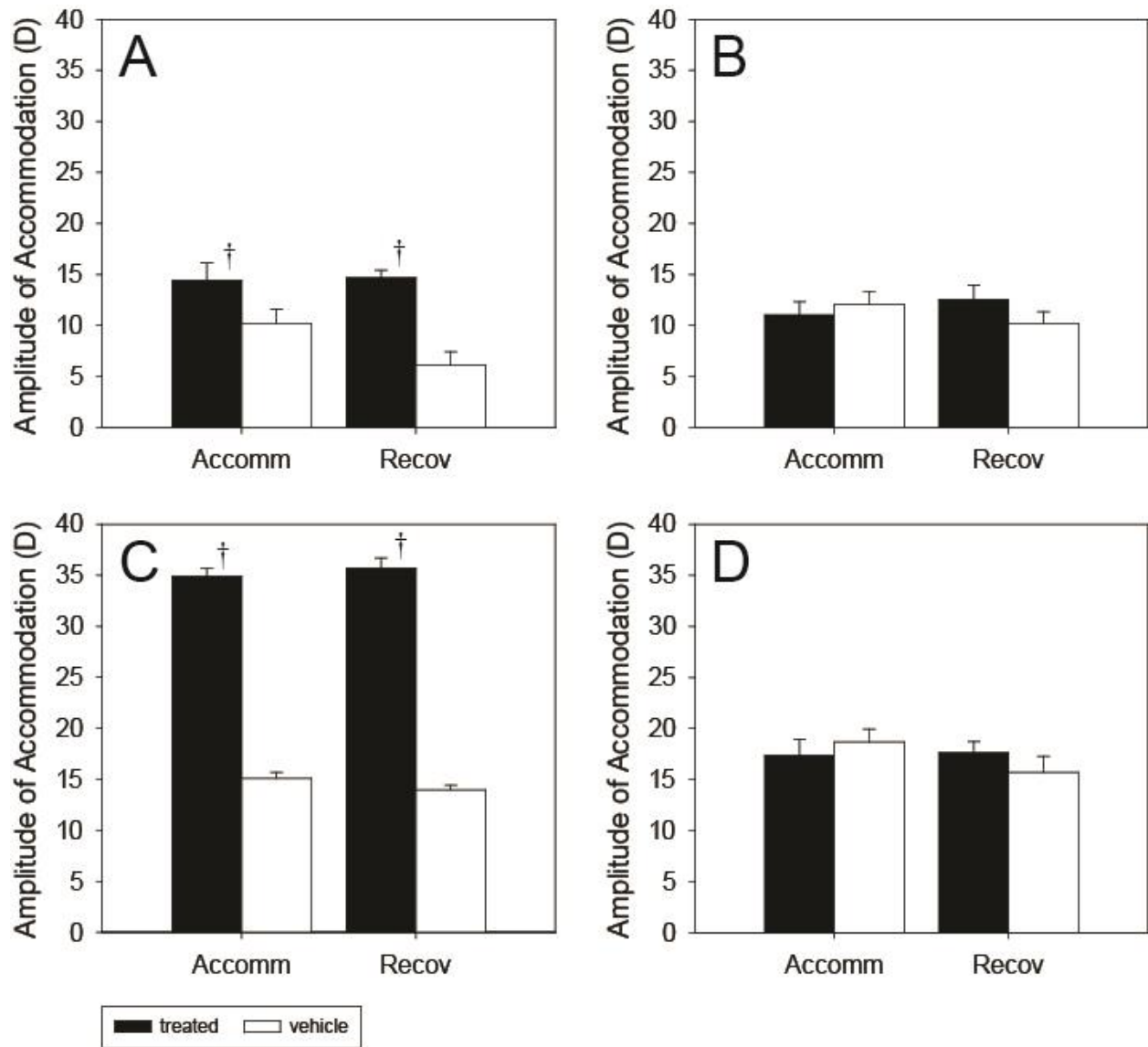
Figure V-5: Mean accommodative and recovery amplitudes (±SEM). Treated lenses (filled bars) and their controls (empty bars) at (A) 1 hour, (B) 2 hour, (C) 4 hour, and (D) 8 hour time points. Daggers denote a significant difference in accommodation or recovery amplitudes between the eyes.

recovery: 17.33 ± 1.62 D vs. 18.66 ± 1.26 D, respectively, $p = 0.386$; control eyes accommodation vs. recovery: 17.63 ± 1.09 D vs. 15.68 ± 1.59 D, respectively, $p = 0.4382$; Fig. V-5D)

To assess the overall specificity and efficacy of b-AQP0Fab, Western blot analysis of lens tissue, as well as various tissues surrounding the lens (cornea, ciliary body, and retina), was

conducted (Fig. V-6) following intravitreal injection of 7-day-old birds with the ADC. As the 4 hour time point was most effective during the accommodation studies, tissues from the 4 hour group were used for the Western blot. Band intensities of myosin heavy chain 9 (MYH9) concentrations were found to be substantially lower in lenticular tissues treated with b-AQP0Fab (10.62 ± 0.40) compared to corneal, ciliary body, and retinal tissues of eyes treated with b-AQP0Fab (33.01 ± 2.47, 35.75 ± 2.09, 30.37 ± 1.89, respetively); untreated retinal tissue had a 90.5% MYH9 to β-actin percentage ratio, while treated lenticular tissue had a 23.3% MYH9 to β-actin percentage ratio. In positive control samples of retinal and lenticular tissues (See Fig. A-1 in appendix), band intensities of MYH9 concentrations were found to be similar, and similarly proportional to β-actin levels (80.5% vs. 70.2% MYH9 to β-actin percentage ratio, respectively; Fig. A-1). Together, these
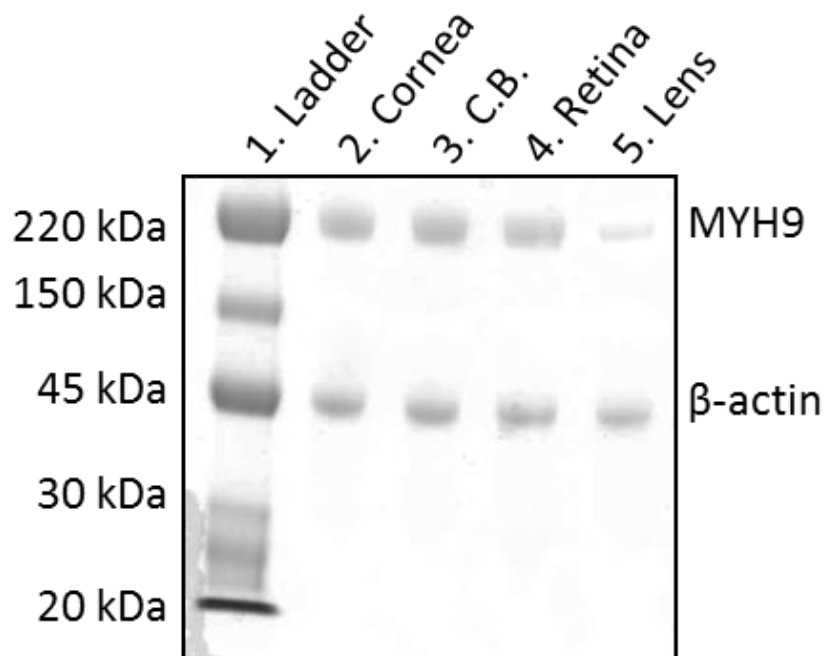
Figure V-6: Western blot of myosin heavy chain 9 (MYH9) levels in corneal, ciliary body (C.B.), retinal and lenticular tissues treated with b-AQP0Fab. Lane 1: molecular weight marker, lane 2: corneal tissue sample, lane 3: ciliary body tissue sample, lane 4: retinal tissue sample, and lane 5: lenticular tissue sample. β-actin was used as a loading control.

results suggest that only lenticular tissue was affected.

Eyes treated with FITC-labeled b-AQP0Fab demonstrated staining specific to the nasal (Fig. V-7A) and temporal (Fig. V-7C) regions of the lens, immediately underneath the capsule, compared to lenses treated with FITC isolate only (data not shown). Eyes counterstained with Texas Red-phalloidin demonstrated the presence of the ciliary body in the same nasal (Fig. V-7B) and temporal (Fig. V-7D) regions of the anterior segment.

Confocal microscopy of lenses treated with b-AQP0Fab demonstrated a substantial loss of myosin organization when compared to control lenses (Fig V-8A and B vs. Fig. V-8C and D, respectively). Nearest neighbour analysis showed that lenses treated with b-AQP0Fab resulted in the dissolution and disorganization of myosin bundles ($R_n = 1.53 \pm 0.16$) when compared to myosin bundles within the control lens (Fig. V-8A and B, $R_n = 2.07 \pm 0.02$, $p = 0.0213$). The hexagonal arrangements of filamentous actin between treated (2.05 ± 0.02) and control lenses (2.05 ± 0.02), however, remained unaffected (Fig. V-8C and D, $p = 0.6747$).

5.5 DISCUSSION

In previous studies (Choh, 2001; Priolo, Sivak, & Kuszak, 1999a; Schaeffel, Glasser, & Howland, 1988), it was demonstrated that emmetropic 7-day-old chicks lenses were non-monotonic and spherical aberrations were negative. Additionally, the lenses maintained negative spherical aberrations during physiological accommodative stimulation and recovery. In the present study, optical scans performed on the anterior segments of 7-day-old chick eyes confirmed these optical traits; except for one pair of eyes (one treated and one control eye) within the 4 hour treatment group, lenses across all time points exhibited negative spherical aberration during all three

131
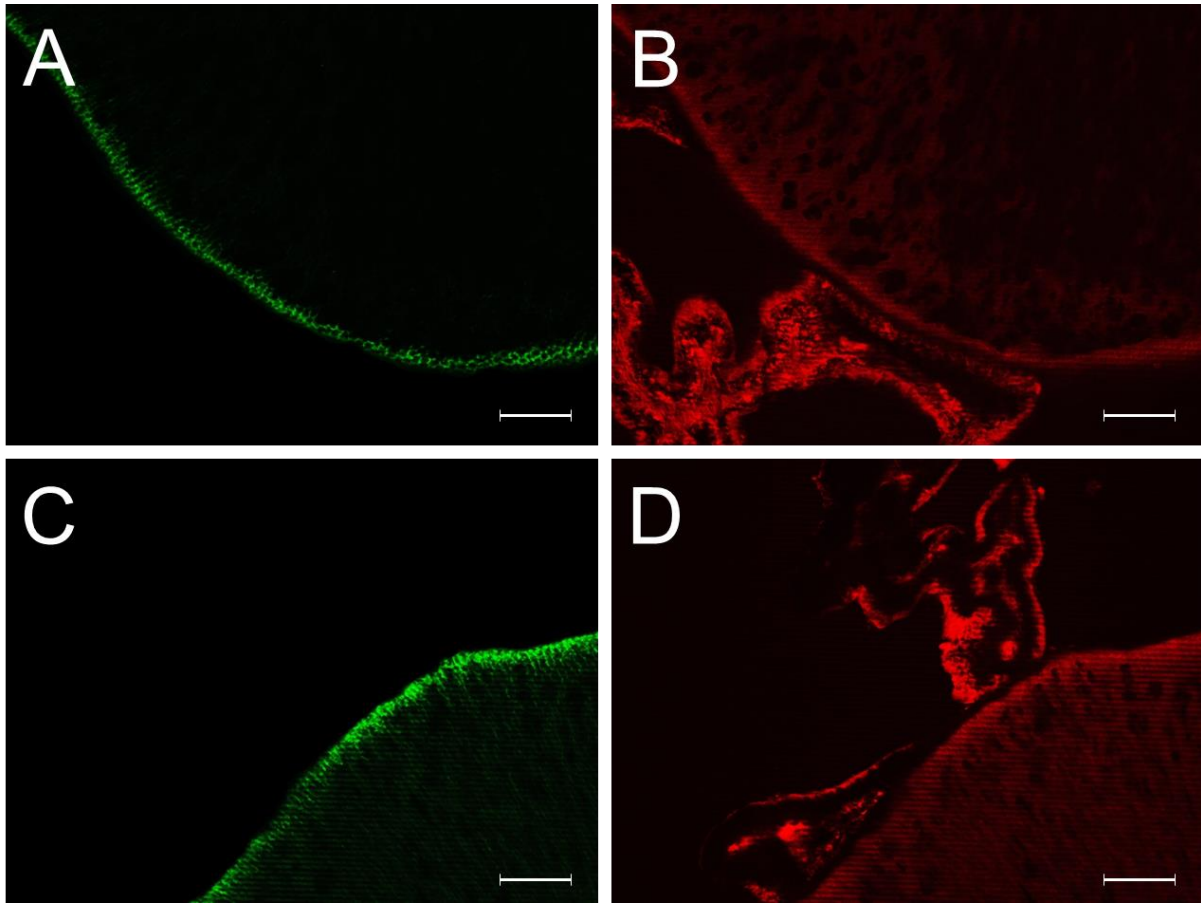
Figure V-7: Light micrographs of lenses treated with FITC-conjugated b-AQP0Fab. FITC-conjugated b-AQP0Fab (green) presence at the anterior (A) nasal, and (B) temporal regions of the lens vs. actin (red) presence at the anterior (A) nasal, and (B) temporal regions of the lens. Scale bars = 100 μm.

physiological states. It is speculated that the bird with positively aberrated lenses had a developmental defect within its lenses. Although the eye of the developing chicken has never been observed to produce a positive spherical aberration (Choh & Sivak, 2000b; V. Choh et al., 2002; Priolo et al., 1999a; West, Sivak, & Doughty, 1991), positively aberrated lenses have been observed in humans as they age (Amano et al., 2004; Guirao, Redondo, & Artal, 2000; McLellan, Marcos, & Burns, 2001), therefore it is possible that a shape or gradient refractive index anomaly existed in this bird. Alternatively, as this pair of eyes was the first in the experiment to be assessed, it is possible
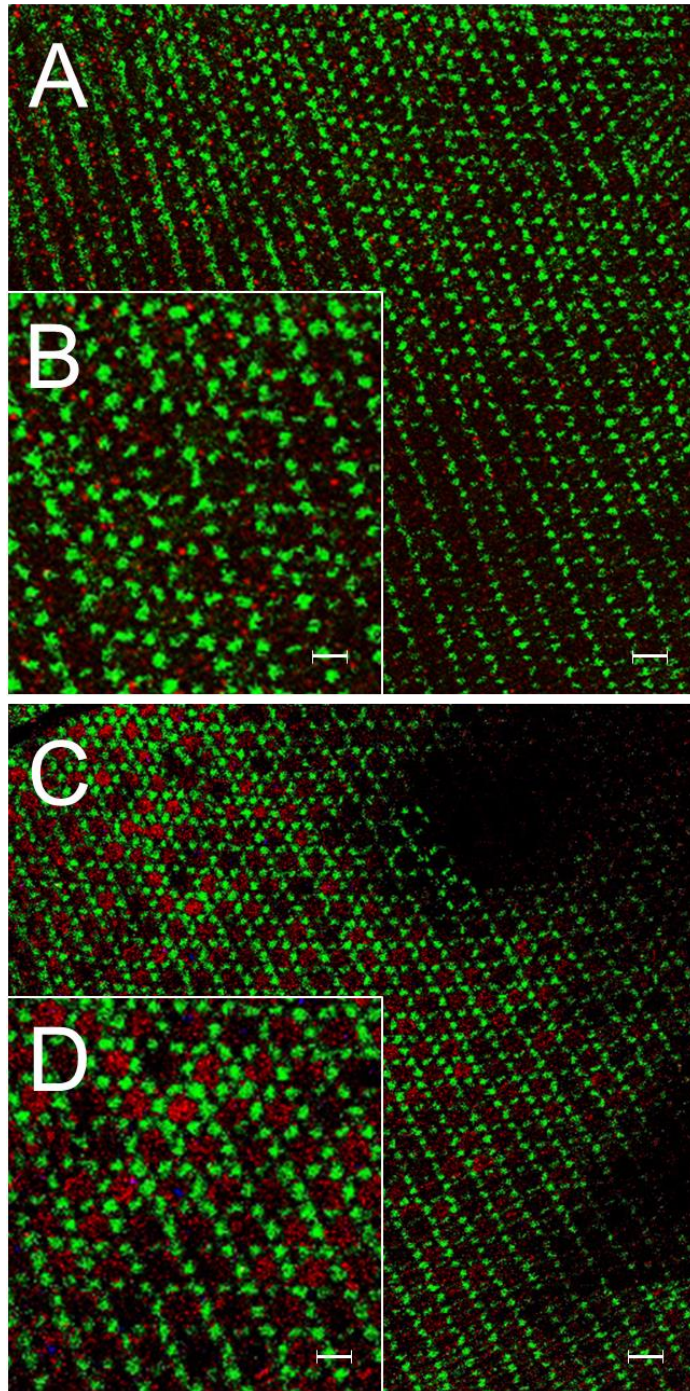
Figure V-8: Confocal micrographs of lens basal membrane complexes after intravitreal injection. (A) b-AQP0Fab, (B) 2x magnification of A, (C) vehicle, and (D) 2x magnification of C. Actin stained in green, myosin stained in red. Scale bars, 10µM for A and C, 5µM for B and D.

that the anterior segment was damaged during the dissection process, although visual inspection of the segments did not indicate any apparent damage. It should be noted that removal from the data of the first pair of eyes did not result in a significant change in the degree of spherical aberration,

however, the trend of increased spherical aberration during stimulation was now apparent for the 4 hour group (compare Fig. V-9A and B), much like the trend observed for other time points (Fig. V-3A, B, and D). Additionally, removal of the data from the aberrant bird did not result in a different statistical result for accommodation and recovery amplitudes between treated and control eyes (treated eye accommodation vs. recovery: 26.49 ± 0.76 D vs. 12.54 ± 0.66 D, respectively, p = 0.0158; control eyes accommodation vs. recovery: 26.94 ± 0.95 D vs. 11.13 ± 0.56 D, respectively, p = 0.0124; compare Fig. V-9C vs. Fig. V-9D). Furthermore, the mean accommodative amplitudes for the 4 hour group were still greater than those for the 1, 2 and 8 hour groups (compare Fig V-9 D with Fig. V-5A, B, and D).

Assessment of mean back vertex focal lengths demonstrated that b-AQP0Fab was most effective at 4 hours. As the function of b-AQP0Fab is to soften the lens, a shortening of the focal lengths during accommodation is to be expected. Furthermore, assessment of focal lengths post-stimulation indicated that treated eyes recovered significantly more than control eyes, although, it should be noted that smaller standard errors were also observed for the post-stimulation values. An increase in focal length at rest might be expected with a softer lens, as the same amount of tension exerted by the zonules on the lens would be expected to result in a flatter surface curvature of the lens, and ultimately less refraction in softer than harder lenses (Maggs, Miller, & Ofri, 2012). In the 8 hour group, the lack of significance in focal lengths between physiological states of both treated and control eyes can be attributed to the large amount of variation between measurements, as stimulation of 7-day old birds has been previously shown to demonstrate significant differences in focal length (Choh & Sivak, 2000a). Alternatively, intravitreal injection of PBS may have a long-term effect on the accommodative mechanism, as it has been shown that Rhesus monkeys injected with saline demonstrate a slight decrease in accommodation compared to no injection (Ostrin,
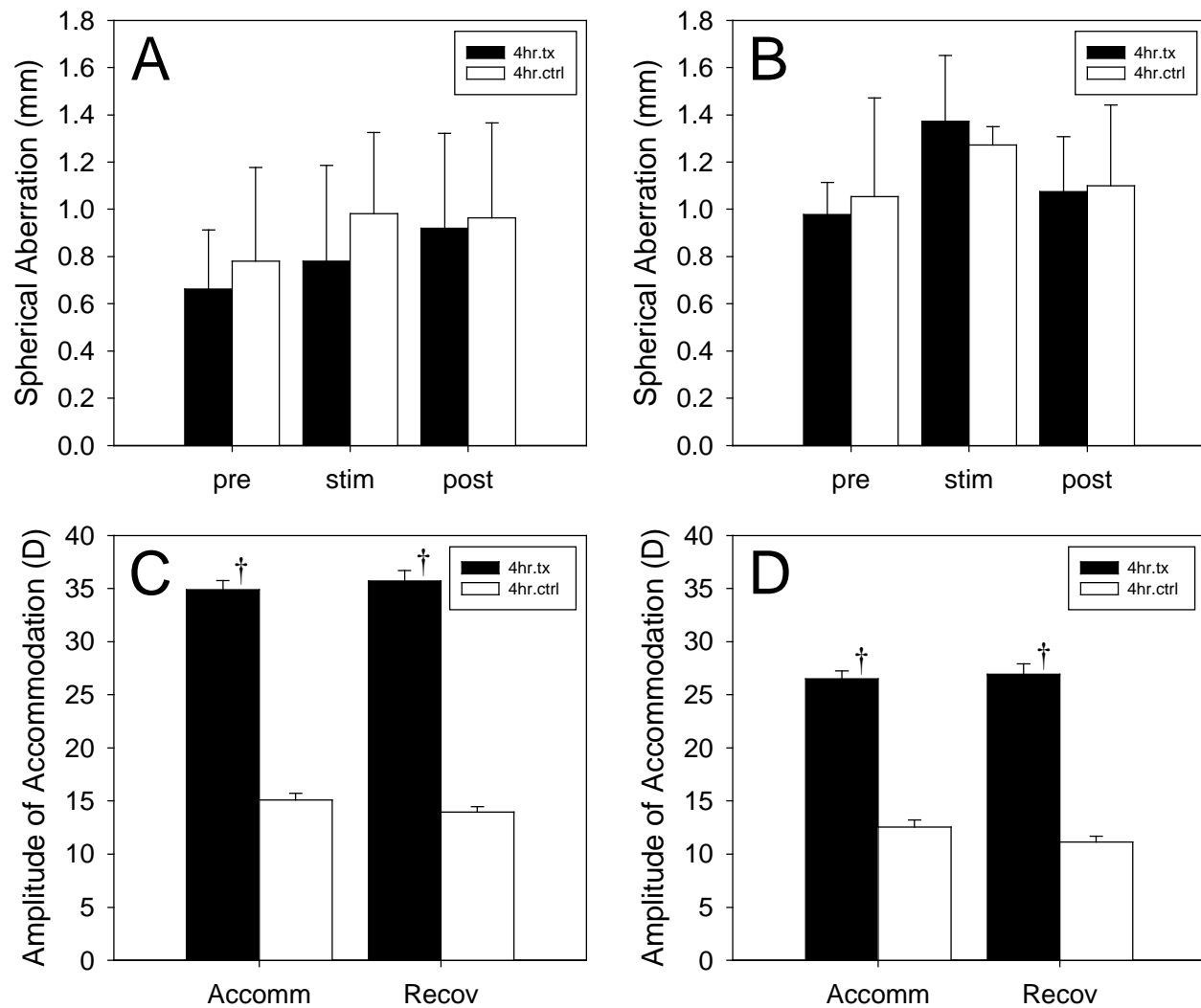
Figure V-9: Comparison of mean spherical aberration and accommodation/recovery amplitude charts at 4 hours. Mean spherical aberrations with (A) and without (B) the first pair of data. Accommodation and recovery charts with (C) and without (D) the first pair of data.

Frishman, & Glasser, 2004).

In a previous study, unbound blebbistatin (at similar concentrations), was demonstrated to soften the lens *in vitro* 15 minutes after treatment (Won et al., 2015) (Chapter 3). Upon removal of the lens from treatment, the lens returned to its initial stiffness state after an hour of equilibration. In the present study, the effects of ADC-associated blebbistatin were not observed *in situ* until 4 hours

after intravitreal injection, indicating that crosslinker cleavage and subsequent tissue saturation with blebbistatin takes approximately that amount of time. Furthermore, clearance of blebbistatin from lenticular tissue and tissue reversibility was demonstrated, as 8 hour treatment groups no longer produced changes in accommodation.

To assess the *in vivo* specificity of b-AQP0Fab after intravitreal injection of the ADC, Western blot analysis was conducted on various ocular tissues to determine myosin heavy chain 9 (MYH9) levels. As the TPAAVRGTLGLSALHPSVG peptide sequence only occurs in the external region of aquaporin-0 (AQP0), and AQP0 water channels only occur in lens fibre cells, the TPAAVRGTLGLSALHPSVG recognition site of b-AQP0Fab should specifically target the lens. As expected, MYH9 levels of lenticular tissue treated with b-AQP0Fab were significantly lower than those of corneal, ciliary body, and retinal tissues, indicating the functional specificity of the ADC to the lens. Furthermore, although other aquaporins that occur ubiquitously throughout the eye have similar homologies to AQP0, b-AQP0Fab did not appear to target their peptide sequences. It should be noted that only tissues within the immediate vicinity of the lens were investigated for adverse reactions. Although further tissues are not expected to be affected by the direct mechanism of b-AQP0Fab, unbound b-AQP0Fab that is expelled systemically, may inadvertently be cleaved, and result in effects on tissue outside of the eye; however, due its concentration, the effects are likely to be minimal. Western blot analyses at various time points and locations are required to further characterize the effects of b-AQP0Fab on ocular tissue.

Light microscopy demonstrated that b-AQP0Fab was specific to lenticular tissue and was able to penetrate the lens capsule, although the penetration depth was not extensive. The shallow penetration of b-AQP0Fab is speculated to be as a result of the large size of the total molecule (approximately 51kDa). Because b-AQP0Fab has a theoretical isoelectric point of 9.1, which is

slightly higher than the pH of the crystalline lens (approximately 7.4), it carries a net positive charge, which has been shown to be beneficial in permeating the lens capsule (Lee et al., 2006). As further digestion of AQP0Fab would eliminate all possible conjugation sites, the size of the ADC can no longer be diminished, therefore, the charge of b-AQP0Fab must be increased in order to optimize penetration. The effect of conjugated blebbistatin (in b-AQP0Fab; Fig. V-9A and B) was found to disrupt the actomyosin distribution of the lens BMC differently than that of unconjugated blebbistatin (Fig. III-6C and D); with b-AQP0Fab treatment, the actin distribution was not found to be affected, however, unconjugated blebbistatin caused a large disruption of both actin and myosin arrays. This difference is speculated to be due to the amount of effective free blebbistatin in solution after treatment, as conjugation of blebbistatin may result in attenuation with or without cleavage of the crosslinker.

In summary, it was found that intravitreal injection of b-AQP0Fab resulted in a significant increase in the amplitude of accommodation and recovery in 7-day-old birds after 4 hours of incubation. Furthermore, Western blot analysis and light microscopy demonstrated a high specificity of b-AQP0Fab to lens tissue, while exhibiting low to no affinity to other ocular tissues. Finally, confocal micrographs revealed that blebbistatin disrupted the actomyosin lattice of the lens basal membrane complex by breaking down the organization of myosin filaments.

VI. CONCLUSION

The findings in this thesis demonstrate that a treatment for the physiological cause of presbyopia is possible; however, pharmacokinetic modelling of b-AQP0Fab is required to determine the drug concentration-time courses in body fluids after its administration. Along with the pharmacodynamics of b-AQP0Fab observed in this thesis, a dose-concentration-response relationship may be established to ultimately predict the effect-time of the ADC after administration (Meibohm & Derendorf, 1997).

In order to translate b-AQP0Fab for use in human eyes, an iteration of the ADC must be synthesized to target the mammalian lens. As the aquaporin-0 (AQP0) water channel that occurs in mammals has a different peptide sequence, an analysis of optimal peptide sequences is once again required in order to synthesize anti-peptides capable of targeting the mammalian lens. Additionally, the long-term effects of binding antibodies to AQP0 must be investigated as it has been demonstrated that the knockout of AQP0 in mice results in significant changes to the lenticular refractive index as well as lens biomechanics (Sindhu Kumari et al., 2015). Furthermore, although the binding of anti-AQP0 to AQP0 did not result in a change in lens integrity, it has been shown that a decrease in AQP0 permeability could reduce fluid fluxes during the shape changes of accommodation, potentially contributing to presbyopia (Gerometta & Candia, 2016). Therefore, using the experimental principles outlined in this thesis, the development of an antibody-drug conjugate to specifically target and soften the crystalline lens in humans is possible; however, several translational milestones must be met in order for this targeted therapy to be successfully realized.

LETTERS OF COPYRIGHT PERMISSIONS

FIGURE II-12 & FIGURE II-13

SINAUER ASSOCIATES, Inc. • Publishers • P.O. Box 407, 23 Plumtree Rd. • Sunderland, MA 01375

Telephone: (413) 549-4300
Fax: (413) 549-1118
Email: permissions@sinauer.com

PERMISSIONS AGREEMENT

September 19, 2016

Permission granted to:
Gah-Jone Won
School of Optometry
University of Waterloo
200 University Avenue West
Waterloo, ON N2L 3G1
CANADA

Email: gwon@uwaterloo.ca

Material to be reproduced:
Oyster: *The Human Eye*
Figure 1.8, page 66 and Figure 1.12, page 69

To be reproduced in the work:
Gah-Jone Won's PhD Thesis entitled "The development of an antibody-drug conjugate to specifically target and soften the crystalline lens *in vivo*" to be published by the University of Waterloo

Sinauer Associates owns copyright to the material described above and hereby grants permission for the one-time use of the material as specified, and for nonexclusive world rights provided that full and appropriate credit is given to the original source and that the work is for NON-COMMERCIAL use only. Please request permission for further use in subsequent editions, translations, or revisions of the work.

Sherri L. Ellsworth   ___September 19, 2016___
Sherri L. Ellsworth   Date
Permissions Coordinator

Please acknowledge your acceptance of these terms by signing one copy of this form and returning it to Sinauer Associates. **Permission Agreement is not valid until signed by applicant and received by Sinauer Associates.**

Signature of Applicant   Oct 4th, 2016
                                          Date

FIGURE II-14

This Agreement between University of Waterloo -- Gah-Jone Won ("You") and Springer ("Springer") consists of your license details and the terms and conditions provided by Springer and Copyright Clearance Center.

License Number	3962050208070
License date	Oct 04, 2016
Licensed Content Publisher	Springer
Licensed Content Publication	Journal of Membrane Biology
Licensed Content Title	The Lens Circulation
Licensed Content Author	Richard T. Mathias
Licensed Content Date	Jan 1, 2007
Licensed Content Volume Number	216
Licensed Content Issue Number	1
Type of Use	Thesis/Dissertation
Portion	Figures/tables/illustrations
Number of figures/tables/illustrations	1
Author of this Springer article	No
Order reference number	
Original figure numbers	Figure 3A
Title of your thesis / dissertation	The Development of an Antibody-Drug Conjugate to Specifically Target and Soften the Crystalline Lens in vivo

Expected completion date	Nov 2016
Estimated size(pages)	215
Requestor Location	University of Waterloo
	200 University Avenue West
	University of Waterloo
	Waterloo, ON N2L3G1
	Canada
	Attn: University of Waterloo
Billing Type	Invoice
Billing Address	University of Waterloo
	200 University Avenue West
	University of Waterloo
	Waterloo, ON N2L3G1
	Canada
	Attn: Gah-Jone Won
Total	0.00 CAD

Terms and Conditions

Introduction

The publisher for this copyrighted material is Springer. By clicking "accept" in connection with completing this licensing transaction, you agree that the following terms and conditions apply to this transaction (along with the Billing and Payment terms and conditions established by Copyright Clearance Center, Inc. ("CCC"), at the time that you opened your Rightslink account and that are available at any time at http://myaccount.copyright.com).

Limited License

With reference to your request to reuse material on which Springer controls the copyright, permission is granted for the use indicated in your enquiry under the following conditions:

- Licenses are for one-time use only with a maximum distribution equal to the

number stated in your request.

- Springer material represents original material which does not carry references to other sources. If the material in question appears with a credit to another source, this permission is not valid and authorization has to be obtained from the original copyright holder.

- This permission

  • is non-exclusive

  • is only valid if no personal rights, trademarks, or competitive products are infringed.

  • explicitly excludes the right for derivatives.

- Springer does not supply original artwork or content.

- According to the format which you have selected, the following conditions apply accordingly:

  • **Print and Electronic:** This License include use in electronic form provided it is password protected, on intranet, or CD-Rom/DVD or E-book/E-journal. It may not be republished in electronic open access.

  • **Print:** This License excludes use in electronic form.

  • **Electronic:** This License only pertains to use in electronic form provided it is password protected, on intranet, or CD-Rom/DVD or E-book/E-journal. It may not be republished in electronic open access.

  For any electronic use not mentioned, please contact Springer at permissions.springer@spi-global.com.

- Although Springer controls the copyright to the material and is entitled to negotiate on rights, this license is only valid subject to courtesy information to the author (address is given in the article/chapter).

- If you are an STM Signatory or your work will be published by an STM Signatory and you are requesting to reuse figures/tables/illustrations or single text extracts, permission is granted according to STM Permissions Guidelines: http://www.stm-assoc.org/permissions-guidelines/

  For any electronic use not mentioned in the Guidelines, please contact Springer

at permissions.springer@spi-global.com. If you request to reuse more content than stipulated in the STM Permissions Guidelines, you will be charged a permission fee for the excess content.

Permission is valid upon payment of the fee as indicated in the licensing process. If permission is granted free of charge on this occasion, that does not prejudice any rights we might have to charge for reproduction of our copyrighted material in the future.
-If your request is for reuse in a Thesis, permission is granted free of charge under the following conditions:
This license is valid for one-time use only for the purpose of defending your thesis and with a maximum of 100 extra copies in paper. If the thesis is going to be published, permission needs to be reobtained.
- includes use in an electronic form, provided it is an author-created version of the thesis on his/her own website and his/her university's repository, including UMI (according to the definition on the Sherpa website: http://www.sherpa.ac.uk/romeo/);
- is subject to courtesy information to the co-author or corresponding author.

Geographic Rights: Scope
Licenses may be exercised anywhere in the world.

Altering/Modifying Material: Not Permitted
Figures, tables, and illustrations may be altered minimally to serve your work. You may not alter or modify text in any manner. Abbreviations, additions, deletions and/or any other alterations shall be made only with prior written authorization of the author(s).

Reservation of Rights
Springer reserves all rights not specifically granted in the combination of (i) the license details provided by you and accepted in the course of this licensing transaction and (ii) these terms and conditions and (iii) CCC's Billing and Payment terms and conditions.

License Contingent on Payment

While you may exercise the rights licensed immediately upon issuance of the license at the end of the licensing process for the transaction, provided that you have disclosed complete and accurate details of your proposed use, no license is finally effective unless and until full payment is received from you (either by Springer or by CCC) as provided in CCC's Billing and Payment terms and conditions. If full payment is not received by the date due, then any license preliminarily granted shall be deemed automatically revoked and shall be void as if never granted. Further, in the event that you breach any of these terms and conditions or any of CCC's Billing and Payment terms and conditions, the license is automatically revoked and shall be void as if never granted. Use of materials as described in a revoked license, as well as any use of the materials beyond the scope of an unrevoked license, may constitute copyright infringement and Springer reserves the right to take any and all action to protect its copyright in the materials.

Copyright Notice: Disclaimer

You must include the following copyright and permission notice in connection with any reproduction of the licensed material:

"Springer book/journal title, chapter/article title, volume, year of publication, page, name(s) of author(s), (original copyright notice as given in the publication in which the material was originally published) "With permission of Springer"

In case of use of a graph or illustration, the caption of the graph or illustration must be included, as it is indicated in the original publication.

Warranties: None

Springer makes no representations or warranties with respect to the licensed material and adopts on its own behalf the limitations and disclaimers established by CCC on its behalf in its Billing and Payment terms and conditions for this licensing transaction.

Indemnity

You hereby indemnify and agree to hold harmless Springer and CCC, and their respective officers, directors, employees and agents, from and against any and all claims arising out of your use of the licensed material other than as specifically authorized pursuant to this license.

No Transfer of License
This license is personal to you and may not be sublicensed, assigned, or transferred by you without Springer's written permission.
No Amendment Except in Writing
This license may not be amended except in a writing signed by both parties (or, in the case of Springer, by CCC on Springer's behalf).

Objection to Contrary Terms
Springer hereby objects to any terms contained in any purchase order, acknowledgment, check endorsement or other writing prepared by you, which terms are inconsistent with these terms and conditions or CCC's Billing and Payment terms and conditions. These terms and conditions, together with CCC's Billing and Payment terms and conditions (which are incorporated herein), comprise the entire agreement between you and Springer (and CCC) concerning this licensing transaction. In the event of any conflict between your obligations established by these terms and conditions and those established by CCC's Billing and Payment terms and conditions, these terms and conditions shall control.

Jurisdiction
All disputes that may arise in connection with this present License, or the breach thereof, shall be settled exclusively by arbitration, to be held in the Federal Republic of Germany, in accordance with German law.

Other conditions:
V 12AUG2015

FIGURE II–15A

Association for Research in Vision and Ophthalmology LICENSE TERMS AND CONDITIONS

Feb 12, 2017

This is a License Agreement between University of Waterloo -- Gah-Jone Won ("You") and Association for Research in Vision and Ophthalmology ("Association for Research in Vision and Ophthalmology") provided by Copyright Clearance Center ("CCC"). The license consists of your order details, the terms and conditions provided by Association for Research in Vision and Ophthalmology, and the payment terms and conditions.

All payments must be made in full to CCC. For payment instructions, please see information listed at the bottom of this form.

License Number	4044300697478
License date	Jan 29, 2017
Licensed content publisher	Association for Research in Vision and Ophthalmology
Licensed content title	Investigative ophthalmology
Licensed content date	Jan 1, 1977
Type of Use	Thesis/Dissertation
Requestor type	Academic institution
Format	Print, Electronic
Portion	image/photo
Number of images/photos requested	1
Title or numeric reference of the portion(s)	Figure 1

Title of the article or chapter the portion is from	Polygonal Arrays of Actin Filaments in Human Lens Epithelial Cells
Editor of portion(s)	N/A
Author of portion(s)	S Yeh; D L Scholz; W Liou; N S Rafferty
Volume of serial or monograph.	Volume 27
Issue, if republishing an article from a serial	Issue 10
Page range of the portion	1535-1540
Publication date of portion	October 1986
Rights for	Main product
Duration of use	Life of current edition
Creation of copies for the disabled	no
With minor editing privileges	yes
For distribution to	Worldwide
In the following language(s)	Original language of publication
With incidental promotional use	no
The lifetime unit quantity of new product	Up to 499
Made available in the following markets	Education/Academia
Specified additional information	Minor Editing Privileges
The requesting person/organization is:	Gah-Jone Won/University of Waterloo
Order reference number	
Author/Editor	Gah-Jone Won
The standard identifier of New Work	Thesis
The proposed price	Free
Title of New Work	The Development of an Antibody-Drug Conjugate to Specifically Target and Soften the Crystalline Lens in vivo

Publisher of New Work	University of Waterloo
Expected publication date	Apr 2017
Estimated size (pages)	215
Total (may include CCC user fee)	0.00 USD
Terms and Conditions	

TERMS AND CONDITIONS

The following terms are individual to this publisher:

None

Other Terms and Conditions:

A reprint of this material must include a full article citation and acknowledge ARVO as the copyright holder.

STANDARD TERMS AND CONDITIONS

1. Description of Service; Defined Terms. This Republication License enables the User to obtain licenses for republication of one or more copyrighted works as described in detail on the relevant Order Confirmation (the "Work(s)"). Copyright Clearance Center, Inc. ("CCC") grants licenses through the Service on behalf of the rightsholder identified on the Order Confirmation (the "Rightsholder"). "Republication", as used herein, generally means the inclusion of a Work, in whole or in part, in a new work or works, also as described on the Order Confirmation. "User", as used herein, means the person or entity making such republication.

2. The terms set forth in the relevant Order Confirmation, and any terms set by the Rightsholder with respect to a particular Work, govern the terms of use of Works in connection with the Service. By using the Service, the person transacting for a republication license on behalf of the User represents and warrants that he/she/it (a) has been duly authorized by the User to accept, and hereby does accept, all such terms and

148

conditions on behalf of User, and (b) shall inform User of all such terms and conditions. In the event such person is a "freelancer" or other third party independent of User and CCC, such party shall be deemed jointly a "User" for purposes of these terms and conditions. In any event, User shall be deemed to have accepted and agreed to all such terms and conditions if User republishes the Work in any fashion.

3. Scope of License; Limitations and Obligations.

3.1 All Works and all rights therein, including copyright rights, remain the sole and exclusive property of the Rightsholder. The license created by the exchange of an Order Confirmation (and/or any invoice) and payment by User of the full amount set forth on that document includes only those rights expressly set forth in the Order Confirmation and in these terms and conditions, and conveys no other rights in the Work(s) to User. All rights not expressly granted are hereby reserved.

3.2 General Payment Terms: You may pay by credit card or through an account with us payable at the end of the month. If you and we agree that you may establish a standing account with CCC, then the following terms apply: Remit Payment to: Copyright Clearance Center, Dept 001, P.O. Box 843006, Boston, MA 02284-3006. Payments Due: Invoices are payable upon their delivery to you (or upon our notice to you that they are available to you for downloading). After 30 days, outstanding amounts will be subject to a service charge of 1-1/2% per month or, if less, the maximum rate allowed by applicable law. Unless otherwise specifically set forth in the Order Confirmation or in a separate written agreement signed by CCC, invoices are due and payable on "net 30" terms. While User may exercise the rights licensed immediately upon issuance of the Order Confirmation, the license is automatically revoked and is null and void, as if it had never been issued, if complete payment for the license is not received on a timely basis either from User directly or through a payment agent, such as a credit card company.

3.3 Unless otherwise provided in the Order Confirmation, any grant of rights to User (i) is

"one-time" (including the editions and product family specified in the license), (ii) is non-exclusive and non-transferable and (iii) is subject to any and all limitations and restrictions (such as, but not limited to, limitations on duration of use or circulation) included in the Order Confirmation or invoice and/or in these terms and conditions. Upon completion of the licensed use, User shall either secure a new permission for further use of the Work(s) or immediately cease any new use of the Work(s) and shall render inaccessible (such as by deleting or by removing or severing links or other locators) any further copies of the Work (except for copies printed on paper in accordance with this license and still in User's stock at the end of such period).

3.4 In the event that the material for which a republication license is sought includes third party materials (such as photographs, illustrations, graphs, inserts and similar materials) which are identified in such material as having been used by permission, User is responsible for identifying, and seeking separate licenses (under this Service or otherwise) for, any of such third party materials; without a separate license, such third party materials may not be used.

3.5 Use of proper copyright notice for a Work is required as a condition of any license granted under the Service. Unless otherwise provided in the Order Confirmation, a proper copyright notice will read substantially as follows: "Republished with permission of [Rightsholder's name], from [Work's title, author, volume, edition number and year of copyright]; permission conveyed through Copyright Clearance Center, Inc. " Such notice must be provided in a reasonably legible font size and must be placed either immediately adjacent to the Work as used (for example, as part of a by-line or footnote but not as a separate electronic link) or in the place where substantially all other credits or notices for the new work containing the republished Work are located. Failure to include the required notice results in loss to the Rightsholder and CCC, and the User shall be liable to pay liquidated damages for each such failure equal to twice the use fee specified in the Order Confirmation, in addition to the use fee itself and any other fees and charges specified.

3.6 User may only make alterations to the Work if and as expressly set forth in the Order Confirmation. No Work may be used in any way that is defamatory, violates the rights of third parties (including such third parties' rights of copyright, privacy, publicity, or other tangible or intangible property), or is otherwise illegal, sexually explicit or obscene. In addition, User may not conjoin a Work with any other material that may result in damage to the reputation of the Rightsholder. User agrees to inform CCC if it becomes aware of any infringement of any rights in a Work and to cooperate with any reasonable request of CCC or the Rightsholder in connection therewith.

4. Indemnity. User hereby indemnifies and agrees to defend the Rightsholder and CCC, and their respective employees and directors, against all claims, liability, damages, costs and expenses, including legal fees and expenses, arising out of any use of a Work beyond the scope of the rights granted herein, or any use of a Work which has been altered in any unauthorized way by User, including claims of defamation or infringement of rights of copyright, publicity, privacy or other tangible or intangible property.

5. Limitation of Liability. UNDER NO CIRCUMSTANCES WILL CCC OR THE RIGHTSHOLDER BE LIABLE FOR ANY DIRECT, INDIRECT, CONSEQUENTIAL OR INCIDENTAL DAMAGES (INCLUDING WITHOUT LIMITATION DAMAGES FOR LOSS OF BUSINESS PROFITS OR INFORMATION, OR FOR BUSINESS INTERRUPTION) ARISING OUT OF THE USE OR INABILITY TO USE A WORK, EVEN IF ONE OF THEM HAS BEEN ADVISED OF THE POSSIBILITY OF SUCH DAMAGES. In any event, the total liability of the Rightsholder and CCC (including their respective employees and directors) shall not exceed the total amount actually paid by User for this license. User assumes full liability for the actions and omissions of its principals, employees, agents, affiliates, successors and assigns.

6. Limited Warranties. THE WORK(S) AND RIGHT(S) ARE PROVIDED "AS IS". CCC HAS THE RIGHT TO GRANT TO USER THE RIGHTS GRANTED IN THE ORDER CONFIRMATION DOCUMENT. CCC AND THE RIGHTSHOLDER

151

DISCLAIM ALL OTHER WARRANTIES RELATING TO THE WORK(S) AND RIGHT(S), EITHER EXPRESS OR IMPLIED, INCLUDING WITHOUT LIMITATION IMPLIED WARRANTIES OF MERCHANTABILITY OR FITNESS FOR A PARTICULAR PURPOSE. ADDITIONAL RIGHTS MAY BE REQUIRED TO USE ILLUSTRATIONS, GRAPHS, PHOTOGRAPHS, ABSTRACTS, INSERTS OR OTHER PORTIONS OF THE WORK (AS OPPOSED TO THE ENTIRE WORK) IN A MANNER CONTEMPLATED BY USER; USER UNDERSTANDS AND AGREES THAT NEITHER CCC NOR THE RIGHTSHOLDER MAY HAVE SUCH ADDITIONAL RIGHTS TO GRANT.

7. Effect of Breach. Any failure by User to pay any amount when due, or any use by User of a Work beyond the scope of the license set forth in the Order Confirmation and/or these terms and conditions, shall be a material breach of the license created by the Order Confirmation and these terms and conditions. Any breach not cured within 30 days of written notice thereof shall result in immediate termination of such license without further notice. Any unauthorized (but licensable) use of a Work that is terminated immediately upon notice thereof may be liquidated by payment of the Rightsholder's ordinary license price therefor; any unauthorized (and unlicensable) use that is not terminated immediately for any reason (including, for example, because materials containing the Work cannot reasonably be recalled) will be subject to all remedies available at law or in equity, but in no event to a payment of less than three times the Rightsholder's ordinary license price for the most closely analogous licensable use plus Rightsholder's and/or CCC's costs and expenses incurred in collecting such payment.

8. **Miscellaneous.**

8.1 User acknowledges that CCC may, from time to time, make changes or additions to the Service or to these terms and conditions, and CCC reserves the right to send notice to the User by electronic mail or otherwise for the purposes of notifying User of such changes or additions; provided that any such changes or additions shall not apply to

permissions already secured and paid for.

8.2 Use of User-related information collected through the Service is governed by CCC's privacy policy, available online here:http://www.copyright.com/content/cc3/en/tools/footer/privacypolicy.html.

8.3 The licensing transaction described in the Order Confirmation is personal to User. Therefore, User may not assign or transfer to any other person (whether a natural person or an organization of any kind) the license created by the Order Confirmation and these terms and conditions or any rights granted hereunder; provided, however, that User may assign such license in its entirety on written notice to CCC in the event of a transfer of all or substantially all of User's rights in the new material which includes the Work(s) licensed under this Service.

8.4 No amendment or waiver of any terms is binding unless set forth in writing and signed by the parties. The Rightsholder and CCC hereby object to any terms contained in any writing prepared by the User or its principals, employees, agents or affiliates and purporting to govern or otherwise relate to the licensing transaction described in the Order Confirmation, which terms are in any way inconsistent with any terms set forth in the Order Confirmation and/or in these terms and conditions or CCC's standard operating procedures, whether such writing is prepared prior to, simultaneously with or subsequent to the Order Confirmation, and whether such writing appears on a copy of the Order Confirmation or in a separate instrument.

8.5 The licensing transaction described in the Order Confirmation document shall be governed by and construed under the law of the State of New York, USA, without regard to the principles thereof of conflicts of law. Any case, controversy, suit, action, or proceeding arising out of, in connection with, or related to such licensing transaction shall be brought, at CCC's sole discretion, in any federal or state court located in the County of New York, State of New York, USA, or in any federal or state court whose geographical

jurisdiction covers the location of the Rightsholder set forth in the Order Confirmation. The parties expressly submit to the personal jurisdiction and venue of each such federal or state court. If you have any comments or questions about the Service or Copyright Clearance Center, please contact us at 978-750-8400 or send an e-mail to info@copyright.com.

v 1.1

FIGURE II-15B

**The Company of Biologists Ltd LICENSE
TERMS AND CONDITIONS**

Jan 29, 2017

This is a License Agreement between University of Waterloo -- Gah-Jone Won ("You") and The Company of Biologists Ltd ("The Company of Biologists Ltd") provided by Copyright Clearance Center ("CCC"). The license consists of your order details, the terms and conditions provided by The Company of Biologists Ltd, and the payment terms and conditions.

All payments must be made in full to CCC. For payment instructions, please see information listed at the bottom of this form.

License Number	3961981345969
License date	Oct 04, 2016
Licensed content publisher	The Company of Biologists Ltd
Licensed content title	Journal of cell science
Licensed content date	Jan 1, 1966
Type of Use	Thesis/Dissertation
Requestor type	Academic institution
Format	Print, Electronic
Portion	image/photo
Number of images/photos requested	1
Title or numeric reference of the portion(s)	Figure 13
Title of the article or chapter the	Molecular architecture of the lens fiber cell basal membrane

portion is from	complex
Editor of portion(s)	n/a
Author of portion(s)	Steven Bassnett, Heather Missey, and Ivica Vucemilo
Volume of serial or monograph.	n/a
Issue, if republishing an article from a serial	n/a
Page range of the portion	Page 2164
Publication date of portion	June 10, 1999
Rights for	Main product
Duration of use	Life of current edition
Creation of copies for the disabled	no
With minor editing privileges	yes
For distribution to	Worldwide
In the following language(s)	Original language of publication
With incidental promotional use	no
The lifetime unit quantity of new product	Up to 499
Made available in the following markets	Academia, Online
The requesting person/organization is:	Gah-Jone Won/University of Waterloo
Order reference number	
Author/Editor	Gah-Jone Won
The standard identifier of New Work	n/a
The proposed price	n/a
Title of New Work	The Development of an Antibody-Drug Conjugate to Specifically Target and Soften the Crystalline Lens in vivo
Publisher of New Work	University of Waterloo
Expected publication date	Nov 2016

Estimated size (pages)	215
Billing Type	Credit Card
Credit card info	Visa ending in 6297
Credit card expiration	08/2020
Total (may include CCC user fee)	3.50 USD
Terms and Conditions	

TERMS AND CONDITIONS

The following terms are individual to this publisher:

The acknowledgement should state "Reproduced / adapted with permission" and give the source journal name. The acknowledgement should either provide full citation details or refer to the relevant citation in the article reference list. The full citation details should include authors, journal, year, volume, issue and page citation.

Where appearing online or in other electronic media, a link should be provided to the original article (e.g. via DOI):

Development: dev.biologists.org

Disease Models & Mechanisms: dmm.biologists.org

Journal of Cell Science: jcs.biologists.org

The Journal of Experimental Biology: jeb.biologists.org

Other Terms and Conditions:
STANDARD TERMS AND CONDITIONS

1. Description of Service; Defined Terms. This Republication License enables the User to obtain licenses for republication of one or more copyrighted works as described in detail on the relevant Order Confirmation (the "Work(s)"). Copyright Clearance Center, Inc. ("CCC") grants licenses through the Service on behalf of the rightsholder identified on the Order Confirmation (the "Rightsholder"). "Republication", as used herein, generally means the inclusion of a Work, in whole or in part, in a new work or works, also as described on the Order Confirmation. "User", as used herein, means the person or entity making such

republication.

2. The terms set forth in the relevant Order Confirmation, and any terms set by the Rightsholder with respect to a particular Work, govern the terms of use of Works in connection with the Service. By using the Service, the person transacting for a republication license on behalf of the User represents and warrants that he/she/it (a) has been duly authorized by the User to accept, and hereby does accept, all such terms and conditions on behalf of User, and (b) shall inform User of all such terms and conditions. In the event such person is a "freelancer" or other third party independent of User and CCC, such party shall be deemed jointly a "User" for purposes of these terms and conditions. In any event, User shall be deemed to have accepted and agreed to all such terms and conditions if User republishes the Work in any fashion.

3. Scope of License; Limitations and Obligations.

3.1 All Works and all rights therein, including copyright rights, remain the sole and exclusive property of the Rightsholder. The license created by the exchange of an Order Confirmation (and/or any invoice) and payment by User of the full amount set forth on that document includes only those rights expressly set forth in the Order Confirmation and in these terms and conditions, and conveys no other rights in the Work(s) to User. All rights not expressly granted are hereby reserved.

3.2 General Payment Terms: You may pay by credit card or through an account with us payable at the end of the month. If you and we agree that you may establish a standing account with CCC, then the following terms apply: Remit Payment to: Copyright Clearance Center, Dept 001, P.O. Box 843006, Boston, MA 02284-3006. Payments Due: Invoices are payable upon their delivery to you (or upon our notice to you that they are available to you for downloading). After 30 days, outstanding amounts will be subject to a service charge of 1-1/2% per month or, if less, the maximum rate allowed by applicable law. Unless otherwise specifically set forth in the Order Confirmation or in a separate written agreement

signed by CCC, invoices are due and payable on "net 30" terms. While User may exercise the rights licensed immediately upon issuance of the Order Confirmation, the license is automatically revoked and is null and void, as if it had never been issued, if complete payment for the license is not received on a timely basis either from User directly or through a payment agent, such as a credit card company.

3.3 Unless otherwise provided in the Order Confirmation, any grant of rights to User (i) is "one-time" (including the editions and product family specified in the license), (ii) is non-exclusive and non-transferable and (iii) is subject to any and all limitations and restrictions (such as, but not limited to, limitations on duration of use or circulation) included in the Order Confirmation or invoice and/or in these terms and conditions. Upon completion of the licensed use, User shall either secure a new permission for further use of the Work(s) or immediately cease any new use of the Work(s) and shall render inaccessible (such as by deleting or by removing or severing links or other locators) any further copies of the Work (except for copies printed on paper in accordance with this license and still in User's stock at the end of such period).

3.4 In the event that the material for which a republication license is sought includes third party materials (such as photographs, illustrations, graphs, inserts and similar materials) which are identified in such material as having been used by permission, User is responsible for identifying, and seeking separate licenses (under this Service or otherwise) for, any of such third party materials; without a separate license, such third party materials may not be used.

3.5 Use of proper copyright notice for a Work is required as a condition of any license granted under the Service. Unless otherwise provided in the Order Confirmation, a proper copyright notice will read substantially as follows: "Republished with permission of [Rightsholder's name], from [Work's title, author, volume, edition number and year of copyright]; permission conveyed through Copyright Clearance Center, Inc. " Such notice must be provided in a reasonably legible font size and must be placed either immediately

adjacent to the Work as used (for example, as part of a by-line or footnote but not as a separate electronic link) or in the place where substantially all other credits or notices for the new work containing the republished Work are located. Failure to include the required notice results in loss to the Rightsholder and CCC, and the User shall be liable to pay liquidated damages for each such failure equal to twice the use fee specified in the Order Confirmation, in addition to the use fee itself and any other fees and charges specified.

3.6 User may only make alterations to the Work if and as expressly set forth in the Order Confirmation. No Work may be used in any way that is defamatory, violates the rights of third parties (including such third parties' rights of copyright, privacy, publicity, or other tangible or intangible property), or is otherwise illegal, sexually explicit or obscene. In addition, User may not conjoin a Work with any other material that may result in damage to the reputation of the Rightsholder. User agrees to inform CCC if it becomes aware of any infringement of any rights in a Work and to cooperate with any reasonable request of CCC or the Rightsholder in connection therewith.

4. Indemnity. User hereby indemnifies and agrees to defend the Rightsholder and CCC, and their respective employees and directors, against all claims, liability, damages, costs and expenses, including legal fees and expenses, arising out of any use of a Work beyond the scope of the rights granted herein, or any use of a Work which has been altered in any unauthorized way by User, including claims of defamation or infringement of rights of copyright, publicity, privacy or other tangible or intangible property.

5. Limitation of Liability. UNDER NO CIRCUMSTANCES WILL CCC OR THE RIGHTSHOLDER BE LIABLE FOR ANY DIRECT, INDIRECT, CONSEQUENTIAL OR INCIDENTAL DAMAGES (INCLUDING WITHOUT LIMITATION DAMAGES FOR LOSS OF BUSINESS PROFITS OR INFORMATION, OR FOR BUSINESS INTERRUPTION) ARISING OUT OF THE USE OR INABILITY TO USE A WORK, EVEN IF ONE OF THEM HAS BEEN ADVISED OF THE POSSIBILITY OF SUCH DAMAGES. In any event, the total liability of the Rightsholder and CCC (including their respective employees and directors) shall not exceed the total amount actually paid by User

for this license. User assumes full liability for the actions and omissions of its principals, employees, agents, affiliates, successors and assigns.

6. Limited Warranties. THE WORK(S) AND RIGHT(S) ARE PROVIDED "AS IS". CCC HAS THE RIGHT TO GRANT TO USER THE RIGHTS GRANTED IN THE ORDER CONFIRMATION DOCUMENT. CCC AND THE RIGHTSHOLDER DISCLAIM ALL OTHER WARRANTIES RELATING TO THE WORK(S) AND RIGHT(S), EITHER EXPRESS OR IMPLIED, INCLUDING WITHOUT LIMITATION IMPLIED WARRANTIES OF MERCHANTABILITY OR FITNESS FOR A PARTICULAR PURPOSE. ADDITIONAL RIGHTS MAY BE REQUIRED TO USE ILLUSTRATIONS, GRAPHS, PHOTOGRAPHS, ABSTRACTS, INSERTS OR OTHER PORTIONS OF THE WORK (AS OPPOSED TO THE ENTIRE WORK) IN A MANNER CONTEMPLATED BY USER; USER UNDERSTANDS AND AGREES THAT NEITHER CCC NOR THE RIGHTSHOLDER MAY HAVE SUCH ADDITIONAL RIGHTS TO GRANT.

7. Effect of Breach. Any failure by User to pay any amount when due, or any use by User of a Work beyond the scope of the license set forth in the Order Confirmation and/or these terms and conditions, shall be a material breach of the license created by the Order Confirmation and these terms and conditions. Any breach not cured within 30 days of written notice thereof shall result in immediate termination of such license without further notice. Any unauthorized (but licensable) use of a Work that is terminated immediately upon notice thereof may be liquidated by payment of the Rightsholder's ordinary license price therefor; any unauthorized (and unlicensable) use that is not terminated immediately for any reason (including, for example, because materials containing the Work cannot reasonably be recalled) will be subject to all remedies available at law or in equity, but in no event to a payment of less than three times the Rightsholder's ordinary license price for the most closely analogous licensable use plus Rightsholder's and/or CCC's costs and expenses incurred in collecting such payment.

8. **Miscellaneous.**

8.1 User acknowledges that CCC may, from time to time, make changes or additions to the Service or to these terms and conditions, and CCC reserves the right to send notice to the User by electronic mail or otherwise for the purposes of notifying User of such changes or additions; provided that any such changes or additions shall not apply to permissions already secured and paid for.

8.2 Use of User-related information collected through the Service is governed by CCC's privacy policy, available online here:http://www.copyright.com/content/cc3/en/tools/footer/privacypolicy.html.

8.3 The licensing transaction described in the Order Confirmation is personal to User. Therefore, User may not assign or transfer to any other person (whether a natural person or an organization of any kind) the license created by the Order Confirmation and these terms and conditions or any rights granted hereunder; provided, however, that User may assign such license in its entirety on written notice to CCC in the event of a transfer of all or substantially all of User's rights in the new material which includes the Work(s) licensed under this Service.

8.4 No amendment or waiver of any terms is binding unless set forth in writing and signed by the parties. The Rightsholder and CCC hereby object to any terms contained in any writing prepared by the User or its principals, employees, agents or affiliates and purporting to govern or otherwise relate to the licensing transaction described in the Order Confirmation, which terms are in any way inconsistent with any terms set forth in the Order Confirmation and/or in these terms and conditions or CCC's standard operating procedures, whether such writing is prepared prior to, simultaneously with or subsequent to the Order Confirmation, and whether such writing appears on a copy of the Order Confirmation or in a separate instrument.

8.5 The licensing transaction described in the Order Confirmation document shall be governed by and construed under the law of the State of New York, USA, without regard to the principles thereof of conflicts of law. Any case, controversy, suit, action, or proceeding arising out of, in connection with, or related to such licensing transaction shall be brought, at CCC's sole discretion, in any federal or state court located in the County of New York, State of New York, USA, or in any federal or state court whose geographical jurisdiction covers the location of the Rightsholder set forth in the Order Confirmation. The parties expressly submit to the personal jurisdiction and venue of each such federal or state court. If you have any comments or questions about the Service or Copyright Clearance Center, please contact us at 978-750-8400 or send an e-mail to info@copyright.com.

v 1.1

FIGURE II-18

**American Society for Clinical Investigation LICENSE
TERMS AND CONDITIONS**

Jan 29, 2017

This is a License Agreement between University of Waterloo -- Gah-Jone Won ("You") and American Society for Clinical Investigation ("American Society for Clinical Investigation") provided by Copyright Clearance Center ("CCC"). The license consists of your order details, the terms and conditions provided by American Society for Clinical Investigation, and the payment terms and conditions.

All payments must be made in full to CCC. For payment instructions, please see information listed at the bottom of this form.

License Number	3962050444868
License date	Oct 04, 2016
Licensed content publisher	American Society for Clinical Investigation
Licensed content title	JOURNAL OF CLINICAL INVESTIGATION. ONLINE
Licensed content date	Dec 31, 1969
Type of Use	Thesis/Dissertation
Requestor type	Academic institution
Format	Print, Electronic
Portion	image/photo
Number of images/photos requested	1
Title or numeric reference of the portion(s)	Figure 3
Title of the article or chapter the portion is from	Functions of the intermediate filament cytoskeleton in the eye lens

Editor of portion(s)	n/a
Author of portion(s)	Shuhua Song, Andrew Landsbury, Ralf Dahm, Yizhi Liu, Qingjiong Zhang, Roy A. Quinlan
Volume of serial or monograph.	n/a
Issue, if republishing an article from a serial	n/a
Page range of the portion	1840
Publication date of portion	July 1, 2009
Rights for	Main product
Duration of use	Life of current edition
Creation of copies for the disabled	no
With minor editing privileges	yes
For distribution to	Worldwide
In the following language(s)	Original language of publication
With incidental promotional use	no
The lifetime unit quantity of new product	Up to 499
Made available in the following markets	Academia, Online
The requesting person/organization is:	Gah-Jone Won/University of Waterloo
Order reference number	
Author/Editor	Gah-Jone Won
The standard identifier of New Work	n/a
The proposed price	n/a
Title of New Work	The Development of an Antibody-Drug Conjugate to Specifically Target and Soften the Crystalline Lens in vivo
Publisher of New Work	University of Waterloo

Expected publication date	Nov 2016
Estimated size (pages)	215
Total (may include CCC user fee)	0.00 USD

Terms and Conditions

<div align="center">

TERMS AND CONDITIONS

The following terms are individual to this publisher:

</div>

None

<div align="center">

Other Terms and Conditions:

STANDARD TERMS AND CONDITIONS

</div>

1. Description of Service; Defined Terms. This Republication License enables the User to obtain licenses for republication of one or more copyrighted works as described in detail on the relevant Order Confirmation (the "Work(s)"). Copyright Clearance Center, Inc. ("CCC") grants licenses through the Service on behalf of the rightsholder identified on the Order Confirmation (the "Rightsholder"). "Republication", as used herein, generally means the inclusion of a Work, in whole or in part, in a new work or works, also as described on the Order Confirmation. "User", as used herein, means the person or entity making such republication.

2. The terms set forth in the relevant Order Confirmation, and any terms set by the Rightsholder with respect to a particular Work, govern the terms of use of Works in connection with the Service. By using the Service, the person transacting for a republication license on behalf of the User represents and warrants that he/she/it (a) has been duly authorized by the User to accept, and hereby does accept, all such terms and conditions on behalf of User, and (b) shall inform User of all such terms and conditions. In the event such person is a "freelancer" or other third party independent of User and CCC, such party shall be deemed jointly a "User" for purposes of these terms and conditions. In

any event, User shall be deemed to have accepted and agreed to all such terms and conditions if User republishes the Work in any fashion.

3. Scope of License; Limitations and Obligations.

3.1 All Works and all rights therein, including copyright rights, remain the sole and exclusive property of the Rightsholder. The license created by the exchange of an Order Confirmation (and/or any invoice) and payment by User of the full amount set forth on that document includes only those rights expressly set forth in the Order Confirmation and in these terms and conditions, and conveys no other rights in the Work(s) to User. All rights not expressly granted are hereby reserved.

3.2 General Payment Terms: You may pay by credit card or through an account with us payable at the end of the month. If you and we agree that you may establish a standing account with CCC, then the following terms apply: Remit Payment to: Copyright Clearance Center, Dept 001, P.O. Box 843006, Boston, MA 02284-3006. Payments Due: Invoices are payable upon their delivery to you (or upon our notice to you that they are available to you for downloading). After 30 days, outstanding amounts will be subject to a service charge of 1-1/2% per month or, if less, the maximum rate allowed by applicable law. Unless otherwise specifically set forth in the Order Confirmation or in a separate written agreement signed by CCC, invoices are due and payable on "net 30" terms. While User may exercise the rights licensed immediately upon issuance of the Order Confirmation, the license is automatically revoked and is null and void, as if it had never been issued, if complete payment for the license is not received on a timely basis either from User directly or through a payment agent, such as a credit card company.

3.3 Unless otherwise provided in the Order Confirmation, any grant of rights to User (i) is "one-time" (including the editions and product family specified in the license), (ii) is non-exclusive and non-transferable and (iii) is subject to any and all limitations and restrictions (such as, but not limited to, limitations on duration of use or circulation) included in the

Order Confirmation or invoice and/or in these terms and conditions. Upon completion of the licensed use, User shall either secure a new permission for further use of the Work(s) or immediately cease any new use of the Work(s) and shall render inaccessible (such as by deleting or by removing or severing links or other locators) any further copies of the Work (except for copies printed on paper in accordance with this license and still in User's stock at the end of such period).

3.4 In the event that the material for which a republication license is sought includes third party materials (such as photographs, illustrations, graphs, inserts and similar materials) which are identified in such material as having been used by permission, User is responsible for identifying, and seeking separate licenses (under this Service or otherwise) for, any of such third party materials; without a separate license, such third party materials may not be used.

3.5 Use of proper copyright notice for a Work is required as a condition of any license granted under the Service. Unless otherwise provided in the Order Confirmation, a proper copyright notice will read substantially as follows: "Republished with permission of [Rightsholder's name], from [Work's title, author, volume, edition number and year of copyright]; permission conveyed through Copyright Clearance Center, Inc. " Such notice must be provided in a reasonably legible font size and must be placed either immediately adjacent to the Work as used (for example, as part of a by-line or footnote but not as a separate electronic link) or in the place where substantially all other credits or notices for the new work containing the republished Work are located. Failure to include the required notice results in loss to the Rightsholder and CCC, and the User shall be liable to pay liquidated damages for each such failure equal to twice the use fee specified in the Order Confirmation, in addition to the use fee itself and any other fees and charges specified.

3.6 User may only make alterations to the Work if and as expressly set forth in the Order Confirmation. No Work may be used in any way that is defamatory, violates the rights of third parties (including such third parties' rights of copyright, privacy, publicity, or other

tangible or intangible property), or is otherwise illegal, sexually explicit or obscene. In addition, User may not conjoin a Work with any other material that may result in damage to the reputation of the Rightsholder. User agrees to inform CCC if it becomes aware of any infringement of any rights in a Work and to cooperate with any reasonable request of CCC or the Rightsholder in connection therewith.

4. Indemnity. User hereby indemnifies and agrees to defend the Rightsholder and CCC, and their respective employees and directors, against all claims, liability, damages, costs and expenses, including legal fees and expenses, arising out of any use of a Work beyond the scope of the rights granted herein, or any use of a Work which has been altered in any unauthorized way by User, including claims of defamation or infringement of rights of copyright, publicity, privacy or other tangible or intangible property.

5. Limitation of Liability. UNDER NO CIRCUMSTANCES WILL CCC OR THE RIGHTSHOLDER BE LIABLE FOR ANY DIRECT, INDIRECT, CONSEQUENTIAL OR INCIDENTAL DAMAGES (INCLUDING WITHOUT LIMITATION DAMAGES FOR LOSS OF BUSINESS PROFITS OR INFORMATION, OR FOR BUSINESS INTERRUPTION) ARISING OUT OF THE USE OR INABILITY TO USE A WORK, EVEN IF ONE OF THEM HAS BEEN ADVISED OF THE POSSIBILITY OF SUCH DAMAGES. In any event, the total liability of the Rightsholder and CCC (including their respective employees and directors) shall not exceed the total amount actually paid by User for this license. User assumes full liability for the actions and omissions of its principals, employees, agents, affiliates, successors and assigns.

6. Limited Warranties. THE WORK(S) AND RIGHT(S) ARE PROVIDED "AS IS". CCC HAS THE RIGHT TO GRANT TO USER THE RIGHTS GRANTED IN THE ORDER CONFIRMATION DOCUMENT. CCC AND THE RIGHTSHOLDER DISCLAIM ALL OTHER WARRANTIES RELATING TO THE WORK(S) AND RIGHT(S), EITHER EXPRESS OR IMPLIED, INCLUDING WITHOUT LIMITATION IMPLIED WARRANTIES OF MERCHANTABILITY OR FITNESS FOR A

PARTICULAR PURPOSE. ADDITIONAL RIGHTS MAY BE REQUIRED TO USE ILLUSTRATIONS, GRAPHS, PHOTOGRAPHS, ABSTRACTS, INSERTS OR OTHER PORTIONS OF THE WORK (AS OPPOSED TO THE ENTIRE WORK) IN A MANNER CONTEMPLATED BY USER; USER UNDERSTANDS AND AGREES THAT NEITHER CCC NOR THE RIGHTSHOLDER MAY HAVE SUCH ADDITIONAL RIGHTS TO GRANT.

7. Effect of Breach. Any failure by User to pay any amount when due, or any use by User of a Work beyond the scope of the license set forth in the Order Confirmation and/or these terms and conditions, shall be a material breach of the license created by the Order Confirmation and these terms and conditions. Any breach not cured within 30 days of written notice thereof shall result in immediate termination of such license without further notice. Any unauthorized (but licensable) use of a Work that is terminated immediately upon notice thereof may be liquidated by payment of the Rightsholder's ordinary license price therefor; any unauthorized (and unlicensable) use that is not terminated immediately for any reason (including, for example, because materials containing the Work cannot reasonably be recalled) will be subject to all remedies available at law or in equity, but in no event to a payment of less than three times the Rightsholder's ordinary license price for the most closely analogous licensable use plus Rightsholder's and/or CCC's costs and expenses incurred in collecting such payment.

8. **Miscellaneous.**

8.1 User acknowledges that CCC may, from time to time, make changes or additions to the Service or to these terms and conditions, and CCC reserves the right to send notice to the User by electronic mail or otherwise for the purposes of notifying User of such changes or additions; provided that any such changes or additions shall not apply to permissions already secured and paid for.

8.2 Use of User-related information collected through the Service is governed by CCC's

privacy policy, available online here:

http://www.copyright.com/content/cc3/en/tools/footer/privacypolicy.html.

8.3 The licensing transaction described in the Order Confirmation is personal to User. Therefore, User may not assign or transfer to any other person (whether a natural person or an organization of any kind) the license created by the Order Confirmation and these terms and conditions or any rights granted hereunder; provided, however, that User may assign such license in its entirety on written notice to CCC in the event of a transfer of all or substantially all of User's rights in the new material which includes the Work(s) licensed under this Service.

8.4 No amendment or waiver of any terms is binding unless set forth in writing and signed by the parties. The Rightsholder and CCC hereby object to any terms contained in any writing prepared by the User or its principals, employees, agents or affiliates and purporting to govern or otherwise relate to the licensing transaction described in the Order Confirmation, which terms are in any way inconsistent with any terms set forth in the Order Confirmation and/or in these terms and conditions or CCC's standard operating procedures, whether such writing is prepared prior to, simultaneously with or subsequent to the Order Confirmation, and whether such writing appears on a copy of the Order Confirmation or in a separate instrument.

8.5 The licensing transaction described in the Order Confirmation document shall be governed by and construed under the law of the State of New York, USA, without regard to the principles thereof of conflicts of law. Any case, controversy, suit, action, or proceeding arising out of, in connection with, or related to such licensing transaction shall be brought, at CCC's sole discretion, in any federal or state court located in the County of New York, State of New York, USA, or in any federal or state court whose geographical jurisdiction covers the location of the Rightsholder set forth in the Order Confirmation. The parties expressly submit to the personal jurisdiction and venue of each such federal or state court. If you have any comments or questions about the Service or Copyright Clearance Center,

please contact us at 978-750-8400 or send an e-mail to info@copyright.com.

v 1.1

Creative Commons

1. Attribution-NonCommercial-NoDerivs 3.0 Unported

2. *License*

THE WORK (AS DEFINED BELOW) IS PROVIDED UNDER THE TERMS OF THIS CREATIVE COMMONS PUBLIC LICENSE ("CCPL" OR "LICENSE"). THE WORK IS PROTECTED BY COPYRIGHT AND/OR OTHER APPLICABLE LAW. ANY USE OF THE WORK OTHER THAN AS AUTHORIZED UNDER THIS LICENSE OR COPYRIGHT LAW IS PROHIBITED.

BY EXERCISING ANY RIGHTS TO THE WORK PROVIDED HERE, YOU ACCEPT AND AGREE TO BE BOUND BY THE TERMS OF THIS LICENSE. TO THE EXTENT THIS LICENSE MAY BE CONSIDERED TO BE A CONTRACT, THE LICENSOR GRANTS YOU THE RIGHTS CONTAINED HERE IN CONSIDERATION OF YOUR ACCEPTANCE OF SUCH TERMS AND CONDITIONS.

1. Definitions

a. **"Adaptation"** means a work based upon the Work, or upon the Work and other pre-existing works, such as a translation, adaptation, derivative work, arrangement of music or other alterations of a literary or artistic work, or phonogram or performance and includes cinematographic adaptations or any other form in which the Work may be recast, transformed, or adapted including in any form recognizably derived from the original, except that a work that constitutes a Collection will not be considered an Adaptation for the purpose of this License. For the avoidance of doubt, where the Work is a musical work, performance or phonogram, the synchronization of the Work in timed-relation with a moving image ("synching") will be considered an Adaptation for the purpose of this License.

b. **"Collection"** means a collection of literary or artistic works, such as encyclopedias and anthologies, or performances, phonograms or broadcasts, or other works or subject matter other than works listed in Section 1(f) below, which, by reason of the selection and arrangement of their contents, constitute intellectual creations, in which the Work is included in its entirety in unmodified form along with one or more other contributions, each constituting separate and independent works in themselves, which together are assembled into a collective whole. A work that constitutes a Collection will not be considered an Adaptation (as defined above) for the purposes of this License.

c. **"Distribute"** means to make available to the public the original and copies of the Work through sale or other transfer of ownership.

d. **"Licensor"** means the individual, individuals, entity or entities that offer(s) the Work under the terms of this License.

e. **"Original Author"** means, in the case of a literary or artistic work, the individual, individuals, entity or entities who created the Work or if no individual or entity can be identified, the publisher; and in addition (i) in the case of a performance the actors, singers, musicians, dancers, and other persons who act, sing, deliver, declaim, play in, interpret or otherwise perform literary or artistic works or expressions of folklore; (ii) in the case of a phonogram the producer being the person or legal entity who first fixes the sounds of a performance or other sounds; and, (iii) in the case of broadcasts, the organization that transmits the broadcast.

f. **"Work"** means the literary and/or artistic work offered under the terms of this License including without limitation any production in the literary, scientific and artistic domain, whatever may be the mode or form of its expression including digital form, such as a book, pamphlet and other writing; a lecture, address, sermon or other work of the same nature; a dramatic or dramatico-musical work; a choreographic work or entertainment in dumb show; a musical composition with or without words; a cinematographic work to which are assimilated works expressed by a process analogous to cinematography; a work of drawing, painting, architecture, sculpture, engraving or lithography; a photographic work to which are assimilated works expressed by a process analogous to photography; a work of applied art; an illustration, map, plan, sketch or three-dimensional work relative to geography, topography, architecture or science; a performance; a broadcast; a phonogram; a compilation of data to the extent it is protected as a copyrightable work; or a work performed by a variety or circus performer to the extent it is not otherwise considered a literary or artistic work.

g. **"You"** means an individual or entity exercising rights under this License who has not previously violated the terms of this License with respect to the Work, or who has received express permission from the Licensor to exercise rights under this License despite a previous violation.

h. **"Publicly Perform"** means to perform public recitations of the Work and to communicate to the public those public recitations, by any means or process, including by wire or wireless means or public digital performances; to make available to the public Works in such a way that members of the public may access these Works from a place and at a place individually chosen by them; to perform the Work to the public by any means or process and the communication to the public of the performances of the Work, including by public digital performance; to broadcast and rebroadcast the Work by any means including signs, sounds or images.

i. **"Reproduce"** means to make copies of the Work by any means including without limitation by sound or visual recordings and the right of fixation and reproducing fixations of the Work, including storage of a protected performance or phonogram in digital form or other electronic medium.

2. Fair Dealing Rights. Nothing in this License is intended to reduce, limit, or restrict any uses free from copyright or rights arising from limitations or exceptions that are provided for in connection with the copyright protection under copyright law or other applicable laws.

3. License Grant. Subject to the terms and conditions of this License, Licensor hereby grants You a worldwide, royalty-free, non-exclusive, perpetual (for the duration of the applicable copyright) license to exercise the rights in the Work as stated below:

a. to Reproduce the Work, to incorporate the Work into one or more Collections, and to Reproduce the Work as incorporated in the Collections; and,

b. to Distribute and Publicly Perform the Work including as incorporated in Collections.

The above rights may be exercised in all media and formats whether now known or hereafter devised. The above rights include the right to make such modifications as are technically necessary to exercise the rights in other media and formats, but otherwise you have no rights to make Adaptations. Subject to 8(f), all rights not expressly granted by Licensor are hereby reserved, including but not limited to the rights set forth in Section 4(d).

4. Restrictions. The license granted in Section 3 above is expressly made subject to and limited by the following restrictions:

a. You may Distribute or Publicly Perform the Work only under the terms of this License. You must include a copy of, or the Uniform Resource Identifier (URI) for, this License with every copy of the Work You Distribute or Publicly Perform. You may not offer or impose any terms on the Work that restrict the terms of this License or the ability of the recipient of the Work to

175

exercise the rights granted to that recipient under the terms of the License. You may not sublicense the Work. You must keep intact all notices that refer to this License and to the disclaimer of warranties with every copy of the Work You Distribute or Publicly Perform. When You Distribute or Publicly Perform the Work, You may not impose any effective technological measures on the Work that restrict the ability of a recipient of the Work from You to exercise the rights granted to that recipient under the terms of the License. This Section 4(a) applies to the Work as incorporated in a Collection, but this does not require the Collection apart from the Work itself to be made subject to the terms of this License. If You create a Collection, upon notice from any Licensor You must, to the extent practicable, remove from the Collection any credit as required by Section 4(c), as requested.

b. You may not exercise any of the rights granted to You in Section 3 above in any manner that is primarily intended for or directed toward commercial advantage or private monetary compensation. The exchange of the Work for other copyrighted works by means of digital file-sharing or otherwise shall not be considered to be intended for or directed toward commercial advantage or private monetary compensation, provided there is no payment of any monetary compensation in connection with the exchange of copyrighted works.

c. If You Distribute, or Publicly Perform the Work or Collections, You must, unless a request has been made pursuant to Section 4(a), keep intact all copyright notices for the Work and provide, reasonable to the medium or means You are utilizing: (i) the name of the Original Author (or pseudonym, if applicable) if supplied, and/or if the Original Author and/or Licensor designate another party or parties (e.g., a sponsor institute, publishing entity, journal) for attribution ("Attribution Parties") in Licensor's copyright notice, terms of service or by other reasonable means, the name of such party or parties; (ii) the title of the Work if supplied; (iii) to the extent reasonably practicable, the URI, if any, that Licensor specifies to be associated with the Work, unless such URI does not refer to the copyright notice or licensing information for the Work. The credit required by this Section 4(c) may be implemented in any reasonable manner; provided, however, that in the case of a Collection, at a minimum such credit will appear, if a credit for all contributing authors of Collection appears, then as part of these credits and in a manner at least as prominent as the credits for the other contributing authors. For the avoidance of doubt, You may only use the credit required by this Section for the purpose of attribution in the manner set out above and, by exercising Your rights under this License, You may not implicitly or explicitly assert or imply any connection with, sponsorship or endorsement by the Original Author, Licensor and/or Attribution Parties, as appropriate, of You or Your use of the Work, without the separate, express prior written permission of the Original Author, Licensor and/or Attribution Parties.

d. For the avoidance of doubt:

176

i. **Non-waivable Compulsory License Schemes**. In those jurisdictions in which the right to collect royalties through any statutory or compulsory licensing scheme cannot be waived, the Licensor reserves the exclusive right to collect such royalties for any exercise by You of the rights granted under this License;

ii. **Waivable Compulsory License Schemes**. In those jurisdictions in which the right to collect royalties through any statutory or compulsory licensing scheme can be waived, the Licensor reserves the exclusive right to collect such royalties for any exercise by You of the rights granted under this License if Your exercise of such rights is for a purpose or use which is otherwise than noncommercial as permitted under Section 4(b) and otherwise waives the right to collect royalties through any statutory or compulsory licensing scheme; and,

iii. **Voluntary License Schemes**. The Licensor reserves the right to collect royalties, whether individually or, in the event that the Licensor is a member of a collecting society that administers voluntary licensing schemes, via that society, from any exercise by You of the rights granted under this License that is for a purpose or use which is otherwise than noncommercial as permitted under Section 4(b).

e. Except as otherwise agreed in writing by the Licensor or as may be otherwise permitted by applicable law, if You Reproduce, Distribute or Publicly Perform the Work either by itself or as part of any Collections, You must not distort, mutilate, modify or take other derogatory action in relation to the Work which would be prejudicial to the Original Author's honor or reputation.

5. Representations, Warranties and Disclaimer

UNLESS OTHERWISE MUTUALLY AGREED BY THE PARTIES IN WRITING, LICENSOR OFFERS THE WORK AS-IS AND MAKES NO REPRESENTATIONS OR WARRANTIES OF ANY KIND CONCERNING THE WORK, EXPRESS, IMPLIED, STATUTORY OR OTHERWISE, INCLUDING, WITHOUT LIMITATION, WARRANTIES OF TITLE, MERCHANTIBILITY, FITNESS FOR A PARTICULAR PURPOSE, NONINFRINGEMENT, OR THE ABSENCE OF LATENT OR OTHER DEFECTS, ACCURACY, OR THE PRESENCE OF ABSENCE OF ERRORS, WHETHER OR NOT DISCOVERABLE. SOME JURISDICTIONS DO NOT ALLOW THE EXCLUSION OF IMPLIED WARRANTIES, SO SUCH EXCLUSION MAY NOT APPLY TO YOU.

6. Limitation on Liability. EXCEPT TO THE EXTENT REQUIRED BY APPLICABLE LAW, IN NO EVENT WILL LICENSOR BE LIABLE TO YOU ON ANY LEGAL THEORY FOR ANY SPECIAL, INCIDENTAL, CONSEQUENTIAL, PUNITIVE OR EXEMPLARY DAMAGES ARISING OUT OF THIS LICENSE OR THE USE OF THE WORK, EVEN IF LICENSOR HAS BEEN ADVISED OF THE POSSIBILITY OF SUCH DAMAGES.

7. Termination

a. This License and the rights granted hereunder will terminate automatically upon any breach by You of the terms of this License. Individuals or entities who have received Collections from You under this License, however, will not have their licenses terminated provided such individuals or entities remain in full compliance with those licenses. Sections 1, 2, 5, 6, 7, and 8 will survive any termination of this License.

b. Subject to the above terms and conditions, the license granted here is perpetual (for the duration of the applicable copyright in the Work). Notwithstanding the above, Licensor reserves the right to release the Work under different license terms or to stop distributing the Work at any time; provided, however that any such election will not serve to withdraw this License (or any other license that has been, or is required to be, granted under the terms of this License), and this License will continue in full force and effect unless terminated as stated above.

8. Miscellaneous

a. Each time You Distribute or Publicly Perform the Work or a Collection, the Licensor offers to the recipient a license to the Work on the same terms and conditions as the license granted to You under this License.

b. If any provision of this License is invalid or unenforceable under applicable law, it shall not affect the validity or enforceability of the remainder of the terms of this License, and without further action by the parties to this agreement, such provision shall be reformed to the minimum extent necessary to make such provision valid and enforceable.

c. No term or provision of this License shall be deemed waived and no breach consented to unless such waiver or consent shall be in writing and signed by the party to be charged with such waiver or consent.

d. This License constitutes the entire agreement between the parties with respect to the Work licensed here. There are no understandings, agreements or representations with respect to the Work not specified here. Licensor shall not be bound by any additional provisions that may appear in any communication from You. This License may not be modified without the mutual written agreement of the Licensor and You.

e. The rights granted under, and the subject matter referenced, in this License were drafted utilizing the terminology of the Berne Convention for the Protection of Literary and Artistic Works (as amended on September 28, 1979), the Rome Convention of 1961, the WIPO Copyright Treaty of 1996, the WIPO Performances and Phonograms Treaty of 1996 and the Universal Copyright Convention (as revised on July 24, 1971). These rights and subject matter

take effect in the relevant jurisdiction in which the License terms are sought to be enforced according to the corresponding provisions of the implementation of those treaty provisions in the applicable national law. If the standard suite of rights granted under applicable copyright law includes additional rights not granted under this License, such additional rights are deemed to be included in the License; this License is not intended to restrict the license of any rights under applicable law.

3. Creative Commons Notice

Creative Commons is not a party to this License, and makes no warranty whatsoever in connection with the Work. Creative Commons will not be liable to You or any party on any legal theory for any damages whatsoever, including without limitation any general, special, incidental or consequential damages arising in connection to this license. Notwithstanding the foregoing two (2) sentences, if Creative Commons has expressly identified itself as the Licensor hereunder, it shall have all rights and obligations of Licensor.

Except for the limited purpose of indicating to the public that the Work is licensed under the CCPL, Creative Commons does not authorize the use by either party of the trademark "Creative Commons" or any related trademark or logo of Creative Commons without the prior written consent of Creative Commons. Any permitted use will be in compliance with Creative Commons' then-current trademark usage guidelines, as may be published on its website or otherwise made available upon request from time to time. For the avoidance of doubt, this trademark restriction does not form part of this License.

Creative Commons may be contacted at **https://creativecommons.org/**.

REFERENCES

Abdelkader, A. (2015). Improved presbyopic vision with miotics. *Eye & Contact Lens, 41*(5), 323-327.

Al-Ghadyan, A. A., & Cotlier, E. (1986). Rise in lens temperature on exposure to sunlight or high ambient temperature. *British Journal of Ophthalmology, 70*(6), 421-426.

Alberts, B., Bray, D., Lewis, J., Raff, M., Roberts, K., Watson, J. D., & Grimstone, A. (1995). Molecular Biology of the Cell (Third Edition). *Trends in Biochemical Sciences, 20*(5), 210-210.

Alberts, B., Johnson, A., Lewis, J., Morgan, D., Raff, M., Roberts, K., Walter, P., Wilson, J., Hunt, T. Molecular Biology of the Cell (Sixth Edition).

Alm, A. (2000). Uveoscleral outflow. *Eye, 14*(3b), 488-491.

Amano, S., Amano, Y., Yamagami, S., Miyai, T., Miyata, K., Samejima, T., & Oshika, T. (2004). Age-related changes in corneal and ocular higher-order wavefront aberrations. *American Journal Ophthalmology, 137*(6), 988-992.

Atchison, D. A. (2002). Accommodation and presbyopia. *Opthalmic and Physiological Optics, 15*(4), 255-272.

Bäck, I., Donner, K., & Reuter, T. (1965). The screening effect of the pigment epithelium on the retinal rods in the frog. *Vision Research, 5*(4-5).

Bantseev, V. L., Herbert, K. L., Trevithick, J. R., & Sivak, J. G. (1999). Mitochondria of rat lenses: distribution near and at the sutures. *Current Eye Research, 19*(6), 506-516.

Barrett, J. (1938). Accommodation in the eyes of mammals. *British Journal of Ophthalmology, 22*(3), 148-153.

Bassnett, S., Missey, H., & Vucemilo, I. (1999). Molecular architecture of the lens fiber cell basal membrane complex. *Journal of Cell Science, 112*(13), 2155-2165.

Bassnett, S., & Winzenburger, P. A. (2003). Morphometric analysis of fibre cell growth in the developing chicken lens. *Experimental Eye Research, 76*(3), 291-302.

Baylor, D. (1996). How photons start vision. *Proceedings of the National Academy of Sciences, 93*(2), 560-565.

Beebe, D. C., & Truscott, R. J. W. (2010). Reply to: a critical appraisal of the lens circulation model—an experimental paradigm for understanding the maintenance of lens transparency? *Investigative Ophthalmology and Visual Science, 51*(5), 2312-2312.

Beers, A., & Van der Heijde, G. (1996). Age-related changes in the accommodation mechanism. *Optometry and Visual Science, 73*(4), 235-242.

Best, A., & Nicol, J. (1967). Reflecting cells of elasmobranch tapetum lucidum. *Contributions in Marine Science,* 172.

Bettelheim, F. A. (1985). Physical basis of lens transparency in the ocular lens: structure, function, and pathology. New York: Marcel Dekker Inc.

Bill, A. (1984). Physiology of the outflow mechanism. *Glaucoma: Applied Pharmacology in Medical Treatment. New York: Grune and Stratton*.

Bill, A., & Hellsing, K. (1965). Production and drainage of aqueous humor in the cynomolgus monkey (Macaca irus). *Investigative Ophthalmology and Visual Science, 4*(5), 920-926.

Bito, L. Z. (1988). Presbyopia. *Archives of Ophthalmology, 106*(11), 1526-1527.

Bjork, I., & Tanford, C. (1971). Recovery of native conformation of rabbit immunoglobulin G upon recombination of separately renatured heavy and light chains at near-neutral pH. *Biochemistry, 10*(8), 1289-1295.

Bloemendal, H. (1981). *Molecular and cellular biology of the eye lens*: John Wiley & Sons.

Bloemendal, M., & Bloemendal, H. (1998). Hydrophobicity and flexibility of αA- and αB-crystallin are different. *International Journal of Biological Macromolecules, 22*(3), 239-245.

Bochow, T. W., West, S. K., Azar, A., Munoz, B., Sommer, A., & Taylor, H. R. (1989). Ultraviolet light exposure and risk of posterior subcapsular cataracts. *Archives of Ophthalmology, 107*(3), 369-372.

Borcherding, M. S., Blacik, L. J., Sittig, R. A., Bizzell, J. W., Breen, M., & Weinstein, H. G. (1975). Proteoglycans and collagen fibre organization in human corneoscleral tissue. *Experimental Eye Research, 21*(1), 59-70.

Boström, J. E., Dimitrova, M., Canton, C., Håstad, O., Qvarnström, A., & Ödeen, A. (2016). Ultra-rapid vision in birds. *PLOS ONE, 11*(3), e0151099.

Bowmaker, J., & Martin, G. (1978). Visual pigments and colour vision in a nocturnal bird, Strix aluco (tawny owl). *Vision Research, 18*(9), 1125-1130.

Boycott, B. B., Dowling, J. E., & Kolb, H. (1969). Organization of the primate retina: light microscopy. *Philosophical Transactions of the Royal Society of London. Series B, Biological Sciences*, 109-184.

Braekevelt, C. R. (1986). Fine structure of the tapetum cellulosum of the grey seal (Halichoerus grypus). *Acta Anatomica (Basel), 127*(2), 81-87.

Braekevelt, C. R. (1990). Fine structure of the feline tapetum lucidum. *Anatomia, Histologia, Embryologia, 19*(2), 97-105.

Broekhuyse, R., Kuhlmann, E., & Winkens, H. (1979). Lens membranes VII. MIP is an immunologically specific component of lens fiber membranes and is identical with 26K band protein. *Exprimental Eye Research, 29*(3), 303-313.

Brucke, E. (1846). Ueber den musculus Cramptonianus und den spannmuskel der choroidea. *Archiv für Anatomie, Physiologie und Wissenschaftliche Medicine, 1*, 370-378.

Burnside, B., & Nagle, B. (1983). Retinomotor movements of photoreceptors and retinal pigment epithelium: mechanisms and regulation. *Progress in Retinal Research, 2*, 67-109.

Burridge, K., & Wennerberg, K. (2004). Rho and Rac take center stage. *Cell, 116*(2), 167-179.

Burton, D. R. (1985). Immunoglobulin G: functional sites. *Molecular Immunology, 22*(3), 161-206.

Campbell, F. W., Robson, J. G., & Westheimer, G. (1959). Fluctuations of accommodation under steady viewing conditions. *The Journal of Physiology, 145*(3), 579-594.

Carver, J. A., Nicholls, K. A., Aquilina, A. J., & Truscott, R. J. W. (1996). Age-related changes in bovine α-crystallin and high-molecular-weight protein. *Experimental Eye Research, 63*(6), 639-647.

Chan, L. M., & Cathou, R. E. (1977). The role of the inter-heavy chain disulfide bond in modulating the flexibility of immunoglobulin G antibody. *Journal of Molecular Biology, 112*(4), 653-656.

Charman, W. N. (2014). Developments in the correction of presbyopia II: surgical approaches. *Ophthalmic and Physiologic Optics, 34*(4), 397-426.

Cheng, H.-M., & Chylack, L. (1985). Lens metabolism. *The Ocular Lens: Structure, Function and Pathology. New York: Marcel Dekker*, 223-264.

Chepelinsky, A. B. (2003). The ocular lens fiber membrane specific protein MIP/Aquaporin 0. *Journal of Experimental Zoology, Part A: Comparative Experimental Biology, 300A*(1), 41-46.

Chieffi, G., Baccari, G. C., Di Matteo, L., d'Istria, M., Marmorino, C., Minucci, S., & Varriale, B. (1992). The Harderian gland of amphibians and reptiles. *Harderian Glands* (pp. 91-108):

Springer.

Chiou, S. H., Chang, W. P., Lo, C. H., & Chen, S. W. (1987). Sequence comparison of γ-crystallins from the reptilian and other vertebrate species. *FEBS Letters, 221*(1), 134-138.

Choh, V., & Sivak, J. G. (2000a, February 11 - 14, 2000). An *in situ* physiological model to measure lenticular changes during accommodation. Paper presented at the *Vision Science and Its Applications* meeting, Santa Fe, NM.

Choh, V., & Sivak, J. G. (2000b, July 7 - 10, 2000). Optical changes of accommodating lenses in myopic chicks. Paper presented at the *VIII International Conference on Myopia*, Boston, MA.

Choh, V., Sivak, J. G., & Meriney, S. D. (2002). A physiological model to measure effects of age on lenticular accommodation and spherical aberration in chickens. *Investigative Ophthalmology and Visual Science, 43*(1), 92-98.

Choh, V., Sivak, J. G., & Meriney, S. D. (2002). A physiological model to measure effects of age on lenticular accommodation and spherical aberration in chickens. *Investigative Ophthalmology and Visual Science, 43*(1), 92-98.

Clark, J. I., Matsushima, H., David, L. L., & Clark, J. M. (1999). Lens cytoskeleton and transparency: a model. *Eye (Lond), 13 (Pt 3b)*, 417-424.

Clout, N. J., Kretschmar, M., Jaenicke, R., & Slingsby, C. (2001). Crystal structure of the calcium-loaded spherulin 3a dimer sheds light on the evolution of the eye lens βγ-crystallin domain fold. *Structure, 9*(2), 115-124.

Cohen, A. (1965). The electron microscopy of the normal lens. *Investigative Ophthalmology and Visual Science, 4*, 433-446.

Collin, S. P. (2009). Early evolution of vertebrate photoreception: lessons from lampreys and

lungfishes. *Integrative Zoology, 4*(1), 87-98.

Collin, S. P., & Collin, H. B. (2001). The fish cornea: adaptations for different aquatic environments.

Crawford, K. S., Garner, W. H., & Burns, W. (2014). Dioptin™: A novel pharmaceutical formulation for restoration of accommodation in presbyopes. *Investigative Ophthalmology and Visual Science, 55*(13), 3765-3765.

Danysh, B. P., Czymmek, K. J., Olurin, P. T., Sivak, J. G., & Duncan, M. K. (2008). Contributions of mouse genetic background and age on anterior lens capsule thickness. *Anatomical record (Hoboken, N.J. : 2007), 291*(12), 1619-1627.

Davidson, R. S., Dhaliwal, D., Hamilton, D. R., Jackson, M., Patterson, L., Stonecipher, K., Donaldson, K. (2016). Surgical correction of presbyopia. *Journal of Cataract and Refractive Surgery, 42*(6), 920-930.

Davies, L. N., Croft, M. A., Papas, E., & Charman, W. N. (2016). Presbyopia: physiology, prevention and pathways to correction. *Ophthalmic and Physiological Optics, 36*(1), 1-4.

Davies, W. L., Cowing, J. A., Bowmaker, J. K., Carvalho, L. S., Gower, D. J., & Hunt, D. M. (2009). Shedding light on serpent sight: the visual pigments of henophidian snakes. *The Journal of Neuroscience, 29*(23), 7519-7525.

Delaye, M., & Tardieu, A. (1982). Short-range order of crystallin proteins accounts for eye lens transparency. *Nature, 302*(5907), 415-417.

Demer, L. L., & Yin, F. C. (1983). Passive biaxial mechanical properties of isolated canine myocardium. *The Journal of Physiology, 339*, 615-630.

Derham, B. K., & Harding, J. J. (1997). Effect of aging on the chaperone-like function of human alpha-crystallin assessed by three methods. *Biochemical Journal, 328*(Pt 3), 763-768.

Donaghy, H. (2016). Effects of antibody, drug and linker on the preclinical and clinical toxicities of antibody-drug conjugates. *MAbs, 8*(4), 659-671. doi: 10.1080/19420862.2016.1156829

Donaldson, P. J., Musil, L. S., & Mathias, R. T. (2010). Point: A Critical Appraisal of the Lens Circulation Model—An Experimental Paradigm for Understanding the Maintenance of Lens Transparency? *Investigative Ophthalmology and Visual Science, 51*(5), 2303-2306.

Douglas, R., Collett, T., & Wagner, H.-J. (1986). Accommodation in anuran Amphibia and its role in depth vision. *Journal of Comparative Physiology A, 158*(1), 133-143.

Dowling, J., & Boycott, B. (1966). Organization of the primate retina: electron microscopy. *Proceedings of the Royal Society of London B: Biological Sciences, 166*(1002), 80-111.

Drews, R. C. (1979). Posterior subcapsular cataracts. *Archives of Ophthalmology, 97*(8), 1543-1543.

Duane, A. (1908). An attempt to determine the normal range of accommodation at various ages, being a revision of Donder's experiments. *Transactions of the American Ophthalmological Society, 11*(Pt 3), 634-641.

Duane, A. (1925). Are the current theories of accommodation correct? *American Journal of Ophthalmology, 8*(3), 196-202.

Duane, A. (1931). Accommodation. *Archives of Ophthalmology, 5*(1), 1-14.

E, Hemaprabha. (2012). Chemical crosslinking of proteins: a review. *Journal of Pharmaceutical and Scientific Innovation*.

Ehrlich, P., & Herter, C. (1904). Über einige verwendungen der naphtochinonsulfosäure. *Hoppe-Seyler´s Zeitschrift für Physiologische Chemie, 41*(5), 379-392.

Farnsworth, P. N., Shyne, S. E., Caputo, S. J., Fasano, A. V., & Spector, A. (1980). Microtubules: a major cytoskeletal component of the human lens. *Experimental Eye Research, 30*(5), 611-615.

Fincham, E. F. (1937). *The mechanism of accommodation*: G. Pulman & Sons, Limited.

Fincham, E. F. (1951). The accommodation reflex and its stimulus. *British Journal of Ophthalmology, 35*(7), 381.

Fisher, R. (1977). The force of contraction of the human ciliary muscle during accommodation. *The Journal of Physiology, 270*(1), 51.

Fisher, R. (1988). The mechanics of accommodation in relation to presbyopia. *Eye, 2*(6), 646-649.

Frahm, N., Korber, B. T., Adams, C. M., Szinger, J. J., Draenert, R., Addo, M. M., Brander, C. (2004). Consistent cytotoxic-T-lymphocyte targeting of immunodominant regions in human immunodeficiency virus across multiple ethnicities. *Journal of Virology, 78*(5), 2187-2200.

Freddo, T. F. (1996). Ultrastructure of the iris. *Microscopy Research and Technique, 33*(5), 369-389.

Fudge, D. S., McCuaig, J. V., Van Stralen, S., Hess, J. F., Wang, H., Mathias, R. T., & FitzGerald, P. G. (2011). Intermediate filaments regulate tissue size and stiffness in the murine lens. *Investigative Ophthalmology and Visual Science, 52*(6), 3860-3867.

Gabbott, S. E., & Donoghue, P. C. (2016). Pigmented anatomy in Carboniferous cyclostomes and the evolution of the vertebrate eye. *Proceedings of the Royal Society B: Biological Sciences, 283*(1836).

Garner, L. F. (1983). Mechanisms of accommodation and refractive error. *Ophthalmic and Physiological Optics, 3*(3), 287-293.

Garner, W. H., Garner, M., Crawford, K. S., & Burns, W. (2014). Dioptin™ Eye Drop to Treat Presbyopia: corneal penetration and ocular pharmacokinetics. *Investigative Ophthalmology and Visual Science, 55*(13), 3766-3766.

Gaudana, R., Ananthula, H. K., Parenky, A., & Mitra, A. K. (2010). Ocular Drug Delivery. *The*

AAPS Journal, 12(3), 348-360.

Gerkema, M. P., Davies, W. I. L., Foster, R. G., Menaker, M., & Hut, R. A. (2013). The nocturnal bottleneck and the evolution of activity patterns in mammals. *Proceedings of the Royal Society B: Biological Sciences, 280*(1765).

Gerometta, R., & Candia, O. A. (2016). A decrease in the permeability of aquaporin zero as a possible cause for presbyopia. *Medical Hypotheses, 86*, 132-134.

Ghosh, S., Thorogood, P., & Ferretti, P. (1994). Regenerative capability of upper and lower jaws in the newt. *International Journal of Developmental Biology, 38*(3), 479-490.

Giblin, F. J. (2000). Glutathione: a vital lens antioxidant. *Journal of Ocular Pharmacology and Therapeutics, 16*(2), 121-135.

Gil-Cazorla, R., Shah, S., & Naroo, S. A. (2016). A review of the surgical options for the correction of presbyopia. *British Journal of Ophthalmology, 100*(1), 62-70.

Glasser, A., & Campbell, M. C. (1998). Presbyopia and the optical changes in the human crystalline lens with age. *Vision Research, 38*(2), 209-229.

Glasser, A., & Howland, H. C. (1995). *In vitro* changes in back vertex distance of chick and pigeon lenses: species differences and the effects of aging. *Vision Research, 35*(13), 1813-1824.

Glasser, A., & Kaufman, P. L. (1999). The mechanism of accommodation in primates. *Ophthalmology, 106*(5), 863-872.

Glasser, A., Murphy, C. J., Troilo, D., & Howland, H. C. (1995). The mechanism of lenticular accommodation in chicks. *Vision Research, 35*(11), 1525-1540.

Glasser, A., Pardue, M. T., Andison, M. E., & Sivak, J. G. (1997). A behavioral study of refraction, corneal curvature, and accommodation in raptor eyes. *Canadian journal of zoology, 75*, 2010-2020.

Glasser, A., Troilo, D., & Howland, H. C. (1994). The mechanism of corneal accommodation in chicks. *Vision Research, 34*(12), 1549-1566.

Godwin, J. W., & Brockes, J. P. (2006). Regeneration, tissue injury and the immune response. *Journal of Anatomy, 209*(4), 423-432.

Goodenough, D. A. (1979). Lens gap junctions: a structural hypothesis for nonregulated low-resistance intercellular pathways. *Investigative Ophthalmology and Visual Science, 18*(11), 1104-1122.

Guirao, A., Redondo, M., & Artal, P. (2000). Optical aberrations of the human cornea as a function of age. *Journal of the Optical Society of America, A, Optics, image science, and vision, 17*(10), 1697-1702.

Gullstrand, A., & von Helmholtz, H. (1909). *Handbuch der physiologischen Optik. 1. Die Dioptrik des Auges*: Voss.

Gullstrand, v. A. (1924). Mechanism of accommodation.

Hai, C. M., & Murphy, R. A. (1988). Cross-bridge phosphorylation and regulation of latch state in smooth muscle. *American Journal of Physiology, 254*(1 Pt 1), C99-106.

Hall, A. (1998). Rho GTPases and the actin cytoskeleton. *Science, 279*(5350), 509-514.

Hall, S. M., & Haworth, S. G. (1996). Effect of cold preservation on pulmonary arterial smooth muscle cells. *American Journal of Physiology, 270*(3 Pt 1), L435-445.

Hall, S. M., Komai, H., Reader, J., & Haworth, S. G. (1994). Donor lung preservation: effect of cold preservation fluids on cultured pulmonary endothelial cells. *American Journal of Physiology, 267*(5 Pt 1), L508-517.

Hanson, S. R., Hasan, A., Smith, D. L., & Smith, J. B. (2000). The major in vivo modifications of the human water-insoluble lens crystallins are disulfide bonds, deamidation, methionine

oxidation and backbone cleavage. *Experimental Eye Research, 71*(2), 195-207.

Harris, R. J. (2005). Heterogeneity of recombinant antibodies: linking structure to function. *Developmental Biology (Basel), 122*, 117-127.

Haslbeck, M., Peschek, J., Buchner, J., & Weinkauf, S. (2016). Structure and function of α-crystallins: Traversing from in vitro to in vivo. *Biochimica et Biophysica Acta (BBA) - General Subjects, 1860*(1, Part B), 149-166.

Heath, A. R. (1990). The ocular tapetum lucidum: a model system for interdisciplinary studies in elasmobranch biology. *Journal of Experimental Zoology, 256*(S5), 41-45.

Helmholtz, H. (1855). Über die Akkommodation des Auges. *Albrecht v Graefes Arch Ophthalmol 1855, 1: 1–74., 1*(1), 1-74.

Helmholtz, H. v. (1962). *Helmholtz's treatise on physiological optics* (Translated from the 3d German ed.). New York,: Dover Publications.

Helmholtz, H. v., & Southall, J. P. (1924). Mechanism of accommodation.

Higashita, R., Sugawara, M., Kondoh, Y., Kawai, Y., Mitsui, K., Ohki, S., Suma, K. (1996). Changes in diastolic regional stiffness of the left ventricle before and after coronary artery bypass grafting. *Heart Vessels, 11*(3), 145-151.

Hocking, B., & Mitchell, B. (1961). Owl vision. *Ibis, 103*(2), 284-288.

Hodgson, E. S., & Mathewson, R. F. (1978). Sensory biology of sharks, skates, and rays: DTIC Document.

Holden, B. A., Fricke, T. R., Ho, S., & et al. (2008). Global vision impairment due to uncorrected presbyopia. *Archives of Ophthalmology, 126*(12), 1731-1739.

Holly, F. J., & Lemp, M. A. (1977). Tear physiology and dry eyes. *Survey of Ophthalmology, 22*(2), 69-87.

Hopp, T. P., & Woods, K. R. (1981). Prediction of protein antigenic determinants from amino acid sequences. *Proceedings of the National Academy of Sciences of the United States of America, 78*(6), 3824-3828.

Horwitz, J. (1992). Alpha-crystallin can function as a molecular chaperone. *Proceedings of the National Academy of Sciences of the United States of America, 89*(21), 10449-10453.

Horwitz, J. (2003). Alpha-crystallin. *Experimental Eye Research, 76*(2), 145-153.

Horwitz, J. (2009). Alpha crystallin: The quest for a homogeneous quaternary structure. *Experimental Eye Research, 88*(2), 190-194.

Hozic, A., Rico, F., Colom, A., Buzhynskyy, N., & Scheuring, S. (2012). Nanomechanical characterization of the stiffness of eye lens cells: a pilot study. *Investigative Ophthalmology and Visual Science, 53*(4), 2151-2156.

Imokawa, Y., & Brockes, J. P. (2003). Selective activation of thrombin is a critical determinant for vertebrate lens regeneration. *Current Biology, 13*(10), 877-881.

Ireland, M., Lieska, N., & Maisel, H. (1983). Lens actin: Purification and localization. *Experimental Eye Research, 37*(4), 393-408.

Ireland, M., & Maisel, H. (1983). Identification of native actin filaments in chick lens fiber cells. *Experimental Eye Research, 36*(4), 531-536.

Jakob, U., Gaestel, M., Engel, K., & Buchner, J. (1993). Small heat shock proteins are molecular chaperones. *Journal of Biological Chemistry, 268*(3), 1517-1520.

Ji, Y., Cai, L., Zheng, T., Ye, H., Rong, X., Rao, J., & Lu, Y. (2015). The mechanism of UVB irradiation induced-apoptosis in cataract. *Molecular and Cellular Biochemistry, 401*(1-2), 87-95.

Jones, M. P., Pierce, K. E., & Ward, D. (2007). Avian vision: a review of form and function with

special consideration to birds of prey. *Journal of Exotic Pet Medicine, 16*(2), 69-87.

Jordan, M., Luthardt, G., Meyer-Naujoks, C., & Roth, G. (1980). The role of eye accommodation in the depth perception of common toads. *Zeitschrift für Naturforschung C, 35*(9-10), 851-852.

Kamm, K. E., & Stull, J. T. (1985). The function of myosin and myosin light chain kinase phosphorylation in smooth muscle. *Annual Review of Pharmacology and Toxicology, 25*, 593-620.

Kaufman, P. L. (2008). Enhancing trabecular outflow by disrupting the actin cytoskeleton, increasing uveoscleral outflow with prostaglandins, and understanding the pathophysiology of presbyopia: Interrogating Mother Nature: asking why, asking how, recognizing the signs, following the trail. *Experimental Eye Research, 86*(1), 3-17.

Kibbelaar, M. A., Ramaekers, F. C., Ringens, P. J., Selten-Versteegen, A. M., Poels, L. G., Jap, P. H., Bloemendal, H. (1980). Is actin in eye lens a possible factor in visual accomodation? *Nature, 285*(5765), 506-508.

Kibbelaar, M. A., Selten-Versteegen, A.-M. E., Dunia, I., Benedetti, E. L., & Bloemendal, H. (1979). Actin in Mammalian Lens. *European Journal of Biochemistry, 95*(3), 543-549.

Klemenz, R., Fröhli, E., Steiger, R. H., Schäfer, R., & Aoyama, A. (1991). Alpha B-crystallin is a small heat shock protein. *Proceedings of the National Academy of Sciences of the United States of America, 88*(9), 3652-3656.

Kolega, J., & Kumar, S. (1999). Regulatory light chain phosphorylation and the assembly of myosin II into the cytoskeleton of microcapillary endothelial cells. *Cell Motility and the Cytoskeleton, 43*(3), 255-268.

Komai, Y., & Ushiki, T. (1991). The three-dimensional organization of collagen fibrils in the human cornea and sclera. *Investigative Ophthalmology and Visual Science, 32*(8), 2244-2258.

Koretz, J. F., & Cook, C. A. (2001). Aging of the optics of the human eye: lens refraction models and principal plane locations. *Optometry and Vision Science, 78*(6), 396-404.

Koretz, J. F., Cook, C. A., & Kaufman, P. L. (2002). Aging of the human lens: changes in lens shape upon accommodation and with accommodative loss. *Journal of the Optical Society of America A, 19*(1), 144-151.

Koretz, J. F., & Handelman, G. H. (1982). Model of the accommodative mechanism in the human eye. *Vision Research, 22*(8), 917-927.

Kovacs, K. M., Toth, J., Hetenyi, C. Malnasi-Csizmadia, A., Sellers, J. R. (2004). Mechanism of Blebbistatin Inhibition of Myosin II. *The Journal of Biological Chemistry, 279*(34), 35557-35563.

Kruse, F. E. (1994). Stem cells and corneal epithelial regeneration. *Eye, 8*(2), 170-183.

Kuhn, J. R., & Pollard, T. D. (2005). Real-time measurements of actin filament polymerization by total internal reflection fluorescence microscopy. *Biophysical Journal, 88*(2), 1387-1402.

Kusak, J. R., & Brown, H. G. (1994). Embryology and anatomy of the lens. *Principles and Practice of Ophthalmology, 12*(11), 82.

Kuszak, J. R. (1995). The ultrastructure of epithelial and fiber cells in the crystalline lens. *International Review of Cytology, 163*, 305-350.

Kuszak, J. R., Bertram, B. A., Macsai, M. S., & Rae, J. L. (1984). Sutures of the crystalline lens: a review. *Scanning Electron Microscopy* (Pt 3), 1369-1378.

Kuszak, J. R., Zoltoski, R. K., & Tiedemann, C. E. (2004). Development of lens sutures. *International Journal of Developmental Biology, 48*(8-9), 889-902.

Kuwabara, T. (1975). The maturation of the lens cell: a morphologic study. *Experimental Eye Research, 20*(5), 427-443.

Lee, B. S., Huang, J. S., Jayathilaka, G. D., Lateef, S. S., & Gupta, S. (2010). Production of antipeptide antibodies. *Methods of Molecular Biology, 657*, 93-108.

Lee, C. J., Vroom, J. A., Fishman, H. A., & Bent, S. F. (2006). Determination of human lens capsule permeability and its feasibility as a replacement for Bruch's membrane. *Biomaterials, 27*(8), 1670-1678.

Lee, D. C., Gonzalez, P., Rao, P. V., Zigler, J. S., Jr., & Wistow, G. J. (1993). Carbonyl-metabolizing enzymes and their relatives recruited as structural proteins in the eye lens. *Advances in Experimental Medicine and Biology, 328*, 159-168.

Leong, Y. Y., & Tong, L. (2015). Barrier function in the ocular surface: from conventional paradigms to new opportunities. *The Ocular Surface, 13*(2), 103-109.

Lesurtel, M., Graf, R., Aleil, B., Walther, D. J., Tian, Y., Jochum, W., Clavien, P. A. (2006). Platelet-derived serotonin mediates liver regeneration. *Science, 312*(5770), 104-107.

Levine, J. S., & MacNichol, E. F. (1979). Visual pigments in teleost fishes: effects of habitat, microhabitat, and behavior on visual system evolution. *Sensory Processes*.

Levine, R. P., Monroy, J. A., & Brainerd, E. L. (2004). Contribution of eye retraction to swallowing performance in the northern leopard frog, Rana pipiens. *Journal of Experimental Biology, 207*(8), 1361-1368.

Levy, B., & Sivak, J. (1980). Mechanisms of accommodation in the bird eye. *Journal of Comparative Physiology, 137*(3), 267-272.

Li, W.-C., & Spector, A. (1996). Lens epithelial cell apoptosis is an early event in the development of UVB-induced cataract. *Free Radical Biology and Medicine, 20*(3), 301-311.

Li, W., Hayashida, Y., Chen, Y. T., & Tseng, S. C. (2007). Niche regulation of corneal epithelial stem cells at the limbus. *Cell Research, 17*(1), 26-36.

Linetsky, M., & Ortwerth, B. J. (1996). Quantitation of the Reactive Oxygen Species Generated by the UVA Irradiation of Ascorbic Acid-Glycated Lens Proteins. *Photochemistry and Photobiology, 63*(5), 649-655.

Lodish, H., Berk, A., Zipursky, S. L., Matsudaira, P., Baltimore, D., & Darnell, J. (2000). Protein structure and function.

Lowenstein, O., & Loewenfeld, I. E. (1950). Role of sympathetic and parasympathetic systems in reflex dilatation of the pupil: Pupillographic studies. *Archives of Neurology & Psychiatry, 64*(3), 313-340.

Lubsen, N., Aarts, H., & Schoenmakers, J. (1988). The evolution of lenticular proteins: the β-and γ-crystallin super gene family. *Progress in biophysics and molecular biology, 51*(1), 47-76.

Luck, S., & Choh, V. (2010). Effects of a myosin light chain kinase inhibitor on the optics and accommodation of the avian crystalline lens. *Molecular Vision, 17*, 2759-2764.

Lyall, A. (1957). The Growth of the Trout Reina. *Journal of Cell Science, 3*(41), 101-110.

Maddala, R., Deng, P. F., Costello, J. M., Wawrousek, E. F., Zigler, J. S., & Rao, V. P. (2004). Impaired cytoskeletal organization and membrane integrity in lens fibers of a Rho GTPase functional knockout transgenic mouse. *Lab Invest, 84*(6), 679-692.

Maggs, D. J., Miller, P., & Ofri, R. (2012). *Slatter's fundamentals of veterinary ophthalmology*: Elsevier Health Sciences.

Maisel, H., & Perry, M. M. (1972). Electron microscope observations on some structural proteins of the chick lens. *Experimental Eye Research, 14*(1), 7-12.

Martens, J. C., & Radmacher, M. (2008). Softening of the actin cytoskeleton by inhibition of myosin II. *Pflugers Archiv, 456*(1), 95-100.

Mathias, R. T., Kistler, J., & Donaldson, P. (2007). The lens circulation. *Journal of Membrane*

Biology, 216(1), 1-16.

Mathias, R. T., & Rae, J. L. (2004). The lens: local transport and global transparency. *Exp Eye Res, 78*(3), 689-698.

Matthews, J. N., Yim, P. B., Jacobs, D. T., Forbes, J. G., Peters, N. D., & Greer, S. C. (2005). The polymerization of actin: extent of polymerization under pressure, volume change of polymerization, and relaxation after temperature jumps. *Journal of Chemical Physics, 123*(7), 074904.

Maurice, D. M. (1957). The structure and transparency of the cornea. *The Journal of Physiology, 136*(2), 263-286.261.

Maurice, D. M. (1970). The transparency of the corneal stroma. *Vision Research, 10*(1), 107-108.

McAuley, A., Jacob, J., Kolvenbach, C. G., Westland, K., Lee, H. J., Brych, S. R., Matsumura, M. (2008). Contributions of a disulfide bond to the structure, stability, and dimerization of human IgG1 antibody C(H)3 domain. *Protein Science : A Publication of the Protein Society, 17*(1), 95-106.

McAvoy, J. W., & Chamberlain, C. G. (1989). Fibroblast growth factor (FGF) induces different responses in lens epithelial cells depending on its concentration. *Development, 107*(2), 221-228.

McLellan, J. S., Marcos, S., & Burns, S. A. (2001). Age-related changes in monochromatic wave aberrations of the human eye. *Investigative Ophthalmology and Visual Science, 42*(6), 1390-1395.

Meibohm, B., & Derendorf, H. (1997). Basic concepts of pharmacokinetic/pharmacodynamic (PK/PD) modelling. *International Journal of Clinical Pharmacology and Therapeutics, 35*(10), 401-413.

Meister, D. J., & Fisher, S. W. (2008). Progress in the spectacle correction of presbyopia. Part 1: Design and development of progressive lenses. *Clinical and Experimental Optometry, 91*(3), 240-250.

Mills, J. K., & Needham, D. (1999). Targeted drug delivery. *Expert Opinion on Therapeutic Patents, 9*(11), 1499-1513.

Mitashov, V. I. (1996). Mechanisms of retina regeneration in urodeles. *International Journal of Developmental Biology, 40*(4), 833-844.

Mitsuda, S., Yoshii, C., Ikegami, Y., & Araki, M. (2005). Tissue interaction between the retinal pigment epithelium and the choroid triggers retinal regeneration of the newt Cynops pyrrhogaster. *Developmental Biology, 280*(1), 122-132.

Mollon, J., & Bowmaker, J. (1992). The spatial arrangement of cones in the primate fovea. *Nature, 360*(6405), 677-679.

Moore, D. T. (1980). Gradient-index optics: a review. *Applied Optics, 19*(7), 1035-1038.

Morton, W. M., Ayscough, K. R., McLaughlin, P. J. (2000). Latrunculin alters the actin-monomer subunit interface to prevent polymerization. *Nature Cell Biology, 2*.

Muchowski, P. J., Valdez, M. M., & Clark, J. I. (1999). AlphaB-crystallin selectively targets intermediate filament proteins during thermal stress. *Investigative Ophthalmology and Visual Science, 40*(5), 951-958.

Nathans, J. (1987). Molecular biology of visual pigments. *Annual review of neuroscience, 10*(1), 163-194.

Németh-Cahalan, K. L., Kalman, K., & Hall, J. E. (2004). Molecular Basis of pH and Ca(2+) Regulation of Aquaporin Water Permeability. *The Journal of General Physiology, 123*(5), 573-580.

197

Nolte, J. (2002). The human brain: an introduction to its functional anatomy.

O'Day, K. (1952). Observations on the eye of the monotreme. *Transactions of the Opthalmological Society of Australia, 12*, 95-104.

Ollivier, F. J., Samuelson, D. A., Brooks, D. E., Lewis, P. A., Kallberg, M. E., & Komáromy, A. M. (2004). Comparative morphology of the tapetum lucidum (among selected species). *Veterinary Ophthalmology, 7*(1), 11-22.

Ong, H. S., Evans, J. R., & Allan, B. D. (2014). Accommodative intraocular lens versus standard monofocal intraocular lens implantation in cataract surgery. *The Cochrane Database of Systemic Reviews*(5), Cd009667.

Ostrin, L. A., Frishman, L. J., & Glasser, A. (2004). Effects of Pirenzepine on Pupil Size and Accommodation in Rhesus Monkeys. *Investigative Ophthalmology and Visual Science, 45*(10), 3620-3628.

Ostrin, L. A., & Glasser, A. (2010). Autonomic drugs and the accommodative system in rhesus monkeys. *Experimental Eye Research, 90*(1), 104-112.

Ott, M. (2006). Visual accommodation in vertebrates: mechanisms, physiological response and stimuli. *Journal of Comparative Physiology A, 192*(2), 97-111.

Ouellette, D., Alessandri, L., Chin, A., Grinnell, C., Tarcsa, E., Radziejewski, C., & Correia, I. (2010). Studies in serum support rapid formation of disulfide bond between unpaired cysteine residues in the VH domain of an immunoglobulin G1 molecule. *Analytical Biochemistry, 397*(1), 37-47.

Oyster, C. W. (1999). *The human eye: structure and function*. Sunderland, Mass.: Sinauer Associates.

Pardue, M. T., & Sivak, J. G. (1997). The functional anatomy of the ciliary muscle in four avian

species. *Brain, Behavior and Evolution, 49*(6), 295-311.

Payne, A. (1994). The harderian gland: a tercentennial review. *Journal of anatomy, 185*(Pt 1), 1.

Pearce, T. L., & Zwaan, J. (1970). A light and electron microscopic study of cell behavior and microtubules in the embryonic chicken lens using Colcemid. *Development, 23*(2), 491-507.

Pellegrini, G., Golisano, O., Paterna, P., Lambiase, A., Bonini, S., Rama, P., & De Luca, M. (1999). Location and clonal analysis of stem cells and their differentiated progeny in the human ocular surface. *The Journal of cell biology, 145*(4), 769-782.

Perng, M.-D., Zhang, Q., & Quinlan, R. A. (2007). Insights into the beaded filament of the eye lens. *Experimental Cell Research, 313*(10), 2180-2188.

Phillips, R. (2009). Sensory Physiology: Evolution and Anatomy of Snake Eyes.

Piatigorsky, J. (1981). Lens Differentiation in Vertebrates. *Differentiation, 19*(1-3), 134-153.

Piatigorsky, J. (1981). Lens differentiation in vertebrates. A review of cellular and molecular features. *Differentiation, 19*(3), 134-153.

Piatigorsky, J. (1984). Delta crystallins and their nucleic acids. *Molecular and Cellular Biochemistry, 59*(1), 33-56.

Piatigorsky, J. (1993). Puzzle of crystallin diversity in eye lenses. *Developmental Dynamics, 196*(4), 267-272.

Piatigorsky, J., O'Brien, W. E., Norman, B. L., Kalumuck, K., Wistow, G. J., Borras, T., Wawrousek, E. F. (1988). Gene sharing by delta-crystallin and argininosuccinate lyase. *Proceedings of the National Academy of Sciences of the United States of America, 85*(10), 3479-3483.

Piatigorsky, J., Webster, H. d. F., & Wollberg, M. (1972). Cell elongation in the cultured embryonic chick lens epithelium with and without protein synthesis. Involvement of microtubules.

Journal of Cell Biology, 55(1), 82-92.

Pierscionek, B. K., & Chan, D. Y. C. (1989). Refractive Index Gradient of Human Lenses. *Optometry and Vision Science, 66*(12), 822-829.

Pollard, T. D. (1986). Rate constants for the reactions of ATP- and ADP-actin with the ends of actin filaments. *The Journal of Cell Biology, 103*(6 Pt 2), 2747-2754.

Prince, J. H. (1956). *Comparative anatomy of the eye*: Thomas.

Priolo, S., Sivak, J. G., & Kuszak, J. R. (1999). Effect of age on the morphology and optical quality of the avian crystalline lens. *Experimental Eye Research, 69*(6), 629-640.

Quinlan, R. A., Sandilands, A., Procter, J. E., Prescott, A. R., Hutcheson, A. M., Dahm, R., Carter, J. M. (1999a). The eye lens cytoskeleton. *Eye, 13*(3b), 409-416.

Rafferty, N. (1985). *Lens Morphology*. New York: Marcel Decker.

Rafferty, N. S., Rafferty, K. A., & Ito, E. (1994). Agonist-induced rise in intracellular calcium of lens epithelial cells: effects on the actin cytoskeleton. *Experimental Eye Research, 59*(2), 191-201.

Rafferty, N. S., Scholz, D. L., Goldberg, M., & Lewyckyj, M. (1990). Immunocytochemical evidence for an actin-myosin system in lens epithelial cells. *Experimental Eye Research, 51*(5), 591-600.

Rajchard, J. (2009). Ultraviolet (UV) light perception by birds: a review. *Veterinarni Medicina, 54*(8), 351-359.

Ramaekers, F. C., Poels, L. G., Jap, P. H., & Bloemendal, H. (1982). Simultaneous demonstration of microfilaments and intermediate-sized filaments in the lens by double immunofluorescence. *Experimental Eye Research, 35*(4), 363-369.

Rao, P. V., Huang, Q.-l., Horwitz, J., & Zigler, J. S. (1995). Evidence that α-crystallin prevents non-

specific protein aggregation in the intact eye lens. *Biochimica et Biophysica Acta (BBA) - General Subjects, 1245*(3), 439-447.

Rao, P. V., & Maddala, R. (2006). The role of the lens actin cytoskeleton in fiber cell elongation and differentiation. *Seminars in Cell & Developmental Biology, 17*(6), 698-711.

Reddy, V. N. (1990). Glutathione and its function in the lens--an overview. *Experimental Eye Research, 50*(6), 771-778.

Reyer, R. W. (1954). Regeneration of the lens in the amphibian eye. *The Quarterly Review of Biology, 29*(1), 1-46.

Reyer, R. W. (1977). The Amphibian Eye: Development and Regeneration. In F. Crescitelli (Ed.), *The Visual System in Vertebrates* (pp. 309-390). Berlin, Heidelberg: Springer Berlin Heidelberg.

Richdale, K., Sinnott, L. T., Bullimore, M. A., Wassenaar, P. A., Schmalbrock, P., Kao, C. Y., Zadnik, K. (2013). Quantification of age-related and per diopter accommodative changes of the lens and ciliary muscle in the emmetropic human eye. *Invest Ophthalmol Vis Sci, 54*(2), 1095-1105.

Ridley, A. J., Schwartz, M. A., Burridge, K., Firtel, R. A., Ginsberg, M. H., Borisy, G., Horwitz, A. R. (2003). Cell migration: integrating signals from front to back. *Science, 302*(5651), 1704-1709.

Roberts, J. E. (2011). Ultraviolet Radiation as a Risk Factor for Cataract and Macular Degeneration. *Eye Contact Lens, 37*(4), 246-249.

Rosner, L., Farmer, C. J., & Bellows, J. (1938). Biochemistry of the lens: Xii. studies on glutathione in the crystalline lens. *Archives of Ophthalmology, 20*(3), 417-426.

Roy, D., & Spector, A. (1976). Absence of low-molecular-weight alpha crystallin in nuclear region

of old human lenses. *Proceedings of the National Academy of Sciences of the United States of America, 73*(10), 3484-3487.

Saponara, S., Fabio, F., Sgaragli, G., Maurizio, C., Hopkins, B., Bova, S. (2012). Effects of commonly used protein kinase inhibitors on vascular contraction and L-type calcium current. *Biochemical Pharmacology*.

Sassoon, I., & Blanc, V. (2013). Antibody–Drug Conjugate (ADC) Clinical Pipeline: A Review. In L. Ducry (Ed.), *Antibody-Drug Conjugates* (pp. 1-27). Totowa, NJ: Humana Press.

Schachar, R. A. (1992). Cause and treatment of presbyopia with a method for increasing the amplitude of accommodation. *Annals of ophthalmology, 24*(12), 445.

Schachar, R. A. (2015). Human Accommodative Ciliary Muscle Configuration Changes Are Consistent With Schachar's Mechanism of Accommodation. *Investigative Ophthalmology and Visual Science, 56*(10), 6075.

Schaeffel, F., Glasser, A., & Howland, H. C. (1988). Accommodation, refractive error and eye growth in chickens. *Vision Research, 28*(5), 639-657.

Schaeffel, F., & Howland, H. C. (1991). Properties of the feedback loops controlling eye growth and refractive state in the chicken. *Vision Research, 31*(4), 717-734.

Schroeder, D. D., Tankersley, D. L., & Lundblad, J. L. (1981). A new preparation of modified immune serum globulin (human) suitable for intravenous administration. I. Standardization of the reduction and alkylation reaction. *Vox Sanguinis, 40*(6), 373-382.

Schumacher, D., Hackenberger, C. P., Leonhardt, H., & Helma, J. (2016). Current Status: Site-Specific Antibody Drug Conjugates. *36 Suppl 1*, 100-107.

Shestopalov, V. I., & Bassnett, S. (2000). Expression of autofluorescent proteins reveals a novel protein permeable pathway between cells in the lens core. *Journal of Cell Science, 113 (Pt*

11), 1913-1921.

Shestopalov, V. I., & Bassnett, S. (2003). Development of a macromolecular diffusion pathway in the lens. *Journal of Cell Science, 116*(Pt 20), 4191-4199.

Shirama, K., Kikuyama, S., Takeo, Y., Shimizu, K., & Maekawa, K. (1982). Development of Harderian gland during metamorphosis in anurans. *The Anatomical Record, 202*(3), 371-378.

Sillman, A. J. (1973). Avian vision. *Avian biology, 3*, 349-387.

Silverthorn, D. U., Ober, W. C., Garrison, C. W., Silverthorn, A. C., & Johnson, B. R. (2009). *Human physiology: an integrated approach*: Pearson/Benjamin Cummings San Francisco, CA, USA.

Simon, A., & Brockes, J. P. (2002). Thrombin activation of S-phase reentry by cultured pigmented epithelial cells of adult newt iris. *Experimental Cell Research, 281*(1), 101-106.

Sinard, J. H., & Pollard, T. D. (1990). Acanthamoeba myosin-II minifilaments assemble on a millisecond time scale with rate constants greater than those expected for a diffusion limited reaction. *The Journal of Biological Chemistry, 265*(7), 3654-3660.

Sindhu Kumari, S., Gupta, N., Shiels, A., FitzGerald, P. G., Menon, A. G., Mathias, R. T., & Varadaraj, K. (2015). Role of Aquaporin 0 in lens biomechanics. *Biochemical and Biophysical Research Communications, 462*(4), 339-345.

Sivak, J. (1978). Refraction and accommodation of the elasmobranch eye. *Sensory Biology of Sharks, Skates and Rays (ed. ES Hodgson and RF Mathewson)*, 107-116.

Sivak, J. (1990). Elasmobranch visual optics. *Journal of Experimental Zoology, 256*(S5), 13-21.

Sivak, J., & Woo, G. (1975). Accommodative lens movement in holosteans (Amia calva and Lepisosteus osseus oxyurus) and in the sea lamprey (Petromyzon marinus). *Canadian journal of zoology, 53*(5), 516-520.

Sivak, J. G. (1975). Accommodative mechanisms in aquatic vertebrates *Vision in fishes* (pp. 289-297): Springer.

Sivak, J. G. (1977). The role of the spectacle in the visual optics of the snake eye. *Vision Res, 17*(2), 293-298.

Sivak, J. G. (1980). Accommodation in vertebrates: a contemporary survey. *Current Topics in Eye Research, 3*, 281-330.

Sivak, J. G., Herbert, K. L., Peterson, K. L., & Kuszak, J. R. (1994). The interrelationship of lens anatomy and optical quality. I. Non- primate lenses. *Experimental Eye Research, 59*(5), 505-520.

Sivak, J. G., & Kreuzer, R. O. (1983). Spherical aberration of the crystalline lens. *Vision Research, 23*(1), 59-70.

Sivak, J. G., Ryall, L. A., Weerheim, J., & Campbell, M. C. (1989a). Optical constancy of the chick lens during pre- and post-hatching ocular development. *Investigative Ophthalmology and Visual Science, 30*(5), 967-974.

Sivak, J. G., Ryall, L. A., Weerheim, J., & Campbell, M. C. (1989b). Optical constancy of the chick lens during pre- and post-hatching ocular development. *Investigative Ophthalmology and Visual Science, 30*(5), 967-974.

Slingsby, C., Wistow, G. J., & Clark, A. R. (2013). Evolution of crystallins for a role in the vertebrate eye lens. *Protein Science : A Publication of the Protein Society, 22*(4), 367-380.

Somiya, H. (1987). Dynamic mechanism of visual accommodation in teleosts: structure of the lens muscle and its nerve control. *Proceedings of the Royal Society of London B: Biological Sciences, 230*(1258), 77-91.

Somiya, H., & Tamura, T. (1973). Studies on the visual accommodation in fishes. *Japanese Journal*

of Ichthyology, 20, 193-206.

Song, S., Landsbury, A., Dahm, R., Liu, Y., Zhang, Q., & Quinlan, R. A. (2009). Functions of the intermediate filament cytoskeleton in the eye lens. *The Journal of Clinical Investigation, 119*(7), 1837-1848.

Spector, N. R., Shochet, Y., Kashman, A. (1983). Latrunculins: novel marine toxins that disrupt microfilament organization in cultured cells. *Science, 219*(4584), 493-495.

Sperduto, R. D., & Hiller, R. (1984). The Prevalence of Nuclear, Cortical, and Posterior Subcapsular Lens Opacities in a General Population Sample. *Ophthalmology, 91*(7), 815-818.

Srinivasan, A. N., Nagineni, C. N., & Bhat, S. P. (1992). alpha A-crystallin is expressed in non-ocular tissues. *Journal of Biological Chemistry, 267*(32), 23337-23341.

Stone, L., & Farthing, T. (1942). Return of vision four times in the same adult salamander eye (Triturus viridescens) repeatedly transplanted. *Journal of Experimental Zoology, 91*(2), 265-285.

Strenk, S. A., Strenk, L. M., & Koretz, J. F. (2005). The mechanism of presbyopia. *Progress in Retinal and Eye Research, 24*(3), 379-393.

Takemoto, L., & Boyle, D. (1994). Molecular chaperone properties of the high molecular weight aggregate from aged lens. *Current Eye Research, 13*(1), 35-44.

Takizawa, N., Ikebe, R., Ikebe, M., & Luna, E. J. (2007). Supervillin slows cell spreading by facilitating myosin II activation at the cell periphery. *Journal of Cell Science, 120*(Pt 21), 3792-3803.

Tamm, S., Tamm, E., & Rohen, J. W. (1992). Age-related changes of the human ciliary muscle. A quantitative morphometric study. *Mechanisms of ageing and development, 62*(2), 209-221.

Tamura, T. (1957). A study of visual perception in fish, especially on resolving power and

accommodation. *Bulletin of the Japanese Society of Scientific Fisheries, 22*(9), 536-557.

Tanaka, E. M., & Brockes, J. P. (1998). A target of thrombin activation promotes cell cycle re-entry by urodele muscle cells. *Wound Repair Regen, 6*(4), 371-381.

Tapon, N., & Hall, A. (1997). Rho, Rac and Cdc42 GTPases regulate the organization of the actin cytoskeleton. *Current Opinion in Cell Biology, 9*(1), 86-92.

Tassava, R. A., & Huang, Y. (2005). Tail regeneration and ependymal outgrowth in the adult newt, Notophthalmus viridescens, are adversely affected by experimentally produced ischemia. *Journal of experimental zoology. Part A, Comparative experimental biology, 303*(12), 1031-1039.

Taylor, V. L., al-Ghoul, K. J., Lane, C. W., Davis, V. A., Kuszak, J. R., & Costello, M. J. (1996). Morphology of the normal human lens. *Investigative Ophthalmology and Visual Science, 37*(7), 1396-1410.

The Eye Diseases Prevalence Research, G. (2004). The prevalence of refractive errors among adults in the united states, western europe, and australia. *Archives of Ophthalmology, 122*(4), 495-505.

Thies, M. J., Mayer, J., Augustine, J. G., Frederick, C. A., Lilie, H., & Buchner, J. (1999). Folding and association of the antibody domain CH3: prolyl isomerization preceeds dimerization. *Journal of Molecular Biology, 293*(1), 67-79.

Thoft, R. A., & Friend, J. (1983). The X, Y, Z hypothesis of corneal epithelial maintenance. *Investigative Ophthalmology and Visual Science, 24*(10), 1442-1443.

Tian, B., Brumback, L. C., & Kaufman, P. L. (2000). ML-7, chelerythrine and phorbol ester increase outflow facility in the monkey eye. *Experimental Eye Research, 71*(6), 551-566.

Tripathi, R. C. (1971). Mechanism of the aqueous outflow across the trabecular wall of Schlemm's

canal. *Experimental Eye Research, 11*(1), 116-121.

Troy, A. B. (2015). Targeted Cancer Therapy: The Next Generation of Cancer Treatment. *Current Drug Discovery Technologies, 12*(1), 3-20.

van der Zypen, E. (1978). The arrangement of the connective tissue in the stroma iridis of man and monkey. *Experimental Eye Research, 27*(3), 349-357.

van Heyningen, R. (1969). The lens: metabolism and cataract. *The Eye, 1*, 381-488.

Walls, G. L., & Cranbrook Institute of Science. (1942). *The vertebrate eye and its adaptive radiation*. Bloomfield Hills, Mich.: Cranbrook Institute of Science.

Wang, K., & Spector, A. (1994). The chaperone activity of bovine alpha crystallin. Interaction with other lens crystallins in native and denatured states. *Journal of Biological Chemistry, 269*(18), 13601-13608.

Wang, X., Garcia, C. M., Shui, Y.-B., & Beebe, D. C. (2004). Expression and regulation of α-, β-, and γ-crystallins in mammalian lens epithelial cells. *Investigative Ophthalmology and Visual Science, 45*(10), 3608-3619.

Watson, D. (1918). *On Seymouria, the most primitive known reptile*. Paper presented at the Proceedings of the Zoological Society of London.

Weale, R. (1962). Presbyopia. *British Journal of Ophthalmology, 46*(11), 660.

Weeber, H. A., & van der Heijde, R. G. (2008). Internal deformation of the human crystalline lens during accommodation. *Acta Ophthalmologica, 86*(6), 642-647.

Weinreb, R. N. (2000). Uveoscleral outflow: the other outflow pathway. *Journal of Glaucoma, 9*(5), 343-345.

Wendt, M., He, L., & Glasser, A. (2013). Comparison between carbachol iontophoresis and intravenous pilocarpine stimulated accommodation in anesthetized rhesus monkeys.

Experimental Eye Research, 115, 123-130.

West, J. A., Sivak, J. G., & Doughty, M. J. (1991). Functional morphology of lenticular accommodation in the young chicken (*Gallus domesticus*). *Canadian journal of zoology, 69*(8), 2183-2193.

Williams, T., & Wilkinson, J. (1992). Position of the fovea centralis with respect to the optic nerve head. *Optometry and Visiual Science, 69*(5), 369-377.

Willner, D., Trail, P. A., Hofstead, S. J., King, H. D., Lasch, S. J., Braslawsky, G. R., Firestone, R. A. (1993). (6-Maleimidocaproyl)hydrazone of doxorubicin--a new derivative for the preparation of immunoconjugates of doxorubicin. *Bioconjugate Chemistry, 4*(6), 521-527.

Wistow, G. (1993). Lens crystallins: gene recruitment and evolutionary dynamism. *Trends in Biochemical Sciences, 18*(8), 301-306.

Won, G.-J., Fudge, D. S., & Choh, V. (2015). The effects of actomyosin disruptors on the mechanical integrity of the avian crystalline lens. *Molecular Vision, 21*, 98-109.

Woolner, S., & Bement, W. M. (2009). Unconventional myosins acting unconventionally. *Trends in cell biology, 19*(6), 245-252.

y Cajal, S. R. (1893). *La rétine des vertébrés*: Typ. de Joseph van In & Cie.

Yeh, S. D. L. S., W. Liou, N. S. Rafferty. (1986). Polygonal Arrays of Actin Filaments in Human Lens Epithelial Cells. *Investigative Opthalmology and Visual Science, 27*, 1535-1539.

Yuen, S. L., Ogut, O., & Brozovich, F. V. (2009). Nonmuscle myosin is regulated during smooth muscle contraction. *American Journal of Physiology Heart and Circulatory Physiology, 297*(1), H191-199.

Yurchenco, P. D., & Schittny, J. C. (1990). Molecular architecture of basement membranes. *The FASEB Journal, 4*(6), 1577-1590.

Zigman, S. (2000). Lens UVA photobiology. *Journal of Ocular Pharmacology and Therapeutics, 16*(2), 161-165.

Zinn, J. G., & Wrisberg, H. A. (1780). *Descriptio anatomica oculi humani iconibus illustrata*. Goettingae: Apud viduam B. Abrami Vandenhoeck.

Zolot, R. S., Basu, S., & Million, R. P. (2013). Antibody-drug conjugates. *Nature Reviews Drug Discovery, 12*(4), 259-260.

APPENDIX

In Figure V-6, untreated retinal tissue had a 90.5% MYH9 to β-actin percentage ratio, while treated lenticular tissue had a 23.3% MYH9 to β-actin percentage ratio. In positive control samples of retinal and lenticular tissues, band intensities (±SEM) of MYH9 concentrations were found to be similar to one another, and similarly proportional to β-actin levels. Untreated retinal and lenticular tissues from 7 day old chickens were collected and processed for western blot as previously described (Section 5.3.5.). In Figure A-1, untreated retinal tissue had a 80.5% MYH9 to β-actin percentage ratio, while untreated lenticular tissue had a 70.2% MYH9 to β-actin percentage.
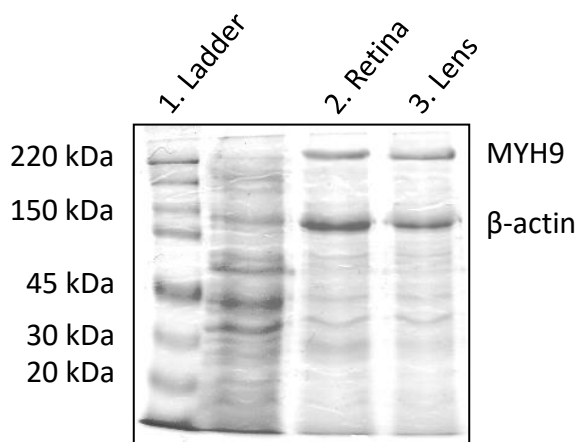

Figure A-1: Western blot of myosin heavy chain 9 (MYH9) levels in untreated retinal and lenticular tissues. Lane 1: molecular weight marker, lane 2: retinal tissue sample, lane 3: lenticular tissue sample. β-actin was used as a loading control.